

EVALUATION OF THE IMPACT OF ENVIRONMENTAL CONDITIONS
ON CONSTITUENT LEACHING FROM GRANULAR MATERIALS
DURING INTERMITTENT INFILTRATION

By

Sarynna López Meza

Dissertation

Submitted to the Faculty of the
Graduate School of Vanderbilt University
in partial fulfillment of the requirements

for the degree of

DOCTOR IN PHILOSOPHY

in

Environmental Engineering

May, 2006

Nashville, Tennessee

Approved:

Professor David S. Kosson

Professor Florence Sanchez

Professor Andrew C. Garrabrants

Professor John C. Ayers

Professor Hans van der Sloot

© 2006

Sarynna López Meza

ALL RIGHTS RESERVED

To all my family,
with love.

*Para toda mi familia,
con cariño.*

ACKNOWLEDGEMENTS

This research project was funded through a Cooperative Agreement (DTFH61-98-X-00095) between the Federal Highway Administration (FHWA) and the University of New Hampshire (Recycled Materials Resource Center – Project 11), and partially with the support of the U.S. Department of Energy, under Award No. DE-FG01-03EW15336 to the Institute for Responsible Management, Consortium for Risk Evaluation with Stakeholder Participation II. However, any opinions, findings, conclusions, or recommendations expressed herein are those of the author and do not necessarily reflect the views of the DOE, IRM/CRESP II, or the FHWA.

I thank the members of my committee for allowing me to take some of their time, and for their valuable contributions. Dr. David Kosson, my advisor, has been a true mentor. I am grateful for the opportunity to work under his direction in such a fascinating project and for making me grow as an engineer. I thank him for his support during difficult times. Drs. Florence Sanchez and Andy Garrabrants were very helpful in the lab and in the writing process, and I thank them for their insights and suggestions. Dr. John Ayers helped me understand geochemical speciation modeling and showed me the fun side of geochemistry. Dr. Hans van der Sloot was extremely helpful with the modeling process, and I am thankful for his long-distance participation in this committee.

I thank Dr. Frank Parker from the Civil and Environmental Engineering Department and Dr. David Ernst from the Physics Department for giving me the opportunity to come to Vanderbilt. Thanks also to Debra Stephens, Rick Stringer-Hye, Kitty Porter, Jon Erickson, John Whelan, and Sherre Harrington for giving me the

opportunity to help them serve the Vanderbilt community as part of the Science and Engineering Library crew during my first four years at the University.

I thank the professors and office staff of the Department of Civil and Environmental Engineering for their help and support. Karen Page has always taken really good care of me and has helped with endless forms, last-minute crises and fun conversations. Mary Jean Morris is a wonderful lab manager and I thank her enormously for making my years in the lab run smoothly. Dr. Jim Clarke provided advice and helped make sure all the proper forms and notices were submitted when needed. Thanks also to Elaine Chisum, Joyce Jones, Dale Rogers, Danny Riley, Whitney Crouch, and Nicole Comstock.

I thank all the people that contributed their time and effort to this project. John Fellenstein from the Physics Machine Shop helped design and put the columns together. Bob Agassie at the University of Wisconsin at Madison did neutron activation analysis on my materials. PSI Laboratories in Nashville crushed my 200 pounds of concrete. Mike Austin helped me set up my aging experiments. Vincent Chatain, Kati Young, Christine Switzer, Kate Langley, Rossane Delapp, and Walter Clark helped me collect samples from my columns or take carbonation measurements while I was running around in Mexico. Special thanks go to Rossane Delapp; without her ICP-MS expertise it would have taken forever to get all my samples analyzed. Alan Wiseman from the Earth and Environmental Sciences Department helped me with SEM analysis. I thank the Chemistry Department for the use of instruments for SEM microscopy and X-ray diffraction analyses, and John Ayers and the Earth and Environmental Sciences Department for allowing me to use their laboratories to further crush my material and

prepare my samples for SEM analysis. The LeachXS crew from ECN in The Netherlands was extremely helpful, and I especially thank Andre van Zomeren and Hans van der Sloot for helping me with my simulations through multiple e-mail conversations.

During my time at Vanderbilt, I have shared an office with a number of interesting people: Kati Young, Christine Switzer, Leslie Shor, Terra Baranowski, Paul Martin, Wei Wang, Wenying Li, Kate Langley, Ned Mitchell, Janey Smith, Derek Bryant, Becky Hinton, and Francesca Maier. While all foreign graduate students must endure the cultural shock of being in a new land, I am grateful to them for introducing me to a wide range of American culture (and other cultures) in a fun way, especially Kati, Christine, Leslie, and Terra.

Nashville has offered many good things, including many friends that have made this experience more enjoyable. Mike, Leslie, Jake and Ellie Shor deserve special thanks: you guys have made me feel at home while being many miles and months away from my family. I thank Jake and Ellie particularly for all the free therapy that I got at their expense. Edgar, Fabiola, and Ana (*Familia Terán Cruz*) also deserve my gratitude for many good times together, even if they were talking on the phone. Thanks also to Christine “LL” Switzer, Terra Baranowski, Hugo Valle, Isa Asensio, Robert Guratzsch, Ned Mitchell, Simon Mudd, Robin Cathcart, René López, Mayra Fortes, Audrey Copeland, Megan Keen, Krissy Shepherd, Caryll and Harris Schenker, Florence Sanchez, Andy Garrabrants, Heather McDonald, Rossane Delapp, and Dave Knickerbocker for sharing all sorts of scholarly, emotional, intellectual, culinary, cultural, musical, traveling, running, dancing, pampering, honky-tonk, political, moving, outdoor and off-road adventures and conversations all through this time.

And even though Mexico was far and I did not get to go as often as I would have liked to, some friends stayed in touch and encouraged me through this time. Daniel Torres is a special friend and I thank him for being there for me. Thanks also to Tere Martínez and Idalia Caballero. I thank my cousins Moni Meza and Lucre García for all of our crazy e-mail conversations, without them I would have lost my sanity long ago. I thank *Tío Lico*, *Tía Yolanda*, and Carmen (*Familia Meza Blanco*) for their support through all my years of school, and Charley, Dianne, and Suzy Boulware for cheering for me from South Carolina.

I want to thank my parents, Juan Francisco and Azucena, for your constant support, for never letting me give up, for always having high expectations, and for all the sacrifices you have made through the years to get me standing here. Thanks also to my siblings, Tania, Claudia, and Julián, for always being there for me. I am sorry I have missed so many important things while being away, but I am grateful distance only seems to have strengthened our bonds. Thanks to all of you for all your love and encouragement in the long periods without seeing each other. *Los quiero mucho.*

The last words I leave for the most important person of all, my wonderful husband, Chase Boulware. Thank you for patiently bearing the long months of hard research and writing work, the weeks of sleep deprivation, and for always having a happy smile and a warm hug to make me feel comforted, supported and loved. There are no words to express the joy of sharing my life with you; taking the scenic route of life to find you was well worth it. I love you.

AGRADECIMIENTOS

Este proyecto fué auspiciado por la *Federal Highway Administration* (FHWA) y el *RMRC* de la Universidad de New Hampshire (Proyecto # 11) por medio del fondo DTFH61-98-X-00095, y en parte por el *U.S. Department of Energy*, bajo el fondo No. DE-FG01-03EW15336 para el *Institute for Responsible Management, Consortium for Risk Evaluation with Stakeholder Participation II*. Sin embargo, cualquier opinion, conclusion, o recomendación expresada aquí es solamente la del autor, y no necesariamente refleja los puntos de vista de DOE, IRM/CRESP II, o la FHWA.

Quiero agradecer a los miembros de mi comité de tesis por permitirme robarles un poco de su tiempo y por sus valiosas contribuciones. El Dr. Kosson, mi asesor, ha sido un gran mentor. Estoy agradecida por la oportunidad de trabajar bajo su tutela en un proyecto tan fascinante, y por motivarme a ser una mejor ingeniera. Le agradezco su apoyo durante tiempos difíciles. Los Dres. Sanchez y Garrabrants me ayudaron mucho en el laboratorio y en el proceso de escribir la tesis, y por eso les agradezco sus comentarios y sugerencias. El Dr. Ayers me ayudó a entender modelación y especiación geoquímica y me enseñó la parte divertida de la geoquímica. El Dr. van der Sloot me ayudó en el proceso de modelación y le agradezco su participación a larga distancia en este comité.

Quiero agradecer al Dr. Parker del Depto. de Ingeniería Civil y Ambiental y al Dr. Ernst del Depto. de Física por darme la oportunidad de venir a Vanderbilt. Gracias también a Debra, Rick, Kitty, Jon, John, Sherre y el resto del personal de la Biblioteca de

Ciencias e Ingeniería por darme la oportunidad de ayudarlos a servir a la comunidad de Vanderbilt durante mis primeros 4 años en la Universidad.

Agradezco a los profesores y el personal del Depto. de Ingeniería Civil y Ambiental por su ayuda y apoyo. Karen ha cuidado siempre de mí y me ha ayudado con el llenado de muchas solicitudes y papeles, crisis de último minuto y conversaciones entretenidas. Mary Jean es una excelente coordinadora del laboratorio y le agradezco que mis años en el laboratorio hayan sido fáciles. El Dr. Clarke se aseguró que todos los documentos para la graduación fueran entregados a tiempo. Gracias también a Elaine, Joyce, Dale, Danny, Whitney y Nicole.

Agradezco a toda la gente que contribuyó con su tiempo y esfuerzo a este proyecto. John Fellenstein, del Taller de Física, ayudó a diseñar y construir las columnas. Bob Aggassie, de la Universidad de Wisconsin en Madison, hizo *NAA* en mis materiales. Los Laboratorios *PSI* en Nashville trituraron mis 200 libras de concreto. Mike me ayudó a hacer mis experimentos de envejecimiento de materiales. Vincent, Kati, Christine, Kate, Rossane, y Walter me ayudaron a tomar muestras de mis columnas o tomar medidas de carbonatación mientras yo andaba en México. Gracias especialmente a Rossane, porque sin su experiencia con el *ICP-MS* me hubiera llevado muchísimo tiempo analizar mis muestras. Alan Wiseman del Depto. de Ciencias Terrestres y Ambientales me ayudó a hacer análisis *SEM*. Agradezco al Depto. de Química por dejarme usar el microscopio electrónico y el difractor de rayos X, y a John Ayers y el Depto. de Ciencias Terrestres y Ambientales por dejarme usar sus laboratorios para triturar mis materiales y preparar mis muestras para el análisis de *SEM*. El personal de *LeachXS* en *ECN* en Holanda me ayudó muchísimo con mi modelación, y agradezco especialmente a

Andre van Zomeren y Hans van der Sloot por ayudarme en mis simulaciones por medio de múltiples conversaciones electrónicas.

Durante mi tiempo en Vanderbilt, he compartido una oficina con mucha gente interesante: Kati, Christine, Leslie, Terra, Paul, Wei, Wenying, Kate, Ned, Janey, Derek, Becky, y Francesca. Aunque es cierto que los estudiantes foráneos deben enfrentar el choque cultural de estar en tierra desconocida, les estoy agradecida a estas personas por introducirme a un gran espectro de la cultura americana (y otras culturas) de una forma divertida, sobre todo a Kati, Christine, Leslie, y Terra.

Nashville ha ofrecido muchas cosas buenas, incluyendo muchas amistades que han hecho esta experiencia más agradable. Mike, Leslie, Jake y Ellie merecen un agradecimiento especial: me han hecho sentir en casa, a pesar de estar a muchas millas y pasar muchos meses lejos de mi familia. Agradezco particularmente a Jake y Ellie por toda la terapia gratuita que tuve a costa suya. Edgar, Fabiola y Ana también merecen mi gratitud por muchos buenos momentos, aunque fueran hablando por teléfono. Gracias también a Christine “LL”, Terra, Hugo, Isa, Robert, Ned, Ramesh, Simon, Robin, René, Mayra, Audrey, Megan, Krissy, Caryll y Harris, Florence, Andy, Heather, Rossane, y Dave por compartir toda clase de aventuras y conversaciones escolares, emocionales, intelectuales, culinarias, culturales, musicales, viajeras, de baile, consentidoras, *honky-tonk*, políticas, de campamento y caminata, y por ayudarme a cambiarme de casa un par de veces.

Y aunque mi México estuvo lejos y no pude ir tan seguido como me hubiera gustado, algunos amigos se mantuvieron en contacto y me apoyaron en todo este tiempo. Daniel es un amigo especial y le agradezco su apoyo constante. Gracias también a Tere e

Idalia. Les agradezco a mis primas Moni y Lucre nuestras conversaciones electrónicas, sin ellas hubiera perdido la cordura hace tiempo. Gracias también a Tío Lico, Tía Yolanda, y Carmen por su cariño y apoyo en todo este tiempo, y a Charley, Dianne, y Suzy for echarme porras desde Carolina del Sur.

Quiero agradecer a mis papás, Juan Francisco y Azucena, por su apoyo constante, por no dejarme vencer por los obstáculos, por siempre esperar lo mejor de mí, y por todos los sacrificios que han hecho para que yo pueda estar en donde estoy ahora. Gracias también a mis hermanitos, Tania, Claudia, y Julián, por siempre estar ahí cuando los necesito. Lamento no haber estado presente en tantas cosas importantes en sus vidas al estar lejos, pero estoy agradecida que la distancia sólo parece haber reforzado nuestros lazos. Gracias a todos por su amor y su apoyo en los largos períodos sin vernos. Los quiero mucho.

Las últimas palabras las dejo para la persona más importante de todas, mi maravilloso marido, Chase Boulware. Gracias por aguantar los largos meses de arduo trabajo y de estar escribiendo la tesis, las últimas semanas de cansancio continuo, y por siempre tener una sonrisa y un abrazo para hacerme sentir tranquila, apoyada y amada. No hay palabras para describir la alegría de compartir mi vida contigo; tomar la ruta escénica de la vida para encontrarte valió *la* pena. Te amo.

TABLE OF CONTENTS

	Page
DEDICATION	iii
ACKNOWLEDGEMENTS	iv
LIST OF FIGURES	xvi
LIST OF TABLES	xx
LIST OF ABBREVIATIONS.....	xxi
Chapter	
I. OVERVIEW	1
Introduction.....	1
Objectives	2
General Background	3
Reuse of materials in construction.....	3
General approach to leaching assessment.....	6
Aging.....	6
Carbonation.....	8
Leaching tests.....	11
Equilibrium tests	13
Dynamic tests.....	13
Geochemical speciation modeling	15
Research Approach	16
Dissertation Structure.....	18
References.....	21
II. ESTIMATION OF FIELD BEHAVIOR BASED ON LABORATORY BATCH DATA.....	27
Abstract	27
Introduction.....	28
Modeling.....	31

Model-based extrapolation of batch tests to long-term release	31
Empirical.....	32
LeachXS.....	36
Methodology	38
Uncertainties	44
Conclusions.....	46
References.....	47

III. THE EFFECTS OF INTERMITTENT UNSATURATED WETTING
ON THE RELEASE OF CONSTITUENTS FROM
CONSTRUCTION DEMOLITION DEBRIS49

Abstract.....	49
Introduction.....	50
Materials and Methods.....	55
Materials	55
Methods.....	58
Results and Discussion	62
pH and Conductivity	62
Major constituents.....	63
Minor constituents	65
Conclusions.....	66
References.....	68

IV. COMPARISON OF THE RELEASE OF CONSTITUENTS OF CONCERN
FROM A GRANULAR MATERIAL UNDER BATCH AND COLUMN
TESTING.....70

Abstract.....	70
Introduction.....	72
Materials and Methods.....	74
Materials	74
Coal Fly Ash	75
Aluminum Recycling Residue	79
Methods.....	81
Batch testing.....	82
Solubility and release as a function of pH	82
Solubility and release as a function of LS	83
Column testing.....	84
Results and Discussion	84
Coal Fly Ash # 1	86
pH and Conductivity	86

Major constituents.....	87
Minor constituents	89
Coal Fly Ash # 2	91
pH and Conductivity	91
Major constituents.....	92
pH Dependent constituents	94
Aluminum Recycling Residue	95
pH and Conductivity	95
Major constituents.....	97
Minor constituents	99
Geochemical speciation modeling results.....	101
Conclusions.....	105
References.....	107

V. THE EFFECTS OF CARBONATION IN THE RELEASE OF
CONSTITUENTS FROM LABORATORY FORMULATED CONCRETE..... 109

Abstract.....	109
Introduction.....	110
Leaching evaluation.....	112
Geochemical speciation modeling.....	113
Objectives	113
Materials and Methods.....	114
Materials	114
Methods.....	118
Carbonation.....	118
Batch testing.....	121
Column testing.....	121
Results and Discussion	121
Carbonation.....	122
pH and Conductivity	124
Major constituents.....	126
Minor constituents	129
Geochemical speciation modeling results.....	134
Conclusions.....	141
References.....	144

VI. THE EFFECTS OF DIFFERENT WEATHERING CONDITIONS IN
THE RELEASE OF CONSTITUENTS FROM MSWI BOTTOM ASH 146

Abstract.....	146
Introduction.....	147

Materials and Methods.....	150
Materials	150
Methods.....	154
Aging.....	154
Batch testing.....	155
Column testing.....	155
Results and Discussion	156
pH and Conductivity	157
Major constituents.....	160
Minor constituents	162
Geochemical speciation modeling results.....	167
Conclusions.....	175
References.....	178
VII. SUMMARY AND CONCLUSIONS	180
Summary of Results.....	180
Primary Conclusions.....	183
Significance and applications	187
Future directions	188
Appendix	
A. DEFINING CONDITIONS FOR MATERIAL CARBONATION.....	190
B. EXPERIMENTAL RESULTS.....	197
C. GEOCHEMICAL SPECIATION MODELING RESULTS.....	259
D. MINERAL TABLE.....	281
CURRICULUM VITA	284

LIST OF FIGURES

Figure	Page
1.1. Environmental factors affecting the aging of a material.....	7
1.2. Factors affecting the leaching of constituents from a material.....	12
1.3. LeachXS.....	16
2.1. Comparison of ionic strength-conductivity correlation.....	34
2.2. LeachXS.....	36
2.3. ANC comparison from LeachXS.....	40
2.4. Saturation index table in LeachXS.....	41
2.5. Aqueous concentration diagram in LeachXS.....	42
2.6. Residual plot example.....	44
3.1 SEM image for CD “light” component.....	57
3.2. SEM image for CD “dark” component.....	57
3.3. SEM image for CD “brick” component.....	57
3.4. Particle size distribution for CD.....	58
3.5. Column experiments.....	60
3.6. pH and conductivity of CD column samples as a function of LS ratio.....	63
3.7. Na release from CD column testing as a function of LS ratio.....	64
3.8. Ca release from CD column testing as a function of LS ratio.....	64
3.9. SO ₄ release from CD column testing as a function of LS ratio.....	64
3.10. Ba release from CD column testing as a function of pH and LS ratio.....	65
3.11. Fe release from CD column testing as a function of pH and LS ratio.....	65
3.12. Pb release from CD column testing as a function of pH and LS ratio.....	66
3.13. Sr release from CD column testing as a function of pH and LS ratio.....	66
4.1. SEM image for CFA#1.....	79
4.2. SEM image from ARR.....	81
4.3. Particle size distribution for ARR.....	81
4.4. pH of CFA #1 batch testing as a function of LS Ratio.....	87
4.5. pH and conductivity of CFA#1 column testing as a function of LS ratio.....	87

4.6.	Ca release from CFA#1 as a function of LS ratio.....	88
4.7.	K release from CFA#1 as a function of LS ratio	89
4.8.	Al release from CFA#1 as a function of pH and LS ratio	90
4.9.	Fe release from CFA#1 as a function of pH and LS ratio	90
4.10.	pH of CFA #2 batch testing as a function of LS ratio	91
4.11.	pH and conductivity of CFA#2 column testing as a function of LS ratio	92
4.12.	Ca release from CFA#2 as a function of LS ratio.....	93
4.13.	K release from CFA#2 as a function of LS ratio	93
4.14.	Al release from CFA#2 as a function of pH and LS ratio	94
4.15.	Fe release from CFA#2 as a function of pH and LS ratio	95
4.16.	pH and conductivity of ARR titration curve.....	96
4.17.	pH and conductivity of ARR batch testing as a function of LS ratio	96
4.18.	pH and conductivity of ARR column testing as a function of LS ratio.....	97
4.19.	Ca release from ARR as a function of LS ratio	98
4.20.	Cl release from ARR as a function of LS ratio.....	98
4.21.	Na release from ARR as a function of LS ratio	99
4.22.	Al release from ARR as a function of pH and LS ratio	100
4.23.	Mg release from ARR as a function of pH and LS ratio	100
4.24.	Sr release from ARR as a function of pH and LS ratio	101
4.25.	Al prediction from ARR as a function of pH.....	103
4.26.	Ca prediction from ARR as a function of pH	103
4.27.	Mg prediction from ARR as a function of pH.....	103
4.28.	Sr prediction from ARR as a function of pH	104
5.1.	SEM image from LFC	117
5.2.	Particle size distribution for LFC.....	117
5.3.	Carbonation experiment.....	119
5.4.	Carbonation degree measurement.....	120
5.5.	Carbonation data for LFC	123
5.6.	pH and conductivity of LFC titration curve.....	124
5.7.	pH and conductivity of LFC batch testing as a function of LS ratio	125
5.8.	pH and conductivity of LFC column testing as a function of LS ratio.....	126

5.9.	Ca release from LFC as a function of LS ratio	127
5.10.	Cl release from LFC as a function of LS ratio.....	128
5.11.	Na release from LFC as a function of LS ratio.....	128
5.12.	K release from LFC as a function of LS ratio.....	129
5.13.	As release from LFC as a function of pH and LS ratio	131
5.14.	Cd release from LFC as a function of pH and LS ratio	132
5.15.	Cu release from LFC as a function of pH and LS ratio	132
5.16.	Pb release from LFC as a function of pH and LS ratio.....	133
5.17.	Zn release from LFC as a function of pH and LS ratio	134
5.18.	Ca prediction from LFC as a function of pH	137
5.19.	Cd prediction from LFC as a function of pH.....	138
5.20.	Cu prediction from LFC as a function of pH.....	139
5.21.	Pb prediction from LFC as a function of pH	140
5.22.	Zn prediction from LFC as a function of pH	140
6.1.	Mixing of bottom ash.....	151
6.2.	SEM image from BA	153
6.3.	Particle size distribution for BA	154
6.4.	Aging of BA.....	155
6.5.	pH and conductivity of BA titration curve	157
6.6.	pH and Conductivity of BA batch testing as a function of LS Ratio.....	158
6.7.	pH and conductivity of all BA cases IC column testing as a function of pH and LS ratio.....	159
6.8.	pH and conductivity of all BA cases SC column testing as a function of LS ratio.....	159
6.9.	pH and conductivity of all BA cases SC column testing as a function of LS ratio.....	160
6.10.	Ca release from BA as a function of pH and LS ratio	161
6.11.	Cl release from BA as a function of pH and LS ratio.....	161
6.12.	Na release from BA as a function of pH and LS ratio	162
6.13.	Ba release from BA as a function of pH and LS ratio	163
6.14.	Cd release from BA as a function of pH and LS ratio	165

6.15.	Cu release from BA as a function of pH and LS ratio	165
6.16.	Pb release from BA as a function of pH and LS ratio	166
6.17.	Zn release from BA as a function of pH and LS ratio	167
6.18.	Ca prediction from BA as a function of pH.....	171
6.19.	Cd prediction from BA as a function of pH.....	172
6.20.	Cu prediction from BA as a function of pH.....	173
6.21.	Pb prediction from BA as a function of pH	174
6.22.	Zn prediction from BA as a function of pH.....	174
7.1.	Statistical data for all residual values.....	185
7.2.	Statistical data for residual values of LS 10 samples.....	186
A.1.	Carbonation experiment.....	191
A.2.	Carbonation degree measurement.....	193
A.3.	Carbonation data for BA.....	194
A.4.	Carbonation data for LFC	195
A.5.	Carbonation data for CD.....	196
B.1.	Relationship between activity coefficient, ionic strength and conductivity.....	198
B.2. - B.21.	ARR experimental data	198
B.22. - B.41.	BA experimental data.....	208
B.42. - B.60.	CFA # 1 experimental data.....	217
B.61. - B.79.	CFA # 2 experimental data.....	226
B.80. - B.99.	CD experimental data.....	235
B.100. - B.119.	LFC experimental data.....	245
B.120 – B.123.	Mean and standard deviation data for residual values.....	256
C.1.	Example of phase partitioning diagram	260
C.2. - C.11.	Constituent solubility and phase partitioning for ARR.....	261
C.12. - C.28.	Constituent solubility and phase partitioning for BA.....	266
C.29. - C.39.	Constituent solubility and phase partitioning for LFC.....	275

LIST OF TABLES

Table	Page
1.1. Experimental design.....	17
3.1. Total composition for CD from XRF analysis.....	56
4.1. Total composition for CFA from XRF analysis	77
4.2. Total composition for CFA (EPA Method 3052B).....	77
4.3. Total composition for CFA#1 from NAA analysis.....	78
4.4. Total composition for ARR from XRF analysis	80
4.5. Total composition for ARR from NAA analysis	80
5.1. LFC composition	115
5.2. Total composition for LFC from XRF analysis.....	116
5.3. Assumed Si concentration for non-aged LFC.....	135
5.4. Assumed Si concentration for carbonated LFC	135
5.5. Solubility controlling minerals for LFC	136
6.1. Total composition for BA from XRF analysis.....	151
6.2. Total composition for BA from NAA analysis.....	152
6.3. Initial assumptions for Si and CO ₃ for BA.....	168
6.4. Solubility controlling minerals for BA	169
A.1. Humidity of samples carbonation experiment	194
B.1. Statistical data for residual values.....	255
B.2. Statistical data for residual values of LS 10 samples	257
D.1. Table of minerals considered for geochemical speciation	281

LIST OF ABBREVIATIONS

ANC	Acid Neutralization Capacity
ARR	Aluminum Recycling Residue
ASTM	American Society for Testing and Material
BA	Bottom Ash
CD	Construction Debris
CFA	Coal Fly Ash
CPC	Constituents of Potential Concern
HPIC	High Performance Ion Chromatography
IC	Intermittent Unsaturated Column
ICP-MS	Inductively Coupled Plasma Mass Spectrometer
LFC	Laboratory Formulated Concrete
LS	Liquid to Solid Ratio
MSWI	Municipal Solid Waste Incinerator
NAA	Neutron Activation Analysis
SC	Continuous Saturated Column
SEM	Scanning Electron Microscope
SI	Solubility Index
XRD	X-Ray Diffraction
XRF	X-Ray Fluorescence

CHAPTER I

OVERVIEW

Introduction

Many secondary materials are being considered for use as aggregate substitutes in highway construction applications. Such applications may include use in road base, shoulders, embankments, landscape materials, and other fill applications. During use, these materials may experience intermittent infiltration as a consequence of precipitation events. Additionally, as a result of exchange with the atmosphere, the materials also will be subjected to changing conditions. Typically, the release of contaminants from these materials is estimated by leaching of continuously saturated material, and therefore the impacts of intermittent wetting and changing environmental conditions are not considered. Understanding the relationships among testing and interpretation techniques, including uncertainties associated with necessary extrapolation, is critical to avoiding erroneous or misleading long-term performance assessments.

Previous research suggests that constituent leaching will be affected by both the intermittent nature of infiltration and changing environmental conditions. However, the relationships between these factors and actual leaching have not been well established. Test methods are needed to assess the potential impact of changing conditions on long-term release to evaluate potential environmental impacts. Finally, given that some of these test methods can be prohibitively time consuming, appropriate and reliable leaching models based on initial measurement of intrinsic material properties and simplified

testing are needed to predict the release of constituents of concern from secondary materials.

Objectives

The overall goal of this dissertation is to further develop testing and interpretation protocols to estimate constituent leaching from granular waste materials that are utilized as aggregate in highway construction applications. These protocols will be used to calibrate a model that, given basic pH-solubility information of a secondary material, can predict the release of constituents from that material under field utilization conditions.

The specific objectives of this dissertation are:

- 1) Evaluate the relationships between laboratory batch and column leaching tests under saturated conditions to column leaching that occurs under unsaturated, intermittent flow.
- 2) Evaluate the impact of aging by carbonation on constituent leaching from alkaline materials.
- 3) Recommend a specific approach for laboratory evaluation of leaching from secondary granular materials to be used in construction or highway applications under conditions of unsaturated, intermittent flow.
- 4) Evaluate geochemical speciation modeling using LeachXS to predict the release of constituents based on batch testing data from secondary materials.

General Background

This section reviews previous research in the areas of use of recycled materials in construction, general approaches to leaching assessment, accelerated aging of materials, equilibrium leaching tests, dynamic leaching tests and geochemical modeling.

Reuse of materials in construction

Given the large amounts of secondary materials currently being disposed in landfills, several alternatives have been proposed to find different applications for these materials, and thus, reduce the material that is being disposed, as well as the cost that this represents (Edinçliler et al. 2004). One of these alternatives is to use the materials in highway applications. This alternative also has an added value, because obtaining soils and other construction materials of good quality at reasonable prices has become more difficult. Therefore, reusing materials that are currently being produced in large quantities has become more attractive to construction businesses.

The various secondary materials considered for construction present different advantages. Municipal solid waste (MSW) incinerator residues, like fly and bottom ash have been widely studied for reuse (Styron et al. 1993; Lu 1996; IAWG et al. 1997; Bruder-Hubscher et al. 2001). Some types of fly ash have cementitious or binding characteristics that allow them to be used for construction purposes (Georgakopoulos et al. 2002). Coal combustion fly ash has been the most widely used secondary material since the early 70's until the late 80's (Vipulanandan et al. 1998; Edinçliler et al. 2004). Scrap tires have also been used in embankment construction; this practice eventually encouraged tire shredding into tire chips that have been incinerated for energy recovery,

production of crumb rubber for use as binder in pavements and bulk usage such as in embankments.

There has been extensive research regarding MSW incinerator residue (Sawell et al. 1988; Sawhney et al. 1991; Styron et al. 1993; Eighmy et al. 1994; Eighmy et al. 1995; Fällman 1996; IAWG et al. 1997). MSW bottom ash also has been studied for reuse in highway applications. One study in particular (Bruder-Hubscher et al. 2001) tested the release of constituents from a road constructed with a sub-layer of bottom ash and compared the results to those obtained from a road constructed with natural gravel materials. The experiment ran for 3 years and analysis of the results showed that minimal leaching of pollutants from the bottom ash had occurred. Furthermore, the amounts of leached constituents from the road constructed with bottom ash were not very different from the amounts leached from the road constructed with natural materials.

Other applications include the use of recovered construction and demolition debris, scrubber base, fluorogypsum, and other industrial by-products as soil amendment or alternative cover at landfills and fill material in roads, embankments and other construction projects (Vipulanandan et al. 1998; López Meza et al. 1999; Bruder-Hubscher et al. 2001; Eighmy et al. 2001; Jang et al. 2001). However, the beneficial use of secondary materials must consider the potential environmental impact that such materials can pose to their surrounding environment. Constituents of potential concern present in the materials are subject to leaching, as runoff and water percolating through the materials carries these metals and compounds into the ground, and eventually into the aquifers or surface streams.

Some primary constituents in secondary materials do not pose the same type of environmental risk as other trace pollutants; however, in the case of chloride or sulfate, they can impact surrounding vegetation. These two compounds are of particular importance when considering the reuse of the material in construction applications. Chloride diffusion into reinforced concrete is also associated with depassivation and corrosion of reinforcing steel (Jensen 1999; Griffiths 2002). Sulfate diffusion into cementitious materials leads to decalcification and expansive cracking (Collivignarelli 2001).

In an attempt to decrease the leachability of some materials, stabilization / solidification (S/S) of the matrices has been considered. S/S typically involves the formation of a solid material (e.g., brick, blocks) using waste as a component along with Portland cement or other binders, with the purpose of decreasing the mobility of the constituents of potential concern by precipitating them into the solid material (EPA 1996). A review of various S/S techniques and tests has been presented elsewhere (Alba et al. 2001). Most of these tests have successfully shown that heavy metals and sulfates usually are immobilized within the solidified matrix, whereas chlorides are retained only partially due to their higher solubility. Blast furnace slags and fly ash/lime mixtures, which have pozzolanic properties that would aid to solidification, also have been considered for S/S of MSW residue (Albino et al. 1996). Soils contaminated with mining residues have been studied for the purpose of stabilizing waste material (Weng et al. 1994).

General approach to leaching assessment

This research is being carried out in the context of an overarching framework for evaluation of leaching from wastes and secondary materials for disposal and beneficial use decisions (Kosson et al. 2002). This framework provides a philosophical basis of testing materials to determine intrinsic leaching properties and using mass transfer models to develop estimates of constituent release through leaching under field scenarios, rather than to develop a variety test methods to mimic individual field scenarios. Intrinsic properties of a material include availability, constituent partitioning between phases, acid neutralization capacity, and mass transfer rate. The framework also provides specific leaching test methods for evaluation of intrinsic leaching properties and a hierarchical approach to testing and evaluation that allow for a balance between release estimate, amount of testing provided, and the resources required to complete the evaluation.

This framework presents a series of material testing protocols under continuously saturated conditions, but there is still a need for understanding release of constituents under unsaturated, intermittent conditions. The research being completed here extends this approach to recommend specifications for evaluating materials under consideration for use in construction applications under unsaturated, intermittent infiltration conditions.

Aging

When developing testing methods it is important to consider that environmental conditions have a significant effect on the leaching of constituents. Direct contact with the atmosphere, intermittent wetting and reducing conditions in the ground impact the

chemical behavior of constituents, as well as the mineralogy of the material and the physical properties of the material (e.g., pore structure). Primary aging processes include oxidation, reduction, and carbonation of alkali materials (Figure 1.1). Other environmental factors that can be considered as aging processes include thawing and freezing, percolation/infiltration, and evaporation. Methods for environmental testing used to assess these changes on materials can be separated in two kinds: 1) long-term field testing, and 2) artificially accelerated laboratory aging (Gwynne 1996).

When a material is naturally aged, it is subjected to changes of different environmental conditions, such as temperature and relative humidity (Andrade et al. 1999). Even though the long-term methods provide accurate results, the testing time required can be prohibitive, as the reaction rates for aging processes may be on a geological time scale.

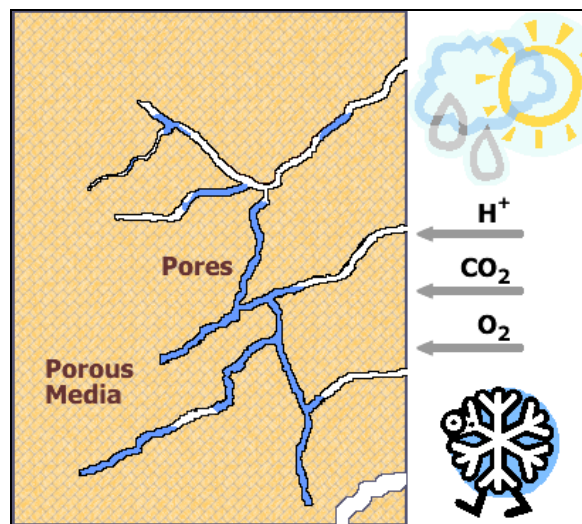


Figure 1.1. Environmental factors affecting the aging of a material (Sanchez 2000)

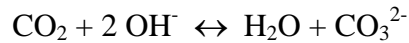
Methods carried out artificially in the laboratory can be run in shorter periods of time, but because of interaction with other materials and the inability to duplicate the

randomness of a field scenario, the results should be viewed as a limiting case for field data. General artificial aging techniques found in the literature include thermal aging (Wood et al. 2000; Eighmy et al. 2002; Carter et al. 2003), aging under different atmospheres (Carter et al. 2003; Polettini et al. 2004), outdoor weathering (River 1994; Gwynne 1996), indoor weathering (Gwynne 1996), cyclic loading, for stress-induced failure of a material (Eighmy et al. 2002) and freezing-thawing (Eighmy et al. 2002; White 2005). Carbonation is another aging process that has been widely considered, as it is the most likely environmental condition that the material will experience while in use for highway or construction applications, and is the process that was selected to study in this dissertation.

Carbonation

Carbonation is a relevant process for initially alkaline materials ($\text{pH} > 9$) and is one of the most common chemical reactions that an alkaline material will experience while in contact with the environment (Garrabrants 2001; Freyssinet et al. 2002). Atmospheric carbon dioxide diffuses into the matrix, reacts to produce carbonates, and decreases the pH value of the system. Calcite (CaCO_3) is the predominant carbonate formed in the carbonation process, and this occurs for most alkaline materials with high Ca content (e.g., cement, concrete, fly ash, bottom ash). Carbonation has been found to affect the chemical composition and physical properties of cementitious matrices and other secondary materials, thus affecting the release of constituents of potential concern. (Macias et al. 1997). Carbonation occurs through reaction of the alkaline materials

present in a sample with the atmospheric carbon dioxide, according to the following overall reaction (Snoeyink et al. 1980):



A detailed review of the steps in the carbonation reaction for cement-based materials has been presented elsewhere (Van Gerven 2005). These reactions involve the the transfer of CO₂ from the gas into the aqueous phase, reacting with water to produce carbonic acid, and upon the pH of the solution, the eventual dissociation of the carbonic acid into carbonate ions (CO₃²⁻). The dissolution of the CO₂ in the gas phase into the aqueous phase can lead to the precipitation of the carbonate ions with cations in the solution, being Ca the most important cation, and leading to the formation of calcite.

There has been extensive research done focusing on carbonation of concrete materials (Dias 2000; Krajci et al. 2000; Garrabrants 2001) and bottom ash (Meima et al. 2002; Fernández Bertos et al. 2004; Poletini et al. 2004; Van Gerven et al. 2005), finding that in most cases, a carbonated matrix exhibits lower release of constituents of concern. Depth of carbonation in concrete and its consequences have been widely studied; typically finding reductions in sorptivity and increase in concrete degradation rate for specimens that had been carbonated by air-drying (Krajci et al. 2000). Carbonation effects also have been studied in lime mortars (Cazalla et al. 2000) and the tests showed that non-aged lime had a slower carbonation rate and needed a higher binder-aggregate ratio.

Carbonation does not occur as significantly in water-saturated pores, because of the poor diffusion of CO₂ in the water-filled pores. Completely dry pores will also slow the carbonation reaction, because this reaction is more likely to occur in the liquid phase. Therefore, the degree of wetting is very important for the rate of carbonation; partially filled pores lead to a faster carbonation because of the higher diffusion rate of carbon dioxide in air than in water and the presence of a water film on the solid pore surface (van der Sloot et al. 1997; Garrabrants 2001; Van Gerven 2005). Research suggests that changes in relative humidity and temperature induced continuous non-steady state conditions in the interior of concrete: temperature being the most influential factor in sheltered samples and rain being the most influential in unsheltered samples (Andrade et al. 1999).

Carbonation studies have also included aging for concrete composites (MacVicar et al. 1999), where it was found that the induced laboratory testing was able to simulate natural aging. Scrubber residues have also been the focus of carbonation studies, finding that lead solubility was reduced when leaching residues had been previously aged (Alba et al. 2001).

Bottom ash has been also widely studied for carbonation effects. When calcite (CaCO₃) is formed during bottom ash aging, lead and zinc are trapped by newly formed carbonates (Speiser et al. 2000; Freyssinet et al. 2002; Poletini et al. 2004). These studies showed that new mineralogical phases of these metals are formed due to the aging. Carbonation increases the leachability of SO₄²⁻ and heavy metals such as Zn and Cr (Alba et al. 2001). The effect of carbonation in the “aging” of bottom ash is of particular importance, since bottom ash usually has to be stored a few months between

production and reuse in public works (Dugenest et al. 1999); a 12-month study showed that aging leads to natural biodegradation of organic matter available in bottom ash, and would eventually improve its quality for reuse. Another bottom ash study analyzed the differences in trace metals leachability from bottom ash at different stages of weathering (Meima et al. 1999). The weathering was carried out analyzing samples that had been left in contact with the atmosphere for 1.5 to 12 years. A reduction in leaching of the metals was observed as the weathering continued, due to the neutralization of the bottom ash and the formation of less soluble species of these elements. Chapter 5 and 6 of this dissertation present more detailed aging and carbonation background for concrete and bottom ash, respectively.

Leaching Tests

Rain and waterways provide a pathway for potential constituents of concern to contaminate groundwater. Leaching tests are a useful tool for estimating the intrinsic properties of constituents of concern that leach from a particular material. Along with mathematical modeling, leaching tests estimate the release under field management scenarios (Kosson et al. 2002). Figure 1.2 shows the factors affecting the leaching of constituents from a material. These factors are related to matrix characteristics (e.g., mineralogy of material, permeability, acid neutralization capacity), environmental conditions (e.g., infiltration rate, leachant composition), and reactions between the material and its surrounding environment (e.g., acid or sulfate attack, carbonation) (Garrabrants et al. 2005). Furthermore, it is also important to consider the hydraulic regime of the road application. For granular materials that are used in road base and

embankments, it is most likely that solubility, as opposed to advection, will be the controlling factor for the release of the constituents (Apul et al. 2003).

Because the leaching process is very complex, no one single leaching test or single set of leaching conditions is appropriate for a wide variety of leach testing objectives and applications (Garrabrants et al. 2005). For this reason, several leaching tests have been developed in order to try to evaluate the different leaching parameters and conditions being tested.

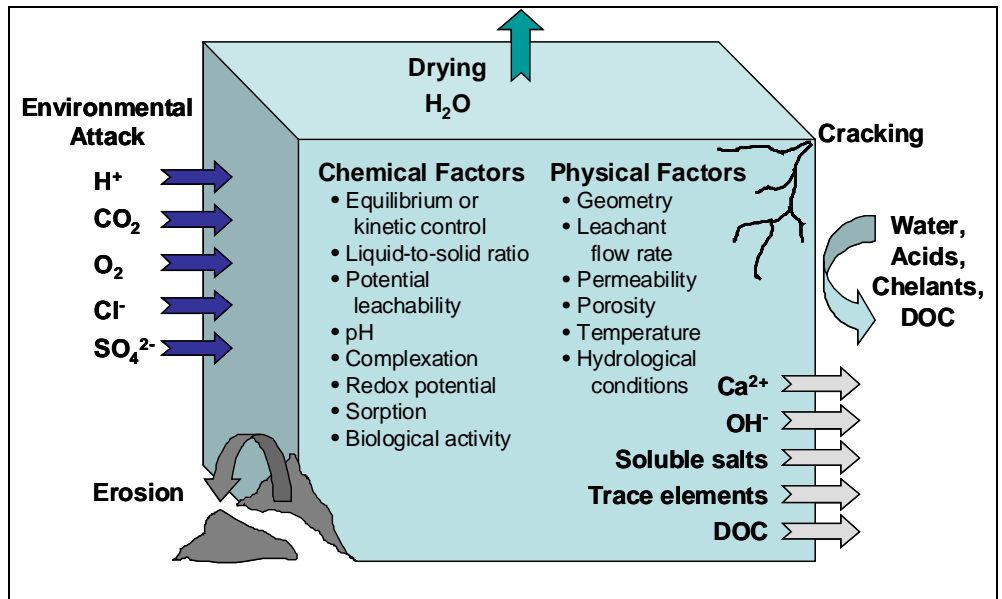


Figure 1.2. Factors affecting the leaching of constituents from a material (Garrabrants et al. 2005).

There are two groups of leaching tests that can be used to study secondary materials: equilibrium tests and dynamic tests. Equilibrium tests are designed to evaluate the release of constituents in the limiting case when the material is in chemical equilibrium with its surroundings; dynamic tests are designed to evaluate the release of constituents as a function of time. Equilibrium testing offers the advantage of greater

reproducibility and simpler design; dynamic testing provides more realistic simulation of leaching processes that occur in field conditions (Jackson et al. 1984; Caldwell et al. 1990; Kjeldsen et al. 1990; Förstner et al. 1991; Sawhney et al. 1991; Wasay 1992; van der Sloot et al. 1996).

Equilibrium Tests

Equilibrium tests were developed to study the equilibrium between a solid phase and a leachant solution. There are several approaches to equilibrium tests, including: single batch extractions with and without pH control, single batch extractions with some form of complexation by organic constituents, and single batch extractions at low LS ratios (van der Sloot et al. 1997). As a general rule for equilibrium tests, the material is in contact with the leaching solution and the variables include: contact time, agitation rate, pH of the leachant solution, and LS ratio. Equilibrium leaching tests have been discussed extensively elsewhere (Garrabrants et al. 2005). In this dissertation, the term “batch test” refers to equilibrium testing.

Dynamic Tests

Dynamic tests include multiple or serial batch test, and percolation and flow through (i.e., column) tests. While serial batch testing can provide leaching information of heavy metals for a given material, it is not possible to rely on serial batch testing for predicting the movement of these metals through the ground. In order to predict and model the behavior of the metals in the ground (i.e., under the highway layers), it is necessary to have a testing method that can practically and adequately simulate the soil

conditions, including the soil and leachate interactions. Column tests typically consist of a leachant (e.g., deionized water, acidified water) percolating through a column packed with the material of study. A detailed review of column tests is given in Chapter 3.

Column leaching tests provide a better way of evaluating the soil sorption performance and the effects of partial soil saturation (Jang et al. 1998; Anderson et al. 2000). Column tests give an indication of the time-dependent leaching behavior, and can be useful to quantify the retention in the matrix of the element of interest (i.e., heavy metals) relative to the inert constituents of the matrix.

Another approach for percolation studies has been with lysimeters. Lysimeter leaching experiments are large-scale column leaching test where the column has an open surface. The column or container has a drainage system at the bottom, to collect the leachate (Hansen et al. 2000). Lysimeters are usually carried out under field conditions and with higher quantities of material and for longer periods of time (typical duration of lysimeter studies is one to several years), in order to better estimate the behavior of the material in the ground. An important characteristic of lysimeters is that they are open to the atmosphere, so the balance of rainfall and evaporation provides natural infiltration as the leaching solution. These experiments are mostly used for studies of the fate and movement of water, pesticides, salts, trace elements and heavy metals in the soil (Hansen et al. 2000). Other lysimeter studies have been conducted for bottom ash (Stegemann 1995; Bruder-Hubscher et al. 2001). Lysimeters are an important link between laboratory leaching tests and leaching behavior under field conditions. No lysimeter testing has been standardized to date.

Geochemical speciation modeling

In order to predict the release of constituents of potential concern (CPC) from secondary materials appropriately, it is necessary to understand the factors controlling the release of these constituents. Many processes affect the movement and distribution of CPCs, including but not limited to: chemical reactions, transport, biological processes, fluid flow, and heat transport (Zhu et al. 2002). Depending on the area of interest, it is important that geochemical speciation models include the most important of these factors. For leaching assessment, chemical reactions, transport, and fluid flow are relevant.

Geochemical speciation models can be categorized depending on their characteristics. Speciation-solubilization models describe, given the initial concentration of constituents in the system, the concentrations and activities of species in an aqueous solution, the saturation states of the minerals present in the system, and the stable species of these minerals that are at equilibrium with the aqueous solution. Reaction path models simulate processes where there is a mass transfer of constituents between the various phases of a system. These types of models are based on mass balance and thermodynamic equilibrium principles. Coupled mass transport models include models where two sets of processes, chemical and physical, affecting the speciation and transport of constituents are solved together. These processes include partitioning of constituents, chemical reactions, heat transport, and fluid flow.

The model used in this dissertation is LeachXS (van der Sloot et al. 2003). The capabilities of this program include chemical equilibrium and transport modeling through the ORCHESTRA modeling environment (Meeussen 2003). The materials database of this system consists of results from a variety of batch and column leaching tests that have

been performed in a wide range of different materials, including soil, waste and construction materials. Although the characteristics obtained from each test might differ, they all provide the database with concentration of constituents as a function of pH and/or LS ratio as a minimum. With this information, these results are interpreted by the expert system to predict the long-term behavior of the materials in different applications (Figure 1.3). A detail review of geochemical speciation modeling, as well as a background for LeachXS and ORCHESTRA, is presented in Chapter 2.

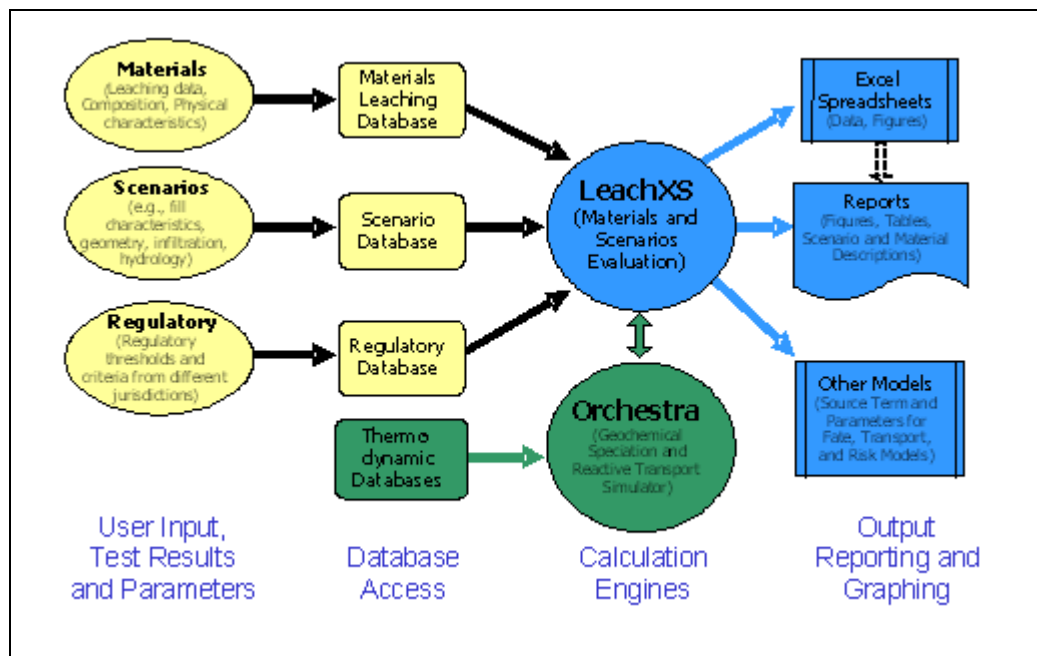


Figure 1.3. LeachXS.

Research Approach

The approach to satisfy the objectives in this dissertation was to obtain different materials that have been considered for use in highway applications and evaluate their leaching characteristics. The materials used were Municipal Solid Waste Incinerator Bottom Ash (BA), Aluminum Recycling Residue (ARR), Laboratory Formulated

Concrete (LFC), Coal Fly Ash (CFA), and Construction Debris (CD). These particular materials were chosen because of their availability in the Nashville area (BA, CD, ARR), their significance to other studies previously performed (LFC), and their relevance to other studies currently being carried out (CFA).

These materials were tested under different environmental conditions, including material “as received” or non-aged (ARR, CFA, and CD), and material aged under accelerated conditions in a carbonated atmosphere (BA and LFC). All materials were also tested under batch and column testing, including solubility and release as a function of pH and LS ratio for the batch testing, and continuously saturated and intermittent unsaturated column flow conditions (Table 1.1).

Table 1.1. Experimental design.

Material	Batch testing (pH, LS ratio)	Column testing	
		IC	SC
Bottom ash	Non-aged (D)	Non-aged (D)	Non-aged (D)
	Carbonated (D)	Carbonated (D)	Carbonated (D)
	N ₂ -aged (D)	N ₂ -aged (D)	N ₂ -aged (D)
	Air-aged (D)	Air-aged (D)	Air-aged (D)
Aluminum recycling residue	Non-aged (D)	Non-aged (D)	Non-aged (D)
Laboratory formulated concrete	Non-aged (D)	Non-aged (D)	Non-aged (D)
	Carbonated (D)	Non-aged, 4-4	Carbonated
Coal fly ash	Completed by US-EPA	CFA # 1	CFA # 1
	CFA # 1, CFA #2	CFA # 2	CFA # 2
Construction debris	Non-aged (D)	Non-aged Non-aged, 4-4	Non-aged (D)

Notes:

IC-Intermittent unsaturated columns

SC-Continuously saturated columns

D-Duplicates

4-4, Intermittent unsaturated columns, 4 days on, 4 days off

The results from this experimental work provide a better understanding of material behavior and are used to evaluate the types of tests necessary for material characterization. These results also will provide a reliable foundation for calibrating a geochemical speciation “leaching” model. The input for the leaching model will be the data obtained from batch testing. The ability of the model to predict long-term release of constituents from a secondary material will be evaluated by comparing simulation results and results obtained from column testing. This comparison is possible under the assumption that column leaching tests are at local equilibrium, and this equilibrium condition can be compared to the batch equilibrium tests.

It is not the purpose of this dissertation to thoroughly review each material presented and study its constituent release mechanisms. Instead, the purpose is to fulfill the objectives of this dissertation by testing the materials via batch and column leaching tests and characterizing their leaching properties to test the hypothesis presented in this research: that batch testing can be used as the basis to provide a reasonable estimate of constituent leaching under intermittent percolation conditions.

Dissertation Structure

This dissertation is organized as different manuscripts. Some chapters are to be submitted as manuscripts to peer-reviewed journals. For this reason, there might be repetitive explanations in some chapters, especially when describing background and methodologies. When possible, repeating explanations was avoided by referencing a previous chapter.

Chapter 2 explains the modeling methodology used in this research, including a theoretical background of an empirical calculation of solubility-controlling minerals, as well as the theory behind the simulation software LeachXS, its capabilities and uncertainties.

Chapter 3 presents an in-depth analysis of column leaching tests, focusing on the effects of unsaturated intermittent wetting testing versus saturated continuous flow experiments in the release of constituents from Construction Debris.

Chapter 4 compares the release of constituents from two different types of Coal Fly Ash and Aluminum Recycling Residue when tested via column testing under both intermittent unsaturated and continuously saturated flow conditions (as explained in Chapter 2) to the release that occurs under batch testing as a function of LS ratio and pH. It also presents preliminary simulation and speciation results for Aluminum Recycling Residue from batch data. Both Chapters 3 and 4 focus on materials that have been tested “as received” or have been naturally exposed to weathering conditions.

Chapter 5 introduces the effect of accelerated aging conditions and presents how carbonation affects the leaching of constituents released from “non-aged” and carbonated Laboratory Formulated Concrete when tested under batch and both intermittent unsaturated and continuously saturated column tests. It also presents simulation and geochemical speciation results from batch data.

Chapter 6 explores the effects of different types of accelerated aging under 3 different atmospheres (Air, N₂, CO₂-N₂) on the release of constituents from Bottom Ash under batch and column testing conditions, as well as simulation and geochemical speciation results from batch data.

Chapter 7 presents a set of overall dissertation conclusions, significance of the research presented, and recommendations for future research.

References

- Alba, N., E. Vazquez, S. Gasso and J. M. Baldasano (2001). "Stabilization/solidification of MSW incineration residues from facilities with different air pollution control systems. Durability of matrices versus carbonation." Waste Management **21**(4): 313-323.
- Albino, V., R. Cioffi, L. Santoro and G. L. Valenti (1996). "Stabilization of residue containing heavy metals by means of matrices generating calcium trisulphoaluminate and silicate hydrates." Waste Management & Research **14**: 29-41.
- Anderson, P., C. M. Davidson, A. L. Duncan, D. Littlejohn, A. M. Ure and L. M. Garden (2000). "Column leaching and sorption experiments to assess the mobility of potentially toxic elements in industrially contaminated land." JEM.
- Andrade, C., J. Sarria and C. Alonso (1999). "Relative humidity in the interior of concrete exposed to natural and artificial weathering." Cement and Concrete Research **29**(8): 1249-1259.
- Apul, D. S., K. H. Gardner, T. T. Eighmy, J. Benoit and L. Brannaka (2003). A review of water movement in the highway environment: Implications for recycled materials use. Beneficial use of recycled materials in transportation applications. T. T. Eighmy, Air and Waste Management Association Press: 195-204.
- Bruder-Hubscher, V., F. Lagarde, M. J. F. Leroy, C. Coughanowr and F. Enguehard (2001). "Utilisation of bottom ash in road construction: a lysimeter study." Waste Management & Research **19**(6): 557-566.
- Bruder-Hubscher, V., F. Lagarde, M. J. F. Leroy, C. Coughanowr and F. Enguehard (2001). "Utilisation of bottom ash in road construction: evaluation of the environmental impact." Waste Management & Research **19**(6): 545-556.
- Caldwell, R., T. W. Constable, P. Cote, J. McLellan, S. E. Sawell and J. Stegemann (1990). Compendium of Waste Leaching Tests, Environmental Protection Series.
- Carter, R. K., K. H. Gardner, O. Hjelm, S. Lopez and D. S. Kosson (2003). Mineralogical and Leaching Characteristics of Weathered Industrial Ash. Fifth International Conference on the Environmental and Technical Implications of Construction with Alternative Materials, San Sebastian, Spain.
- Cazalla, O., C. Rodriguez-Navarro, E. Sebastian, G. Cultrone and M. J. De la Torre (2000). "Aging of lime putty: Effects on traditional lime mortar carbonation." Journal of the American Ceramic Society **83**(5): 1070-1076.
- Collivignarelli, C., Sorlini, S. (2001). "Optimisation of industrial wastes reuse as construction material." Waste Management & Research **19**: 539-544.
- Dias, W. P. S. (2000). "Reduction of concrete sorptivity with age through carbonation." Cement and Concrete Research **30**(8): 1255-1261.

- Dugenes, S., J. Combrisson, H. Casabianca and M. F. Grenier-Loustalot (1999). "Municipal solid waste incineration bottom ash: Characterization and kinetic studies of organic matter." Environmental Science & Technology **33**: 1110-1115.
- Edinçliler, A., G. Baykal and K. Dengili (2004). "Determination of static and dynamic behavior of recycled materials for highways." Resources, Conservation and Recycling **42**(3): 223-237.
- Eighmy, T. T., R. A. Cook, D. L. Gress, A. Coviello, J. C. M. Spear, K. Hover, R. Pinto, S. Hobbs, D. S. Kosson, F. Sanchez, H. A. van der Sloot, C. Korhonen and M. Simon (2002). "Use of accelerated aging to predict behavior of recycled materials in concrete pavements." Journal of the Transportation Research Board(1792).
- Eighmy, T. T., J. D. Eusden, J. E. Krzanowski, D. S. Domingo, D. Stämpfli, J. R. Martin and P. M. Erickson (1995). "Comprehensive approach toward understanding element speciation and leaching behavior in municipal solid waste incineration electrostatic precipitator ash." Environmental Science & Technology **29**(3): 629-646.
- Eighmy, T. T., J. D. Eusden, K. Marsella, J. Hogan, D. Domingo, J. E. Krzanowski and D. Stämpfli (1994). Particle petrogenesis and speciation of elements in MSW incineration bottom ashes. International Conference on Environmental Implications of Construction Materials and Technology Developments, The Netherlands, Elsevier.
- Eighmy, T. T. and B. J. Magee (2001). "The road to reuse." Civil Engineering **71**(9): 66-71,81.
- EPA (1996). Stabilization/Solidification processes for mixed waste. Washington, DC, United States Environmental Protection Agency: 91.
- Fällman, A.-M. (1996). "Aspects of the performance and design of the availability test for measurement of potentially leachable amounts from ash." Environmental Science & Technology.
- Fernández Bertos, M., X. Li, S. J. R. Simons, C. D. Hills and P. J. Carey (2004). "Investigation of accelerated carbonation for the stabilisation of MSW incinerator ashes and the sequestration of CO₂." The Royal Society of Chemistry **6**: 428-436.
- Förstner, U., W. Calmano and W. Kienz (1991). "Assessment of long-term metal mobility in heat-processing wastes." Water, Air and Soil Pollution(57-58): 319-328.
- Freyssinet, P., P. Piantone, M. Azaroual, Y. Itard, B. Clozel-Leloup, D. Guyonnet and J. C. Baubron (2002). "Chemical changes and leachate mass balance of municipal solid waste bottom ash submitted to weathering." Waste Management **22**: 159-172.
- Garrabrants, A. C. (2001). Assessment of inorganic constituent release from a portland cement matrix as a result of intermittent wetting, drying and carbonation. Chemical and Biochemical Engineering. New Brunswick, NJ, Rutgers, the State University of New Jersey.

Garrabrants, A. C. and D. S. Kosson (2005). Leaching processes and evaluation tests for inorganic constituent release from cement-based matrices. Stabilization and solidification of hazardous, radioactive and mixed waste. R. Spence and C. Shi. Boca Raton, CRC Press: 229-280.

Georgakopoulos, A., A. Filippidis, A. Kassoli-Fournaraki, J.-L. Fernández-Turiel, J.-F. Llorens and F. Mousty (2002). "Leachability of major and trace elements of fly ash from Ptolemais power station, Northern Greece." Energy Sources **24**: 103-113.

Griffiths, C. T., Krstulovich, J.M. (2002). Utilization of Recycled Materials in Illinois Highway Construction, Federal Highway Administration: 27.

Gwynne, P. (1996). "Environmental testing firms make fast work of natural aging." Research and Development **38**(11): 25-.

Hansen, J. B., P. E. Holm, E. A. Hansen and O. Hjelmar (2000). Use of lysimeters for characterisation of leaching from soil and waste materials. Hørsholm, Denmark, DHI.

IAWG, A. J. Chandler, T. T. Eighmy, J. Hartlen, O. Hjelmar, D. S. Kosson, S. E. Sawell, H. A. van der Sloot and J. Vehlow (1997). Municipal Solid Waste Incinerator Residues. Studies in Environmental Science 67. Elsevier. New York.

Jackson, D. R., B. C. Garrett and T. A. Bishop (1984). "Comparison of batch and column methods for assessing leachability of hazardous waste." Environmental Science & Technology **18**: 668-673.

Jang, A., Y. S. Choi and I. S. Kim (1998). "Batch and column tests for the development of an immobilization technology for toxic heavy metals in contaminated soils of closed mines." Water Science and Technology **37**(8): 81-88.

Jang, Y.-C. and T. Townsend (2001). "Sulfate leaching from recovered construction and demolition debris fines." Advances in Environmental Research **5**: 203-217.

Jensen, O. M., Hansen, P.F., Coats, A.M., Glasser, F.P. (1999). "Chloride ingress in cement paste and mortar." Cement and Concrete Research **29**: 1497-1504.

Kjeldsen, P. and T. H. Christensen (1990). "Leaching tests to evaluate pollution potential of combustion residues from an iron recycling industry." Waste Management & Research(8): 277-192.

Kosson, D. S., H. A. van der Sloot, F. Sanchez and A. C. Garrabrants (2002). "An integrated framework for evaluating leaching in waste management and utilization of secondary materials." Environmental Engineering Science **19**(3): 159-204.

Krajci, L. and I. Janotka (2000). "Measurement techniques for rapid assessment of carbonation in concrete." ACI Materials Journal: 168-171.

- López Meza, S. and B. Treviño (1999). Integración de un residuo proveniente de la producción de carbonato de estroncio en la fabricación de bloques para construcción. Environmental Engineering. Monterrey, México, Instituto Tecnológico y de Estudios Superiores de Monterrey.
- Lu, C. (1996). "A model of leaching behaviour from MSW incinerator residue landfills." Waste Management & Research **14**: 51-70.
- Macias, A., A. Kindness and F. P. Glasser (1997). "Impact of carbon dioxide on the immobilization potential of cemented wastes: chromium." Cement and Concrete Research **27**(2): 215-225.
- MacVicar, R., L. M. Matuana and J. J. Balatinecz (1999). "Aging mechanisms in cellulose fiber reinforced cement composites." Cement and Concrete Composites **21**(3): 189-196.
- Meeussen, J. C. L. (2003). "ORCHESTRA: An Object-oriented framework for implementing chemical equilibrium models." Environmental Science & Technology **37**(6): 1175-1182.
- Meima, J. A. and R. N. J. Comans (1999). "The leaching of trace elements from municipal solid waste incinerator bottom ash at different stages of weathering." Applied Geochemistry **14**(2): 159-171.
- Meima, J. A., R. D. van der Weijden, T. T. Eighmy and R. N. J. Comans (2002). "Carbonation process in municipal solid waste incinerator bottom ash and their effect on the leaching of copper and molybdenum." Applied Geochemistry **17**: 1503-1513.
- Polettini, A. and R. Pomi (2004). "The leaching behavior of incinerator bottom ash as affected by accelerated ageing." Journal of Hazardous Materials **113**(1-3): 209-215.
- River, B. H. (1994). "Outdoor aging of wood-based panels and correlation with laboratory aging." Forest Products Journal **44**(11/12): 55-.
- Sanchez, F. (2000). Environmental factors affecting the aging of a material: Figure.
- Sawell, S. E., T. R. Bridle and T. W. Constable (1988). "Heavy metal leachability from solid waste incinerator ashes." Waste Management & Research **6**: 227-238.
- Sawhney, B. L. and C. R. Frink (1991). "Heavy metals and their leachability in incinerator ash." Water, Air and Soil Pollution **57-58**: 289-296.
- Snoeyink, V. L. and D. Jenkins (1980). Water Chemistry. New York, John Wiley & Sons, Inc.
- Speiser, C., T. Baumann and R. Niessner (2000). "Morphological and chemical characterization of calcium hydrate phases formed in alteration processes of deposited

municipal solid waste incinerator bottom ash." Environmental Science & Technology **34**(23): 5030-5037.

Stegemann, J. A., Schneider, J., Baetz, B.W., Murphy, K.L. (1995). "Lysimeter washing of MSW incinerator bottom ash." Waste Management & Research **13**: 149-165.

Styron, R. W., F. H. Gustin and T. L. Viness, Eds. (1993). MSW ash aggregate for use in asphalt concrete. Use of Waste Materials in Hot-Mix Asphalt Concrete. Philadelphia, American Society for Testing and Materials.

van der Sloot, H. A., R. N. J. Comans and O. Hjelm (1996). "Similarities in the leaching behaviour of trace contaminants from waste, stabilized waste, construction materials and soils." The Science of the Total Environment **178**: 111-126.

van der Sloot, H. A., L. Heasman and P. Quevauviller, Eds. (1997). Harmonization of leaching/extraction tests. Studies in Environmental Science. Amsterdam, Elsevier.

van der Sloot, H. A., A. van Zomeren, P. Seignette, J. J. Dijkstra, R. N. J. Comans, H. Meeussen, D. S. Kosson and O. Hjelm (2003). Evaluation of Environmental Aspects of Alternative Materials Using an Integrated Approach Assisted by a Database/Expert System. Advances in Waste Management and Recycling.

Van Gerven, T. (2005). Leaching of heavy metals from carbonated waste-containing construction material. Chemical Engineering. Heverlee (Leuven), Katholieke Universiteit Leuven: 25.

Van Gerven, T., E. Van Keer, S. Arickx, M. Jaspers, G. Wauters and C. Vandecasteele (2005). "Carbonation of MSWI-bottom ash to decrease heavy metal leaching, in view of recycling." Waste Management **25**(3): 291-300.

Vipulanandan, C. and M. Basheer (1998). Recycled materials for embankment construction. Recycled Materials in Geotechnical Applications: Proceedings of sessions sponsored by the Soil Properties Committee of the Geo-Institute of the ASCE in conjunction with the ASCE National Convention, co-sponsored by the CIGMAT, Boston, Massachusetts.

Wasay, S. A. (1992). "Leaching study of toxic trace elements from fly ash in batch and column experiment." Journal of Environmental Science and Health A **27**(3): 697-712.

Weng, C. H., C. P. Huang, H. E. Allen, A. H.-D. Cheng and P. F. Sanders (1994). "Chromium leaching behavior in soil derived from chromite ore processing waste." The Science of the Total Environment **154**: 71-86.

White, K. L. (2005). Leaching from granular waste materials used in highway infrastructures during infiltration coupled with freezing and thawing. Civil and Environmental Engineering Department. Nashville, TN, Vanderbilt University.

Wood, J. E., R. B. Plunkett, P. H. Tsang, K. N. E. Verghese and J. Lesko (2000). "Assessment of residual composites properties as influenced by thermal mechanical aging." Journal of Composites Technology & Research **22**(2): 82-90.

Zhu, C. and G. Anderson (2002). Environmental Applications of Geochemical Modeling. Cambridge, Cambridge University Press.

CHAPTER II

ESTIMATION OF FIELD BEHAVIOR BASED ON LABORATORY BATCH DATA

Abstract

The use of recycled materials in different construction applications is a widespread approach that can save both resources for use in other applications and landfill space for other materials that do not have the potential for reuse. However, when these materials are first obtained, little is known about their particular leaching characteristics and the potential leaching of constituents to the surrounding environment. Usually, these characteristics are obtained from leaching tests, with individual testing regimes having a range of requirements. Several chemical equilibrium speciation models have been developed to evaluate the characteristics of these materials from short leaching tests and predict the chemical transformations that the materials and their leachates will undergo when in use. This speciation modeling approach describes the mineralogy of the material and serves as the basis for estimating long-term behavior. This chapter presents the modeling methodology used in this research, including background on empirical calculation of equilibrium solubility from conductivity and ionic strength correlations. Equilibrium solubilities are used to calculate the saturation index of various minerals in the leachate. It also presents background and discussion of the simulation software LeachXS, which was used in this research, as well as its capabilities and uncertainties.

Introduction

When considering the use of waste materials for construction or highway applications, it is important to know whether these materials have constituents that might be of potential concern when exposed to the environment. In order to predict the release of constituents of potential concern (CPC) from secondary materials in an accurate way, it is necessary to understand the factors controlling the release of these constituents. Many processes (e.g., chemical reactions, transport, biological processes, heat transport, fluid flow) affect the movement and distribution of CPCs (Zhu et al. 2002). Depending on the desired use for the material and the characteristics of the environment surrounding it, a given process may have a greater effect on the release of CPCs than another process. Although there are many experimental protocols that cover various conditions of possible use for a material, including different pH, flow or temperature conditions, it would be a constraint, in terms of budget and time, to run all these tests in the laboratory before making a decision about the use of the material. For this reason, it is important to have accurate geochemical models that have the capability to simulate what would most likely happen in the field.

Depending on their characteristics, geochemical speciation models can be categorized as speciation-solubilization, reaction path, or coupled-mass transfer models (Zhu et al. 2002). Based on initial concentrations of constituents in the system, speciation-solubilization models describe the concentrations and activities of species in an aqueous solution and the saturation states of the minerals that could potentially be in the system. Reaction path models simulate processes where there is a mass transfer of constituents between the various phases of a system. These types of models are based on

mass balance and thermodynamic equilibrium principles. Coupled mass transport models include models where two sets of processes (i.e., chemical reactions, transport, fluid flow) affecting the speciation and transport of constituents are solved together.

There are various commercial geochemical speciation computer-modeling programs available. Currently, MINTEQA2 (Allison et al. 1991), PHREEQC (Parkhurst et al. 1999), and The Geochemist's Workbench (Bethke 2002) are among the most widely used programs. MINTEQA2 is capable of calculating equilibria between dissolved, adsorbed, solid, and gas phases in a system. The necessary data to predict equilibrium composition includes total concentrations of constituents of interest, as well as pH, pe, and partial pressures for the gases present in the system. PHREEQC is capable of speciation and saturation-index calculations, batch reaction and 1D transport calculations involving reversible reactions and irreversible reactions, and inverse modeling. Reversible reactions include aqueous, mineral, gas, solid solution, surface-complexation, and ion-exchange equilibria. Irreversible reactions include specified mole transfers of reactants, reactions controlled kinetically, solution mixing, and effects of temperature. PHREEQC uses the Davies equation or an extended form of the Debye-Hückel equation depending on the ionic strength of the species. The main difference between these two programs is PHREEQC's ability to include reaction path modeling. Both programs include an extensive database of thermodynamic data. The Geochemist's Workbench has similar capabilities to both PHREEQC and ORCHESTRA, but in addition, its Act2 package provides predominance and stability diagrams that show the dominant species and mineral phases that are stable in a given region.

There are also several programs that have been developed for specific academic research purposes. These programs have been constructed from an entirely original code, or based on an existing computer program, such as MINTEQA2. To mention a few, SOLTEQ (Park et al. 1999) and SBLEM (Park et al. 2002) have been tested extensively for predicting release of constituents from stabilized/solidified wastes. Of these two models, SBLEM is of relative importance because it has the ability to predict the release of constituents based on the pH-solubility data, thus replacing longer experimental leaching tests.

ORCHESTRA (Meeussen 2003) is a Java-based program that can create geochemical models including adsorption and surface complexation models. One of the differences between ORCHESTRA and other models, such as PHREEQC, is that ORCHESTRA lacks built-in model equations and a database. This results in a model where the source of equations and definitions is more easily accessible to users. This model has been used to predict leaching of constituents from soils at various pH values, obtaining generally good predictions for the behavior of constituents, except for higher alkaline pH values, where the model failed to accurately describe the release of constituents (Dijkstra et al. 2004). The ability of this model to predict chemical speciation has been compared to that obtained from PHREEQC and the Geochemist's Workbench, obtaining very similar results (Kinniburgh et al. 2005).

The model used in this research is LeachXS (van der Sloot et al. 2003; van der Sloot et al. 2006). The capabilities of this program include chemical equilibrium (ORCHESTRA based) and transport modeling based on pH-solubility batch data. LeachXS also includes organic matter interaction with the matrix, which has not been

considered by other geochemical speciation models. The long-term prediction is done by using advective data obtained from column testing under the assumption that the columns are at a state of local equilibrium. The purpose of this chapter is to provide a summary of LeachXS as applied in the research presented in this dissertation. This model is used in Chapters 4, 5 and 6 for predicting the solubility of the constituents present in the materials studied in those specific chapters.

Modeling

Model-based extrapolation of batch tests to long-term release

Based on batch and/or column experiments approximating local equilibrium, it is possible to have an estimate of the release of constituents from a granular material in the long term. When trying to predict the long-term release of CPCs from a granular material, it is imperative to understand the factors that are controlling that release. Batch leaching tests provide important information to understand the leaching behavior that would occur under different pH conditions (solubility and release as a function of pH, where the pH ranges from 2 to 12), and at different scenario applications, such as embankments with low LS ratios ($LS < 1 \text{ mL/g}$), and road base applications with high LS ratios (solubility and release as a function of LS ratio, where the LS ratio ranges from 0.1 to 10 mL/g). Batch testing at very low LS ratios (i.e., $LS < 0.5$) can be difficult, and if the desired application requires a low LS ratio, then it is also important to consider running a column test where the leaching behavior at lower LS ratios can be easily studied.

Empirical

It is reasonable to assume that batch experiments overestimate the release of CPCs from the field utilization, as the batch experiment allows for the material and leachant to come to equilibrium. In the batch experiments conducted as a function of pH, the possible changes in the solubility of the species due to pH changes can be estimated, as is the case for the batch experiments as a function of LS ratio (Methods - Chapter 3). LS ratio can also be used as a measure of time, so based on batch experiments a cumulative release could be predicted over time. When time needed to characterize material behavior is not a constraint, column experiments provide a more realistic approach of release in flow-through conditions, similar to the conditions that the material would be subjected to when in use, allowing for the depletion of controlling phases. The release of constituents is plotted against LS ratio (or time) and an extrapolation could be made for longer periods of time. However, none of these experiments would show in an obvious way which minerals and liquid-solid partitioning processes are actually controlling the concentrations of CPCs in the fluid, i.e., the leach rates.

Once the available field liquid samples or experimental leachates have been analyzed, the steps to predict which species will be controlling the solubility of the species are relatively straightforward. The activities of the dissolved species in solution are calculated based on the molar concentration of the species and the ionic strength of the solution. Once activities are calculated, they are used to compute the saturation index of all the possible minerals present in the system. The saturation index calculation can also consider other phenomena, such as liquid-phase complexation (e.g., by dissolved organic carbon), and adsorption processes (e.g., on iron surfaces). The saturation index is

important because it measures the saturation state of the mineral in the system: supersaturated, undersaturated or at equilibrium. Further study and geochemistry knowledge and expertise are needed to choose the relevant minerals based on their saturation index, as not all the ones that are saturated or supersaturated are actually present in the original material or even possible in a regular environment.

When concentrations of every particular species in a sample are available, the ionic strength of the solution is calculated using Equation 2.1.

$$I = \frac{1}{2} \sum m_i z_i^2 \quad (2.1)$$

where m is the molar concentration (mol/L) and z is the charge of the ion/element entered. However, because it is not always possible to have a full analysis of all the ionic species present in the leachate, it is necessary to have an estimate of ionic strength based on the measured conductivity of the samples. Two correlations were found between ionic strength (I) and conductivity and are shown in Equation 2.2 (Marion et al. 1976) and Equation 2.3 (Russell 1976):

$$\log I = -1.841 + \log EC \quad (2.2)$$

$$I = 1.6 \times 10^{-5} \times \text{specific conductance} \quad (2.3)$$

where I is the ionic strength, specific conductance ($\mu\text{mho/cm}$) is the same as conductivity for this particular case, as $\mu\text{mho/cm} = \mu\text{S/cm}$, and EC (mS/cm) stands for electrical conductivity. These correlations were derived from waters with a wide

composition range. Both correlations were compared and the results were very similar as can be observed in Figure 2.1.

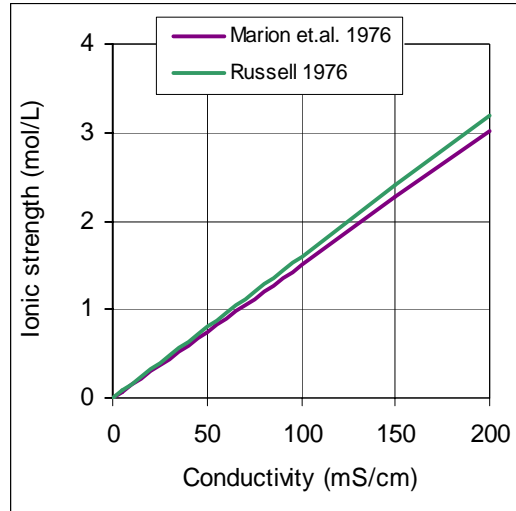


Figure 2.1. Comparison of ionic strength-conductivity correlations.

Activity of the ions is calculated using one of the I -conductivity correlations presented previously (Equations 2.1, 2.2 and 2.3) to calculate I based on conductivity measured from the sample. Depending on the ionic strength of the solution, an activity-coefficient model is selected. The extended Debye -Hückel equation (Equation 2.4) is a suitable model for solutions with low ionic strength (0-0.1 mol/L):

$$\log \gamma_i = \frac{-Az_i^2 I^{1/2}}{1 + Ba_i I^{1/2}} \quad (2.4)$$

The Davies equation (Equation 2.5) is an empirical correlation that can be used for low ionic strengths (0.1-0.5 mol/L)

$$\log \gamma_i = -Az_i^2 \left(\frac{I^{1/2}}{1+I^{1/2}} - 0.3I \right) \quad (2.5)$$

The Truesdell-Jones model (Equation 2.6) can be used for higher ionic strength solutions (0-2 mol/L):

$$\log \gamma_i = \frac{-Az_i^2 I^{1/2}}{1+Ba_i I^{1/2}} + bI \quad (2.6)$$

where γ_i is the activity coefficient, z_i is the charge of the ion, and A and B are constants depending on temperature and pressure. For the Debye-Hückel model, a_i is the hydrated radius of a particular ion (Kielland 1937); for the Truesdell-Jones model, a_i and b are determined from experimental data (Truesdell et al. 1974; Parkhurst 1990). This activity coefficient is used later to calculate the activity for each ion, according to Equation 2.7:

$$\alpha = \gamma_i m_i \quad (2.7)$$

where α is the activity of the ion.

The activity is an important factor in the calculation of the saturation index (SI), which determines the saturation conditions of a solution with respect to a particular mineral. A value of 0 for SI implies that the solution is in equilibrium with a particular mineral according to Equation 2.8:

$$SI = \log \frac{IAP}{K_{sp}} \quad (2.8)$$

where IAP is the ion activity product and K_{sp} is the solubility product constant. A positive value means that the solution is oversaturated with respect to that mineral; a negative value shows undersaturation.

LeachXS

LeachXS is a database system that has been developed for the characterization of a broad range of material types, leaching evaluations, and field release conditions (van der Sloot et al. 2003).

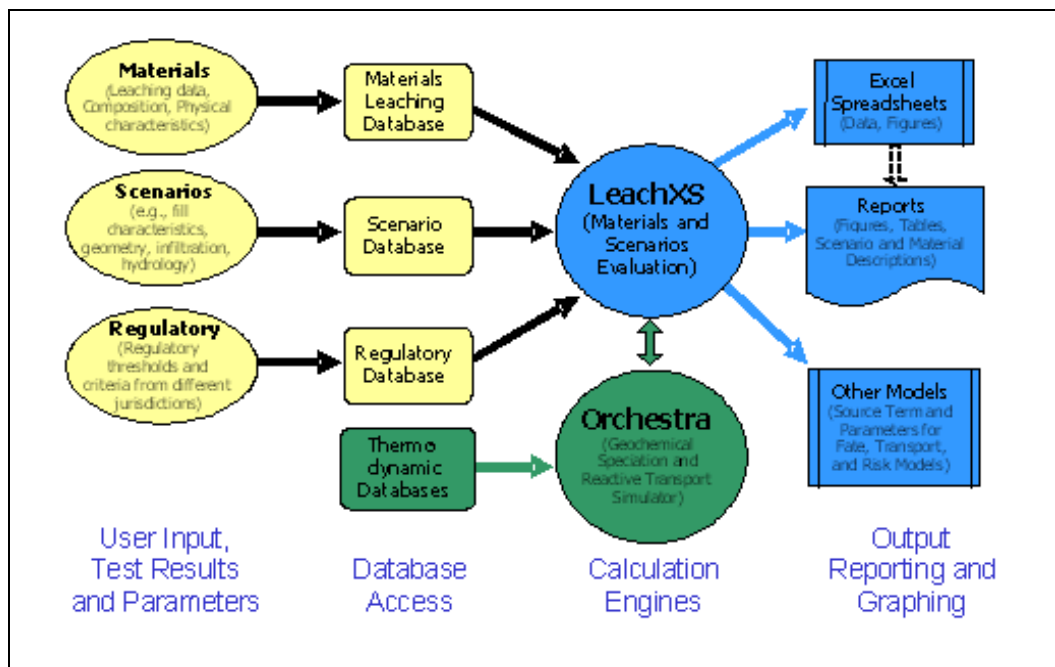


Figure 2.2. LeachXS.

Figure 2.2 shows how the expert system works. The system allows for user input, and test results and parameters entering separately into three databases: a materials leaching database, a database that considers the different scenarios for use, and a regulatory database. The information contained in these databases is used by LeachXS. Similarly, ORCHESTRA uses the thermodynamic database from MINTEQA2 3.11 (Allison et al. 1991) to support its chemical equilibrium capabilities. LeachXS and ORCHESTRA operate together to then obtain the prediction results in a user-friendly graphical interface, consisting of spreadsheets that can be use as basis for reporting prediction results, and these results can also be used as input parameters for other type of modeling.

To calculate the ionic strength of a solution, ORCHESTRA uses the Davies equation (Equation 2.4). The calculations in ORCHESTRA are done in 4 stages: 1) calculation of activities of all chemical entities, 2) calculation of concentrations of all chemical entities using the activities previously calculated and ion activity correction models, 3) calculation of cumulative mass balances of chemical entities for each system phase, using concentrations calculated in stage2, and 4) calculation of cumulative mass balances for all phases. In addition, ORCHESTRA implements other models for adsorption of ions to organic and oxide surfaces, including the NICA-Donnan model for metal-ion binding to humic substances (Benedetti et al. 1995; Kinniburgh et al. 1996; Kinniburgh et al. 1999; Milne et al. 2003). This model includes the non-ideal competitive adsorption (NICA) isotherm description of the binding of a heterogeneous material, coupled with a Donna electrostatic sub-model that describes the electrostatic interactions between the ions and the humic materials. This is useful in ORCHESTRA to

calculate the fractions of the species that are bound to dissolved organic carbon (DOC) and soil humic acid (SHA) or particulate organic matter (POM). The two-layer model (Dzomback et al. 1990) is used for specific binding of metal cations and (oxy)anions to hydrous ferric oxide (HFO) and hydrous aluminum oxide (Dijkstra et al. 2004). HFO is used as a surrogate sorbant in the system, and this approach has been justified by other research (Meima et al. 1998).

The information needed by ORCHESTRA to calculate saturation indices of potentially solubility controlling minerals includes total solution concentrations and DOC measurements. For the solubility prediction of metals, via adsorption models mentioned in the previous paragraph, ORCHESTRA also needs information about concentrations of different reactive surfaces in the solid and the solution (i.e., SHA, DOC, HFO, clay), the available concentrations of species at low pH ranges, the pH of system, and total solution concentrations (Dijkstra et al. 2004).

Methodology

The scope of this project is mainly for leaching characterization of materials, so the focus of this methodology is primarily to the materials leaching database of LeachXS. The materials leaching database consists of results from a variety of batch and column leaching tests that have been performed in a wide range of different materials, including soil, waste and construction materials. Although the characteristics obtained from each test might differ, they all provide the database with concentration of constituents as a function of pH and/or LS ratio as a minimum. With this information, these results are

interpreted by the expert system to predict the long-term behavior of the materials in different applications.

For each material, a dataset is composed in Excel including the type of leaching test (e.g., batch and percolation/column tests), constituent concentration, pH, conductivity, and LS ratio values. Acid or base added for batch experiments is also included. This basic spreadsheet is converted to an extended spreadsheet that is standardized for the LeachXS database. This dataset is then added to the LeachXS database. LeachXS is composed of several wizards for different modeling purposes: each of these wizards provides significant results that can be exported into Excel for easy data handling.

The first wizard is used for comparing constituent results from different materials tested under the same type of leaching tests. This wizard is useful to compare the leaching behavior of materials based on release of constituents. For example, when a material is considered for use and a similar material has been previously tested, this wizard might provide information that allows for decision-making regarding the use of the new material without extensive testing.

The second wizard is for comparison of acid neutralization capacities (ANCs) of different materials. The ANC of a material describes the ability of a solution in equilibrium with the material to resist changes in pH when acid or base is added (Garrabrants et al. 2005). This wizard is useful when comparing ANCs of different type of materials. Figure 2.2 shows a comparison of ANCs from aged and non-aged bottom ash.

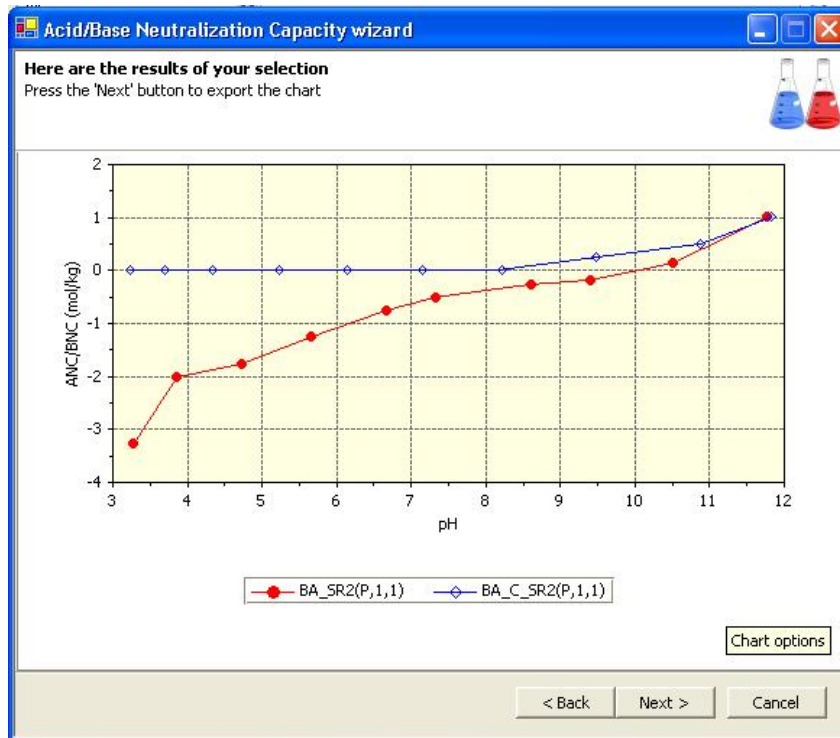


Figure 2.3. ANC comparison from LeachXS.

The third wizard is for long-term leaching behavior calculations. This wizard converts test time to LS ratio, including factors such as infiltration rate and density of the material.

The fourth wizard is for chemical reactions and transport, and it is divided into chemical speciation of the fluid sample and prediction of the fluid composition, including solubility controlling minerals, based on the chemical speciation results.

For the chemical speciation, the first step is to select a material (material tested under pH-dependent conditions, percolation conditions, or both). The chemical speciation is based on the saturation index (*SI*) of the potential constituents and minerals present in the solid pre-leached material. The main constituents are chosen based on XRF and/or NAA analyses; minerals are identified by XRD and/or SEM analyses. The

SIs are calculated using ORCHESTRA and thermodynamic values from the MINTQA2

3.11 database. Figure 2.4 shows the stage of the modeling program at which *SI* are

chosen. The darker *SIs* are the ones closer to 0 (−1.5 to 1.5), which are the possible

solubility controlling minerals based on measured elements.

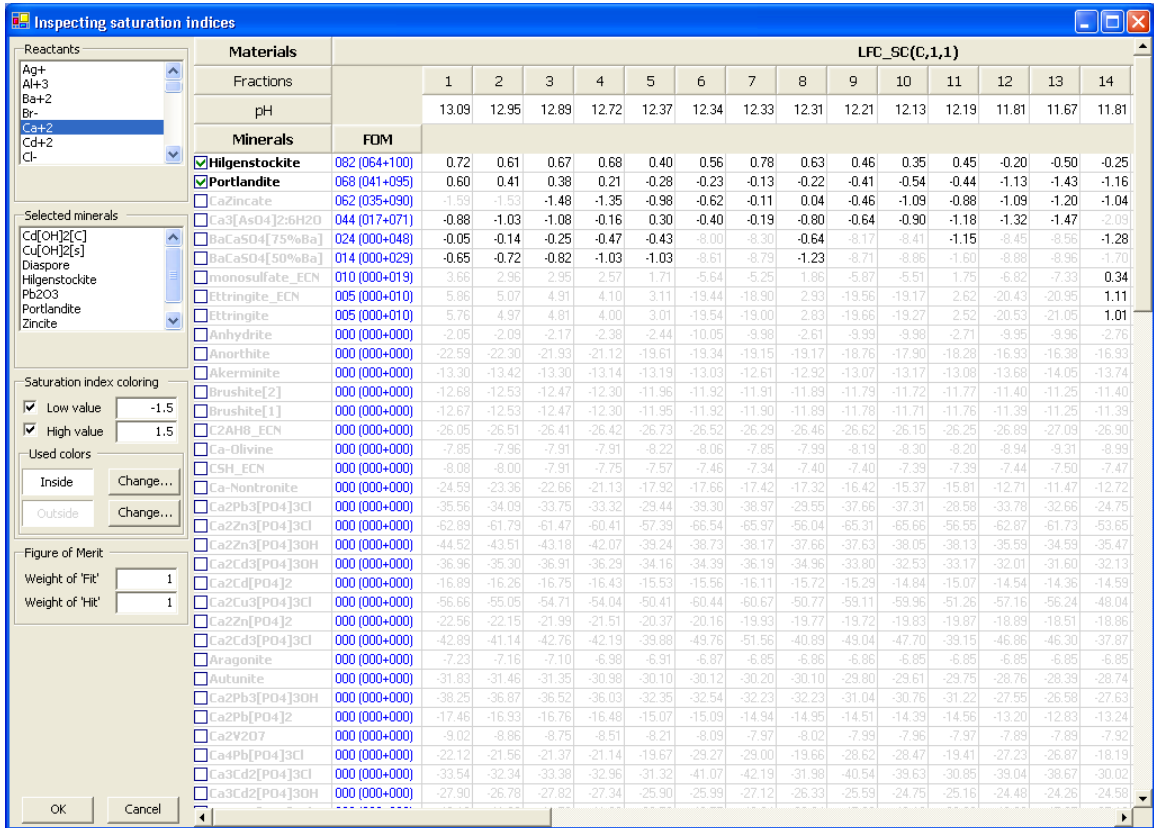


Figure 2.4. Saturation index table in LeachXS

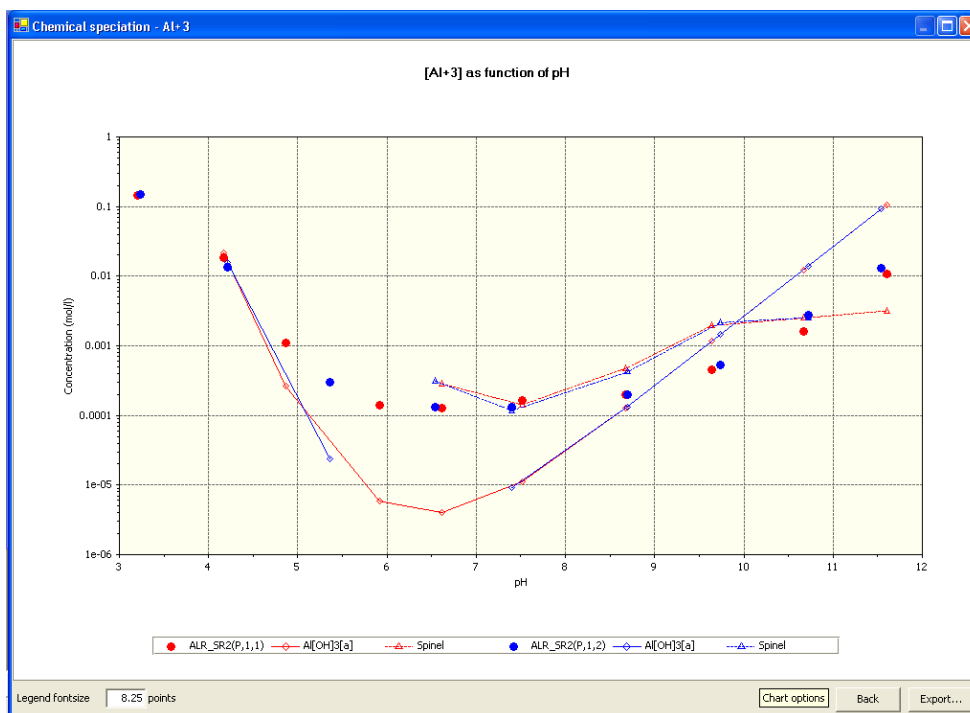


Figure 2.5. Aqueous concentration diagram in LeachXS.

The model calculates the chemical speciation based on data generated by the pH-dependence test and LS dependence test. Figure 2.5 shows the aqueous concentration diagram obtained from the chemical speciation on LeachXS; this diagram shows the different minerals that are controlling the solubility of the constituent at different pH values.

The information obtained from the “chemical speciation” part of the wizard is used to calculate the solubility data for the particular constituent. For this calculation, the wizard gives the option of adjusting other parameters, including availabilities of all the constituents present in the sample, HFO (hydrated ferric oxide), SHA (soil humic acid), and DOC (dissolved organic carbon). After obtaining the predicted aqueous concentration data from LeachXS, these data are compared to the actual concentration of

the constituent (as measured by ICP-MS or IC) at each pH step by means of a “discrepancy” comparison, or residual (Equation 2.9).

$$Residual = \log\left(\frac{Predicted}{Actual}\right) \quad (2.9)$$

To clarify, this is not a residual from a fitting process, given that actual model characteristics do not allow a change of parameters other than choosing the potential phase-controlling minerals. The predicted value is the aqueous concentration based on the controlling mineral and other processes as predicted by the LeachXS. The actual concentration is the measured concentration of the ion in solution from laboratory testing. A residual of 0 means the predicted and actual values were the same, a residual of ± 1 means they were different by 1 order of magnitude. A negative value implies that the actual value is less than the predicted value; a positive value means the actual value is higher than the predicted value. These residuals were plotted as a function of pH for batch experiments, and as a function of LS ratio for column experiments. For example, Figure 2.5 shows the measured and predicted concentration of Ca in a given material, and it also shows the discrepancies between the predicted and measured values.

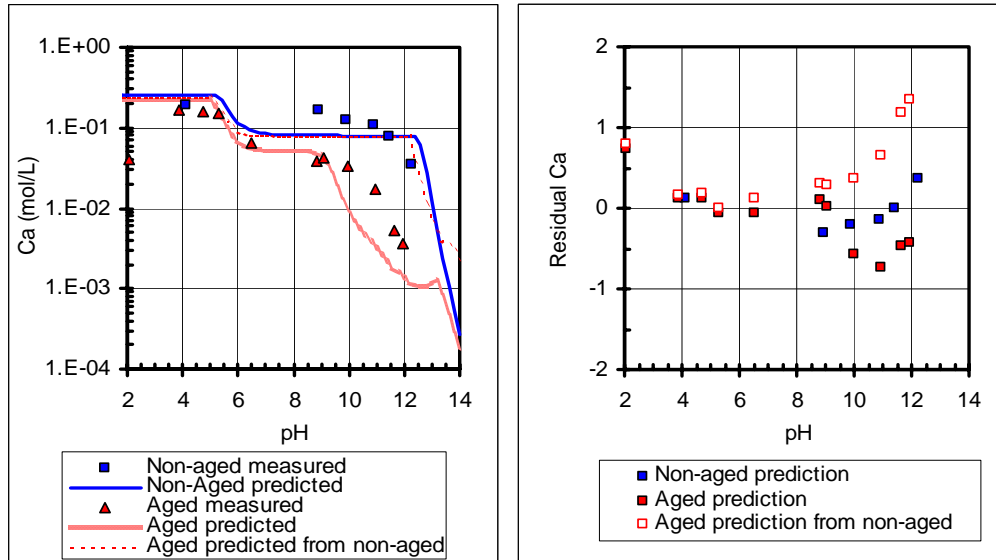


Figure 2.6. Residual plot example.

The purpose of the residual plots is to have a better graphic idea of the discrepancies between the actual data and the predicted data, including any patterns in these discrepancies. It is desired for the discrepancies to not follow a trend, as well as for the values to be as close to zero as possible, which would mean that the actual and predicted values are the same.

Uncertainties

The uncertainties or discrepancies found in using this software in development, as shown by the residual plots, are due to the lack of complete data for modeling purposes. For example, Si and CO₃ were not analyzed for the leachate samples in this project, even though they are the main components of some of the materials (i.e., LFC, CD, BA), because of the lack of available analysis methodologies. Therefore, the concentrations of these components are not present in the database that LeachXS uses to calculate the chemical speciation of those particular materials. The problem becomes evident when

trying to draw conclusions from the modeling data, given that no minerals containing silica or carbonate can be controlling minerals, and as a result, the controlling minerals are readily soluble minerals, such as sulfates. These results emphasize the need for as complete aqueous phase analysis as practical.

In some cases it might be feasible to compare the results from the material of interest to a similar material that has a more complete dataset and see the discrepancies, if any, between both sets of results. This was done for BA and LFC (Chapters 5 and 6); data (e.g., Si and CO₃ data) measured from other similar materials present in the database were used to do extra simulations and observe the change in the saturation indices of the minerals. Si concentrations were found for a range of pH values, whereas CO₃ concentrations were only found for measured reactants in the original solid material, but not for the material in solution. This assumption allowed analysis if the lack of data was resulting in very different simulation results or if it could be assumed that the lack of data did not have a significant effect on the solubility predictions.

Another reason why the lack of complete data might be a problem is in the way the software calculates ionic strength. Ionic strength is calculated in LeachXS using Equation 2.1, considering the concentrations of every ion/element entered in the LeachXS database, and not the actual conductivity measured in the sample (Equation 2.2 and 2.3). This might represent a problem when the concentrations of other ions (e.g., NO₃, PO₄, CO₃) are not entered in the database, especially in the cases where some of these ions might have a significant presence in solution.

Conclusions

Using waste and other types of secondary materials in construction applications can save both resources and landfill space that could be used for materials that do not have another usage application. However, it is imperative to consider the long-term behavior of these waste materials, as they might have constituents of potential concern that could potentially leach out of the material and contaminate other resources. A model that has the ability to quickly predict the long-term behavior based on short-term testing of a material is a very powerful tool. Chemical equilibrium models have the advantage of a vast thermodynamic database that can predict what minerals could be controlling the solubility of a given material when leaching from this material occurs. LeachXS can be a powerful tool to assist in the long-term behavior and solubility prediction of a wide range of materials. It provides a graphical, user-friendly interface to compare data from different materials and different test types, to consider external influences that might affect the conversion of a time-based batch test to a long-time field prediction, and to couple geochemical speciation modeling to transport modeling. Its database can provide data for materials that have been tested extensively, as well as for materials for which limited data are available. This is important when considering use of a material that has not been previously tested or for which data are not complete, as is the case for the materials studied in Chapters 4, 5 and 6.

References

- Allison, J. D., D. S. Brown and K. J. Novo-Gradac (1991). MINTEQA2 / PROEFA2, a geochemical assessment model for environmental systems: version 3.0 EPA/600/3-91/021, U.S. EPA: 108.
- Benedetti, M. F., C. J. Milne, D. G. Kinniburgh, W. H. van Riemsdijk and L. K. Koopal (1995). "Metal ion binding to humic substances: application of the non-ideal competitive adsorption model." Environmental Science & Technology **29**(2): 446-457.
- Bethke, C. M. (2002). The Geochemist's Workbench. Release 4.0. A User's Guide to Rxn, Act2, Tact, React and Gtplot., University of Illinois.
- Dijkstra, J. J., J. C. L. Meeussen and R. N. J. Comans (2004). "Leaching of Heavy Metals from Contaminated Soils: An Experimental and Modeling Study." Environmental Science & Technology **38**: 4390-4395.
- Dzombak, D. A. and F. M. M. Morel (1990). Surface complexation modeling: hydrous ferric oxide. New York, John Wiley & Sons, Inc.
- Garrabrants, A. C. and D. S. Kosson (2005). Leaching processes and evaluation tests for inorganic constituent release from cement-based matrices. Stabilization and solidification of hazardous, radioactive and mixed waste. R. Spence and C. Shi. Boca Raton, CRC Press: 229-280.
- Kielland, J. (1937). "Individual Activity Coefficients of Ions in Aqueous Solutions." Journal of the American Chemical Society **59**: 1675-1735.
- Kinniburgh, D. G. and D. M. Cooper (2005). "Predominance and mineral stability diagrams revisited." Environmental Science & Technology **In print**.
- Kinniburgh, D. G., C. J. Milne, M. F. Benedetti, J. P. Pinheiro, J. Filius, L. K. Koopal and W. H. van Riemsdijk (1996). "Metal ion binding by humic acid: application of the NICA-Donnan model." Environmental Science & Technology **30**(5): 1687-1698.
- Kinniburgh, D. G., W. H. van Riemsdijk, L. K. Koopal, M. Borkovec, M. F. Benedetti and M. J. Avena (1999). "Ion binding to natural organic matter: competition, heterogeneity, stoichiometry and thermodynamic consistency." Colloids and Surfaces A: Physicochemical and Engineering Aspects **151**: 147-166.
- Marion, G. M. and K. L. Babcock (1976). "Predicting specific conductance and salt concentration in dilute aqueous solutions." Soil Science **122**(4): 181-187.
- Meeussen, J. C. L. (2003). "ORCHESTRA: An Object-oriented framework for implementing chemical equilibrium models." Environmental Science & Technology **37**(6): 1175-1182.

- Meima, J. A. and R. N. J. Comans (1998). "Application of surface complexation/precipitation modeling to contaminant leaching from weathered municipal solid waste incinerator bottom ash." Environmental Science & Technology **32**(5): 688-693.
- Milne, C. J., D. G. Kinniburgh, W. H. van Riemsdijk and E. Tipping (2003). "Generic NICA-Donnan model parameters for metal-ion binding by humic substances." Environmental Science & Technology **37**(5): 958-971.
- Park, J.-Y. and B. Batchelor (1999). "Prediction of chemical speciation in stabilized/solidified wastes using a general chemical equilibrium model Part I. Chemical representation of cementitious binders." Cement and Concrete Composites **29**: 361-368.
- Park, J.-Y. and B. Batchelor (2002). "A multi-component numerical leach model coupled with a general chemical speciation code." Water Research **36**: 156-166.
- Parkhurst, D. L., Ed. (1990). Ion-association models and mean activity coefficients of various salts. Chemical Modelling of Aqueous Systems II, American Chemical Society Symposium Series.
- Parkhurst, D. L. and C. A. J. Appelo (1999). User's guide to PHREEQC--A computer program for speciation, batch-reaction, one-dimensional transport, and inverse geochemical calculations: U.S. Geological Survey Water-Resources Investigations Report 99-4259.
- Russell, L. L. (1976). Chemical Aspects of Groundwater Recharge with Wastewaters. Berkeley, University of California.
- Truesdell, A. H. and B. F. Jones (1974). "WATEQ, A computer program for calculating chemical equilibria of natural waters." U.S. Geological Survey, Journal of Research **2**(2): 233-248.
- van der Sloot, H. A., J. C. L. Meeussen, A. van Zomeren and D. S. Kosson (2006). "Developments in the characterisation of waste materials for environmental impact assessment purposes." Journal of Geochemical Exploration **88**: 72-76.
- van der Sloot, H. A., A. van Zomeren, P. Seignette, J. J. Dijkstra, R. N. J. Comans, H. Meeussen, D. S. Kosson and O. Hjelm (2003). Evaluation of Environmental Aspects of Alternative Materials Using an Integrated Approach Assisted by a Database/Expert System. Advances in Waste Management and Recycling.
- Zhu, C. and G. Anderson (2002). Environmental Applications of Geochemical Modeling. Cambridge, Cambridge University Press.

CHAPTER III

THE EFFECTS OF INTERMITTENT UNSATURATED WETTING ON THE RELEASE OF CONSTITUENTS FROM CONSTRUCTION DEMOLITION DEBRIS

Abstract

When used in highway applications, granular materials are submitted to changing environmental conditions. While column testing can provide a closer approximation to field percolation conditions than batch testing, it is still important to develop a column testing procedure that considers realistic conditions. Current column studies are conducted under continuously saturated conditions, without considering unsaturated intermittent flow conditions that exist in the field in response to precipitation events. This study evaluates the effect of different types of column flow on the release of constituents from a granular material. Two different types of intermittent unsaturated flow were studied and compared to continuously saturated flow. Leaching data, including pH, conductivity and constituent release was compared from the three columns. Results showed that there is no difference between the two types of intermittent unsaturated flow, nor is there a significant difference between these two flows and continuously saturated flow, other than higher initial concentrations of salts in intermittent unsaturated flow column testing at low LS ratios. However, this difference is not significant after a LS ratio of 2 mL/g. Release of constituents was similar in all three cases. Also, all three cases show that after a LS ratio of 5 mL/kg there is no significant change in the pH, conductivity or release of constituents.

Introduction

The beneficial use of secondary materials must consider the potential environmental impact that such materials can pose to the surrounding environment. Constituents of potential concern present in the materials are subject to leaching, as runoff and water percolating through the materials carries these metals and compounds into the ground, and eventually into the aquifers or surface streams. In order to better understand the impact of intermittent flow field conditions on a laboratory scale, different types of column leaching tests were evaluated.

A variety of column leaching tests have been reported. Column leaching tests have been used to study the washing and clean-up of soils and materials in order to obtain a product that can be suitable for use without representing an environmental risk; the materials that have been considered under this approach have been MSW bottom ash (Sawhney et al. 1991; Modi et al. 1994; Stegemann 1995), contaminated soils (Futch et al. 1999; Sun 2001), quartz sands (Ubal dini 1996), and ores (Hanson et al. 1993; Vegliò 2001). Different approaches for column testing have involved vertical (van der Sloot et al. 1997; Huang et al. 1998; Jang et al. 1998; O'Grodnick et al. 1998; Jang et al. 2001; Georgakopoulos et al. 2002) and horizontal (Elzahabi 2001) column designs.

The dimensions of the columns have been very different for all the various tests. Inner diameters have ranged from 2 to 33 cm, while length has varied from 10 cm to 1.9 m. Typically, length has been approximately four times the inner diameter. Columns have been constructed out of acrylic, PVC or some other inert material; however, some columns have been constructed with glass (Vegliò 2001) and stainless steel (Jang et al. 2001). Some columns had a silicone sealer bead or ridge on the sides to stop water

movement down the side of the pipe and to prevent “edge flow” or “boundary flow” conditions along the material-wall interface (Futch et al. 1999).

Flow rates for the column studies performed have varied from 2 mL/h to 6000 mL/h. The solution passing through the columns, or leachant, has usually been deionized water, although there have been experiments using a low pH solution (Wasay 1992), a simulated rain solution (Stewart et al. 1997), EDTA (Sun 2001), different concentrations of an oxalic acid solution (Ubal dini 1996), a solution with sulfuric acid and glucose (Vegliò 2001) and tap water (Hanson et al. 1993). Tests have been performed doing extractions with several leachants, such as HNO₃, H₂O₂, NaOAc, DTPA, H₂CO₃, and H₂O. Each leachant extracted different metals. However, the ash samples were taken from different locations and at different aging stages, and therefore, it presented a different chemistry. Therefore, it was not possible to conclude if there was one leachant that was better than the rest of them (Sawhney et al. 1991).

The flow through the columns has varied between up-flow and down-flow. Most of the column studies have been under saturated conditions, and to accomplish this, up flow is usually required to maintain a constant saturated environment. Duration of the column experiments previously mentioned ranged from 48 hrs to 7 yrs. The duration of test is usually selected so it can represent a period of time when the material would become stable. Another way of determining the duration of the test has been by cumulative LS ratio or pore volume flowing through the column combined with the flow rate. Column tests are usually carried out from ½ pore volume to 10 pore volumes. In some studies, the columns were not leached for specific periods of time to simulate drought conditions (Stewart et al. 1997). In the cases where the columns did not have a

constant flow rate (Modi et al. 1994), the leachant solution would be added at the beginning of the test and then, depending on the experiment time, a sample would be taken before adding more leachant solution. The controlled amounts of leachate were usually based on an average monthly or yearly rainfall amount.

Column tests have been studied as closed systems (Jang et al. 2001) and open systems (Lu 1996). In closed systems, the material in the column has no contact with the atmosphere, so carbonation of the sample and evaporation and transpiration losses from the column do not represent an extra variable to consider. In open systems evaporation and transpiration, as well as carbonation, cannot be prevented. Some column studies have involved the use of a thermostatted bath varying from 60°C to 70°C (Ubal dini 1996; Vite et al. 1997) and a water-jacketed glass column connected to a thermostatted bath at 80°C (Vegliò 2001). Temperature had a positive effect on the extraction of some of the heavy metals in the early stages of the leaching process (e.g, Mn, Fe).

The packing of the column also has varied between experiments. In most cases, a layer of glass beads or ceramic material is placed underneath and above the material of interest. The top layer, usually consisting of glass beads, helps distribute the flow above the column evenly (Stewart et al. 1997; Huang et al. 1998). The bottom layer, usually consisting of sand or glass beads, nylon mesh, filter paper, glass wool or synthetic cloth, helps filter the leachate and prevent the material inside the column from exiting the system (Wasay 1992; Ubal dini 1996; Stewart et al. 1997; Huang et al. 1998; O'Gro dnick et al. 1998; Sun 2001). The packing of the columns has not followed a specific method, and only a couple of studies mentioned tapping the column to pack the material (O'Gro dnick et al. 1998; Vegliò 2001).

The sampling times for column studies have ranged from hourly to daily for columns that are running continuously. For some of the studies simulating drought conditions, the samples are only taken before adding more leachant to the columns. The leachate samples are usually analyzed for pH, conductivity and concentrations of metals by atomic absorption spectrometry or ICP-AES and ICP-MS and anions by IC. For some studies, after the leaching phase of the experiment has ended, the columns are cut open and examined for evidence of oxidation and weathering features (Stewart et al. 1997). Results from leaching column tests on clay have shown that heavy metals solubility is highly pH dependent, usually increasing as the pH of the material decreases (Farrah et al. 1977).

In most of the previously mentioned cases, batch testing overestimated or had a similar metal release pattern as the column leaching data; one study in particular (Wasay 1992) concluded that the average percentage leachable trace elements was 44.7% in batch experiments at a leachant pH of 6 and 35% in column experiments at a leachant pH of 5. However, there were studies that showed that when using EDTA as the leachant, the heavy metal extraction resulted in different patterns of metal release when comparing batch and column data, and this depends on the fractions of the heavy metals that are contributing to the metal removal (Sun 2001). In some other cases, the results obtained from the columns for certain metals have been actually lower than the conditions existing in the field (Kjeldsen et al. 1990; Modi et al. 1994; van der Sloot et al. 1997; Sun 2001).

Two standardized column leaching tests are NEN 7343 and NEN 7349 (van der Sloot et al. 1997). Between 0.5 and 0.7 kg of solid material is needed per column. The moisture content should be known, and at least 95% of the dry material should be smaller

than 4 mm. The column size is 5 ± 0.5 cm in diameter and a fillable height of at least 4 times the internal diameter. The column is fitted with shut-off valves where prefilters (1.5 μm) and membrane filters (0.45 μm) can be placed. The column experiment is carried out at room temperature (18-22 °C). A vibration plate for the packing of the column is suggested. The columns are run up-flow with an acidified leachant composed of demineralized water with nitric acid ($\text{pH} = 4 \pm 0.1$). The flow rate through the column is equal to the mass inside the column times a specified factor of 0.025 L/kg·h and the minimum time for the columns to run is three weeks when the flow rate is the maximum permitted by the pump (50 mL/h). Samples are collected at LS ratios of 0.1, 0.2, 0.5, 1, 2, 5, and 10 L/kg. The only difference between NEN 7343 and NEN 7349 is that while NEN 7343 is carried out at LS ratios ranging from 0.1 to 10 L/kg of dry matter, NEN 7349 is carried out from LS ratios ranging from 20 to 100. These procedures were used as the basis for the column experiments designed in this study.

The objective of this research is to study the effects of different types of column flow in the release of constituents of concern from a material. This will be done by studying a naturally aged material and comparing two flow conditions: intermittent unsaturated and continuously saturated. Two types of intermittent unsaturated flow will be studied to see if differences in the flow affect the release of constituents from the aged granular material.

Materials and Methods

Materials

Construction debris (CD), which is mainly composed of pulverized concrete blocks and bricks, was used to study the effect of different types of column flow regimes in the release of constituents from the material. Because of its similarities to concrete debris, construction debris may be used in the same applications as concrete debris. In general, construction debris potentially may be used as an aggregate substitute in pavement construction, as well as an aggregate for cement-treated or lean concrete bases, a concrete aggregate, an aggregate for flowable fill, or an asphalt concrete aggregate (Griffiths 2002).

CD material was collected from the demolition of one of the buildings at Vanderbilt University during renovation in 2001. The material had been part of a building constructed in the late 1960's, and after demolition, it was outside and had been subjected to weathering conditions for a couple of weeks before collection. The material was initially crushed with a hammer and then crushed in a jaw-crusher to a maximum particle size of 2 mm.

Following crushing, a small portion of this material was saved for X-ray fluorescence (XRF) analysis and neutron activation analysis (NAA) for total element analysis, and X-ray diffraction (XRD) and scanning electron microscope (SEM) analysis for possible mineral phases present. Particle size distribution and moisture content were also analyzed. The rest of the material was separated for chemical characterization.

Moisture content of the construction debris was measured “as collected” following ASTM D 2216-92 (ASTM 1992). In this test, a sample is dried in an oven temperature of $110^{\circ}\pm 5^{\circ}\text{C}$ to a constant mass. The measured moisture content was 6.4%. Total composition of construction debris was measured by XRF analysis using a TN Technologies model Spectrace 9000, and results are presented in Table 3.1.

XRD suggested the presence of quartz (SiO_2). For SEM analysis, the material was separated into its three main components (based on appearance): brick (23% wt), a “light” concrete-like component (55% wt), and a “dark” concrete-like component (22% wt). The brick component suggested the presence of Si, K and Fe (Figure 3.1). Both concrete-like samples, “light” (Figure 3.2) and “dark” (Figure 3.3) had Si, Ca, Fe and K as the main components.

Table 3.1. Total composition for CD from XRF analysis.

Element	Concentration (mg/kg)	Standard Deviation
K	5702	575
Ca	155560	1280
Ti	1846	249
Fe	12050	407
Co	284	137
Ni	108	49
Cu	60	30
Zn	77	29
As	47	12
Sr	251	11
Mo	5	3
Rb	54	8
Ba	151	13
Mo	5	3
Ag	29	30

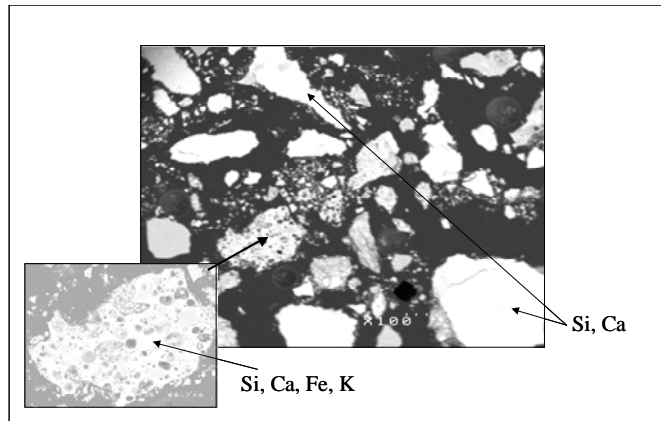


Figure 3.1. SEM image for CD “light” component.

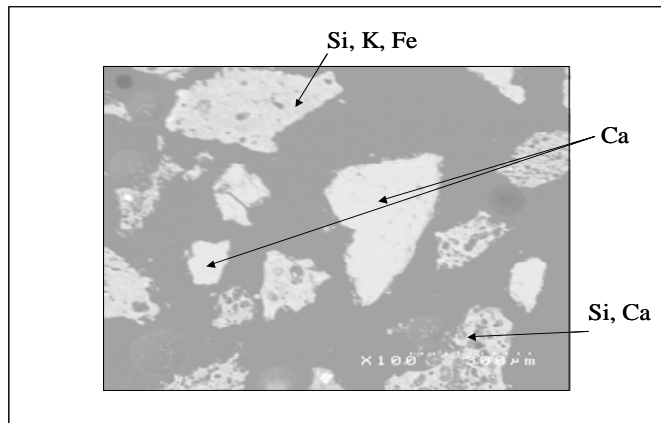


Figure 3.2. SEM image for CD “dark” component.

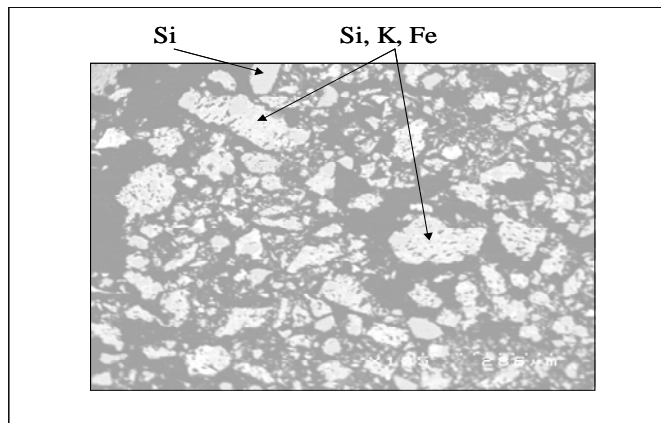


Figure 3.3. SEM image for CD “brick” component.

Particle size distribution of the material was determined using ASTM D 1511-98 (ASTM 1998). In this test, material passing specific mesh sizes was measured. The test

was performed using the original material that had been reduced with the jaw crusher, and Figure 3.4 shows that all material had a maximum particle size than 2 mm, with about 55% of the material having a particle size of 0.9 mm.

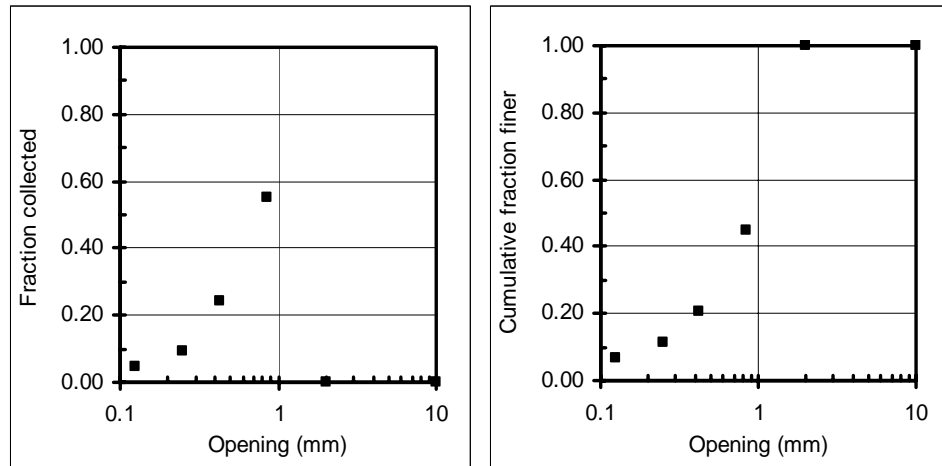


Figure 3.4. Particle size distribution for CD.

Methods

The effect of different types of column flow in the release of constituents from the material was studied by comparing data from continuous saturated flow columns and two different types of intermittent unsaturated flow columns. The column test design was based on the method NEN 7343 (van der Sloot et al. 1997). However, some significant changes were made to this method to provide for the testing under intermittent unsaturated conditions.

The columns were designed to have a 10-cm inner diameter and a length of 40 cm, and were constructed of acrylic with two plastic plates of different mesh sizes to support the material and prevent material losses from the columns, as well as for distribution of the incoming water solution to the columns. The columns were closed

with flanges sealed with an o-ring, and the flanges were kept together with stainless steel nuts and bolts. The flow rate through the columns was set to 220 mL/d, which was based on average precipitation in the Nashville area. The leachant was deionized water. All columns ran concurrently using multi-channel peristaltic pumps

Continuously saturated columns were run up-flow to assure saturation, and intermittent unsaturated columns were run down-flow. Both columns were run as a function of the LS ratios over a range varying from 0.1 to 10 mL/g of dry matter, and in this experiment, LS ratios of 0.1, 0.2, 0.5, 1, 2, 5, and 10 mL/g were originally considered for specific points of sample collection. After previous experiments, it was observed that the change in pH, conductivity and release of constituents was not significant after LS of 5 mL/g, and for this reason, some columns were stopped at this LS ratio. For the continuously saturated columns, every time one of the previously established LS ratios was achieved, a sample was collected. The sample from the first LS ratio was collected entirely, as the plastic collection container was large enough to hold the first fraction (approximately 130 mL). For the following fractions, samples were taken at equal time intervals between the established LS ratios. A collection container was placed on the day before the next LS ratio or sampling interval was reached, according to the volume of leachant exiting the column, and just the last fraction of that interval was collected. When samples were not collected, a container would collect the leachate and the volume would be registered. This leachate was discarded.

For the first case of intermittent unsaturated wetting columns, every time one of the previously established LS ratios was reached, the leachate from the cycle was collected and DI water solution was not added to the column for 4 days. After 4 days of

no-flow conditions, flow was resumed until the next LS ratio was reached. For the second type of intermittent unsaturated wetting column experiments, the columns had intermittent flow, 4 days on, 4 days off, regardless of the particular LS ratio, and they continued to operate in this manner until a LS ratio of 5 mL/g was achieved. A picture of both types of column flow regime, intermittent unsaturated and continuously saturated, is presented in Figure 3.5.

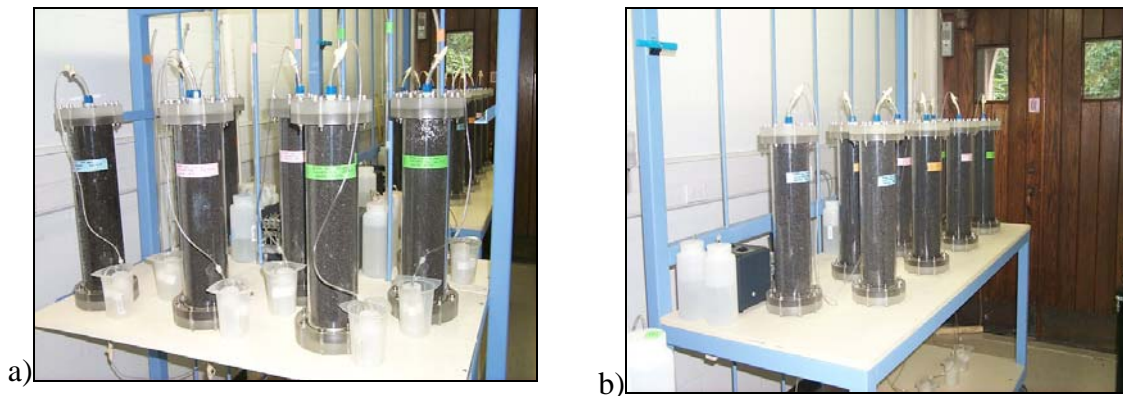


Figure 3.5. Column experiments: a) continuously saturated columns, b) intermittent wetting columns.

At the end of each sample collection, the pH and conductivity of the sample was recorded, followed by sample filtration through a 0.45- μm -pore size polypropylene filtration membrane. pH was measured for all aqueous extracts using a Corning 450 pH/ion meter, accurate to 0.1 pH units. A 3-point calibration was performed using pH buffer solutions. Conductivity of the leachates was measured using an Accumet AR20 pH/ion meter and a standard conductivity probe. The conductivity probe was calibrated using appropriate standard conductivity solutions for the conductivity range of concern. The samples then were collected and separated in two sub-samples; one preserved with nitric acid 2% for metal analysis, and the other unpreserved for anion analysis.

Depending on space availability, samples were stored in a refrigerator at 4°C, or in a constant temperature room at 14°C until analysis.

ICP-MS analyses were completed using a Perkin Elmer model ELAN DRC II. Nine-point standard curves were used for an analytical range between approximately 0.1 µg/L and 500 µg/L. Analytical blanks and analytical check standards at approximately 50 µg/L were run every 10 samples and required to be within 10% of the specified value. Samples for analysis were diluted gravimetrically to within the targeted analytical range using 1 vol% Optima grade nitric acid (Fisher Scientific). A 20-µL aliquot of internal standard was added to every sample. Duplicates and spikes were run every 10 samples to check for element recovery in the instrument. The required spike recovery ranged between 80-120%. If a single data point seemed doubtful, that sample was re-run with an additional spiked sample. Constituents measured included Al, As, Ba, Ca, Cd, Cu, Fe, K, Mg, Na, Pb, Se, Sr, and Zn for cations.

Aqueous concentrations of anions (chloride and sulfate) were determined using a Dionex DX-600 ion chromatograph. The instrument was calibrated with Dionex Five Anion Standard and an independent standard (SPEX Certiprep). The detection limit for chloride and sulfate in aqueous samples is 0.09 and 0.13 mg/L, respectively. Duplicates and spikes were run every 10 samples to check for element recovery in the instrument. The required spike recovery ranged between 80-120 %. If a single data point seemed doubtful, that sample would be re-run with an additional spiked sample.

Results and Discussion

Results presented here show a comparison of the effect that different types of column flow have on the release of constituents from CD. An average of 2 replicates is presented. pH and conductivity of the samples are presented as a function of LS ratio. Elements shown to be present in higher amounts in the solid sample, such as Ca and Fe, are presented. Also shown are elements that are not pH dependent and show the release of highly soluble salts from the material (e.g., Na, SO₄) as a function of LS ratio, as well as elements that are pH-dependant (e.g., Sr, Ba, Pb) as a function of pH. Results for Al, As, Cd, Cu, Cl, K, Mg, Se and Zn are included in Appendix B.

pH and Conductivity

Initial pH values were slightly lower for samples from the intermittent unsaturated column flow regimes, but became constant after a LS ratio of about 2 mL/g, as can be seen in Figure 3.6. The difference between the two unsaturated flow regimes lies in the low initial pH value after a no flow period for the regular intermittent column, where a noticeable decrease in pH is observed at certain LS Ratios (0.2, 0.5, 1, 2 and 5). This may be caused by the flow interruption that allows the material to come into greater contact with air, exposing the carbonate boundry layer of the material, and slightly changing the chemistry of the particles. This effect of intermittent leaching cycles on leachate pH and conductivity has been previously observed (Stewart et al. 1997). pH values from continuously saturated column samples remained at about a constant value of about 10 through out the experiment, which is a result of the carbonation the material experienced while being exposed to the atmosphere.

Initial conductivity values were slightly higher for the intermittent unsaturated column flow regimes as can be seen in Figure 3.6. However, after a LS ratio of 2 mL/g, there is no significant effect of the column flow regime in the conductivity of the column leachates.

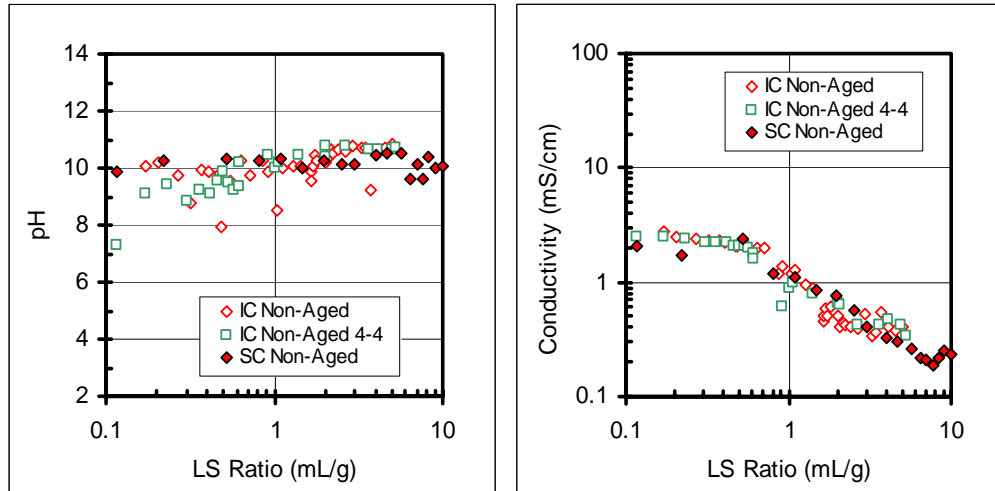


Figure 3.6. pH and Conductivity of CD column samples as a function of LS Ratio.

Major constituents

Major constituents and highly soluble species showed no significant effect of different types of column flow in the release of constituents, as can be seen in the release of Na, Ca, and SO_4 .

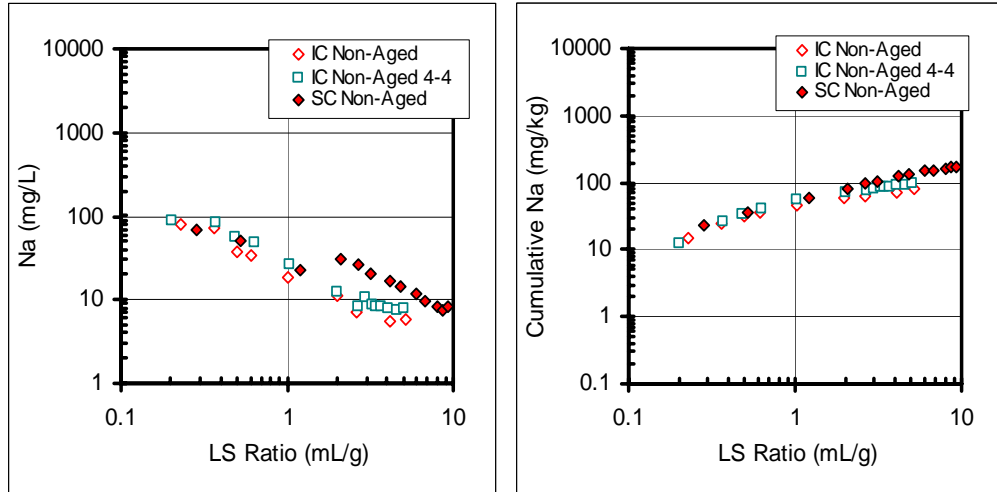


Figure 3.7. Na release from CD column testing as a function of LS Ratio.

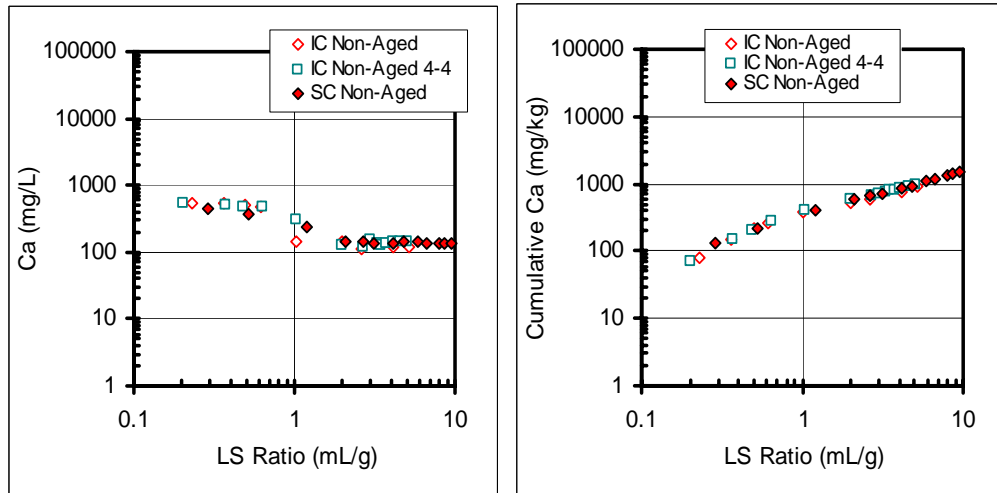


Figure 3.8. Ca release from CD column testing as a function of LS Ratio.

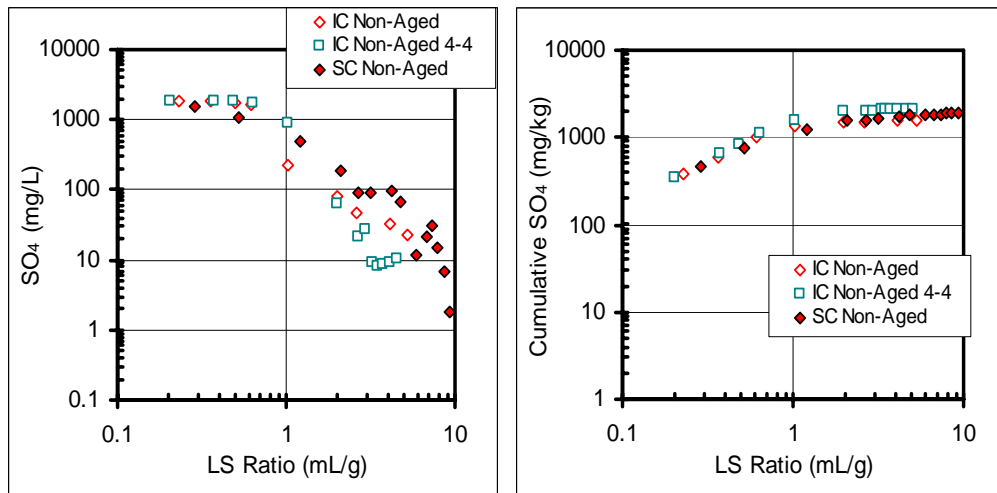


Figure 3.9. SO₄ release from CD column testing as a function of LS Ratio.

Minor constituents

Most of the minor and highly pH dependent materials showed no significant effect of different types of column flow in the release of constituents, as can be seen in the release of Ba, Fe, and Sr. For Pb, the release from 4-4 intermittent unsaturated columns was slightly higher than the release from the other two flow conditions.

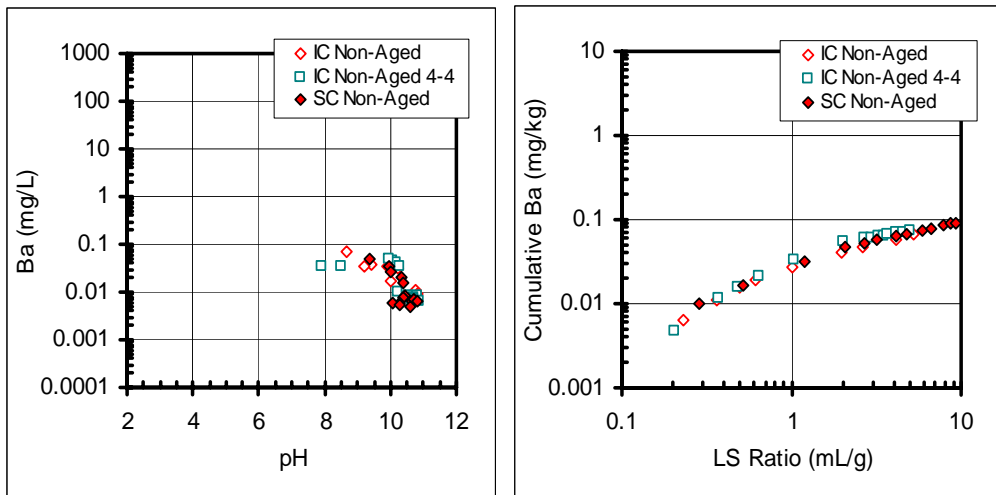


Figure 3.10. Ba release from CD column testing as a function of pH and LS Ratio.

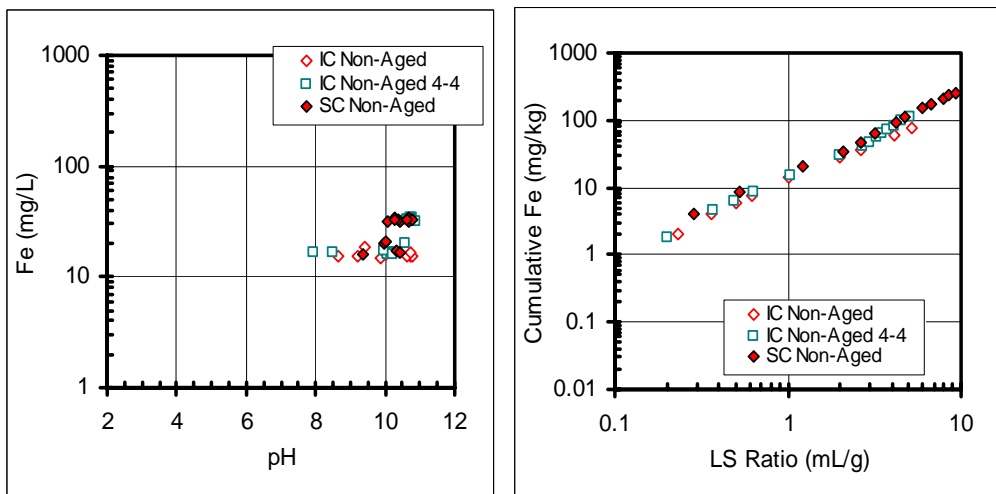


Figure 3.11. Fe release from CD column testing as a function of pH and LS Ratio.

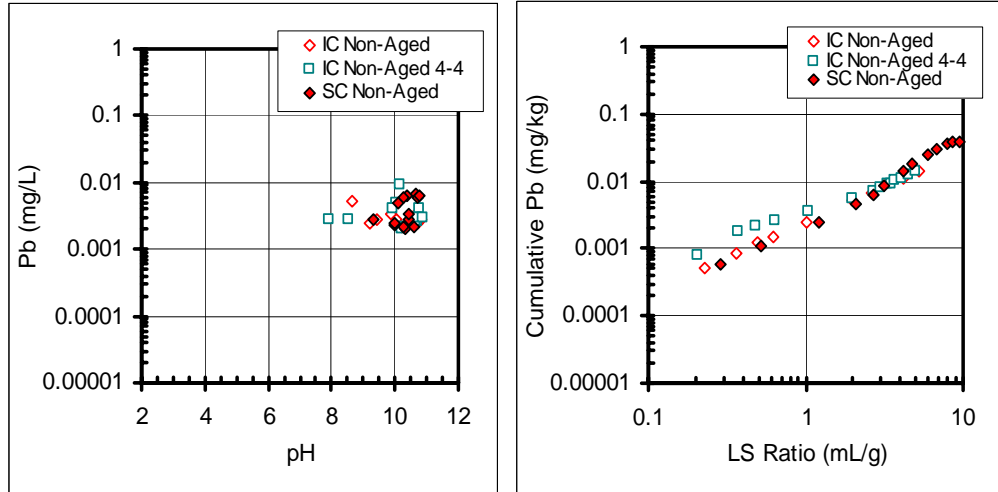


Figure 3.12. Pb release from CD column testing as a function of pH and LS Ratio.

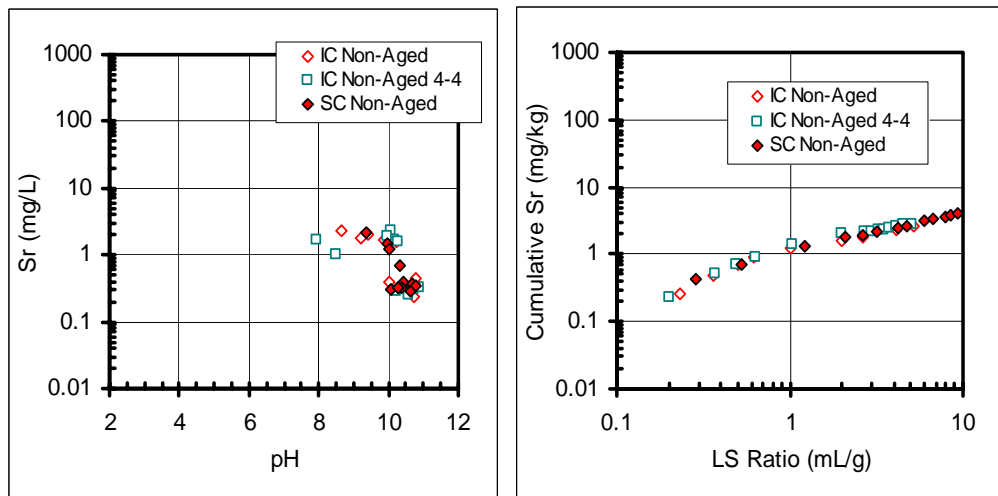


Figure 3.13. Sr release from CD column testing as a function of pH and LS Ratio.

Conclusions

The results presented in this chapter indicate that making the intermittent cycle more frequent has no significant impact on pH, conductivity and release of constituents from column testing than running an intermittent cycle that stops only at specific LS ratios. Also, results show that the only significant difference between intermittent unsaturated flow and continuously saturated flow is the quicker salt release from intermittent unsaturated columns, as shown by conductivity values, at initial LS ratios.

This faster initial release may be due to the presence of preferential flow paths existing in the columns running down flow with intermittent unsaturated flow and constituent wash out at initial LS ratios, and it is more noticeable in the 4-4 columns, where the no flow condition occurs more often. After a LS ratio of 5 mL/kg there is no difference between the different types of column flow regime.

This chapter presents evidence that column experiments performed at continuously saturated conditions, as most standardized column test methods suggest, and as suggested by the protocols presented in the leaching assessment framework, produces similar results to those that what would be obtained under unsaturated conditions. The significance of this observation lies in the shorter column test times required for continuously saturated columns, as well as in the many data available resulting from saturated experiments. The data from these saturated experiments can be considered surrogates for field conditions, even under intermittent unsaturated conditions. This finding will continue to be tested, and supported, in subsequent chapters in this dissertation, considering other materials.

References

- ASTM (1992). Standard Test Method for Laboratory Determination of Water (Moisture) Content of Soil and Rock - D 2216-92. Philadelphia, PA.
- ASTM (1998). Standard Test Method for Carbon Black-Pellet Size Distribution - D1511-98. Philadelphia, PA.
- Elzahabi, M., Yong, R.N. (2001). "pH influence on sorption characteristics of heavy metal in the vadose zone." Engineering Geology **60**: 61-68.
- Farrah, H. and W. F. Pickering (1977). "Influence of clay-solute interactions on aqueous heavy-metal ion levels." Water Air and Soil Pollution **8**(2): 189-197.
- Futch, S. H. and M. Singh (1999). "Herbicide mobility using soil leaching columns." Bulletin of Environmental Contamination and Toxicology **62**: 520-529.
- Georgakopoulos, A., A. Filippidis, A. Kassoli-Fournaraki, J.-L. Fernández-Turiel, J.-F. Llorens and F. Mousty (2002). "Leachability of major and trace elements of fly ash from Ptolemais power station, Northern Greece." Energy Sources **24**: 103-113.
- Griffiths, C. T., Krstulovich, J.M. (2002). Utilization of Recycled Materials in Illinois Highway Construction, Federal Highway Administration: 27.
- Hanson, A. T., B. Dwyer, Z. A. Samani and D. York (1993). "Remediation of chromium-containing soils by heap leaching: Column study." Journal of Environmental Engineering **119**(5): 825-840.
- Huang, C., C. Lu and J. Tzeng (1998). "Model of leaching behavior from fly ash landfills with different age refuses." Journal of Environmental Engineering **124**(8): 767-775.
- Jang, A., Y. S. Choi and I. S. Kim (1998). "Batch and column tests for the development of an immobilization technology for toxic heavy metals in contaminated soils of closed mines." Water Science and Technology **37**(8): 81-88.
- Jang, Y.-C. and T. Townsend (2001). "Sulfate leaching from recovered construction and demolition debris fines." Advances in Environmental Research **5**: 203-217.
- Kjeldsen, P. and T. H. Christensen (1990). "Leaching tests to evaluate pollution potential of combustion residues from an iron recycling industry." Waste Management & Research(8): 277-192.
- Lu, C. (1996). "A model of leaching behaviour from MSW incinerator residue landfills." Waste Management & Research **14**: 51-70.
- Modi, M. and D. W. Kirk (1994). "The effects of codisposal of alkaline hazardous waste with municipal solid waste on leachate contamination." Hazardous Waste & Hazardous Materials **11**(2): 319-332.

- O'Grodnick, J. S., P. G. Wislocki, J. L. Reynolds, M. Wisocky and R. A. Robinson (1998). "Aged soil column leaching of emamectin benzoate (MAB1a)." Journal of Agriculture and Food Chemistry **46**: 2044-2048.
- Sawhney, B. L. and C. R. Frink (1991). "Heavy metals and their leachability in incinerator ash." Water, Air and Soil Pollution **57-58**: 289-296.
- Stegemann, J. A., Schneider, J., Baetz, B.W., Murphy, K.L. (1995). "Lysimeter washing of MSW incinerator bottom ash." Waste Management & Research **13**: 149-165.
- Stewart, B. R., W. L. Daniels and M. L. Jackson (1997). "Evaluation of leachate quality from codisposed coal fly ash and coal refuse." Journal of Environmental Quality **26**: 1417-1424.
- Sun, B., Zhao, F.J., Lombi, E., McGrath, S.P. (2001). "Leaching of heavy metals from contaminated soils using EDTA." Environmental Pollution **113**: 111-120.
- Ubal dini, S., Piga, L., Fornari, P., Massidda, R. (1996). "Removal of iron from quartz sands: A study by column leaching using a complete factorial design." Hydrometallurgy **40**: 369-379.
- van der Sloot, H. A., L. Heasman and P. Quevauviller, Eds. (1997). Harmonization of leaching/extraction tests. Studies in Environmental Science. Amsterdam, Elsevier.
- Vegliò, F., Trifoni, M., Abbruzzese, C., Toro, L. (2001). "Column leaching of a manganese dioxide ore: a study by using fractional factorial design." Hydrometallurgy **59**: 31-44.
- Vite, J., C. Carreño and M. Vite (1997). "Leaching of heavy metals from wastewater sludge, using a thermostatted column." International Journal of Environment and Pollution **8**(1/2): 201-207.
- Wasay, S. A. (1992). "Leaching study of toxic trace elements from fly ash in batch and column experiment." Journal of Environmental Science and Health A **27**(3): 697-712.

CHAPTER IV

COMPARISON OF THE RELEASE OF CONSTITUENTS OF CONCERN FROM A GRANULAR MATERIAL UNDER BATCH AND COLUMN TESTING

Abstract

Under the previously proposed leaching assessment framework, leaching data from batch equilibrium testing as a function of pH and LS is used to provide empirical measurement of aqueous-solid constituent partitioning. The resulting data then is used to estimate constituent release under field percolation conditions, assuming local equilibrium. Column leaching testing can be considered a surrogate for field percolation data to evaluate this approach. In addition, column testing is often carried out as a direct approximation of leaching under field percolation conditions. However, column testing is time-intensive compared to batch testing, and may not always be a viable option when making decisions for material reuse. Therefore, it is important to compare the release that occurs under batch and column testing, and evaluate the uncertainties associated with use of batch data to estimate release under percolation conditions. Two types of coal fly ash (CFA) and an aluminum recycling residue (ARR) were evaluated via batch and column testing, including different column flow regimes (saturated and unsaturated, intermittent flow). Leaching data, including pH, conductivity and constituent release were compared from batch and column tests. Results showed no significant difference between the column flow regimes and agreement in most cases between batch and column testing, including cumulative release. For Al, Fe and K in CFA, however, batch testing underestimates the column constituent release for most LS ratios and on a

cumulative basis. Geochemical speciation modeling results for the solubility prediction of constituents from ARR agree with experimental batch data and, with further sample analysis and software development, these results can be used as a basis for long-term prediction of constituent release from the material.

Introduction

When using secondary materials for highway and construction applications, it is important to consider the potential environmental impact that these materials can have in the surrounding environment. Constituents of potential concern present in the materials are subject to leaching, as runoff and water percolating through the materials carries these metals and compounds into the ground, and eventually into the aquifers or surface streams.

Leaching tests are a very useful tool to estimate the release of constituents of concern from granular materials. However, given the complexity of the leaching process, there is no single leaching test that can provide a complete understanding of the leaching that would occur under different circumstances. Because of this, there are different types of leaching tests that have been developed to provide a better understanding of the leaching processes under different conditions.

Kosson et al. developed a framework for evaluation of leaching from secondary materials that provides specific leaching test methods and a hierarchical approach to testing and evaluation (Kosson et al. 2002). Batch tests proposed in this framework are designed to measure the intrinsic leaching properties of a material, including aqueous-solid equilibrium partitioning of constituents, and evaluate the release of constituents in the limiting case when the material is in chemical equilibrium with its surroundings. The goal of equilibrium batch testing is to represent constituent solubility and release over a range of conditions by varying one parameter (e.g., pH, LS ratio) (Garrabrants et al. 2005). As a general rule for equilibrium tests, the material is in contact with the leaching solution and the variables include: contact time, agitation rate, pH of the leachant

solution, and LS ratio. Equilibrium batch leaching tests have been discussed extensively elsewhere (Garrabrants et al. 2005).

Column tests are designed to evaluate the release of constituents at local equilibrium conditions as a function of time. This local equilibrium condition is approached due to the low flow rates through the column, and is also representative of many field leaching conditions. The goal of column testing is to determine rates of constituent leaching during advective mass transport in order to understand the mechanisms of release at low LS ratios (Garrabrants et al. 2005). Column tests account for constituent wash out at lower LS ratios, and the change in solubility controlling phases that this wash out has as a result (van der Sloot et al. 2001). Column tests give an indication of the time-dependent leaching behavior, and can be useful to quantify the retention in the matrix of the element of interest (i.e., heavy metals) relative to the inert constituents of the matrix. Important parameters considered in column testing and not in batch testing include flow regime and infiltration rate. A more extensive literature review on column testing is presented in Chapter 3.

Batch testing offers the advantage of greater reproducibility and simpler design; column testing provides a closer approximation to leaching processes that occur in field conditions (Jackson et al. 1984; Caldwell et al. 1990; Kjeldsen et al. 1990; Förstner et al. 1991; Sawhney et al. 1991; Wasay 1992; van der Sloot et al. 1996). However, column tests are often time consuming, ranging in duration from a couple of weeks to years. Alternatively, batch tests can be carried in shorter periods of time, varying from a couple of hours to days. For this reason, and in order to provide a better tool for decision-making, it is important to understand the difference between leaching of constituents that

occurs under batch testing and column testing. Furthermore, it is necessary to establish conditions under which constituent release in column testing is accurately predicted by batch testing, and to identify key disagreements between the two testing modes.

The objectives of this research are:

- 1) to understand the relationship between leaching of constituents from granular materials that occurs under batch testing and leaching that occurs under column testing,
- 2) to evaluate the predictability of column results, when considered as a surrogate for field data, based on batch tests,
- 3) to compare the solubility obtained from batch data to the solubility predicted by a geochemical speciation model, and
- 4) to recommend guidelines for batch testing results interpretation of both highly soluble and pH-dependent species.

Materials and Methods

Materials

Three materials are presented in this chapter: two types of Coal Fly Ash (CFA) and one Aluminum Recycling Residue (ARR). Before being collected, the materials had been outside for an unknown period, and had been subjected to weathering conditions.

A small portion of each material was saved for X-ray fluorescence (XRF) analysis and neutron activation analysis (NAA) for total element analysis, and X-ray diffraction (XRD) and scanning electron microscope (SEM) analysis to identify mineral phases

present. Particle size distribution and moisture content were also analyzed. The rest of the material was separated for chemical characterization. Moisture content of the materials was measured “as received” following ASTM D 2216-92 (ASTM 1992). In this test, a sample is dried in an oven temperature of $110^{\circ}\pm 5^{\circ}\text{C}$ to a constant mass. Particle size distribution of the material was determined using ASTM D 1511-98 (ASTM 1998). In this test, material passing specific mesh sizes was measured.

Coal Fly Ash

Coal fly ash (CFA) is produced in the operations of coal-fired power plants. Fly ash is a fine, powder-like residue. Its color depends on the amount of carbon present in it. Gray to black represents higher percentages of carbon, while tan coloring indicates lime and/or calcium content (Hjelmar 1990; Griffiths 2002). Fly ash can be added to concrete to lower the heat of hydration and reduce permeability. Dry fly ash can be used alone or combined with sand as an inert fill material or as an aggregate to improve cohesion and stability to bituminous concrete binder and soil embankments (Griffiths 2002). Because of its carbon composition, some states limit the percentage of ash that can be added as an aggregate.

The fly ash used in this research was obtained from ADA Environmental Solutions under contract from the Department of Energy’s National Energy Technical Laboratory (NETL) field evaluation program. The ash was obtained from Unit 1 in The Brayton Point Plant. There were two types of CFA used in this project. The first type (CFA #1) resulted from carbon injection to the ash hopper; the second type (CFA#2) was the baseline without carbon injection. CFA #1 had a light gray color. CFA #2 had a very

dark, almost black, color. More information on these ashes can be found elsewhere (Sanchez et al. 2006).

The measured moisture content for both ashes was 1.17%. Total composition of the ashes was measured by XRF analysis using a TN Technologies model Spectrace 9000 (Tables 4.1). Digestion results using EPA Method 3052 B for both ashes are shown in Table 4.2. NAA results are shown for CFA #1 (Table 4.3). There was not enough material for NAA analysis for CFA #2. The high Al content of the material caused interferences in the analysis and is the cause of discrepancies between XRF and NAA analytical methods. This explains the different As, Ni and Se results.

Table 4.1. Total composition for CFA from XRF analysis.

Element	CFA #1	CFA #2
	Concentration (mg/kg)	Concentration (mg/kg)
Al	124000	134300
As	BML	BML
Ba	950	100
Br	650	50
Ca	20300	60800
Cl	4400	300
Cr	180	220
Cu	200	220
Fe	25000	46500
I	140	BML
K	15000	18530
Mg	6410	8000
Mn	200	410
Na	2420	5110
Ni	160	150
Pb	100	BML
P _x ²	420	1610
Se	200	50
Si	232400	230800
Sr	830	1240
S _x ³	5820	3510
Ti	1000	10150
V	320	430
Zn	110	210
Zr	310	310

Note: BML=below method limit (As<0.009%, Cl<0.006%, I<0.006%, Pb<0.003%, Se<0.003%)

Table 4.2. Total composition of CFA (EPA Method 3052B).

Element	CFA # 1	CFA # 2
	(mg/kg)	(mg/kg)
As	27.9±2.1	80.5±1.9
Cd	BML	BML
Pb	82.9±2.3	117.3±4.9
Se	151.9±6.2	51.4±1.7

Note: NA = Not Applicable; NT = Not tested; BML = Below ML

Table 4.3. Total composition for CFA # 1 from NAA analysis.

Element	Concentration (mg/kg)
Ag	37
As	1600
Cd	3800
Ce	110
Co	61
Cr	110
Fe	39000
Hf	0.89
In	50
Ir	0.031
K	22000
Mo	190
Na	3500
Nd	100
Ni	6200
Pr	31
Rb	150
Re	68
Ru	140
Se	4600
Sm	29
Sn	1100
Sr	470
Tb	1.8
Th	17
Tm	31
U	65
Yb	14
Zn	55
Zr	400

SEM and XRD analyses were also performed on CFA #1. XRD suggested quartz as the main constituent of the material. SEM confirmed the significant presence of Si, Ca, and Fe as well (Figure 4.1).

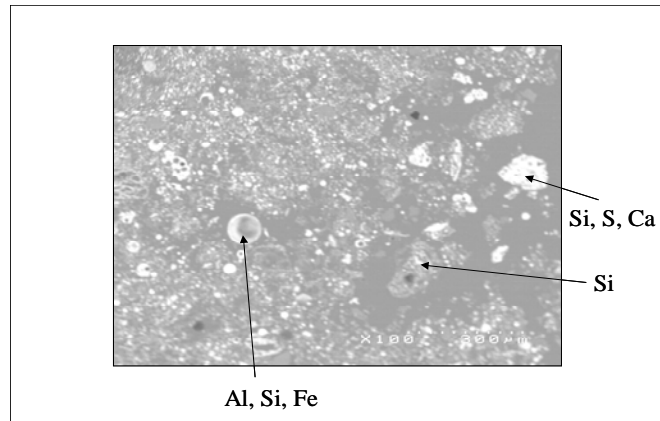


Figure 4.1. SEM image for CFA #1.

Because of the limited amount of material available, it was not possible to perform a particle size distribution test on either type of CFA. However, it is possible to assume that all material passed the 2 mm sieve. This can be confirmed by Figure 4.1, where the particles are all smaller than the 0.3 mm scale bar presented in the figure.

Aluminum Recycling Residue

ARR is generated during the treatment of aluminum scrap in the recycling process. It consists of aluminum metal, spent salt (added to lower the reactivity of aluminum with oxygen), and residue oxides. Approximately one million tons are produced per year (Ghorab et al. 2004). One of its possible uses is as a fill material in highway applications.

The measured moisture content was 0.15%. Total composition of ARR was measured by XRF analysis using a TN Technologies model Spectrace 9000 (Table 4.4), and also by NAA (Table 4.5).

Table 4.4. Total composition for ARR from XRF analysis.

Element	Concentration (mg/kg)	Standard Deviation
Cr	291	91
Fe	2849	252
Mo	7	2
Pb	33	14
Zn	131	32
Zr	38	4

Table 4.5. Total composition for ARR from NAA analysis.

Element	Concentration (mg/kg)
Al	110000
Ba	210
Br	39
Ca	710
Cl	15000
Cu	500
Dy	3.9
Eu	0.72
Ga	120
I	11
In	0.34
K	4000
Mg	37000
Mn	790
Na	8000
Nd	1000
Pd	610
Rb	1700
Sm	9.9
Sn	1800
Sr	380
Th	590
Ti	1600
V	20

SEM and XRD analyses were also performed on ARR. XRD confirmed aluminum oxides as the main constituents of the material, and suggested Mg and Si as major components of the aluminum oxide species. SEM confirmed Al as the main constituent in the material (Figure 4.2).

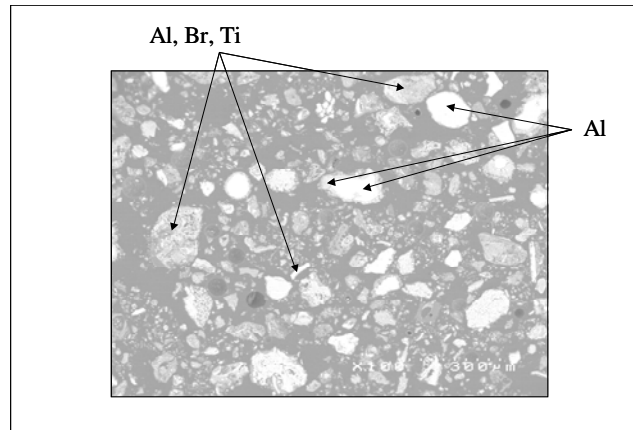


Figure 4.2. SEM image from ARR.

Particle size distribution for ARR is shown in Figure 4.3. This is the material as it was received. The material did not require any particle size reduction before testing. More than 60% of the material was under 0.5 mm.

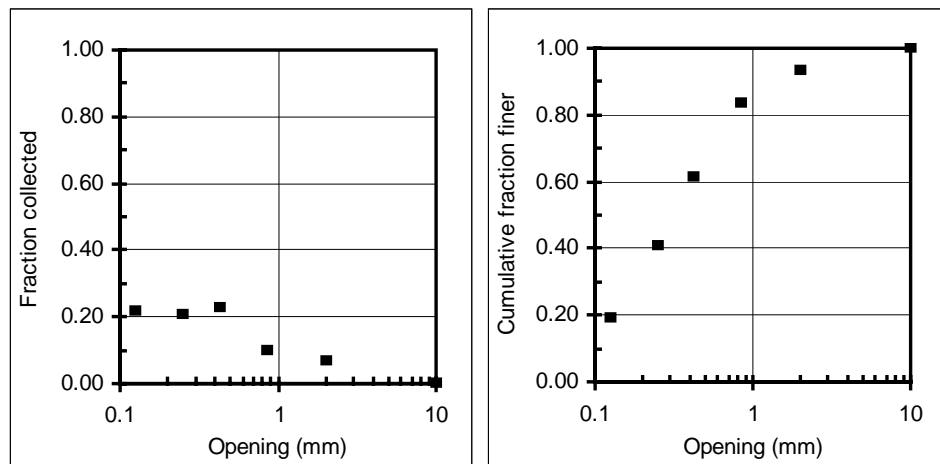


Figure 4.3. Particle size distribution for ARR.

Methods

All materials were tested under batch and column conditions. These tests are described in detail below. The release of constituents from ARR was also modeled using a geochemical speciation model, further explained in the modeling results section.

Batch testing

Batch testing was done to measure the solubility and release of constituents as a function of pH and LS ratio. The batch testing consisted of two tests: solubility and release as a function of pH, SR002.1, and the solubility and release of constituents as a function of LS ratio, SR003.1 (Kosson et al. 2002). Procedures for both protocols are summarized in the following paragraphs. No particle size reduction was needed for the materials, as the particle size was well below 2 mm. Moisture content of the materials was measured before batch testing, so that appropriate adjustments could be made to conduct the test at the specified LS ratio. Batch testing (SR002.1 and SR003.1) for the coal fly ash samples was carried out by Arcadis Laboratories as part of the USEPA evaluation program for leaching of coal combustion residues (Sanchez et al. 2006).

Solubility and release as a function of pH

The SR002.1 (“ANC” in graphs) protocol was followed. The minimum dry equivalent mass (i.e., 40 g dry sample) was placed into each of eleven bottles. Each bottle was labeled with the extraction number or acid addition and the volume of DI water specified in the schedule for LS ratio makeup. The appropriate volume of acid or base was added to each extraction using an adjustable pipette. The bottles were sealed with leak-proof lids and then tumbled in an end-to-end fashion at a room temperature ($20 \pm 2^\circ\text{C}$) for 48 h. At the conclusion of the agitation period, the extraction vessels were removed from the tumbler and the leachates were clarified by allowing the bottles to stand for 15 min. A minimum volume of clear supernatant from each extraction bottle was decanted to measure and record the solution pH and conductivity. For each

extraction, the solid was separated from the liquid by vacuum filtration through a 0.45- μm -pore size polypropylene filtration membrane. The samples then were collected and separated into two sub-samples; one preserved with nitric acid 2% for metal analysis, and the other unpreserved for anion analysis. Samples were stored in a refrigerator at 4°C, or in a constant temperature room at 14°C until their analysis.

Solubility and release as a function of LS Ratio

The SR003.1 (“LS” in graphs) protocol consists of five parallel batch extractions over a range of LS ratios (i.e., 10, 5, 2, 1, and 0.5 mL/g), using DI water as the extractant. The mass of material used for the test was 40 g of dry sample. The minimum equivalent mass required for the test was placed into each of five bottles. The appropriate volume of DI water for each LS ratio was added for each of the LS ratios. For a dry material, this volume was the mass of the aliquot multiplied by the desired LS ratio. The bottles were sealed with leak-proof lids and then tumbled in an end-to-end fashion at a room temperature ($20 \pm 2^\circ\text{C}$) for 48 h. At the conclusion of the agitation period, the extraction vessels were removed from the tumbler and the leachates were clarified by allowing the bottles to stand for 15 min. A minimum volume of clear supernatant from each extraction bottle was decanted to measure and record the solution pH and conductivity. For each extraction, the samples were filtered and preserved as described in the SR002 protocol.

Column testing

The effect of different types of column flow in the release of constituents from the material was studied by comparing data from continuous saturated flow columns and intermittent unsaturated flow columns. The methodology is explained in detail in Chapter 3. Both types of column flow conditions were maintained until a LS ratio of 10 mL/g was achieved. Samples were taken at equidistant points in time between the established LS ratios. Solution pH and conductivity were recorded. Samples were filtered and analyzed as explained previously.

Results and Discussion

Results presented here show the different release of constituents of concern from ARR and both types of CFA when tested under batch and column conditions. pH and conductivity of the samples are presented as a function of LS ratio for column experiments, and as a function of milliequivalents of acid/base added for batch testing. The elements presented are the elements that were present in higher concentrations in the solid samples (i.e., Ca and Fe for CFA and Al for ARR). Also presented are elements that are representative of a certain class of behavior, like highly soluble species (i.e., K for CFA and Ca, Cl and Na for ARR), and pH-dependant species (i.e., Al for CFA and Mg and Sr for ARR). As, Ba, Cu, Cd, Mg, Pb, Se, Sr and Zn are other pH-dependent constituents, and most can be represented by the selected species. SO_4 is a highly soluble species represented. For a complete set of figures for release of constituents from all three materials, refer to Appendix B.

For highly soluble species, the release of constituents in batch and column testing is presented as a function of LS ratio on a concentration basis. These data are integrated to also give cumulative release. Release and cumulative release as a function of LS ratio are also presented for pH-dependent species, as well as release as a function of pH. The equilibrium in batch testing is controlled only by the solubility of the minerals present in the solid material (Kosson et al. 2002). This equilibrium represents a zero flow rate case, and therefore a theoretical upper bound on the release of constituents in low infiltration, local equilibrium controlled column tests (Kosson et al. 2002). Under reuse field applications, cumulative release is the relevant condition. However, the release on a concentration basis as a function of pH or LS ratio can point out potential discrepancies for specific field conditions, even where the estimate of cumulative release is conservative.

A discrepancy or residual plot is presented for each element for a more objective comparison between batch and column data as a function of LS ratio. This residual was obtained similarly as the residuals explained in Chapter 2. Taking the column data as the reference point, the predictive value from batch data is analyzed by calculating the residual as follows (Equation 4.1):

$$Residual = \log\left(\frac{Batch}{Column}\right) \quad (4.1)$$

A positive value for the residual indicates that batch data is a conservative estimate of column release. Negative residual values indicate underprediction of column release. The term “good agreement” is used when the discrepancy between batch and column

tests is within one order of magnitude. Residuals of release as a function of pH are not presented given that the comparison between batch and column data as a function of pH is not of significance, as the column experiments are done at the natural pH of the material, which does not change in more than 1 or 2 pH values throughout the experiment.

Coal Fly Ash # 1

pH and Conductivity

CFA #1 has little buffering capacity; it takes only about 1.5 meq/g of base to change the pH from 10 - 13 (Figure 4.4). This material has a natural pH value of approximately 9 as tested under batch conditions. However, there was an unknown time delay between column testing and batch testing that could have aged the material used for batch testing, and that could be the cause for the lower pH obtained from batch testing. This delay, and the fact that the batch testing was done by a different laboratory, can explain the differences that were observed in constituent release from batch and column testing. No conductivity data are available from batch testing. For column testing, there are no conductivity changes after a LS ratio of 2 mL/g (Figure 4.5).

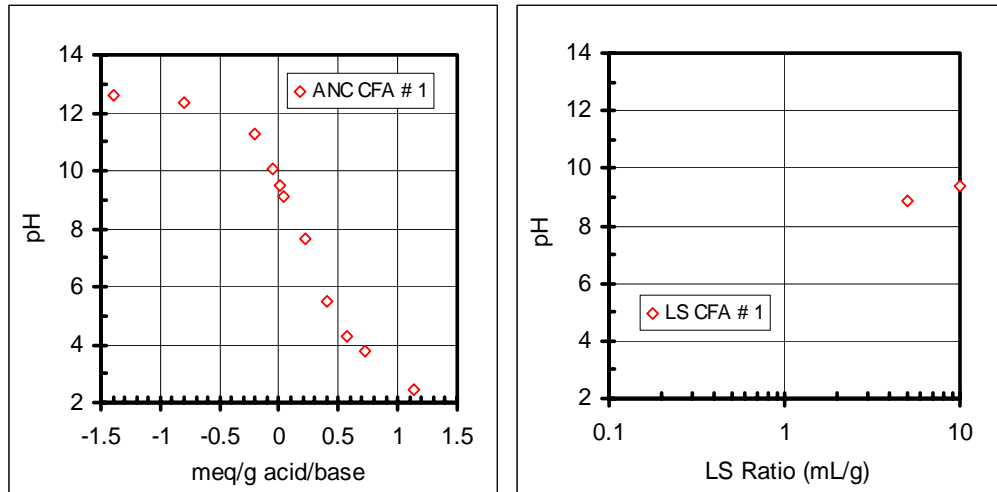


Figure 4.4. pH of CFA #1 batch testing as a function of LS Ratio.

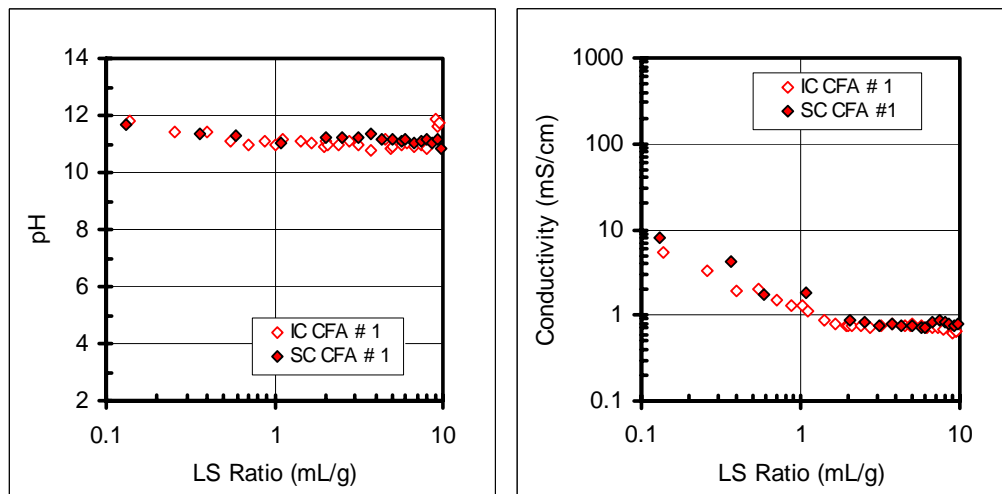


Figure 4.5. pH and Conductivity of CFA #1 column testing as a function of LS Ratio.

Major constituents

Ca and K were considered as the representative major and highly-soluble constituents. No significant effect of column flow regime in the release of constituents is observed for either constituent. For Ca, release under batch testing is a conservative estimate of release from column testing, as observed in the residual values. The cumulative release is well predicted as a function of LS ratio; moreover the release of constituents is overpredicted at each LS ratio (Figure 4.6). For K, release under batch

conditions is underpredictive of the column results at high LS ratios. The cumulative release in columns is also underpredicted, but by less than an order of magnitude (Figure 4.7).

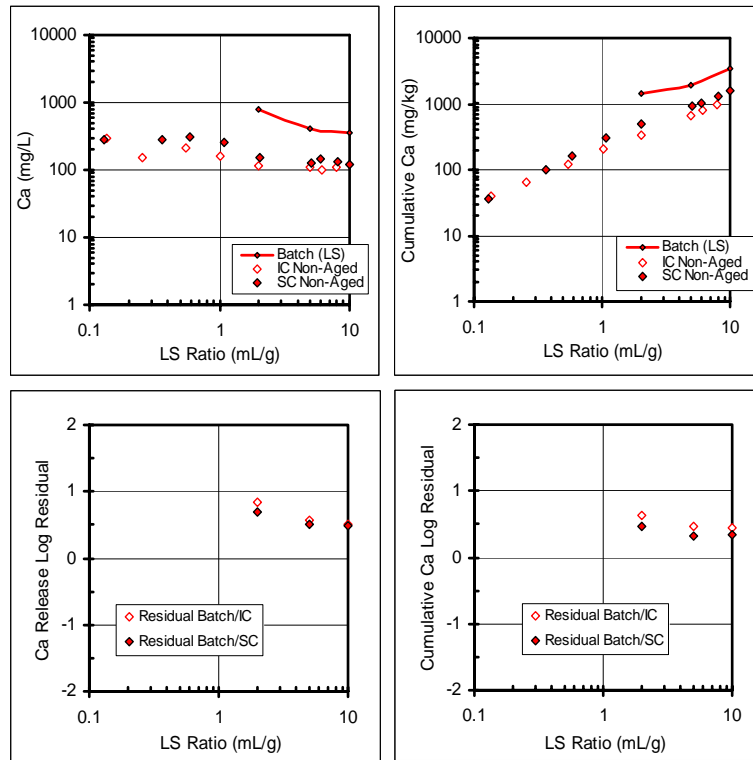


Figure 4.6. Ca release from CFA # 1 as a function of LS Ratio.

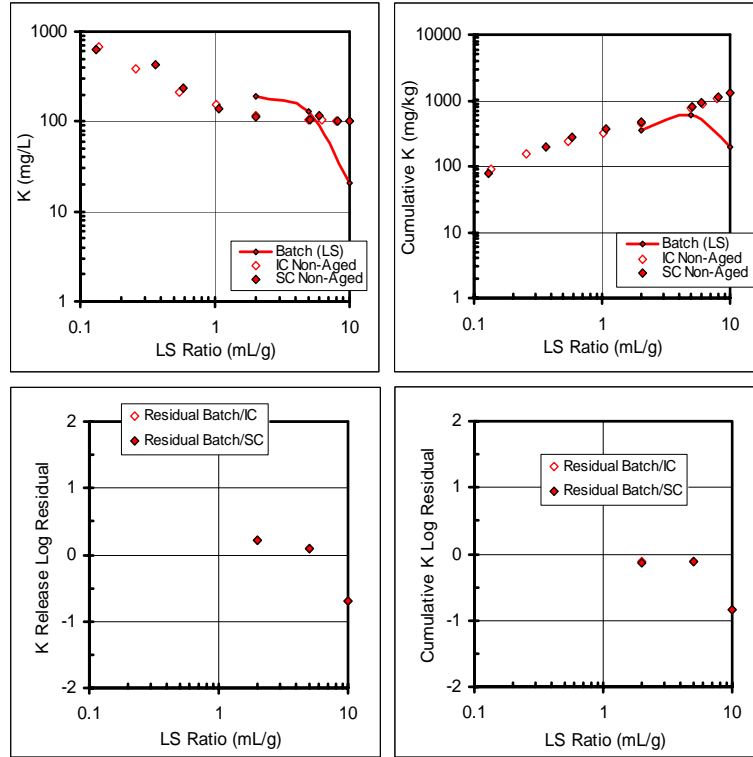


Figure 4.7. K release from CFA # 1 as a function of LS Ratio.

Minor constituents

Al and Fe were considered because they are representative species that show typical minor, pH-dependent cation behavior. The release of constituents from batch testing as a function of pH is in good agreement with the release of constituents from column testing for most of the elements. No significant difference is observed between column flow regimes. For Al, release under batch conditions is underpredictive of the column results as a function of pH and at each LS ratio. The cumulative release in columns is also underpredicted (Figure 4.8). For Fe, there is good agreement between batch and column testing release as a function of pH and at each LS ratio. Cumulative release in columns is also well predicted by the batch testing (Figure 4.9).

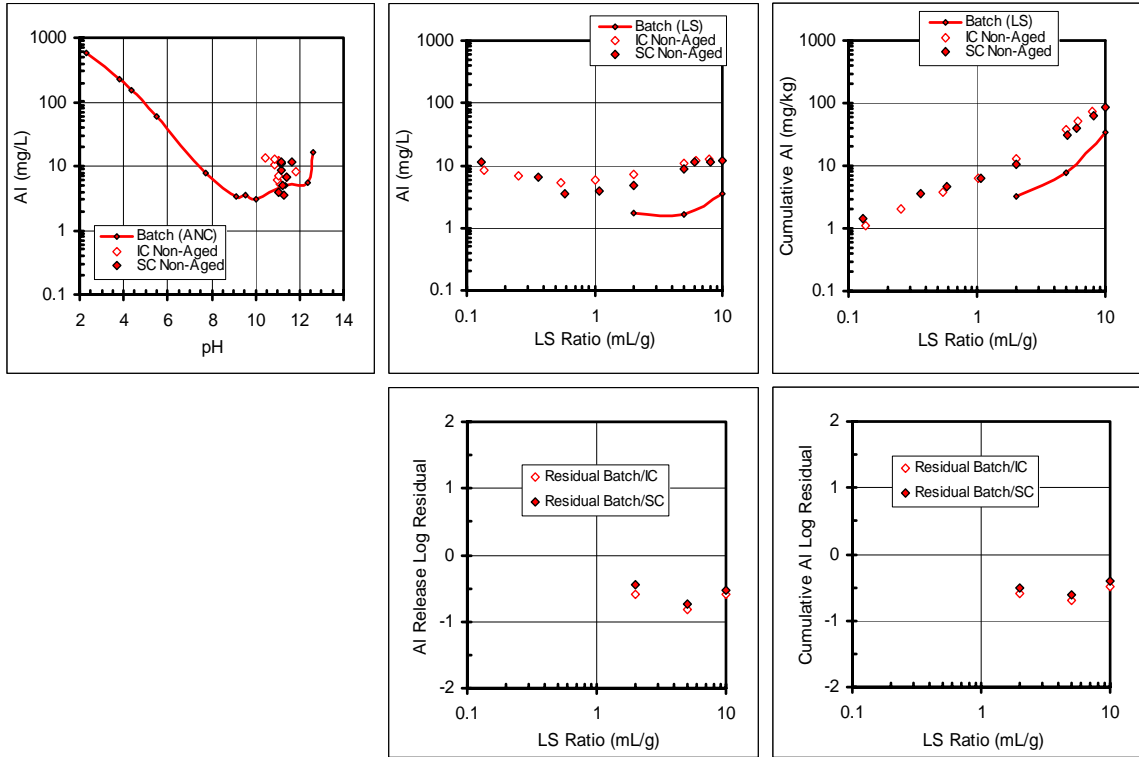


Figure 4.8. Al release from CFA # 1 as a function of pH and LS Ratio.

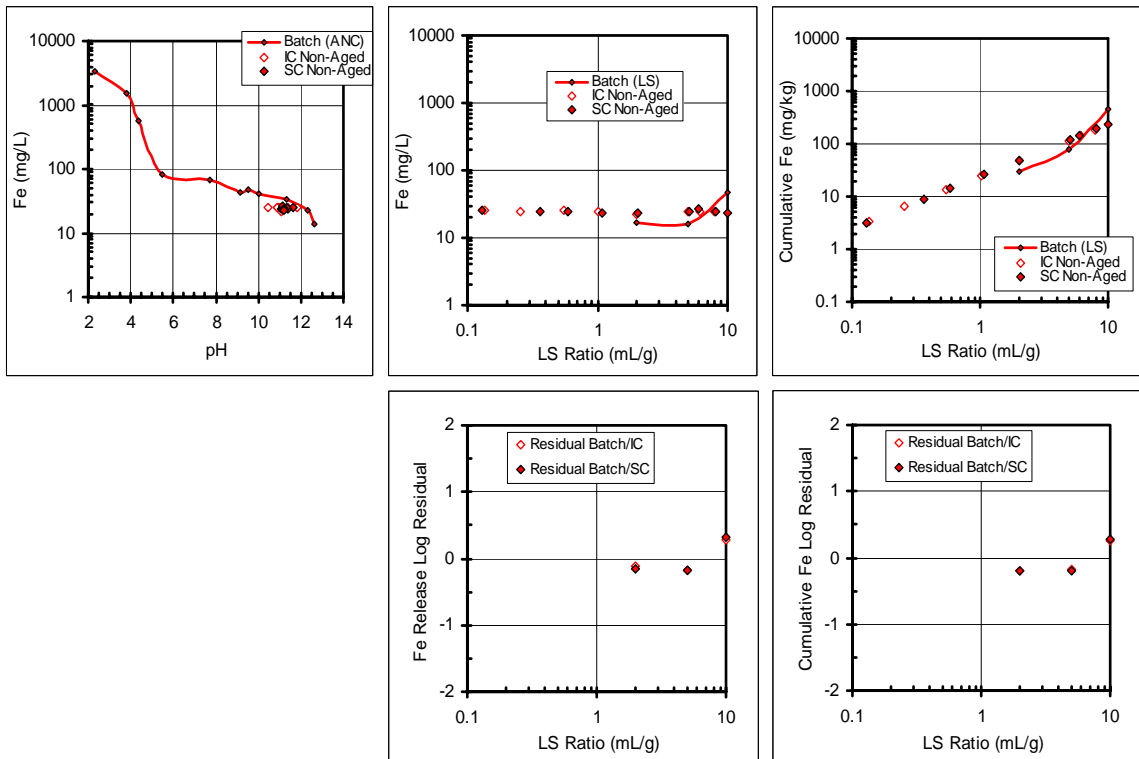


Figure 4.9. Fe release from CFA # 1 as a function of pH and LS Ratio.

Coal Fly Ash # 2

pH and Conductivity

CFA #2 has a high buffering capacity (Figure 4.10). It takes almost 10 meq/g of base to change the pH from 12 to 14. CFA #2 has a natural pH value of 12-13 as measured by batch testing. pH measured from column testing is approximately 10. As for CFA #1, it is possible that the time delay between batch and column testing had some effect on the aging of the material. No conductivity data are available from batch testing. For column testing, there is a significant drop in conductivity after LS ratio of 5 mL/g (Figure 4.11).

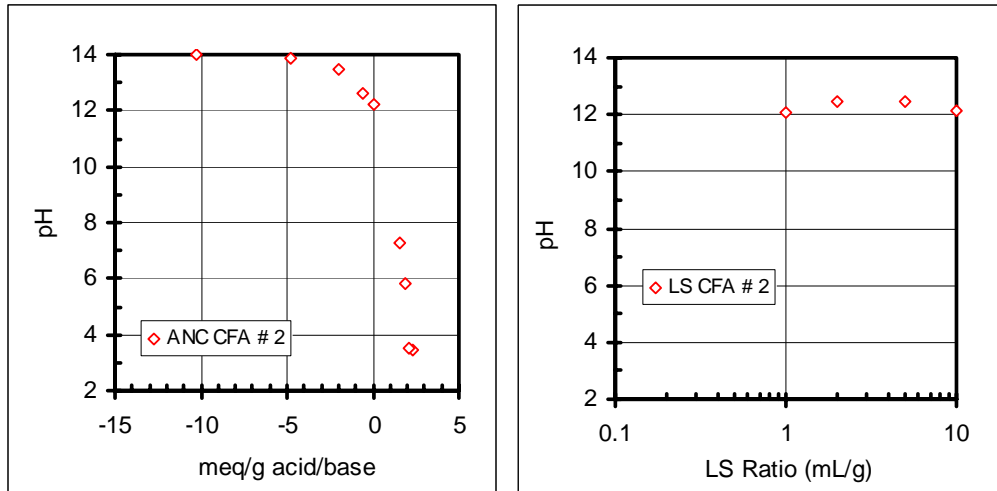


Figure 4.10. pH of CFA #2 batch testing as a function of LS Ratio.

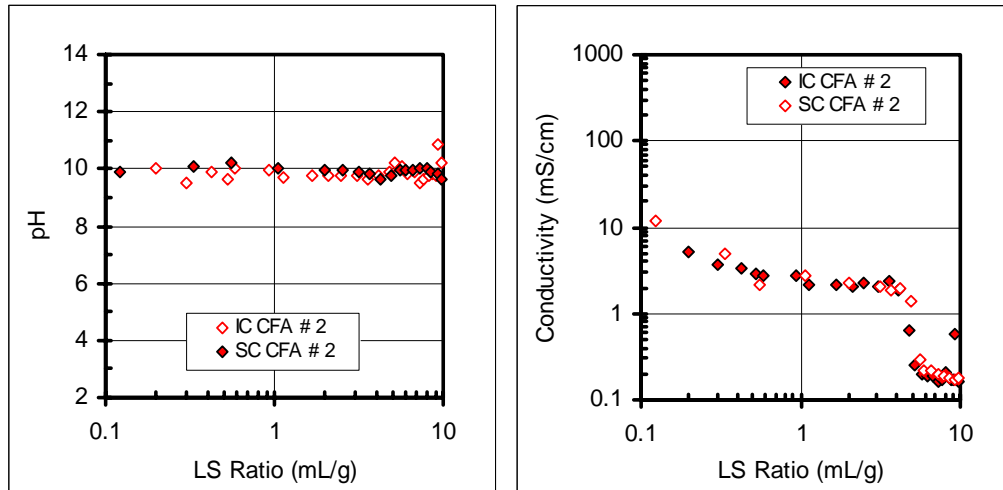


Figure 4.11. pH and Conductivity of CFA #2 column testing as a function of LS Ratio.

Major constituents

Ca and K were considered as the representative major and highly-soluble constituents. No significant effect of column flow regime in the release of constituents is observed for either constituent. For Ca, release under batch testing is a conservative estimate of release from column testing, as observed in the residual values at each LS ratio. Batch testing also gives an accurate prediction of the cumulative release in column testing (Figure 4.12). For K, release under batch conditions gives a conservative prediction of column release at low LS ratios, but is underpredictive of the column results at the highest LS ratio of 10 mL/g. The cumulative release in columns is also underpredicted at the highest LS ratio, but by less than an order of magnitude (Figure 4.13).

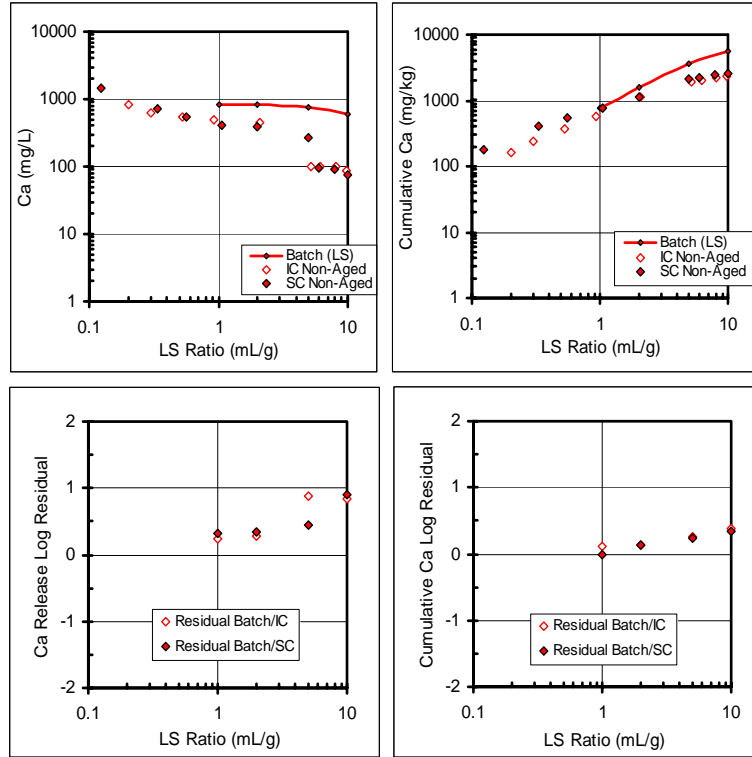


Figure 4.12. Ca release from CFA # 2 as a function of LS Ratio.

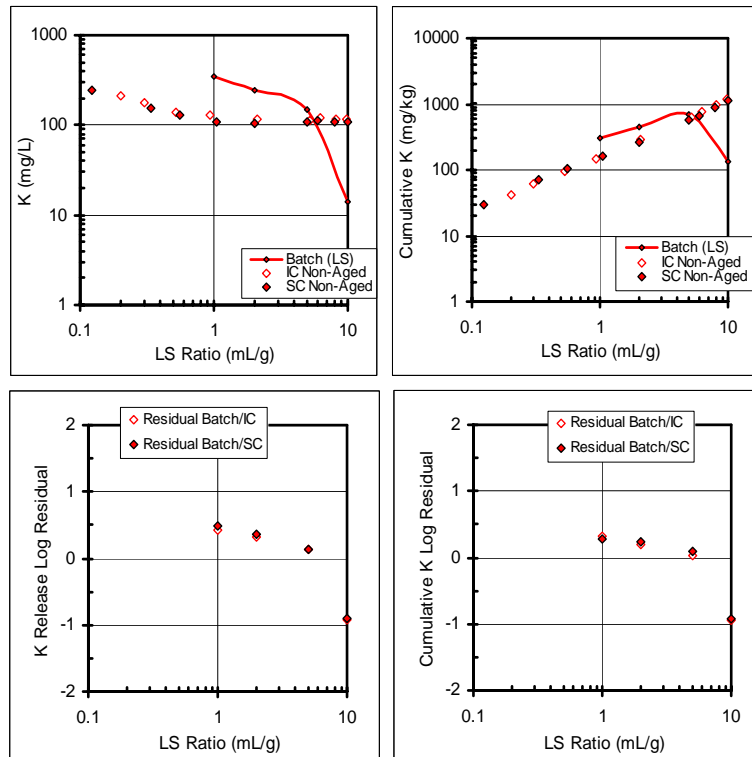


Figure 4.13. K release from CFA # 2 as a function of LS Ratio.

pH Dependent constituents

Al and Fe were considered because they are representative pH-dependent species. Column flow regime does not show significant effect on constituent release. For Al, release under batch conditions is in agreement with column results as a function of pH, but is underpredictive of column results at each LS ratio. Moreover, the cumulative release in columns is also underpredicted, especially at low LS ratios (Figure 4.14). For Fe, there is good agreement between batch and column testing release at low LS ratios, but batch testing is underpredictive of column results as a function of pH; this might be due to the differences in pH for batch and column experiments. Cumulative release in columns is also underpredicted by the batch testing (Figure 4.15). This may be due to the different initial pH of the samples used for batch and column testing.

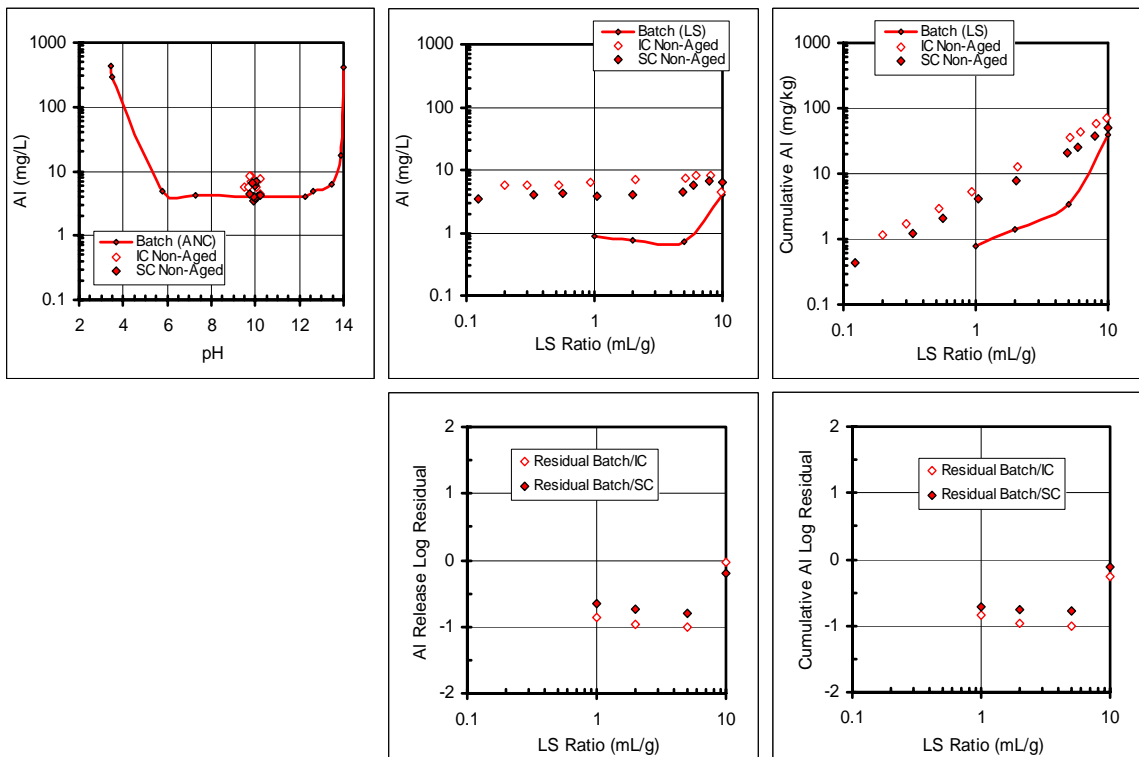


Figure 4.14. Al release from CFA # 2 as a function of pH and LS Ratio.

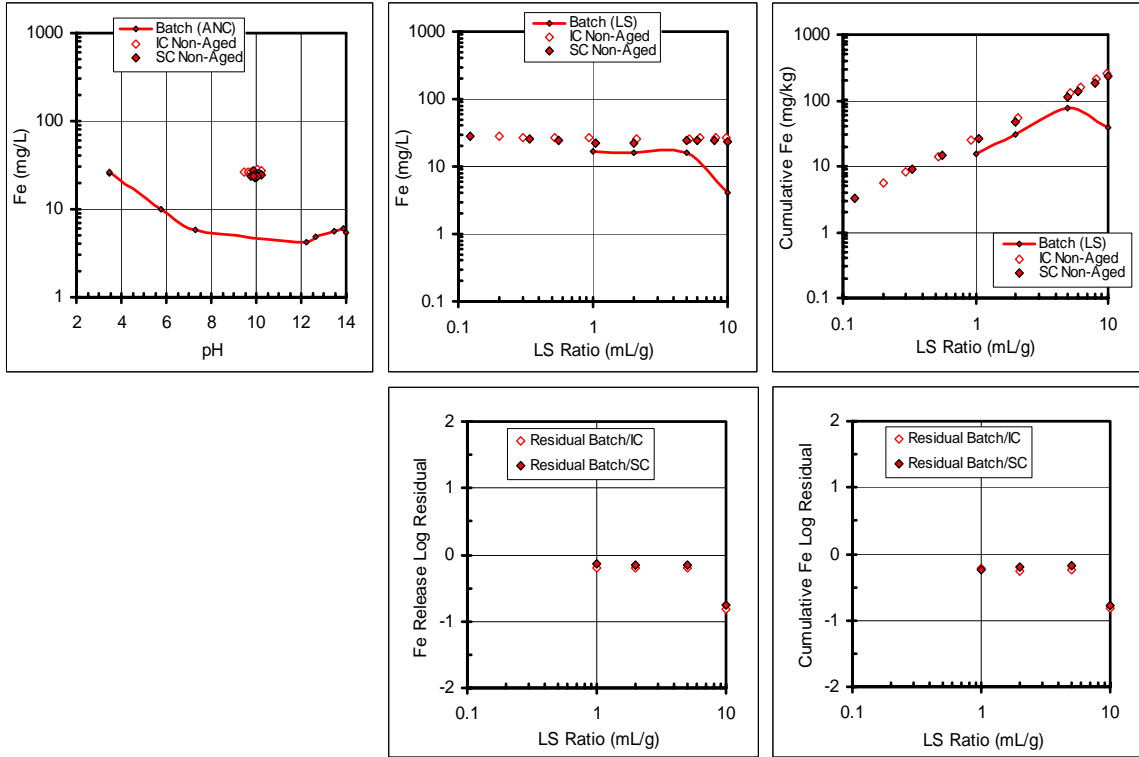


Figure 4.15. Fe release from CFA # 2 as a function of pH and LS Ratio.

Aluminum Recycling Residue

pH and Conductivity

ARR has a high buffering capacity; more than 10 meq acid/g were required to obtain a pH of 3 (Figure 4.16). There is good agreement, in terms of pH values, between batch and column testing at all LS ratios (Figures 4.17 and 4.18). pH from intermittent unsaturated columns is slightly higher than from continuously saturated columns (Figure 4.18). Initial conductivity of samples is higher in batch testing by an order of magnitude. For higher LS ratios, conductivity is overestimated by two orders of magnitude. Conductivity of intermittent unsaturated columns is initially higher than for continuously saturated columns. However, conductivity for IC drops by an order of magnitude lower

than for SC by a LS ratio of 1 mL/g. Final conductivity values are similar for both column flow regimes.

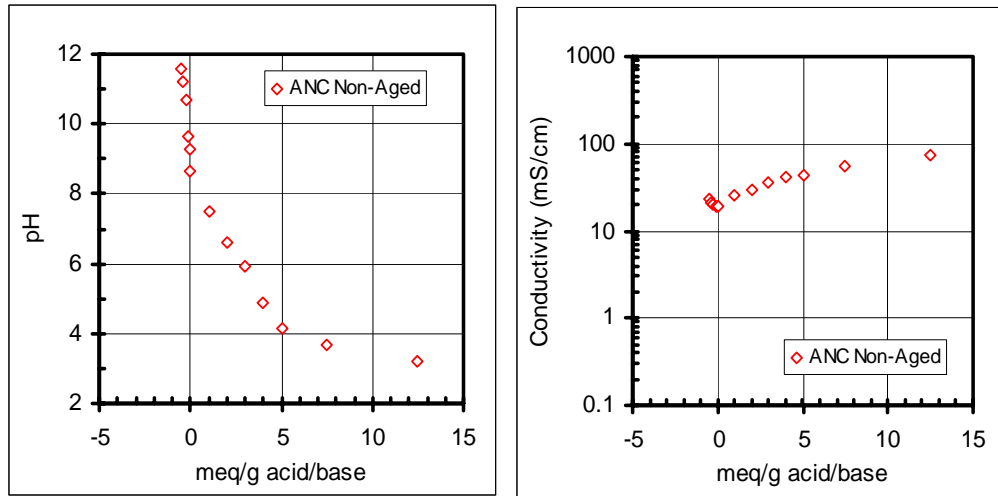


Figure 4.16. pH and Conductivity of ARR titration curve

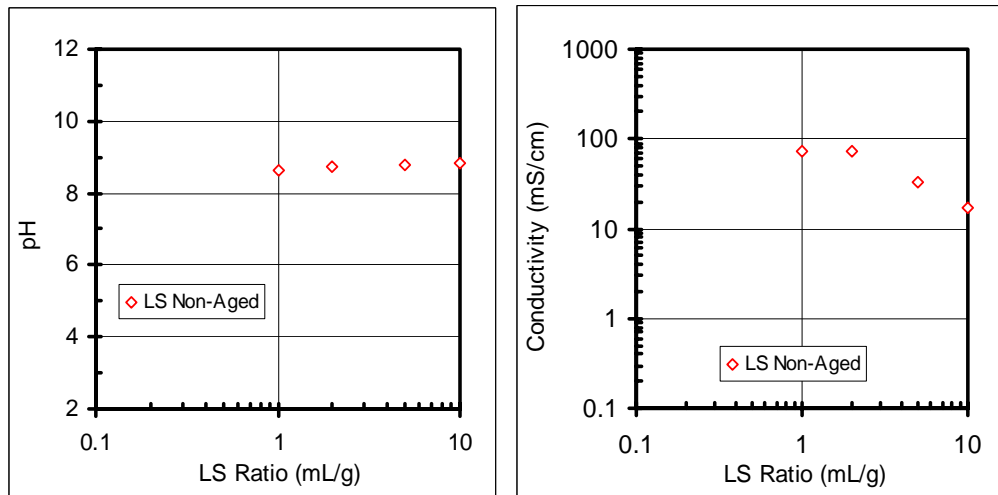


Figure 4.17. pH and Conductivity of ARR batch testing as a function of LS Ratio.

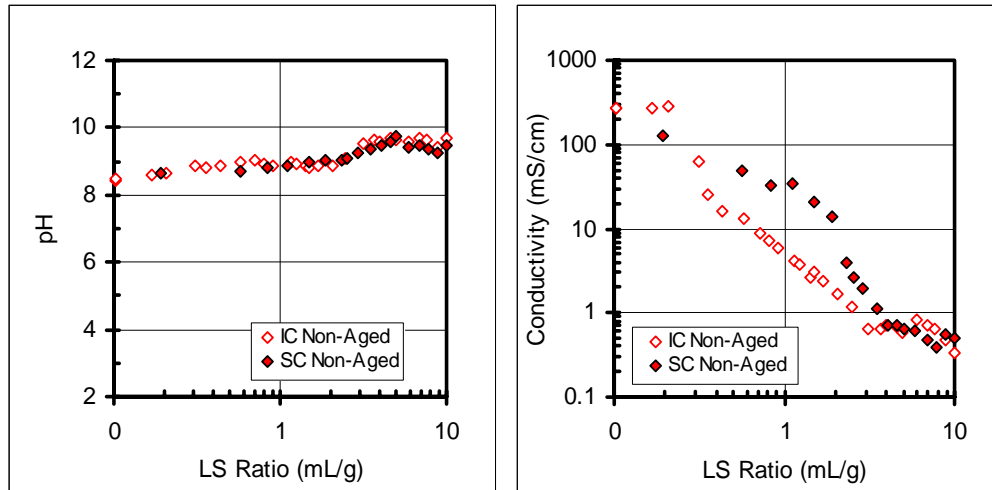


Figure 4.18. pH and Conductivity of ARR column testing as a function of LS Ratio.

Major constituents

Ca, Cl and Na were considered as representative species of major constituents and species with highly soluble behavior. For all elements, batch testing gives a conservative estimate of column results for concentration and cumulative release. Little significant difference in release between column flow regimes is observed for these three constituents. For Ca, the release from continuously saturated columns is slightly higher than from intermittent unsaturated columns (Figure 4.19). For Cl and Na, there is higher initial release in intermittent unsaturated columns. Cumulative release predictions from batch testing are particularly consistent for Cl and Na in both flow regimes (Figures 4.20 and 4.21).

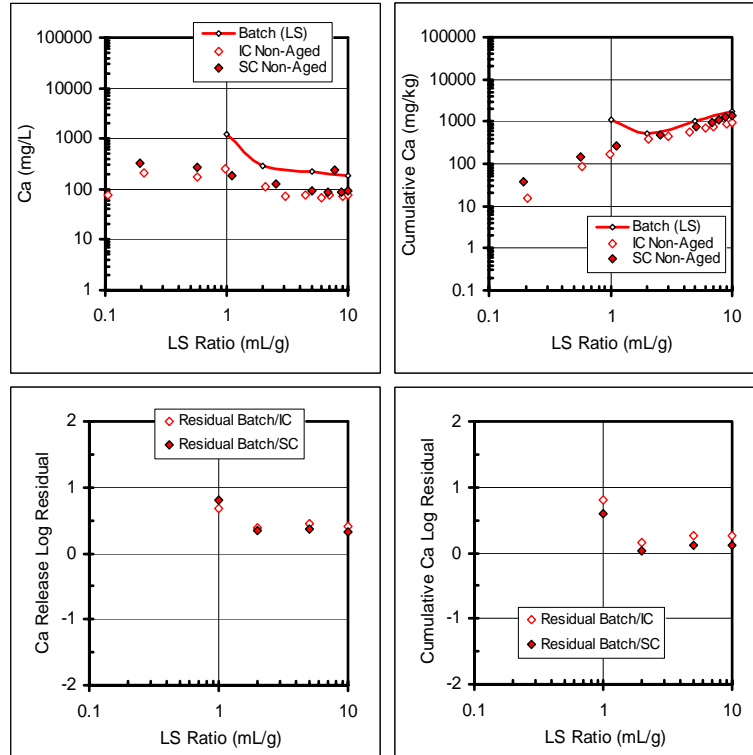


Figure 4.19. Ca release from ARR as a function of LS Ratio.

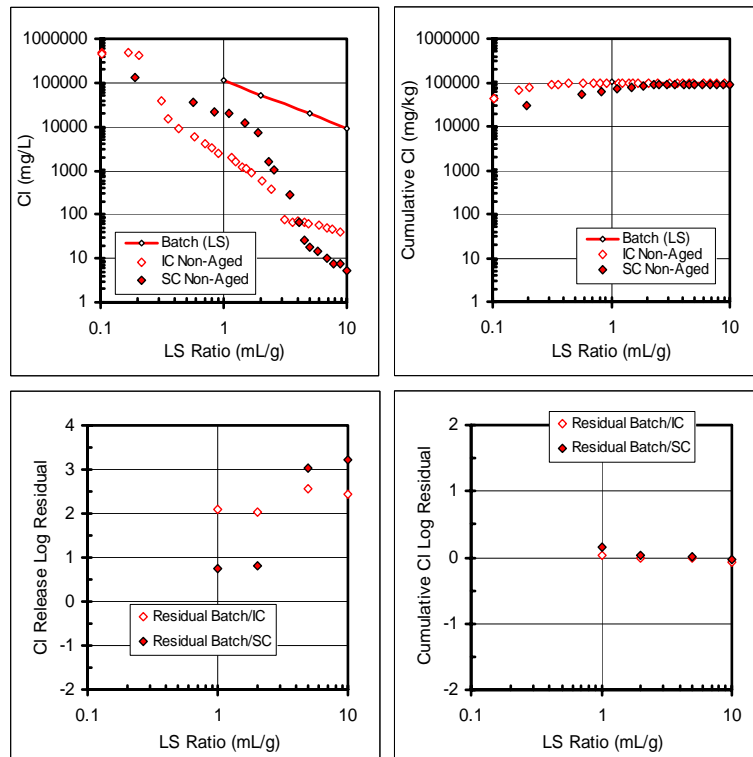


Figure 4.20. Cl release from ARR as a function of LS Ratio.

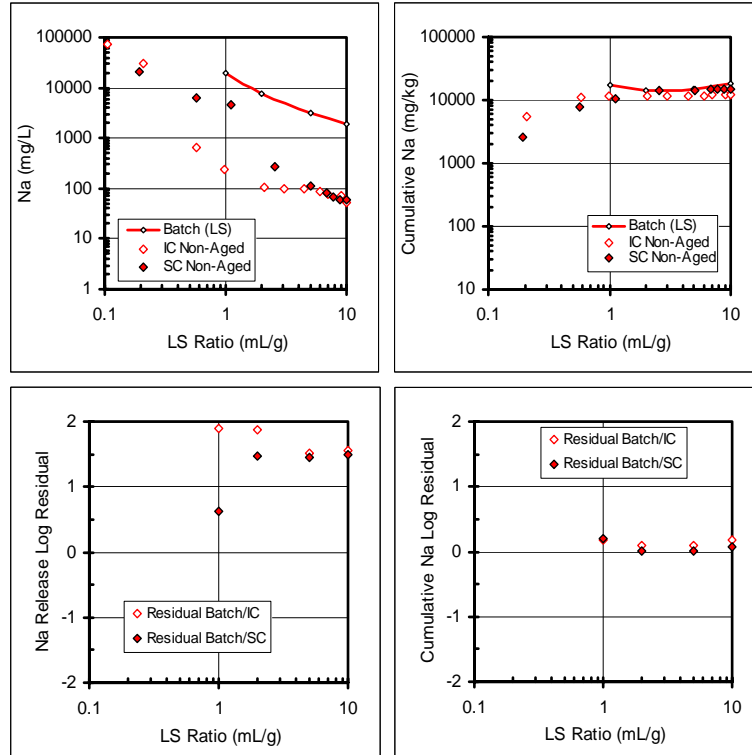


Figure 4.21. Na release from ARR release as a function of LS Ratio.

Minor constituents

Al, Mg and Sr were considered because they are representative species that show typical minor species, pH-dependent behavior. The release of constituents from batch testing as a function of pH is a conservative estimate of the release of constituents from column testing for these selected constituents. There is little effect of the different column flow regimes in the release of constituents. For Al, there is no effect of column flow regime (Figure 4.22). Mg and Sr show a higher release from continuously saturated columns than from intermittent unsaturated columns at very low LS ratios (Figures 4.23 and 4.24). At higher LS ratios, there is no difference between column flow regimes. For most cases, the release of constituents did not change after a LS ratio of 5 mL/g.

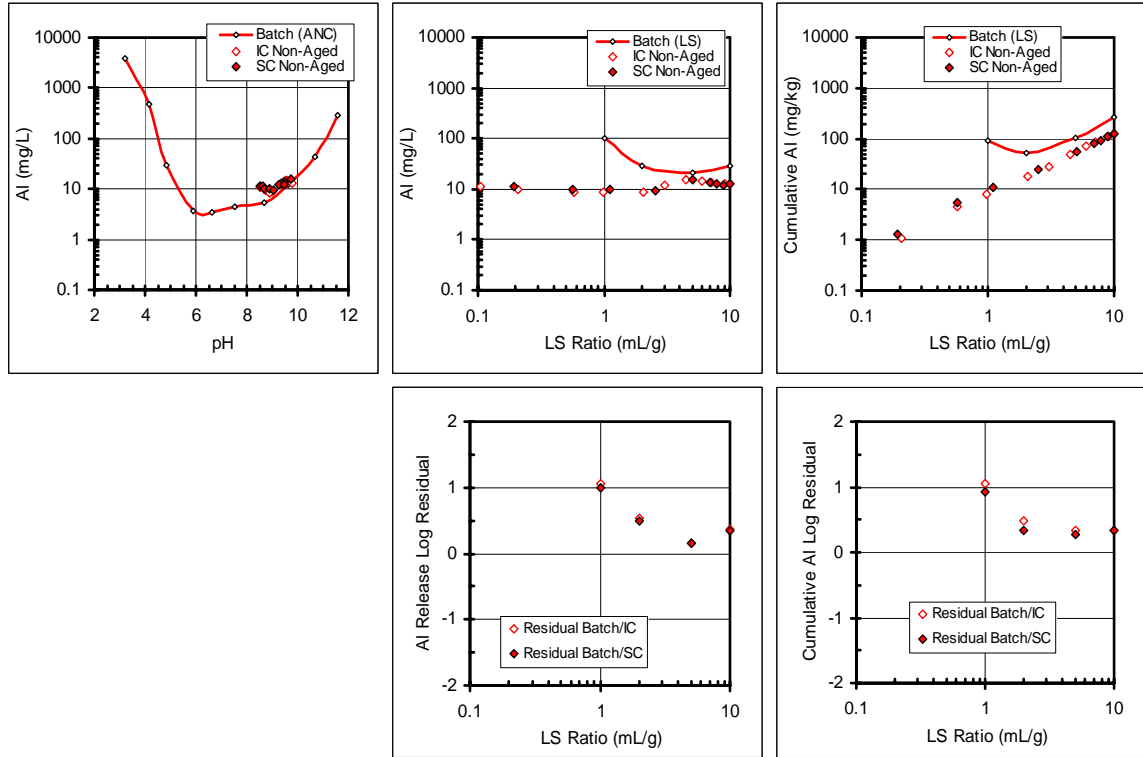


Figure 4.22. Al release from ARR as a function of pH and LS Ratio.

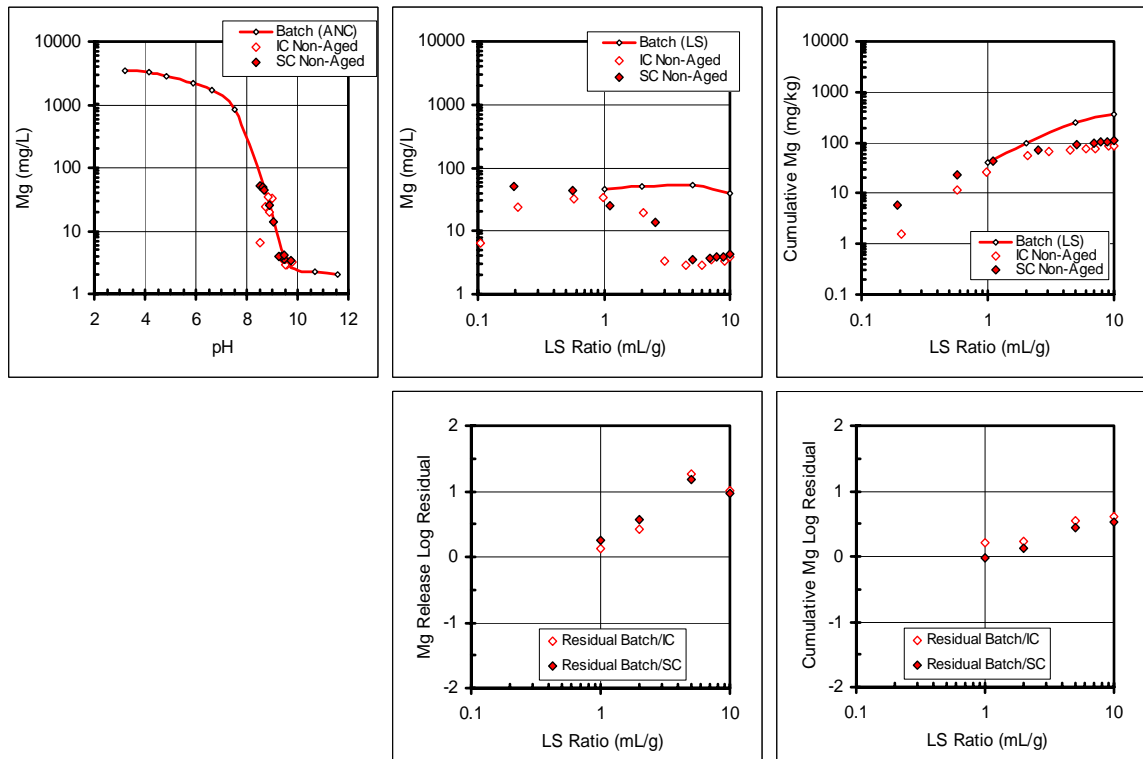


Figure 4.23. Mg release from ARR as a function of pH and LS Ratio

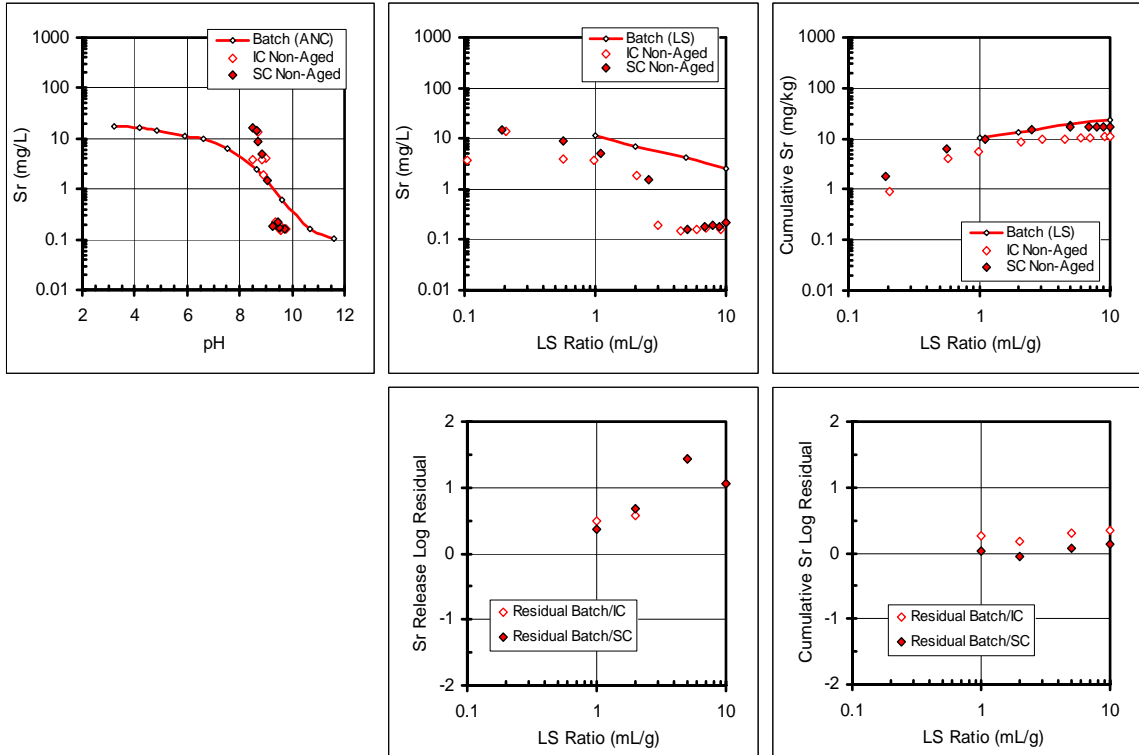


Figure 4.24. Sr release from ARR as a function of pH and LS Ratio.

Geochemical speciation modeling results

The most recent versions of geochemical speciation modeling software LeachXS, 1.0.4.0 and 1.0.4.1, were used to obtain the results presented in this research. This modeling program and its capabilities are discussed in detail in Chapter 2.

The solubility prediction results were based on batch results from protocol SR002 (solubility and release as a function of pH). It was necessary to assume plausible Si concentrations to accurately simulate the material, given that the main constituent of ARR is quartz as confirmed by XRD. Si values were initially assumed to be 1×10^{-8} mol/L Si for all points. Accurate Si concentrations are even more important for long-term prediction in LeachXS.

Using the chemical speciation wizard, and after several solubility prediction iterations, the minerals potentially controlling solubility were selected based on their saturation indices (*SI*). The selected minerals were Al[OH]₃[a], BaSrSO₄[50%Ba], Ba[SCr]O₄[96%SO₄], Ettringite, Anhydrite, Langite, Kaolinite, Muscovite, Birnessite, Pb[OH]₂[C], Strontianite, Zincite, BaCaSO₄[75%Ba], ZnSiO₃, Al₂O₃, Corkite, Brucite, Hercynite, Montmorillonite, Fluorite and ZnO. The nomenclature used in this dissertation for the minerals chosen in LeachXS is strictly the mineralogy as given by LeachXS. For mineral formulas, please refer to the table of minerals in Appendix D. Other changes to the chemistry used by LeachXS included an increase of aluminum availability (5.9×10^{-4} to 9×10^{-4} mg/kg), assumption of a CO₃ value of $1 \times 10^{+3}$ mg/kg (to account for material exposure to the environment) and the addition of 5×10^{-3} mg/kg of hydrous ferric oxide (HFO), and changing the ettringite parameters in ORCHESTRA to 30 orders of magnitude lower to account for ettringite presence.

Results for Al, Ca, Mg and Sr are presented. These constituents were selected to represent both highly soluble and pH-dependent behavior, and to compare directly with experimental results above. A complete set of solubility prediction results, as well as partitioning diagrams showing the minerals that are controlling the solubility of the constituent at specific pH points, is presented in Appendix C.

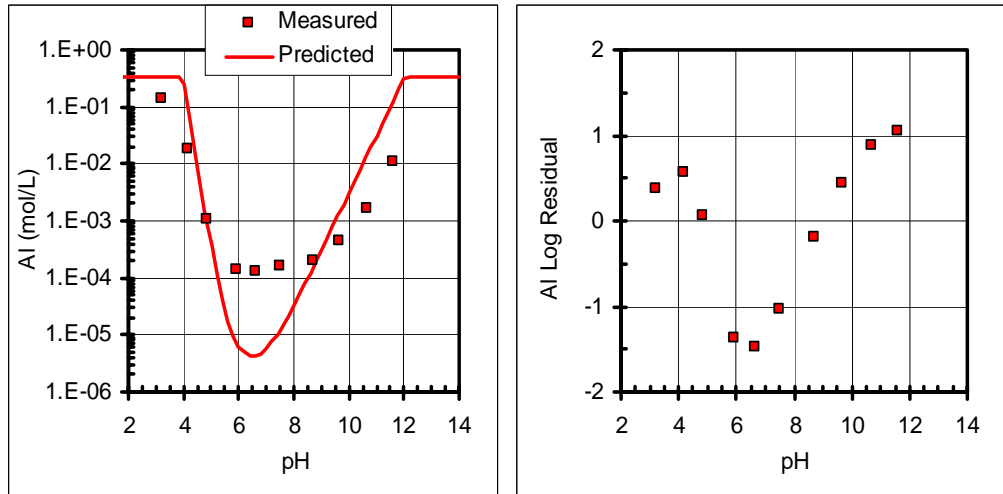


Figure 4.25. AI prediction from ARR as a function of pH.

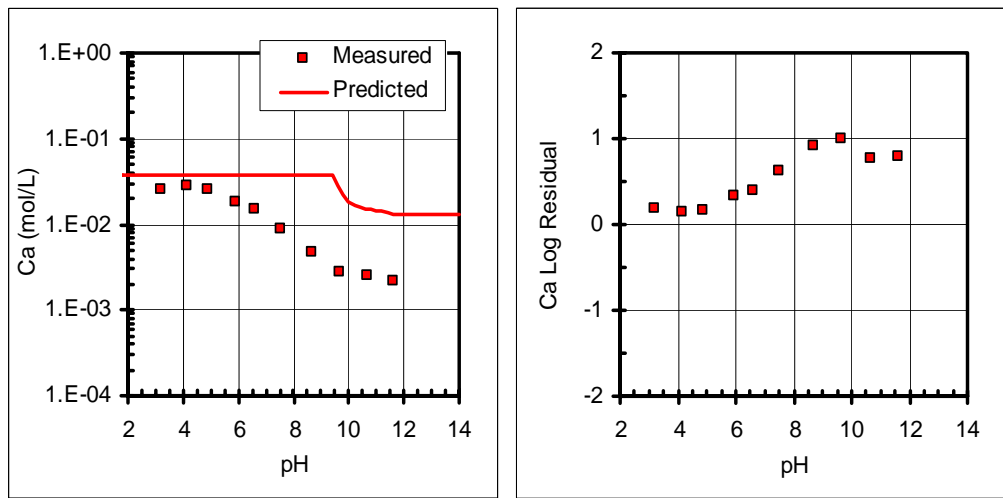


Fig 4.26. Ca prediction from ARR as a function of pH.

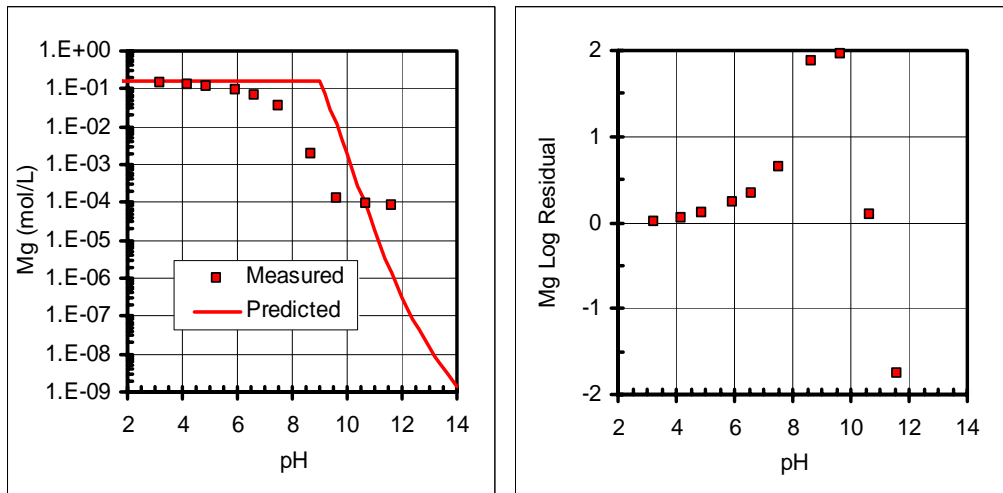


Fig 4.27. Mg prediction from ARR as a function of pH..

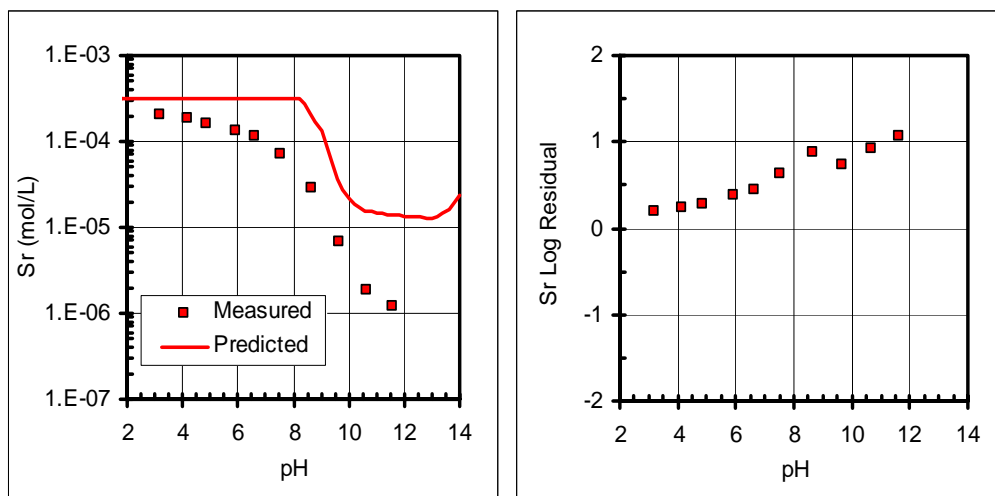


Fig 4.28. Sr prediction from ARR as a function of pH.

Residuals shown in the graphs are discussed in Chapter 2, and are the logarithm of the ratio, in this case, of model prediction to batch experiments. A positive residual value corresponds to model overestimation of constituent solubility.

For Al, the model underestimates the solubility between pH of 5 and 9 (Figure 4.25). The controlling species in this range is $\text{Al}(\text{OH})_3$. Mg solubility is underestimated by the model at pH values above 11 (Figure 4.27). The controlling species in this range is brucite. The model gives conservative estimates for the solubility of Ca and Sr over the entire pH range.

Uncertainties in this modeling are mainly the lack of sufficient data. Si values were assumed for batch samples and account for some of the difference between measured and predicted data. DOC measurements might also improve the modeling results, given that organic matter has a significant impact on complexation of some elements (Meima et al. 1999) and could explain the behavior of Fe leaching prediction (Appendix C). As mentioned previously, these results are preliminary, and the additional measured data (especially Si) will be critical for long-term prediction.

Conclusions

Results indicate that in most cases, there is good agreement between batch and column testing, especially when compared on a cumulative release basis. Also, results indicate that there is no significant difference in the release of constituents when tested under different column flow regimes. Analyzed specifically by constituent, results show that highly soluble species, such as Na, Ca, and Cl, are released slightly faster in intermittent unsaturated columns, as shown by conductivity values. This faster release may be due to the presence of preferential flow paths existing in the columns running down flow with intermittent unsaturated flow. After a LS ratio of 5 mL/kg there is no significant difference between the column flow regimes in terms of pH, conductivity values, or constituent release.

While for most cases batch testing was in agreement with column testing results, there were some cases where release from batch testing was almost an order of magnitude lower than release from column testing. Such was the case for Al at all LS ratios and K at LS ratio of 10 in both types of CFA, and in the case of CFA # 2, for Fe as a function of pH and at LS ratio of 10. For most of the cases, even where there was disagreement between batch and column testing when compared as a function of pH or LS ratio, the agreement is good for cumulative release at higher LS ratios.

As for interpretation protocols, the primary concern is whether or not the cumulative release from batch testing accurately predicts the release of constituents of column testing. Batch testing is an accurate predictor of column results for all ARR species and most of the highly soluble species from CFA. However, even in the cases where cumulative release from batch testing agrees with column testing, it is important to

consider the release as a function of LS ratio for all species, and furthermore, as a function of pH for pH dependent species, and analyze for potential disagreements at specific LS ratios or pH values. An assessment of major environmental parameters in the field, such as infiltration rates, could be used together with these detailed results to analyze potential for leaching of constituents of concern in specific reuse applications.

Preliminary modeling results for ARR indicate a relatively good prediction based on assumed Si data. Modeling failed to successfully predict release at pH values higher than 10 for Mg, and it underestimated release of Al between pH of 5 and 9. These disagreements provided by the simulation have the potential to be improved, with further sample analysis, so the modeling results can provide a strong foundation for long-term prediction of constituent release as the speciation software continues to be developed.

References

- ASTM (1992). Standard Test Method for Laboratory Determination of Water (Moisture) Content of Soil and Rock - D 2216-92. Philadelphia, PA.
- ASTM (1998). Standard Test Method for Carbon Black-Pellet Size Distribution - D1511-98. Philadelphia, PA.
- Caldwell, R., T. W. Constable, P. Cote, J. McLellan, S. E. Sawell and J. Stegemann (1990). Compendium of Waste Leaching Tests, Environmental Protection Series.
- Förstner, U., W. Calmano and W. Kienz (1991). "Assessment of long-term metal mobility in heat-processing wastes." Water, Air and Soil Pollution(57-58): 319-328.
- Garrabrants, A. C. and D. S. Kosson (2005). Leaching processes and evaluation tests for inorganic constituent release from cement-based matrices. Stabilization and solidification of hazardous, radioactive and mixed waste. R. Spence and C. Shi. Boca Raton, CRC Press: 229-280.
- Ghorab, H. Y., M. Rizk, A. Matter and A. A. Salama (2004). "Characterization and Recycling of Aluminum Slag." Polymer-Plastics Technology and Engineering **43**(6): 1663-1673.
- Griffiths, C. T., Krstulovich, J.M. (2002). Utilization of Recycled Materials in Illinois Highway Construction, Federal Highway Administration: 27.
- Hjelmar, O. (1990). "Leachate from land disposal of coal fly ash." Waste Management Research **8**: 429-449.
- Jackson, D. R., B. C. Garrett and T. A. Bishop (1984). "Comparison of batch and column methods for assessing leachability of hazardous waste." Environmental Science & Technology **18**: 668-673.
- Kjeldsen, P. and T. H. Christensen (1990). "Leaching tests to evaluate pollution potential of combustion residues from an iron recycling industry." Waste Management & Research(8): 277-192.
- Kosson, D. S., H. A. van der Sloot, F. Sanchez and A. C. Garrabrants (2002). "An integrated framework for evaluating leaching in waste management and utilization of secondary materials." Environmental Engineering Science **19**(3): 159-204.
- Meima, J. A., A. van Zomeren and R. N. J. Comans (1999). "Complexation of Cu with Dissolved Organic Carbon in Municipal Solid Waste Incinerator Bottom Ash Leachates." Environmental Science & Technology **33**(9): 1424-1429.

Sanchez, F., R. Keeney, D. S. Kosson, R. Delapp and S. Thorneloe (2006). Characterization of Mercury-Enriched Coal Combustion Residues from Electric Utilities Using Enhanced Sorbents for Mercury Control. Research Triangle Park, NC, U.S. Environmental Protection Agency: 232.

Sawhney, B. L. and C. R. Frink (1991). "Heavy metals and their leachability in incinerator ash." Water, Air and Soil Pollution **57-58**: 289-296.

van der Sloot, H. A., R. N. J. Comans and O. Hjelm (1996). "Similarities in the leaching behaviour of trace contaminants from waste, stabilized waste, construction materials and soils." The Science of the Total Environment **178**: 111-126.

van der Sloot, H. A., D. Hoede, D. J. F. Cresswell and J. R. Barton (2001). "Leaching behaviour of synthetic aggregates." Waste Management **21**(3): 221-228.

Wasay, S. A. (1992). "Leaching study of toxic trace elements from fly ash in batch and column experiment." Journal of Environmental Science and Health A **27**(3): 697-712.

CHAPTER V

THE EFFECTS OF CARBONATION IN THE RELEASE OF CONSTITUENTS FROM LABORATORY FORMULATED CONCRETE

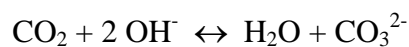
Abstract

Concrete and concrete derived materials have been widely used in construction and highway applications. However, it is known that while in use, concrete will experience intermittent infiltration as a consequence of precipitation events and carbonation, and this will have an effect on its chemistry, decreasing the pH of the material. This study evaluates the effect of carbonation and different types of column flow in the release of constituents from a laboratory formulated concrete, and includes a comparison of release of constituents when tested under both batch and column experiments. This study also presents preliminary geochemical speciation modeling results for the solubility prediction of constituents from laboratory formulated concrete based on batch data. Results from batch and column testing showed that carbonation reduces the pH of the leachates and reduces the release of most constituents, except for As. There is no significant difference between unsaturated, intermittent and continuously saturated column flow regimes. In most cases, there is agreement between batch and column testing release, except for Cl, As and Zn. Solubility predictions were obtained for the non-aged material based on non-aged material data, and for the carbonated material based on non-aged and carbonated data. Predictions based on the existing aging condition were satisfactory, but prediction of the carbonated material based on non-aged data was only satisfactory for Zn.

Introduction

Concrete and concrete derived materials have been extensively used as an aggregate substitute in pavement construction, as well as an aggregate for cement-treated or lean concrete bases, a concrete aggregate, an aggregate for flowable fill, and an asphalt concrete aggregate (Vipulanandan et al. 1998; Griffiths 2002). When using concrete or concrete-like materials in highway and construction applications, it is important to consider the impact that these materials pose to their surrounding environment, especially if the concrete contains constituents of potential concern due to solidification/stabilization treatment of contaminated materials. Constituents of potential concern present in the concrete have the potential to leach, as runoff and water percolating through the granular materials carry these constituents into the ground and eventually into aquifers. Furthermore, the alkaline nature of concrete materials makes them prone to carbonation when used for construction or highway applications, as is the scope presented in this project, and this effect must be considered.

Carbonation is a relevant process for initially alkaline materials ($\text{pH} > 9$) and is one of the most common chemical reactions that an alkaline material will experience while in contact with the environment (Garrabrants 2001; Freyssinet et al. 2002). Atmospheric carbon dioxide diffuses into the matrix, reacts to produce carbonates, and decreases the pH value of the system. Carbonation occurs through reaction of the alkaline materials present in a sample with the atmospheric carbon dioxide, according to the following overall reaction (Snoeyink et al. 1980):



The detailed carbonation reaction has been presented elsewhere (Van Gerven 2005) and is reviewed in Chapter 1. The degree of wetting is very important for the rate of carbonation; partially filled pores lead to a faster carbonation because of the higher diffusion rate of carbon dioxide in air than in water (van der Sloot et al. 1997). Research suggests that sudden changes in relative humidity and temperature induce continuous non-steady state conditions in the interior of concrete, with temperature being the most influential in sheltered samples and rain being the most influential in unsheltered samples (Andrade et al. 1999).

Carbonation has been found to affect the chemical composition and physical properties of cementitious matrices and other secondary materials, affecting the release of constituents of potential concern. (Macias et al. 1997). It becomes very important for materials that have more alkaline pH, such as concrete and construction debris. Carbonation tends to lower the pH of materials by one or two pH units to a pH of 9 - 10, changing mineralogy, and thus, changing the chemistry and the release of certain metals. Also, depending on the carbonation degree, the carbonation of a material can only affect external surfaces, or can change its entire structure. For this reason, it is important to study the effects that carbonation has on the leaching of secondary constituents from waste materials. Carbonation studies have included aging for concrete composites (MacVicar et al. 1999), where it was found that the induced laboratory testing was able to simulate natural aging. A more detailed review of carbonation and its effects in concrete has been discussed elsewhere (Garrabrants 2001).

Leaching evaluation

Leaching tests are a very useful tool to estimate the release of constituents of concern from granular materials, as is the case for concrete and concrete-derived materials used in highway applications. However, given the complexity of the leaching process, there is no single leaching test that can provide a complete understanding of the leaching that would occur under different circumstances. Because of this, there are different types of leaching tests that have been developed to provide a better understanding of the leaching processes under different conditions.

Kosson et al. developed a framework for evaluation of leaching from secondary materials that provides specific leaching test methods and a hierarchical approach to testing and evaluation (Kosson et al. 2002). Batch tests proposed in this framework are designed to measure the intrinsic leaching properties of a material and evaluate the release of constituents in the limiting case when the material is in chemical equilibrium with its surroundings.

Column tests are designed to evaluate the release of constituents at local equilibrium conditions as a function of time. This local equilibrium condition is possible due to the low flow rates through the column (220 mL/day). The goal of column testing is to determine rates of constituent leaching during advective mass transport, assumed to be at local equilibrium, in order to understand the mechanisms of release at low LS ratios (Garrabrants et al. 2005). Column tests account for constituent wash out at lower LS ratios, and the resulting change in solubility controlling phases (van der Sloot et al. 2001). A more extensive literature review on column testing is presented in Chapter 3.

However, column tests are often time consuming, ranging in duration from a couple of weeks to years. Alternatively, batch tests can be carried in shorter periods of time, varying from a couple of hours to days. For this reason, and in order to provide a better tool for decision-making, it is important to understand the difference between leaching of constituents that occurs under batch testing and column testing. Furthermore, it is necessary to establish conditions under which constituent release in batch testing can be extrapolated to obtain release from percolation conditions, and to identify key disagreements between the two testing modes.

Geochemical speciation modeling

Geochemical speciation models become an important tool when only batch data are available for a given material. These models have the ability to predict the possible controlling phases that will determine the behavior of the material in the long-term. LeachXS, a database system created for material characterization, was used to obtain the chemical speciation dictating the solubility of the principal mineral phases, and is being used to evaluate the ability to predict the constituent solubility in the long-term. LeachXS and the modeling background are explained in detail in Chapter 2 and elsewhere (van der Sloot et al. 2003).

Objectives

The objectives of this research are:

- 1) to develop a protocol for laboratory carbonation of granular concrete specimens,

- 2) to evaluate the difference between leaching of constituents from laboratory formulated concrete that occurs under equilibrium testing and leaching that occurs under column testing of “non-aged” concrete and concrete that has been subjected to carbonation,
- 3) to evaluate the predictability of column results, when considered a surrogate for field conditions, based on batch tests, and based on this, to recommend guidelines for batch interpretation of species, and
- 4) to compare the solubility obtained from batch data of “non-aged” and carbonated laboratory formulated concrete to the solubility predicted by geochemical speciation using LeachXS.

Materials and Methods

Materials

Laboratory Formulated Concrete (LFC) is a synthetic matrix composed of cement, sand, and metal oxides. The LFC was made in the laboratory, following a previously tested concrete recipe presented in Table 5.1 (Garrabrants 2001).

Table 5.1. LFC composition.

Component	Weight %
Ordinary Portland Cement	36.0
Sand	49.1
Water	12.7
As ₂ O ₅ (hydrate)	0.45
CdO	0.34
CuO	0.37
PbO	0.29
ZnO	0.37
NaCl	0.29
Water / Cement	0.35
Cement / Waste	0.70

The matrix was created adding metal oxide powders to a mixture of ordinary Portland cement, sand, and water. The oxides added were oxides of the following species: As, Cd, Cu, Pb and Zn. These elements were chosen because of their wide range of solubility behavior at different pH values. Sodium chloride was added as a source of tracer ions (Na, Cl) with high and non-pH-dependent solubility.

The material was poured in plastic rectangular containers and cured, at room temperature (20 ± 3 °C), in the presence of NaOH to scavenge the CO₂ present. After its production, the material was sent to a local laboratory to be crushed using a combination of a jaw crusher and rock hammer. This process took nearly 2 months, due to the amount (200 lbs) and hardness of the material, and it is assumed the aging/carbonation process started in this time, as it was not possible to keep it inside an airtight container with NaOH while at the premises. The material was crushed to a maximum particle size of 1.22 cm, as this was the minimum particle size that could be reduced by the jaw crusher. This material was used in the columns, and further reduced to 2 mm, using a combination of laboratory jaw crusher and mortar and pestle, for batch testing.

A small portion of each material was saved for X-ray fluorescence (XRF) analysis and neutron activation analysis (NAA) for total element analysis, and X-ray diffraction (XRD) and scanning electron microscope (SEM) analysis for possible mineral phases present. Particle size distribution and moisture content were also analyzed. The rest of the material was separated for chemical characterization. Moisture content of the materials was measured “as received” following ASTM D 2216-92 (ASTM 1992). In this test, a sample is dried in an oven temperature of $110^{\circ}\pm 5^{\circ}\text{C}$ to a constant mass. The measured moisture content was 6.3%. Total composition of LFC was measured by XRF analysis using a TN Technologies model Spectrace 9000 (Table 5.2).

XRD suggested the presence of various types of silicates. SEM analysis confirmed Ca and Si as the major components of the sample analyzed and a picture is presented in Figure 5.1.

Table 5.2. Total composition for LFC from XRF analysis.

Element	Concentration (mg/Kg)	Standard deviation
Ag	137	21
As	3030	162
Ba	49	4
Ca	181967	742
Cd	2797	49
Cr	537	103
Cu	2240	164
Fe	6507	479
K	19353	412
Mo	18	5
Pb	1874	91
Sn	32	17
Sr	138	15
Th	40	12
Ti	632	94
Zn	2243	134
Zr	125	10

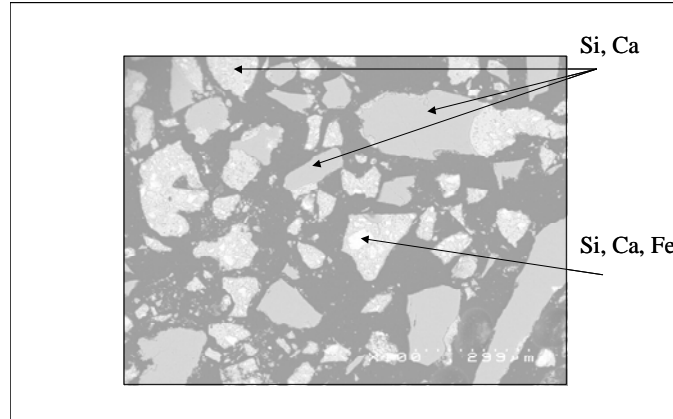


Figure 5.1. SEM image from LFC.

Particle size distribution of the material after crushing was determined using ASTM D 1511-98 (ASTM 1998). In this test, material passing specific mesh sizes was measured (Figure 5.2), with 55% of the material being retained by the 2 mm sieve, and the rest of the material being finer.

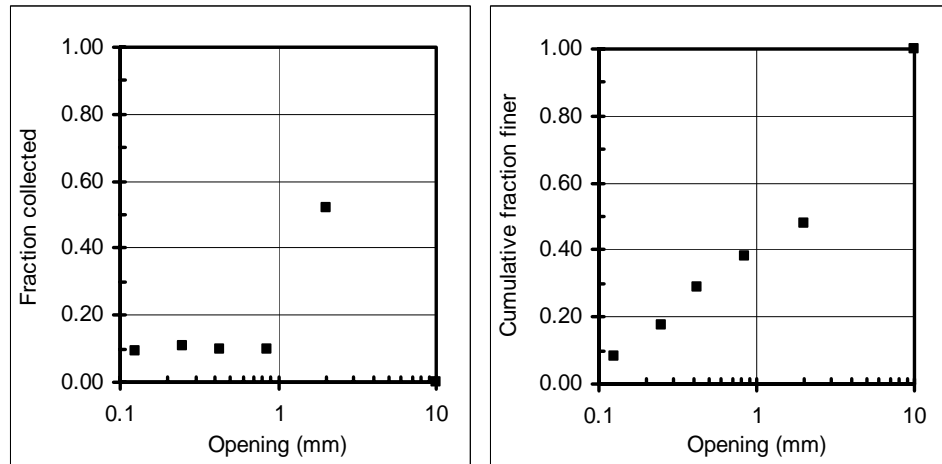


Figure 5.2. Particle size distribution for LFC.

Methods

The total LFC produced and crushed was separated in half. One half was used to start column experiments for that “non-aged” condition immediately. Sample preparation for batch testing took approximately two weeks and most likely minor carbonation of the “non-aged” material occurred at this time. The other half was subjected to the basic carbonation process, which consisted in exposing the material to an atmosphere of a mixture of 20% CO₂-80% N₂. This process was performed in pressurized 2.5 and 5 gal paint tanks (PT 798 Series, Federal Equipment Series, Co.), where conditions of atmosphere could be controlled; the level of CO₂ was maintained at 20% inside the chamber by monitoring the chamber pressure and keeping it constant at 1.36 atm (20 psi). The concrete was carbonated for 3 weeks in a room where the temperature remained constant at 35°C (Figure 5.3). After the carbonation period, column experiments were started, and the remaining material, already carbonated, was crushed to a maximum particle size of 2 mm for batch testing. Carbonation, batch and column testing protocols are explained in the following sections. Geochemical speciation methodology is explained in detail in Chapter 2 and in the modeling results section below.

Carbonation

An experiment was carried out to measure the extent of carbonation and its effects on the particle size of the material. Flow from a 100% CO₂ tank was combined with flow from a 100% air tank passed through a water-saturated sand, in order to obtain a 20% CO₂ humidified gas stream. The expected 20% of CO₂ was achieved by using flow meters to combine the flow of the two streams. There were two containers for

experimentation. The first one only had the humidity (RH) given by the humidified stream of gas. This was accomplished by passing the air stream through a sparger containing sand and glass wool, and filling it with water. The second container contained a beaker filled with water to provide extra humidity (Figure 5.3). The expected conditions were:

- 1) 20% CO₂ – 80% Air, 80% RH
- 2) 20% CO₂ – 80% Air, 40% RH

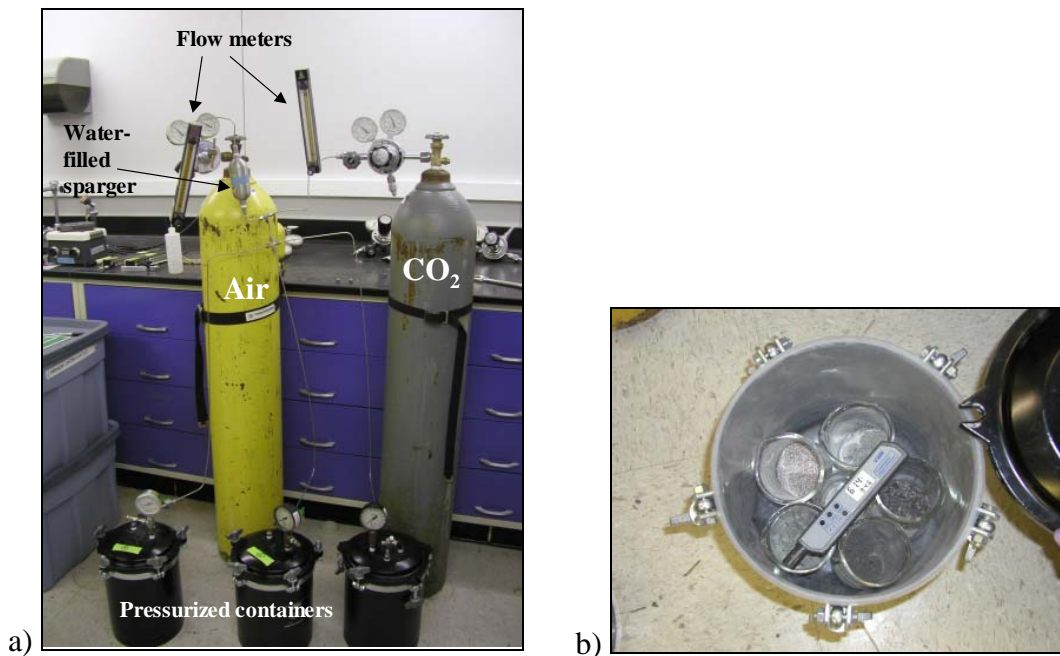


Figure 5.3. Carbonation experiment: a) apparatus, b) pressurized chambers.

In order to investigate the effects of particle size in the carbonation process, two sets of samples were carbonated under each condition:

1. Particle size < 2 mm (batch testing maximum particle size)
2. Particle size < 2 cm (column testing desired particle size)

The carbonation took place in a constant temperature room (35°C) in pressurized containers. Every day while the experiment was in progress, the humidity present in each container was measured with a hygrometer. For the complete humidity measurements refer to Appendix A. The samples were stirred daily (by hand) to maximize the contact of all particle surfaces with the CO₂ atmosphere. The amount of carbonation was measured at different intervals: 3, 7, 14, 21, 28, and 35 days.

For materials with a maximum particle size of 2 mm, a sample of 0.1 g was placed inside a 5 mL vial with a septa lid. A 5 mL syringe was inserted in the lid. Then, 0.1 mL of nitric acid (trace metal grade) was injected into the vial, covering the sample entirely. The volume displaced in the 5 mL syringe was assumed to be the CO₂ produced by the reaction. It was also assumed that there was no friction in the displacement of the syringe. The displacement can be observed in Figure 5.4. For materials with a maximum particle size of 2 cm, the procedure was similar, changing the sample size to 0.3 g, and the volume of acid added to 0.3 mL. The injection took place in a 15 mL vial.

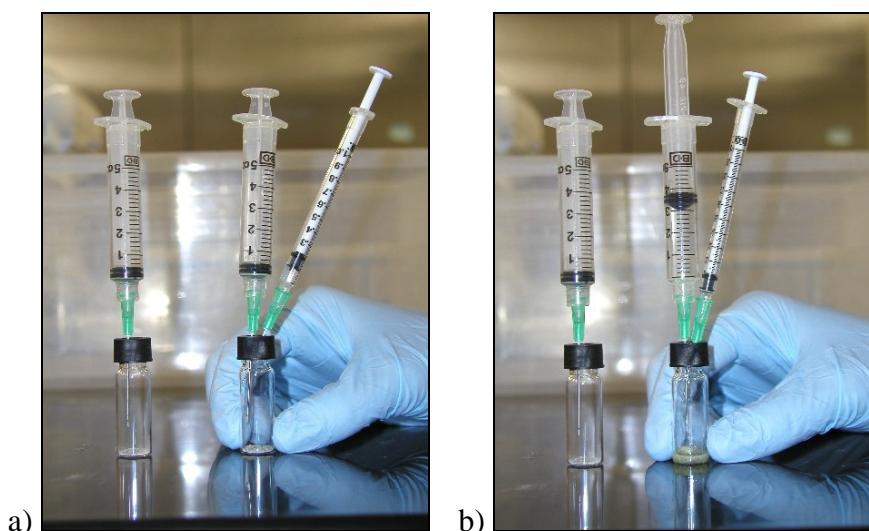


Figure 5.4. Carbonation degree measurement: a) before acid injection, b) displacement after acid injection.

Batch testing

Batch experiments consisted of two tests: solubility and release as a function of pH, SR002.1, and the solubility and release of constituents as a function of LS ratio, SR003.1 (Kosson et al. 2002). Procedures for both protocols were summarized in detail in Chapter 4 and provided in detail elsewhere (Garrabrants et al. 2005).

Column testing

The effect of different types of column flow in the release of constituents from the material was studied by comparing data from continuous saturated flow columns and intermittent unsaturated flow columns. The methodology is explained in detail in Chapter 3. Both types of column flow conditions were carried out until a LS ratio of 10 mL/g was achieved. Samples were taken at equal time intervals between the established LS ratios. Solution pH and conductivity were recorded. Samples were filtered and analyzed as explained previously.

Results and Discussion

Results presented here include carbonation data and the optimal conditions to obtain a carbonated concrete sample. The results also show the different release of constituents of concern from LFC under “non-aged” and “aged” or carbonated conditions. pH and conductivity of the samples are presented as a function of LS ratio for column experiments, and as a function of milliequivalents of acid/base added for batch testing.

The elements presented here are the elements that were shown to be present in higher amounts in the solid samples (e.g., Ca and K). Also shown are elements that are representative of the behavior of highly soluble species (Na and Cl) as a function of LS ratio, as well as elements that are representative of pH-dependent behavior (As, Cd, Cu, Pb and Zn). For each case, a residual is presented for the discrepancy between release of constituents from the material when tested under batch and column conditions as a function of LS ratio. This residual is a tool in the identification of column predictability based on batch tests and its calculation was presented in Chapter 4. A complete set of experimental results, provided in Appendix B, includes other highly soluble species (SO_4) and pH-dependent species (Al, Ba, Fe, Mg, Se and Sr). In this dissertation, the term “good agreement” is used when the difference between batch and column results, or experimental and modeling results, is less than one order of magnitude.

Solubility and speciation results from LeachXS are presented for representative materials. A complete set of modeling results is presented in Appendix C.

Carbonation

It was assumed that all volume displacement after acid injection was due to CO_2 production. Extent of carbonation for LFC (g of CO_2 produced / kg of material) is shown in Figure 5.5. In the sample name “x-LFC-y”, x stands for low (1) or high (2) humidity, and y stands for particle size (2 mm or 2 cm). The average low humidity level was 20% and the high level was 76%. Higher humidity results in a slight increase of carbonation degree in the samples. This is in agreement with previous studies showing that partially filled pores lead to a faster rate of carbonation (Garrabrants 2001).

Replication is fairly good due to the homogeneity of the material for both particle sizes. Smaller particle sizes seem to experience a higher degree of carbonation than large particle sizes, which is expected due to the larger surface area present in smaller particle sizes. Larger particle sizes had a smaller degree of carbonation, and this was later confirmed by the surface carbonation observed in column results. After 15 days, the carbonation degree reached the highest level, so it is possible to assume that a sample that has been carbonated for 15 days or more has reached full carbonation under the conditions provided in this experiment.

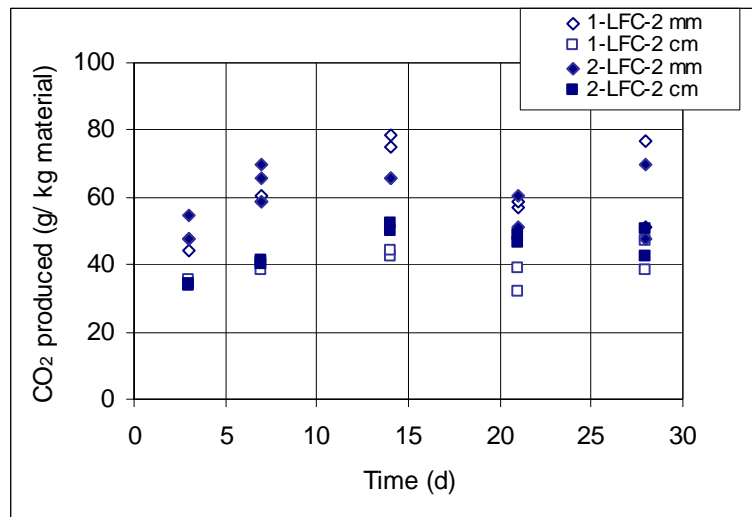


Figure 5.5. Carbonation data for LFC. (1-LFC-2 mm: low humidity; 1-LFC-2 cm: low humidity; 2-LFC-2 mm: high humidity; 2-LFC-2 cm: high humidity).

The recommended conditions for obtaining a carbonated sample are to place the material in a pressurized container with a carbon dioxide enriched atmosphere (20% CO₂-80%N₂) for a minimum time of 15 days and with a relative humidity of at least 60%.

pH and Conductivity

LFC has a high buffering capacity; at least 10 meq acid/g are needed to reach a pH lower than 3 (Figure 5.6). Natural pH is higher for non-aged material than for carbonated material; this difference is more significant at lower LS ratios (Figure 5.7). This may be an effect of carbonation degree through the particles of material, as carbonation occurred mainly in the surface of the larger particles that were later crushed exposing the not-fully-carbonated particle core. Effect of carbonation is observed in the lower conductivity obtained in the carbonated leachates from batch testing (Figure 5.7). This decrease in conductivity can be explained by the loss of alkalinity of the material due to carbonation, and the decrease of ionic strength of the leachates.

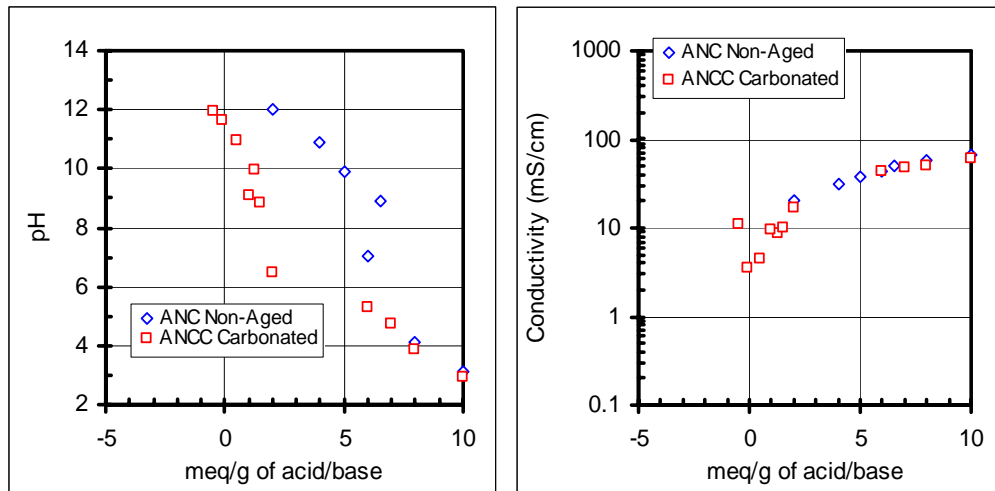


Figure 5.6. pH and conductivity of LFC titration curve.

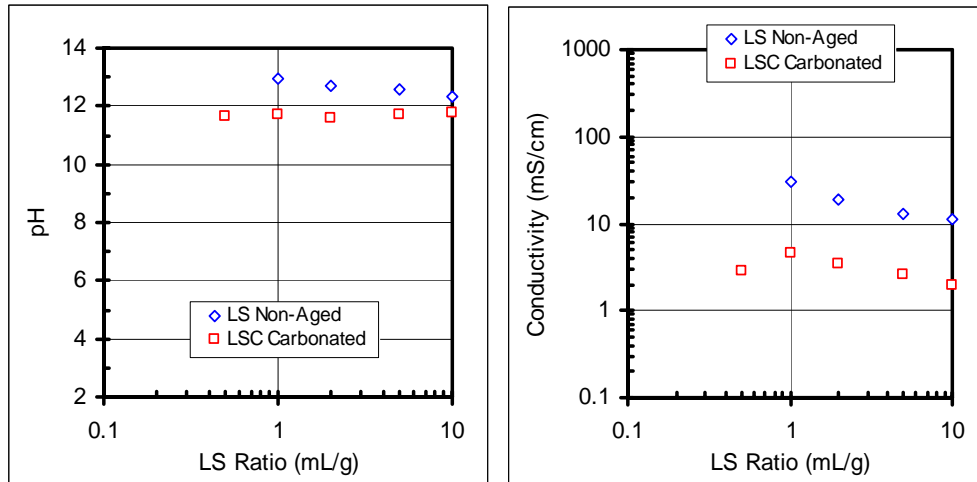


Figure 5.7. pH and Conductivity of LFC batch testing as a function of LS Ratio.

The first carbonation attempt, which resulted in the material used for the 4-4 IC tests, resulted in a very superficial carbonation degree for the particles that only showed carbonation effects at very low LS ratios. This can be observed in the pH and conductivity from the two intermittent carbonated data sets in Figure 5.8. A second carbonation experiment was carried out with the remaining “carbonated” sample and this was used in the carbonated saturated column in the same figure, as well as in the batch characterization of the carbonated sample (Figures 5.6 and 5.7). The drop of pH and conductivity as a result of carbonation can be observed. Overall, the pH difference between the non-aged and the carbonated sample is not as dramatic as expected due to the fact that the non-aged material had been partially carbonated while being crushed by the outside laboratory.

The pH of the samples obtained from the column 4-4 regime is not different than the regular intermittent unsaturated column regime. pH from continuously saturated columns is lower than from intermittent unsaturated column (Figure 5.8). Conductivity of leachates from intermittent unsaturated columns is slightly higher than from

continuously saturated column. No significant difference between the different intermittent regimes is observed (Figure 5.8).

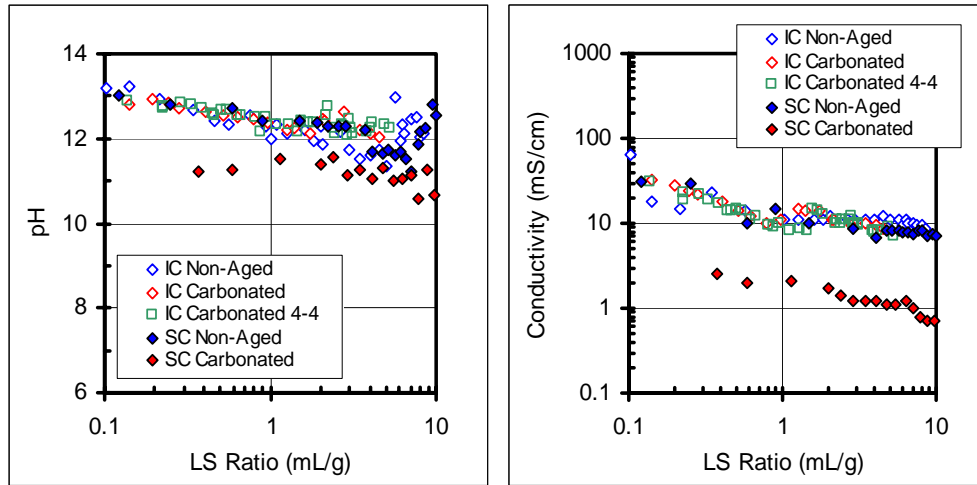


Figure 5.8. pH and Conductivity of LFC column testing as a function of LS Ratio.

Major constituents

Ca, K, Na and Cl were considered representative species of major constituents and species with highly soluble behavior. All elements show a good agreement between column and batch testing based on concentration and cumulative release. Except for Cl, the release of the other non-pH dependent species considered here is lower for the carbonated concrete than from the non-aged concrete. In the case of K (Figure 5.12) the cumulative release from carbonated material under column testing is higher than from batch testing. However, this effect is not as significant when considering release as a function of LS ratio. Most likely, the higher cumulative release for the carbonated case is due to the more constant release of K as a function of LS ratio (as opposed to significant differences between initial and final release). For the rest of the constituents, the release

from column testing is the same (e.g., Na) (Figure 5.11) or lower (e.g., Ca, Cl) (Figures 5.9 and 5.10) than from batch testing.

The column flow regime does not have an effect on the release of constituents, except in the case of Cl, where the release from the 4-4 column flow regime is almost an order a magnitude lower than the regular intermittent unsaturated and continuously saturated columns. However, this could be due to carbonation of the material, as the Cl release from the 4-4 column flow regime is similar to the release from the carbonated material (Figure 5.10). The higher residual values obtained for the carbonated cases are due to the great overestimation of batch testing in the carbonated case. The residual values obtained from the comparison of these highly soluble constituents shows that cumulative release-based comparison is desired.

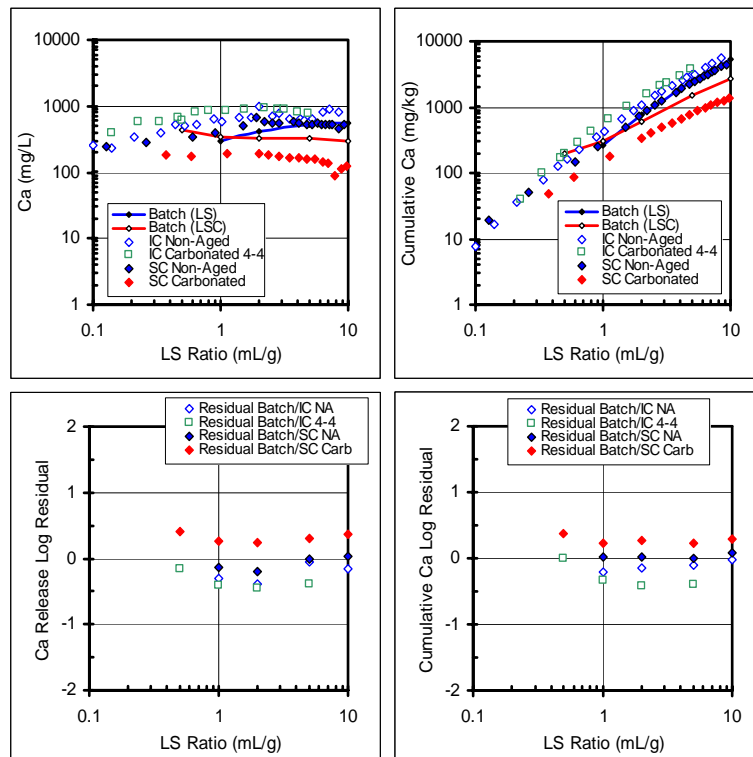


Figure 5.9. Ca release from LFC as a function of LS Ratio.

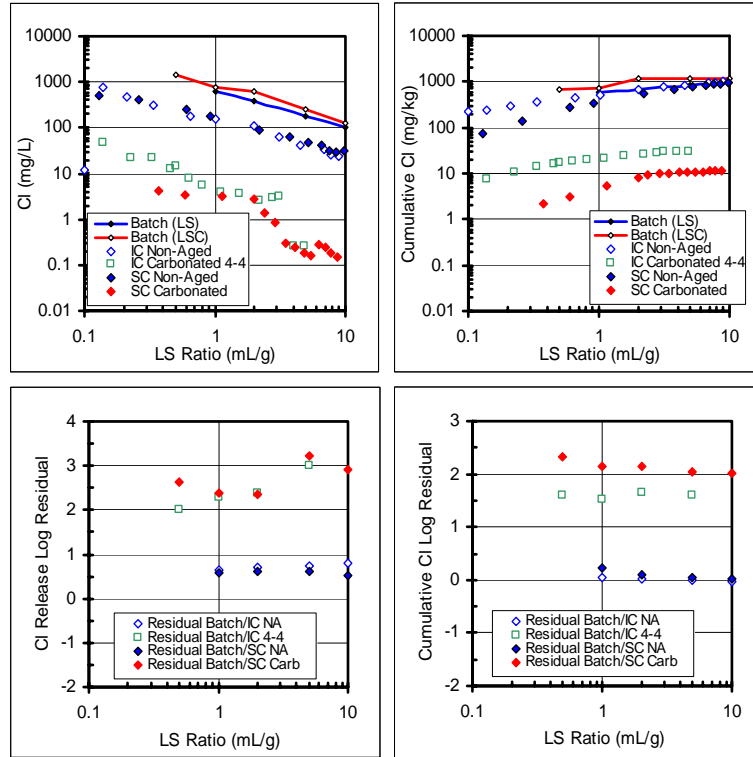


Figure 5.10. Cl release from LFC as a function of LS Ratio.

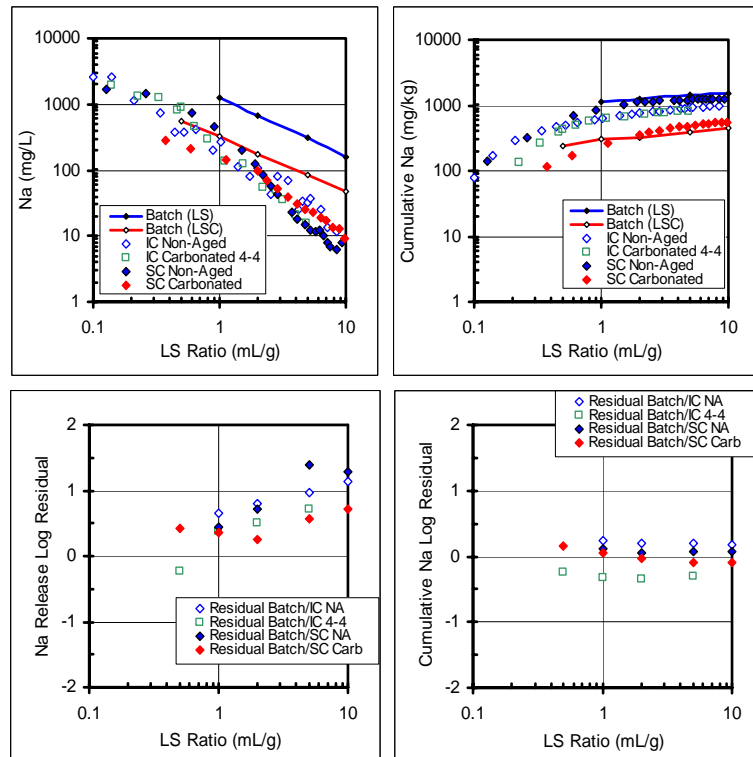


Figure 5.11. Na release from LFC as a function of LS Ratio.

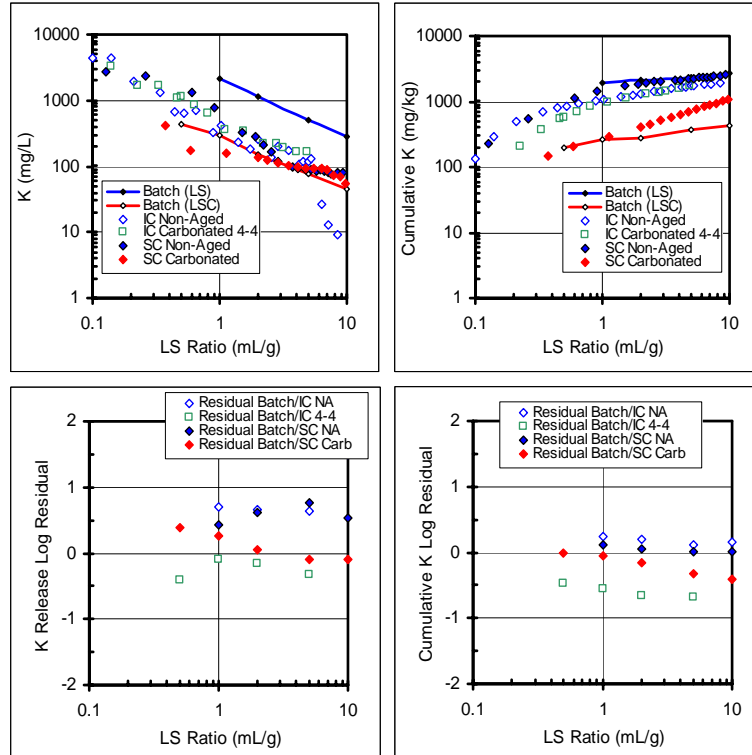


Figure 5.12. K release from LFC as a function of LS Ratio.

Minor constituents

As, Cd, Cu, Pb and Zn were considered the representative species of pH-dependent behavior. Overall, the release of constituents from batch testing as a function of pH is in good agreement with the release of constituents from column testing for most of the elements, except for As release from carbonated material (Figure 5.13). The difference between intermittent unsaturated and continuously saturated column flow is not significant in any of the cases. However, there is a decrease in the release from the 4-4 column flow regime, when compared to the other two flow regimes, as can be observed in all the cases except for Pb (Figure 5.16).

The release from batch experiments from As does not entirely match other analysis of the same concrete recipe (Garrabrants 2001; White 2005). The release from

the non-aged sample is higher and does not have the same behavior, whereas the release from the carbonated matrix is more similar, except for higher release at very low pH values. A possible explanation for this difference between results in this research and those obtained previously might be the pre-carbonation the material was subjected to prior its crushing (i.e., being exposed to the environment for 2 months while crushing was taking place), and the different carbonation methodology used in this research for crushing the larger amounts of concrete. It has been suggested that As can become adsorbed to Ca-bearing hydroxide mineral surfaces and that the increase in solubility upon carbonation is due to the conversion of these materials to calcite (Garrabrants 2001). Re-speciation of Ca into calcite is observed in the carbonated sample modeling in LeachXS, supporting this explanation for the increased As release. Liquid-solid phase partitioning diagrams for Ca obtained from LeachXS modeling are shown in Appendix C.

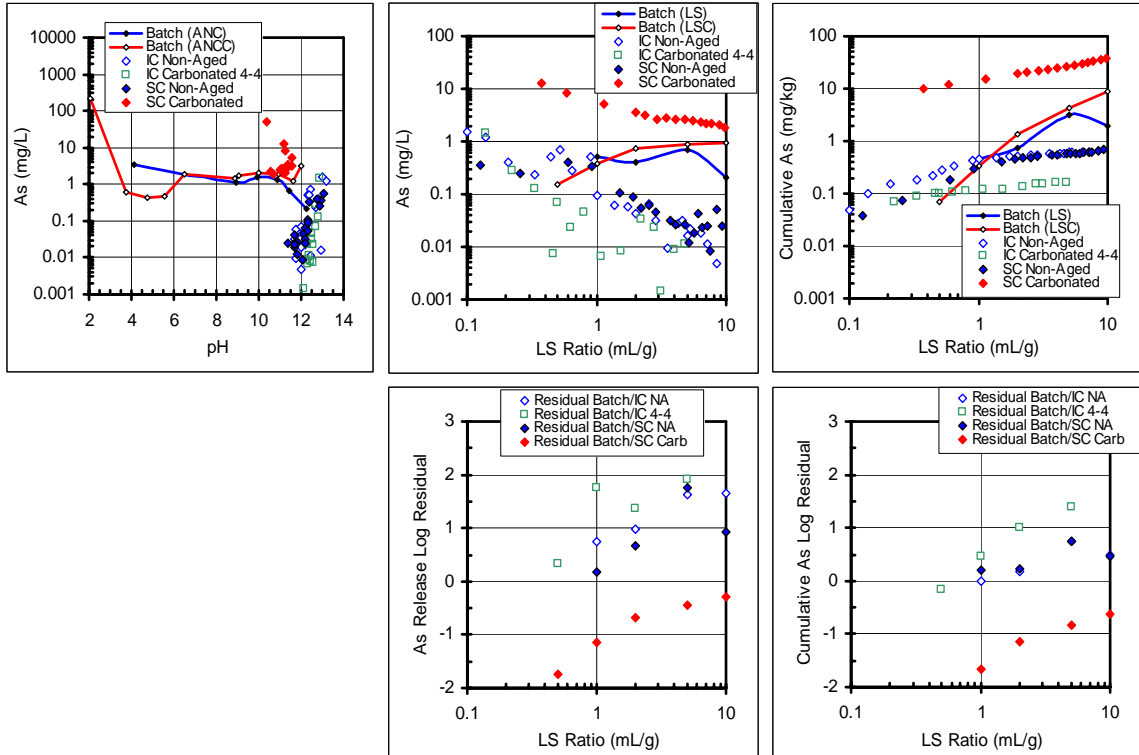


Figure 5.13. As release from LFC as a function of pH and LS Ratio.

Cd release is mostly in agreement with previous testing. The cumulative release from batch testing is in good agreement with release from column testing, and cumulative release from carbonated material is lower than from non-aged material (Figure 5.14).

Cu showed typical behavior except that release is lower at low pH values than previously reported. Carbonation decreased the release of copper from the material by almost an order of magnitude. This is observed in the release from both batch and column testing (Figure 5.15).

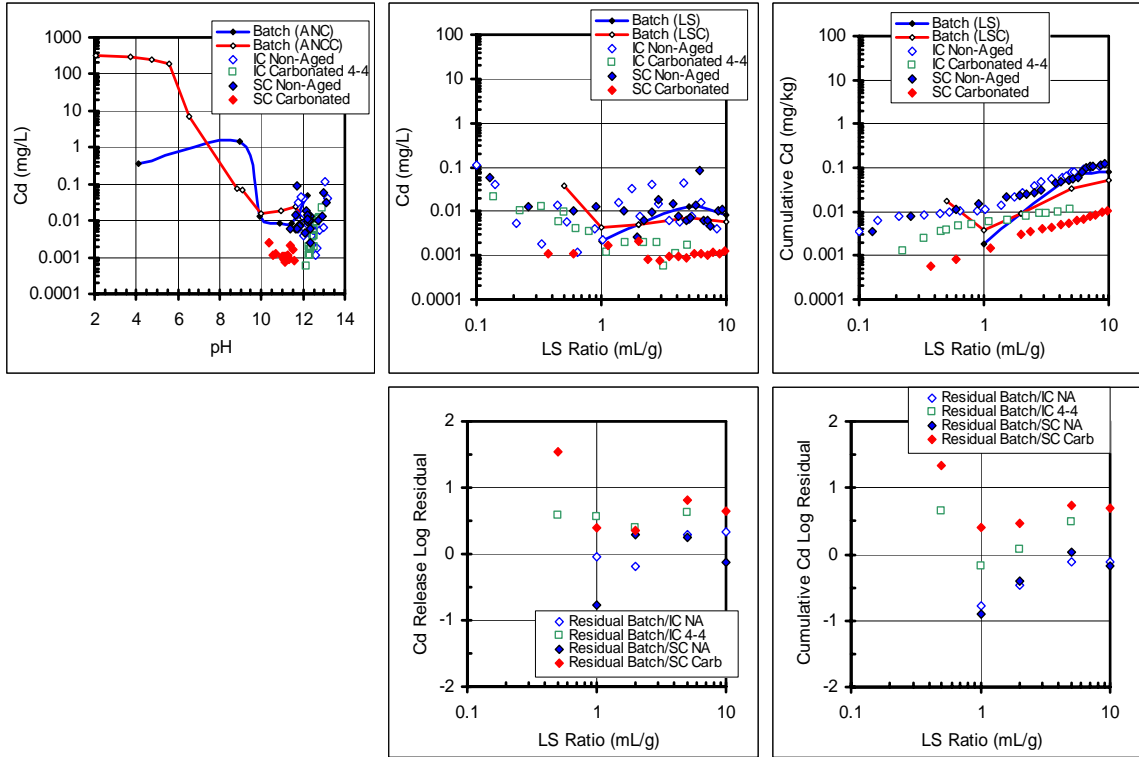


Figure 5.14. Cd release from LFC as a function of pH and LS Ratio.

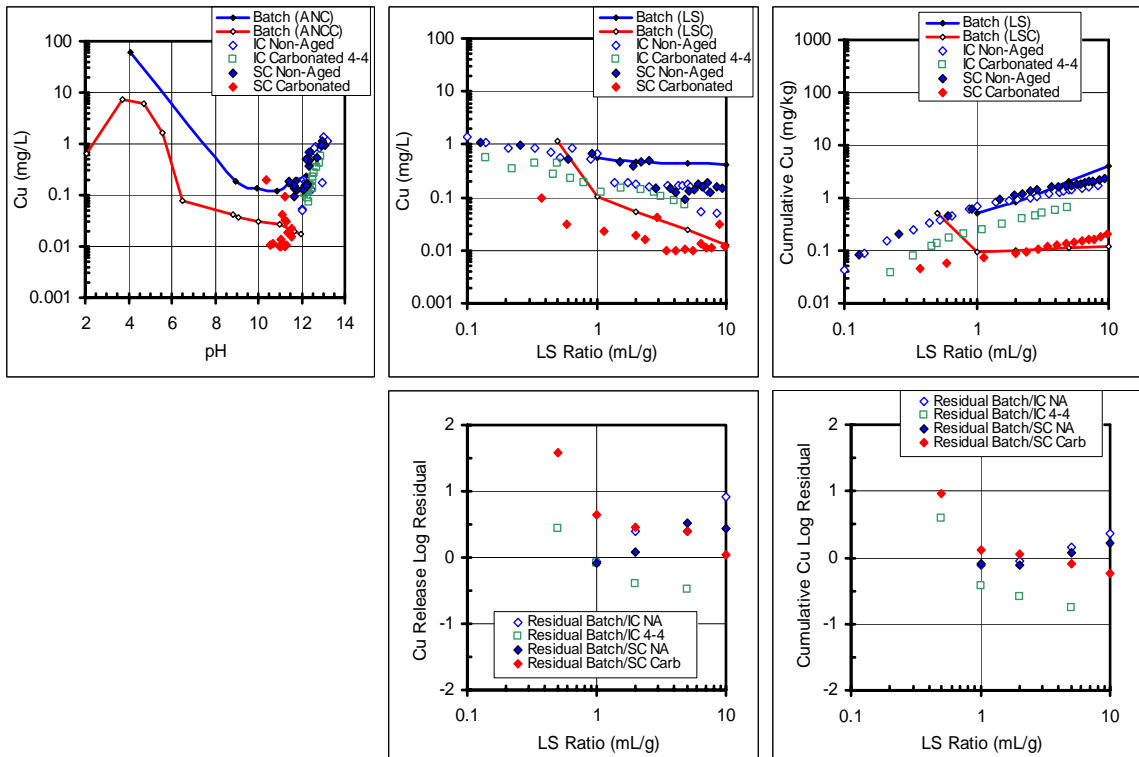


Figure 5.15. Cu release from LFC as a function of pH and LS Ratio.

Pb shows typical behavior of $Pb(OH)_2$ dissolution, and the release is similar to what had been previously reported (Garrabrants 2001; White 2005). The release of Pb is higher from non-carbonated sample at low pH values than from carbonated sample. Release from carbonated material is almost 2 orders of magnitude lower than from non-carbonated material, and there is agreement of batch and column testing results for both aging conditions (Figure 5.16).

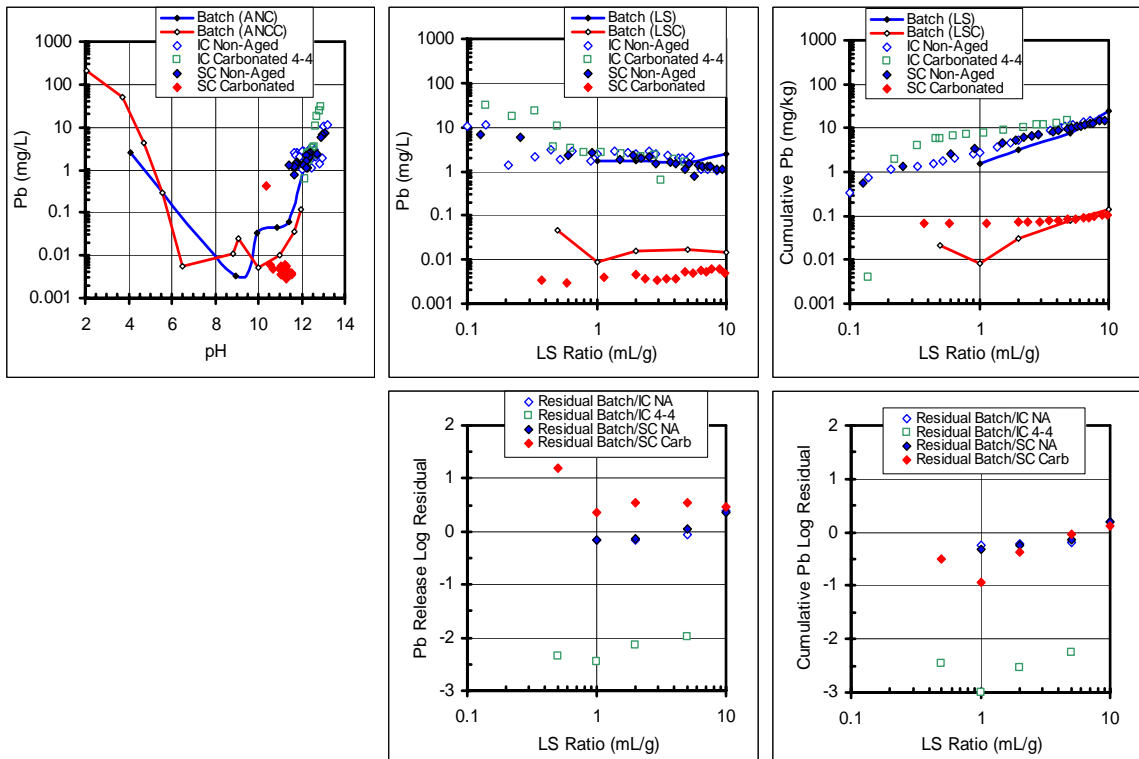


Figure 5.16. Pb release from LFC as a function of pH and LS Ratio.

For Zn, the release from batch testing is in agreement with release of column testing for non-aged and carbonated material (Figure 5.17). Release from carbonated material is over an order of magnitude lower than from non-aged material.

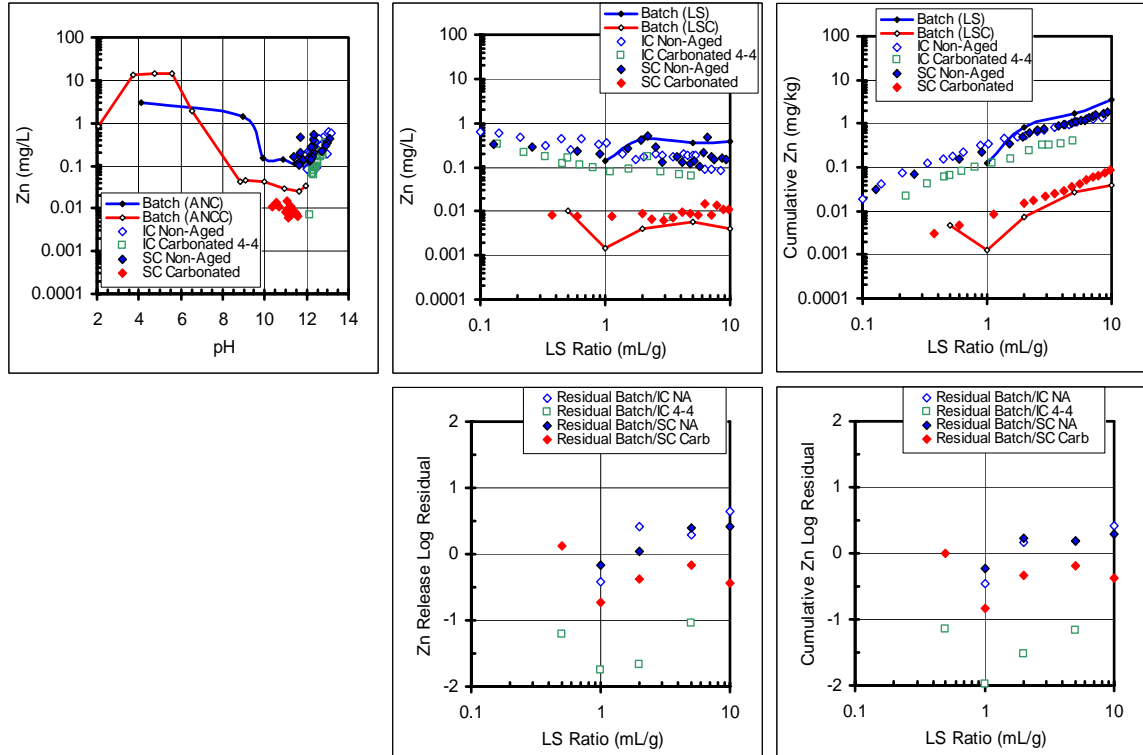


Figure 5.17. Zn release from LFC as a function of pH and LS Ratio.

Geochemical speciation modeling results

The last versions of geochemical speciation modeling software LeachXS, 1.0.4.0 and 1.0.4.1, were used to obtain the results presented in this research. The solubility prediction results were based on batch results of release as a function of pH (SR002). Using the chemical speciation wizard, the minerals potentially controlling solubility were selected based on their saturation indices (*SI*); the species selected had *SI* ranging between -1 and 1 . After several iterations to obtain a better prediction, the minerals selected are shown in Table 5.5. Mineral formulas are shown in Appendix D.

No data were available for Si and CO_3 species in solution, however, values assumed were 1×10^5 mg/kg for CO_3 in the solid sample for both non-aged and carbonated materials, and 1×10^3 mg/kg of Si for non-aged material. Additional

assumed data included Si taken from an average of cement mortars in the LeachXS database (Cement mortar OPC I-F, -B, -can), shown in Table 5.4, and DOC values of 1×10^{-6} kg/L for samples at pH of 10 and above for non-aged material.

Table 5.3. Assumed Si concentration for non-aged LFC.

pH	Si
3.1	8.00×10^3
4.1	4.60×10^3
7.0	2.00×10^3
8.9	1.05×10^3
9.9	1.05×10^3
10.9	7.50×10^2
11.4	3.70×10^2
12.2	1.50×10^2

Table 5.4. Assumed Si concentration for carbonated LFC.

pH	Si
2.1	8.00×10^3
3.9	4.20×10^3
4.7	3.60×10^3
5.3	3.30×10^3
6.5	2.85×10^3
8.9	2.00×10^2
9.1	1.90×10^3
9.9	1.40×10^3
10.9	4.18×10^2
11.9	1.24×10^2

Given that two conditions were evaluated (non-aged and carbonated), two approaches were taken to model the carbonated data. The first approach was to change CO_3 values and other simulation parameters (e.g., HFO, DOC, SHA) in the non-aged simulation to get a prediction similar to the carbonated measured data. The second approach was to do the prediction starting from the carbonated measured data itself.

Table 5.5. Solubility controlling minerals for LFC.

Element	Non-aged LFC	Carbonated LFC
Al	Boehmite, Al(OH) ₃	Al(OH) ₃
Ba	Barite, Ba(SCr)O ₄	Barite, BaSrO ₄
Ca	Portlandite, CSH_ECN, Ca-Olivine, CaMoO ₄ , Ca ₂ V ₂ O ₇ , CaPb ₄ (PO ₄) ₃ OH, CaPb ₃ O(PO ₄) ₂	Portlandite, CSH_ECN, Calcite, Ca-Olivine, Diopside, Anhydrite, α-TCP
Cd	Cd(OH) ₂	Cd(OH) ₂
Cu	Dioptase, Cu(OH) ₂	Dioptase, Cu(OH) ₂
Fe	Fe ₃ (OH) ₈ ,	Fe ₃ (OH) ₈
Mg	Brucite	Brucite, Diopside
Mn	Birnessite, Hausmannite	Birnessite, Manganite
Pb	Pb ₂ SiO ₄ , Pb ₂ O ₃ , Pb(OH) ₂ , Pb ₂ V ₂ O ₇ , PbHPO ₄ , CaPb ₄ (PO ₄) ₃ OH, CaPb ₃ O(PO ₄) ₂ , PbMoO ₄	PbSiO ₃ , Pb ₂ O ₃ , Pb(OH) ₂ , PbMoO ₄ , PbCrO ₄ ,
SO ₄	Celestite, Ba(SCr)O ₄	Anhydrite, BaSrO ₄
Sr	Celestite	Strontianite
Zn	Willemite, Zincite, Zn(OH) ₂	Willemite, Zincite, Zn(OH) ₂

Note: Other minerals included Ni(OH)₂, Bunsenite, Carnotite, Ni₂SiO₄.

Ca, Cd, Cu, Pb and Zn were selected because they were representative of major constituents, highly soluble species and species of pH-dependent behavior, and they are part of the previously selected group of constituents used to study the difference between batch and column testing. In each graph, the measured batch data is presented for non-aged and carbonated material, along with the prediction from the non-aged material to both non-aged and carbonated conditions, and the prediction from the carbonated condition. Discrepancies between predicted and measured data are presented as residuals. These residuals were calculated as previously explained in Chapter 3, and are the logarithm of the ratio of predicted to measured data. A residual of zero means the values are equal, positive values mean the predicted data are higher than the measured data, and negative values mean the predicted data are lower than the measured data.

Changes between non-aged and carbonated material, in terms of prediction assumptions, include controlling the ettringite in solution by decreasing its value in the ORCHESTRA code by 30 orders of magnitude (as the model is under development, there are still some potential problems with ettringite formation, and this value is given to decrease ettringite precipitation in solution and show it as a mineral), and increasing availability values of Al, Ba, Cd, Cu, Fe, and decreasing availability values of SO₄, Zn by $\pm 10\%$ of original values. HFO was decreased from 1×10^{-3} for non-aged material to 5×10^{-4} for carbonated material.

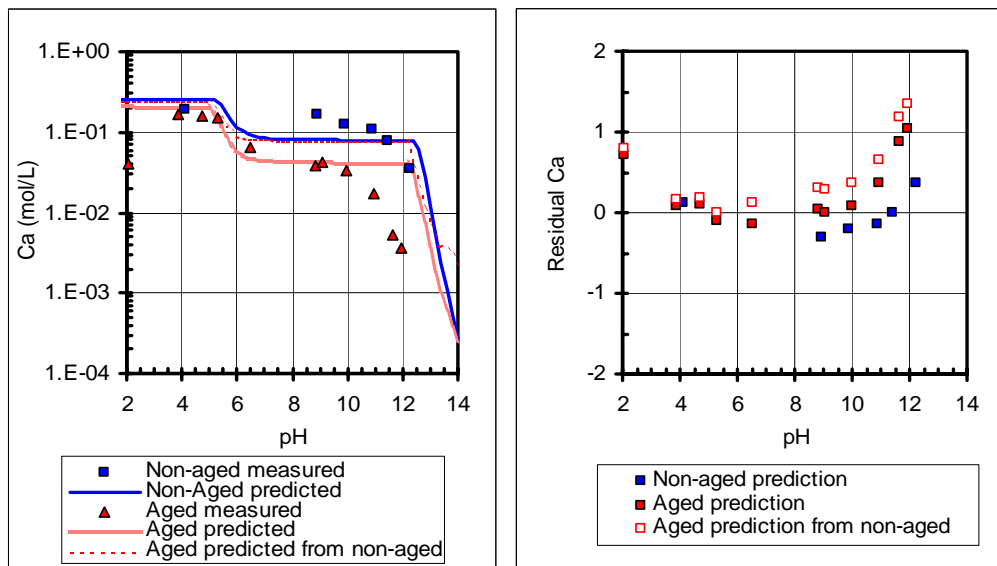


Figure 5.18. Ca prediction from LFC as a function of pH.

For Ca, the prediction from non-aged material is in agreement with the measured data. For the carbonated material, the prediction resulting from both non-aged and carbonated materials is in agreement at pH less than 9. Above that value, the prediction from the non-aged material is higher than the measured carbonated data, and the prediction from the carbonated material is lower than the measured data (Figure 5.18).

Calcite and Portlandite are the dominant species for both conditions, but for the carbonated case, HFO also had an impact on the solubility prediction.

For Cd, the predicted solubility for non-aged and carbonated material is higher than the measured data, but has a similar behavior. The carbonated material solubility predicted from non-aged material is in agreement with the solubility predicted from carbonated material (Figure 5.19). For both aging conditions, Cd(OH)₂ and HFO are the solubility controlling species.

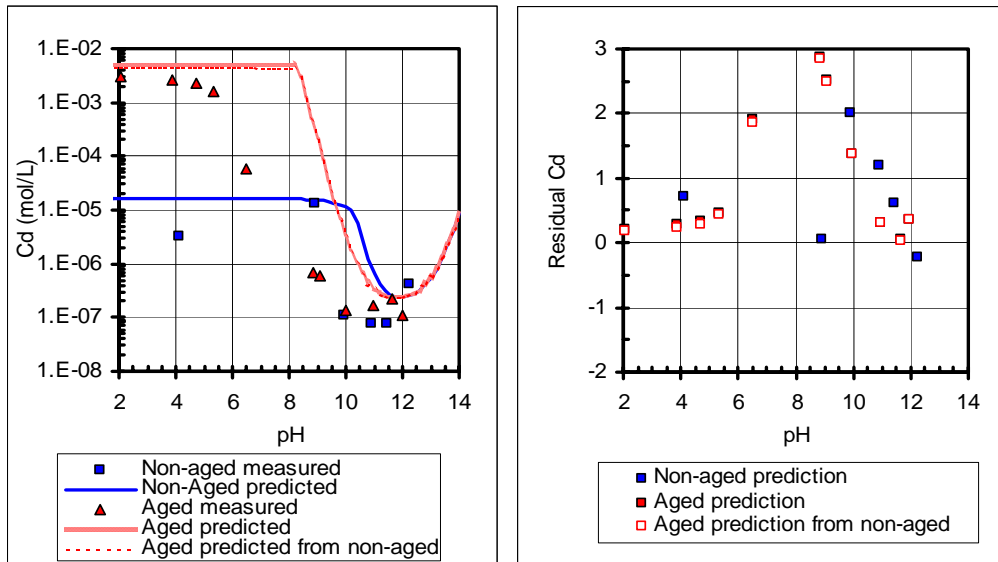


Figure 5.19. Cd prediction from LFC as a function of pH.

In the case of Cu, the predicted solubility for non-aged and carbonated material is higher than the measured data at pH less than 8, and above that, the predicted solubility is lower than measured data. The prediction of solubility in carbonated material from non-aged material is very similar to the non-aged material solubility prediction, and higher than the prediction from carbonated material (Figure 5.20). Solubility controlling species

are $\text{Cu}(\text{OH})_2$ and HFO, and for the non-aged material, while the DOC-bound Cu also contributes to the prediction.

For Pb, the predicted solubility of the non-aged material is in good agreement with the experimentally measured concentration. For the carbonated material, the predicted solubility from non-aged material is lower than the measured data at acidic pH values, and higher at pH values above 5. In the case of the solubility predicted from non-aged material, the prediction is higher than the measured data at acidic pH values, and lower at pH values above 8 (Figure 5.21). The solubility controlling minerals are $\text{Pb}(\text{OH})_2$ and HFO, although in the non-aged material, HFO has a larger impact on the solubility.

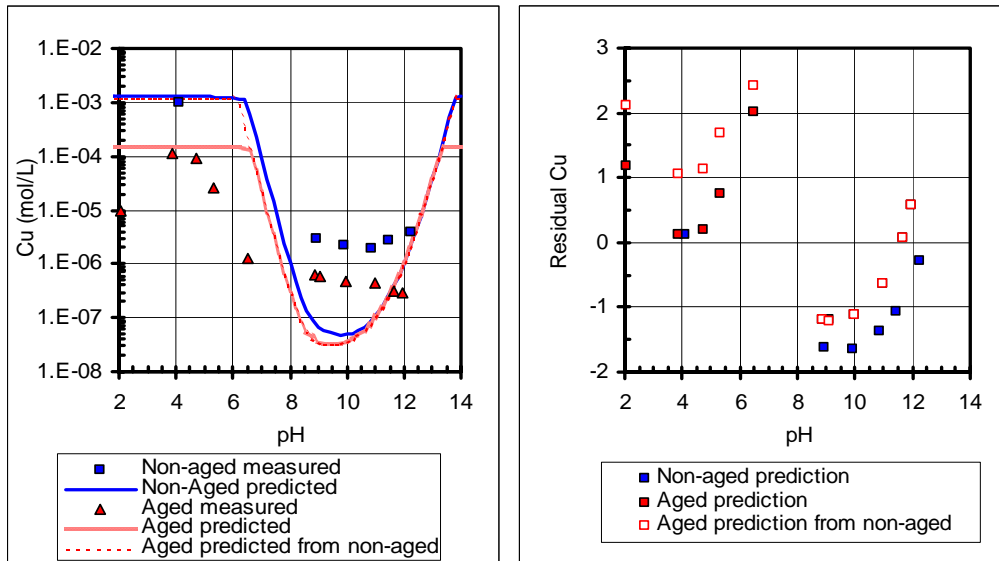


Figure 5.20. Cu prediction from LFC as a function of pH.

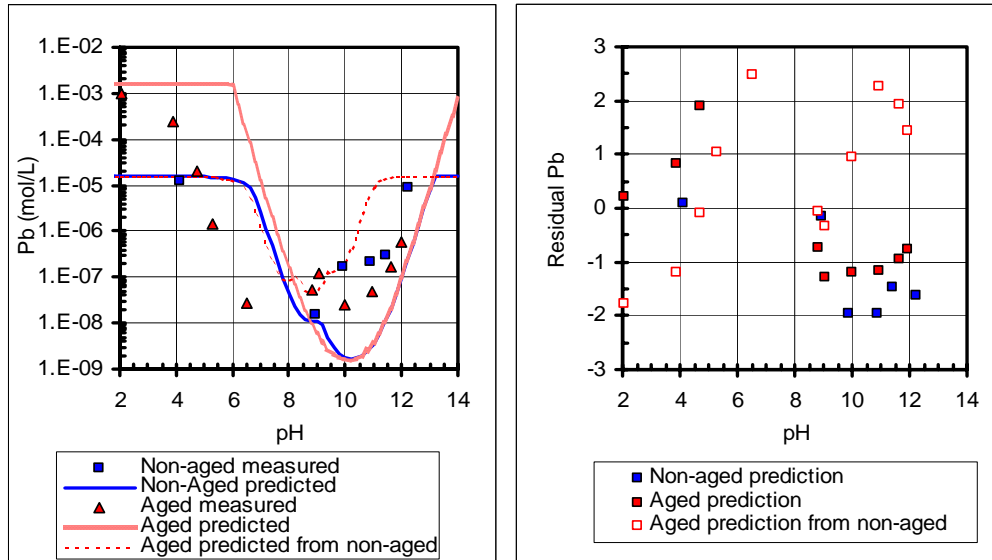


Figure 5.21. Pb prediction from LFC as a function of pH.

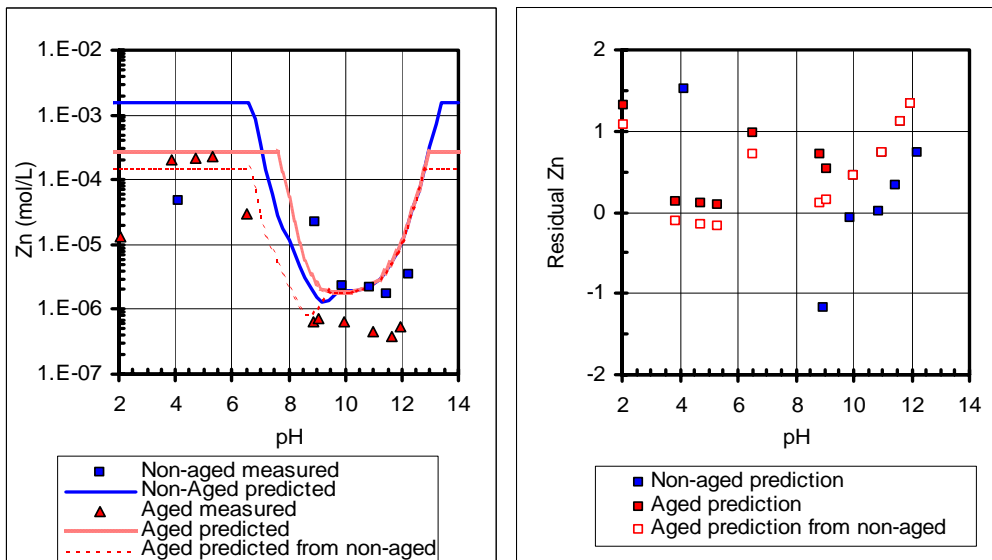


Figure 5.22. Zn prediction from LFC as a function of pH.

For Zn, the solubility prediction for the non-aged material is higher than the measured data for the low and high ends of the pH range. For the carbonated material, the solubility predicted both from the non-aged and the carbonated data is higher than the measured data, and the two predictions are generally in agreement (Figure 5.22). The

mineral phases controlling solubility for Zn are Zincite and HFO for both non-aged and carbonated material, as well as Willemite for non-aged material.

From the presented constituents, only Zn solubility in carbonated material is satisfactorily predicted from non-aged data; for the rest of the constituents, the prediction for the carbonated material based on non-aged material has more similarity to the non-aged material than to the carbonated material. Also, although the prediction and measured solubilities are not exactly the same for non-aged and carbonated materials, the predicted solubility behavior is in agreement with the measured data.

Uncertainties in these prediction results were discussed in Chapter 2, and include mainly the lack of a complete sample analysis (including Si values), as well as the assumptions of Si and CO₃ data for modeling purposes. As mentioned previously, these results are preliminary, and the additional measured data (especially Si) will be critical for long-term prediction.

Conclusions

Results indicate that a carbonated sample can be obtained after being exposed to a 20% CO₂-80% Air stream with a relative humidity of at least 60%. However, at larger particle sizes, it is possible that only surface carbonation will occur, and this can be observed comparing pH values of batch and column testing. The effect of carbonation of the sample was observed by the decrease of pH, from 13 to 11, of the samples resulting from batch and column testing.

When considering release of constituents, results indicate that in most cases, there is good agreement between batch and column testing, and that there is not a significant

difference between testing under different types of column flow (e.g. continuously saturated or intermittent unsaturated). The only disagreement between batch and column data was found for As and K, where release from column testing was higher than from batch testing. Results show that major and highly soluble species, such as Ca, K, Na and Cl are released faster in intermittent unsaturated columns, as shown by conductivity values and actual release from these species. This faster release might be due to the presence of preferential flow paths existing in the columns running down flow with intermittent unsaturated flow. After a LS ratio of 5 mL/g there is no significant difference in the pH and conductivity values, or in constituent release between the different types of column flow regime. The effect of carbonation in the release of highly soluble species can be observed in the lower release of Na and K from batch testing. For column testing, carbonation had a major effect on Cl release, lowering it by almost 2 orders of magnitude and Ca release, lowering it by an order of magnitude.

For the pH-dependent species, the release of Cd, Cu, Pb and Zn from batch testing was lower in the carbonated material than in the non-aged material, as was the case for the release from column testing. However, in the case of As, the release from batch testing was very similar for both aging conditions, and the release from column testing of the carbonated material was almost 2 orders of magnitude higher than from the non-aged material. This higher As solubility in carbonated material has been observed previously and can be explained by calcium minerals re-speciation into calcite and decalcification of the CSH species in the cement.

Preliminary modeling results were obtained for the non-aged material based on the non-aged data, and for the carbonated material based on non-aged and carbonated

data. Solubility prediction results for the non-aged material were reasonable, as were the solubility prediction results for the carbonated material. However, when predicting solubility from carbonated material based on non-aged measured data, only Zn solubility was satisfactory. These disagreements have the potential to be improved with further experimental work and sample characterization. The modeling results provide a strong foundation for long-term prediction of constituent release as the speciation software continues to be developed.

References

- Andrade, C., J. Sarria and C. Alonso (1999). "Relative humidity in the interior of concrete exposed to natural and artificial weathering." Cement and Concrete Research **29**(8): 1249-1259.
- ASTM (1992). Standard Test Method for Laboratory Determination of Water (Moisture) Content of Soil and Rock - D 2216-92. Philadelphia, PA.
- ASTM (1998). Standard Test Method for Carbon Black-Pellet Size Distribution - D1511-98. Philadelphia, PA.
- Freyssinet, P., P. Piantone, M. Azaroual, Y. Itard, B. Clozel-Leloup, D. Guyonnet and J. C. Baubron (2002). "Chemical changes and leachate mass balance of municipal solid waste bottom ash submitted to weathering." Waste Management **22**: 159-172.
- Garrabrants, A. C. (2001). Assessment of inorganic constituent release from a portland cement matrix as a result of intermittent wetting, drying and carbonation. Chemical and Biochemical Engineering. New Brunswick, NJ, Rutgers, the State University of New Jersey.
- Garrabrants, A. C. and D. S. Kosson (2005). Leaching processes and evaluation tests for inorganic constituent release from cement-based matrices. Stabilization and solidification of hazardous, radioactive and mixed waste. R. Spence and C. Shi. Boca Raton, CRC Press: 229-280.
- Griffiths, C. T., Krstulovich, J.M. (2002). Utilization of Recycled Materials in Illinois Highway Construction, Federal Highway Administration: 27.
- Kosson, D. S., H. A. van der Sloot, F. Sanchez and A. C. Garrabrants (2002). "An integrated framework for evaluating leaching in waste management and utilization of secondary materials." Environmental Engineering Science **19**(3): 159-204.
- Macias, A., A. Kindness and F. P. Glasser (1997). "Impact of carbon dioxide on the immobilization potential of cemented wastes: chromium." Cement and Concrete Research **27**(2): 215-225.
- MacVicar, R., L. M. Matuana and J. J. Balatinez (1999). "Aging mechanisms in cellulose fiber reinforced cement composites." Cement and Concrete Composites **21**(3): 189-196.
- Snoeyink, V. L. and D. Jenkins (1980). Water Chemistry. New York, John Wiley & Sons, Inc.
- van der Sloot, H. A., L. Heasman and P. Quevauviller, Eds. (1997). Harmonization of leaching/extraction tests. Studies in Environmental Science. Amsterdam, Elsevier.

van der Sloot, H. A., D. Hoede, D. J. F. Cresswell and J. R. Barton (2001). "Leaching behaviour of synthetic aggregates." Waste Management **21**(3): 221-228.

van der Sloot, H. A., A. van Zomeren, P. Seignette, J. J. Dijkstra, R. N. J. Comans, H. Meeussen, D. S. Kosson and O. Hjelmar (2003). Evaluation of Environmental Aspects of Alternative Materials Using an Integrated Approach Assisted by a Database/Expert System. Advances in Waste Management and Recycling.

Van Gerven, T. (2005). Leaching of heavy metals from carbonated waste-containing construction material. Chemical Engineering. Heverlee (Leuven), Katholieke Universiteit Leuven: 25.

Vipulanandan, C. and M. Basheer (1998). Recycled materials for embankment construction. Recycled Materials in Geotechnical Applications: Proceedings of sessions sponsored by the Soil Properties Committee of the Geo-Institute of the ASCE in conjunction with the ASCE National Convention, co-sponsored by the CIGMAT, Boston, Massachusetts.

White, K. L. (2005). Leaching from granular waste materials used in highway infrastructures during infiltration coupled with freezing and thawing. Civil and Environmental Engineering Department. Nashville, TN, Vanderbilt University.

CHAPTER VI

THE EFFECTS OF DIFFERENT WEATHERING CONDITIONS IN THE RELEASE OF CONSTITUENTS FROM MSWI BOTTOM ASH

Abstract

Bottom ash has been widely used in highway applications. However, it is known that bottom ash undergoes different aging stages, and while in use, these changing aging or carbonating conditions will have an effect on its chemistry, decreasing the pH of the material. Also, during use, bottom ash will experience intermittent infiltration as a consequence of precipitation events. This study evaluates the effect of carbonation and different types of column flow in the release of constituents from a MSWI bottom ash, and includes a comparison of release of constituents when tested under batch and column experiments. This study also presents preliminary geochemical speciation modeling results for the solubility prediction of constituents from bottom ash based on batch data. Results showed that carbonation reduces the pH of the leachates and reduces the release of constituents, except for Ba. There is no significant difference between different types of column flow, and in most cases, there is agreement between batch and column testing release, except for Ba. Solubility predictions were obtained for the non-aged material based on non-aged material data, and for the carbonated material based on both non-aged and carbonated material. Predictions based on the existing aging condition (i.e., non-aged solubility prediction based on non-aged data) were satisfactory, and prediction of the carbonated material based on non-aged data was satisfactory for Ca, Pb and Zn.

Introduction

Bottom ash is derived from municipal solid waste incineration (MSWI). It has a porous, grayish appearance and is mainly composed of grate ash and small amounts of other inert and non-combustible components such as glass, ceramics, and metals (IAWG et al. 1997). Most of the ash produced in the United States is used as a landfill cover material, but there have been extensive studies that have focused on the potential for using bottom ash as an aggregate in concrete, and highway applications both in the United States and Europe. However, there is some concern about the potential impacts that using bottom ash in these applications could pose to the surrounding environment as well as for the usage application itself.

Bottom ash is mainly composed of silica (SiO_2), alumina (Al_2O_3), iron oxide (Fe_2O_3), and calcium oxide (CaO), with smaller quantities of other oxides (Mg, K, Na and S) (Vipulanandan et al. 1998), and has been normally classified as a “non-hazardous” material. However, it has a high salt content and trace metal concentrations, including elements such as Pb, Cd, and Zn, and because the concentrations of these elements are higher in bottom ash than in the typical aggregate materials there is concern for the leaching of these constituents when used in highway applications (Freyssinet et al. 2002).

Also, because of the high sulfate and chloride content, bottom ash has shown corrosive properties when used in contact with metal structures, and a susceptibility to degradation when used in compaction and loading environments. For this reason, bottom ash has not been widely used as aggregate for highway construction, although it has been used for shoulder construction, where the durability and gradation requirements are not as critical. However, MSWI bottom ash that has been processed to remove ferrous and

nonferrous metals, washed to remove salts, and sorted to achieve the appropriate particle size gradation that can be blended with other aggregates for use in an asphalt paving mix with acceptable results (Griffiths 2002). Bottom ash has also been used for ice and snow control, but this has resulted in the plugging of the drainage structures (Griffiths 2002). Also, the high salt content of bottom ash has the potential of interfering with the curing of concrete, and it could affect its strength.

Bottom ash has a high potential for aging, and its characteristics tend to change with time as it is exposed to the atmosphere. There are three major stages of weathering that have been identified in bottom ash: unweathered bottom ash with pH > 12, quenched, non-carbonated bottom ash with pH 10-10.5, and carbonated bottom ash with pH 8-8.5 (Meima et al. 1999). Ca minerals and CO₂ mainly control the pH of bottom ash, as the alkaline material initially takes the CO₂ present in the atmosphere. These effects become more predominant for the unweathered and quenched, non-carbonated bottom ash. The change of pH in these major types of ash plays an important role, as the solubility and complexation of some trace metals is highly dependent on the pH of the solution, and in some cases, a decrease in pH has a positive effect from an environmental point of view. Leaching of Cd, Pb, Cu, and Zn is lower in weathered ash than in other types of ash. This is due to the neutralization of the pH and the formation of less soluble species of these elements as weathering continues (Meima et al. 1999; Freyssinet et al. 2002). Carbonation also leads to solidification or hardening of bottom ash (Freyssinet et al. 2002).

Carbonation, however, is not the only effect that weathering has in bottom ash. As weathering continues, new phases form and lead to secondary mineral species that

have also been studied (Piantone et al. 2004). Extensive information on bottom ash and its properties, as well as weathering effects, can be found elsewhere (IAWG et al. 1997).

As discussed in Chapters 4 and 5, the leaching process is complex, but several effective leaching tests can be used to investigate the release of constituents under different conditions. As proposed in the leaching evaluation framework proposed by Kosson et al. (Kosson et al. 2002), batch tests are designed to measure the intrinsic leaching properties of a material and evaluate its constituent release. Column tests are more appropriate to investigate local equilibrium in field conditions, release at low LS ratios (Garrabrants et al. 2005) and constituent washout, including its effects in the change of solubility controlling phases (van der Sloot et al. 2001).

Column tests often are more time consuming than batch experiments, and so batch experiments are preferred as a decision-making tool. For this reason, it is important to understand the difference between leaching of constituents that occurs under batch testing and column testing. Furthermore, it is necessary to establish conditions under which constituent release in batch testing can be extrapolated to obtain percolation release, and to identify key disagreements between the two testing modes.

Geochemical speciation modeling is also an important tool to predict the possible controlling phases that will affect the behavior of the material in the long term, based only on batch data for a given material. LeachXS, a database system created for material characterization, was used to obtain the chemical speciation dictating the solubility of the principal mineral phases, and is being used to evaluate the ability to predict the constituent solubility in the long-term. LeachXS and the modeling background are explained in detail in Chapter 2 and elsewhere (van der Sloot et al. 2003).

The objectives of this research are:

- 1) to age bottom ash under different conditions,
- 2) to evaluate the difference between leaching of constituents from bottom ash that occurs under equilibrium testing and leaching that occurs under dynamic testing of “non-aged” bottom ash and bottom ash that has been subjected to different aging processes, and
- 3) to evaluate the predictability of column results, when considered as a field simulation, based on batch tests and based on this, to recommend guidelines for batch interpretation of species, and
- 4) to predict the release of constituents from “non-aged” and aged bottom ash using LeachXS.

Materials and Methods

Materials

The bottom ash used in this project is the by-product of in the combustion of municipal solid waste. The bottom ash utilized in this project was freshly quenched as obtained from the Nashville Thermal Plant in 2001. Three samples, collected at approximately 2-3 hour intervals during the course of each day, were collected each day over a period of 5 days. A total of 15 samples were collected. These samples were field-screened to a particle size smaller than 2”, and were collected in plastic 5-gallon buckets. Upon arrival to the laboratory, the material in all buckets was heterogenized by screening it over 4 different containers (Figure 6.1).



Figure 6.1. Mixing of bottom ash.

A small portion of each material was saved for X-ray fluorescence (XRF) analysis and neutron activation analysis (NAA) for total element analysis, and X-ray diffraction (XRD) and scanning electron microscope (SEM) analysis for possible mineral phases present. Particle size distribution and moisture content were also analyzed. The rest of the material was separated for chemical characterization. Moisture content of the materials was measured “as received” following ASTM D 2216-92 (ASTM 1992). In this test, a sample is dried in an oven temperature of $110^{\circ}\pm 5^{\circ}\text{C}$ to a constant mass. The measured moisture content was 25.57%. Total composition of BA was measured by XRF (Table 6.1), and also by NAA (Table 6.2).

Table 6.1. Total composition for BA from XRF analysis.

Element	Concentration (mg/kg)	Standard deviation
Ba	623	26
Ca	133917	870
Cu	1630	146
Pb	1918	99

Table 6.2. Total composition for BA from NAA analysis.

Element	Concentration (mg/kg)
Ag	7.6
As	47
Au	0.11
Br	28
Cd	3500
Ce	4.8
Co	11
Cr	110
Cs	0.58
Eu	0.16
Fe	88000
Hf	2.1
Hg	2.6
Hg	0.83
Hg	1.5
Ho	17
In	24
Ir	0.01
K	60000
La	11
Lu	0.29
Mo	170
Na	31000
Nd	12
Ni	3700
Pr	120
Rb	34
Re	500
Ru	200
Ru	17
Sb	290
Sc	1.8
Se	160
Sm	2.4
Sn	500
Sr	240
Ta	0.61
Tb	1
Te	0.72
Th	2.1
Tm	5.0
U	5.7
W	48
Yb	1.1
Zn	2500
Zr	170

SEM and XRD analyses were also performed on BA. XRD suggested SiO_2 and CaCO_3 as the main species. The presence of calcite in the material suggests that weathering (carbonation) had already started as bottom ash was mixed and heterogenized before testing. SEM suggested Si, Ca and Fe as the main elements in ash particles (Figure 6.2).

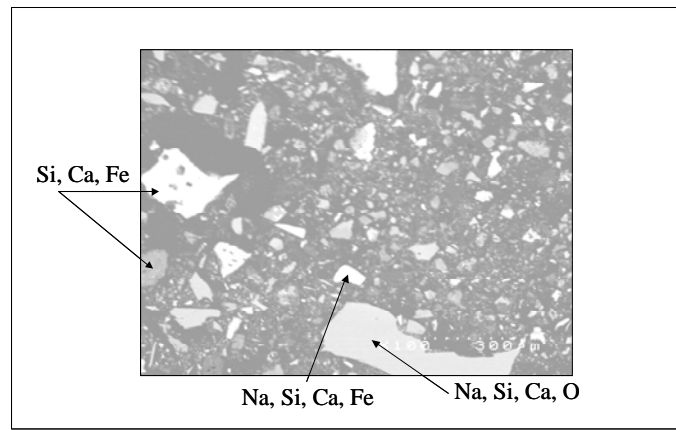


Figure 6.2. SEM image from BA.

Particle size distribution of the material was determined using ASTM D 1511-98 (ASTM 1998). In this test, material passing specific mesh sizes was measured. Results are shown in Figure 6.3. Around 48% of the material was collected by the 2 mm sieve, and 55% of the material was finer than 2 mm.

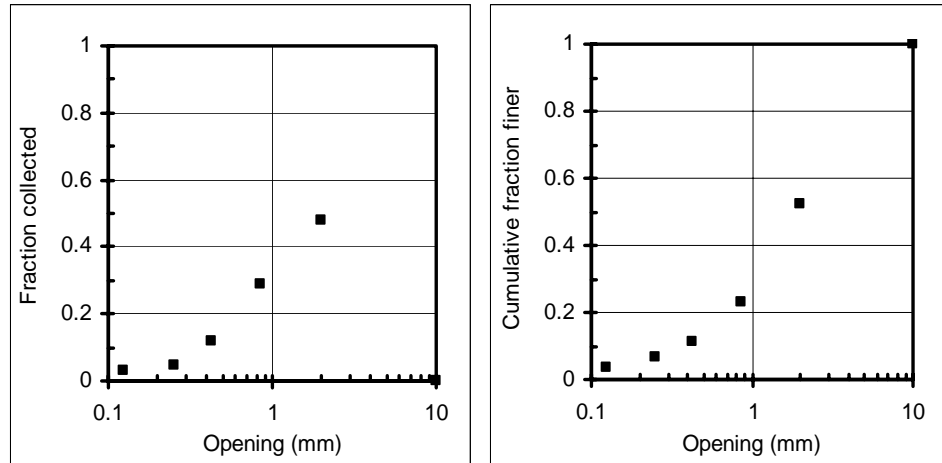


Figure 6.3. Particle size distribution for BA.

Methods

Aging

The aging for bottom ash included exchange with 100% N₂, 100% air, and a mixture of 20% CO₂-80% N₂. These aging processes were performed in pressurized 2.5 and 5 gal paint tanks (PT 798 Series, Federal Equipment Series, Co.), where conditions of atmosphere could be controlled (Figure 6.4). For the 100% N₂ and 100% air atmospheres, the relative humidity was maintained at 100% by passing the inflow gas through a water sparger containing sand and glass wool to keep the moisture. For the 20% CO₂ – 80% N₂ mixture, the level of CO₂ was maintained at 20% inside the chamber by monitoring the chamber pressure and keeping it constant at 1.36 atm (20 psi). The ash was aged under the different environments for 4 weeks in a room where the temperature remained constant at 35°C. Material would be stirred weekly. The results for a more detailed carbonation-only procedure, and the optimum times for obtaining a fully carbonated bottom ash sample are shown in Appendix A.



Figure 6.4. Aging of BA.

Batch testing

Batch testing consisted of two tests: solubility and release as a function of pH, SR002.1, and the solubility and release of constituents as a function of LS ratio, SR003.1 (Kosson et al. 2002). Procedures for both protocols were summarized in Chapter 4 and Chapter 5, and are provided in detail elsewhere (Garrabrants et al. 2005).

Column testing

The effect of different types of column flow on the release of constituents from the material was studied by comparing data from continuous saturated flow columns (SC) and intermittent unsaturated flow columns (IC). Two replicates were run for each material condition (non-aged, aged under N₂, aged under air, and aged under CO₂ atmospheres) and there were a total of 16 columns. All tests were carried out until reaching a LS ratio of 10 mL/g. IC columns were stopped for 4 days every time one of

the following LS ratios was reached: 0.1, 0.2, 0.5, 1, 2, 5 and 10 mL/g. SC columns ran continuously until reaching a LS ratio of 10 mL/g. Samples were taken at equal time intervals between the established LS ratios. Solution pH and conductivity were recorded. Samples were filtered and analyzed as explained previously. The complete methodology is explained in detail in Chapter 3 and Chapter 5.

Results and Discussion

Results presented here show the different release of constituents of concern from batch and column testing of non-aged and aged BA. In terms of aging experiments, BA aging was the first to be tested, and it was concluded that there was no major difference between the “non-aged” and the material aged under a 100% Air, 100% N₂ and 20% CO₂-80%N₂ atmospheres in terms of pH and conductivity, as well as release of constituents in column testing. For this reason, only non-aged and carbonated BA data are shown in the graphs. pH and conductivity of the samples are presented as a function of LS ratio for column experiments, and as a function of milliequivalents of acid/base added for batch testing. The elements presented are the elements that are representative of major constituents and highly soluble constituents (e.g., Ca, Cl, Na) or pH-dependent behavior (e.g., Cd, Cu, Pb, Zn). Results for Al, As, Ba, Fe, K, Mg, Se, SO₄ and Sr can be found in Appendix B. Complete speciation modeling results are presented in Appendix C.

pH and Conductivity

BA has a small buffering capacity; around 5 meq acid/g were required to change the pH of the sample from 12 to 4 (Figure 6.5).

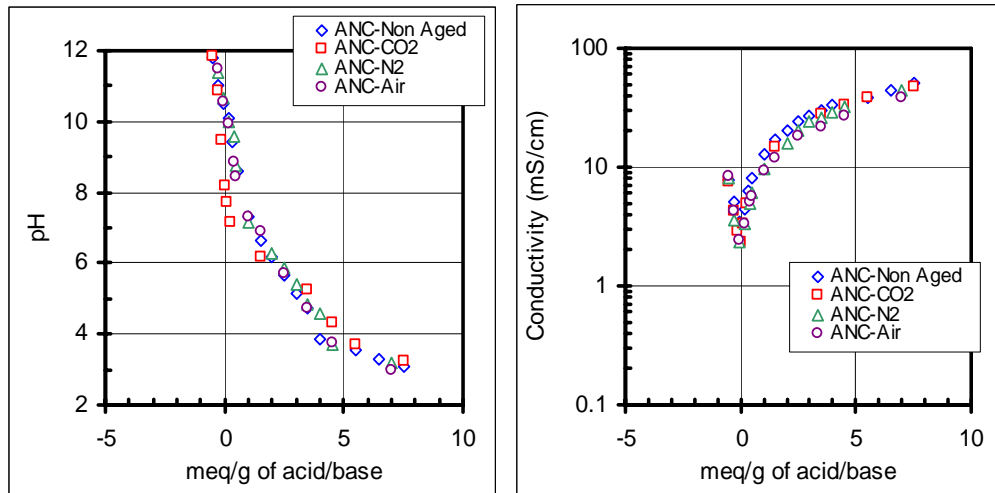


Figure 6.5. pH and conductivity of BA titration curve

There is good agreement, in terms of pH values, between batch and column testing. For the non-aged material and the material aged under air and N₂, the pH in the batch testing is lower; this could be due to the fact that batch testing requires for the material to be particle size reduced, and this was done in an open environment, allowing for some early carbonation process to take place and lowering the pH of the material. Figure 6.6 shows that there is not a significant effect from the type of column flow in the pH values of the solution. These ANC curve is in agreement with other research (Poletini et al. 2004)

Conductivity of the leachates was also measured. For the intermittent unsaturated flow experiments (Figure 6.7) there is a great decrease in conductivity values at low LS ratios from the leachates due to a relaxation of the concentration gradient of the soluble

species (i.e., salts) as they are released from the columns. Above a LS ratio of 2 there is not a significant change in conductivity values, possibly due to the depletion of alkali salts from the material. This also can be seen, to a lesser degree, in the continuous saturated columns (Figure 6.8), where the conductivity reaches a value around 1 mS/cm after a LS ratio of 2-3. Conductivity of samples is higher in batch testing than in column testing by almost an order of magnitude, as can be seen in Figures 6.7 and 6.8. Conductivity of intermittent unsaturated columns is initially higher than for continuously saturated columns. However, near LS ratios of 1 mL/g, the conductivity for IC is lower than for SC by as much as an order of magnitude. Final conductivity values are slightly higher for saturated columns than from intermittent columns.

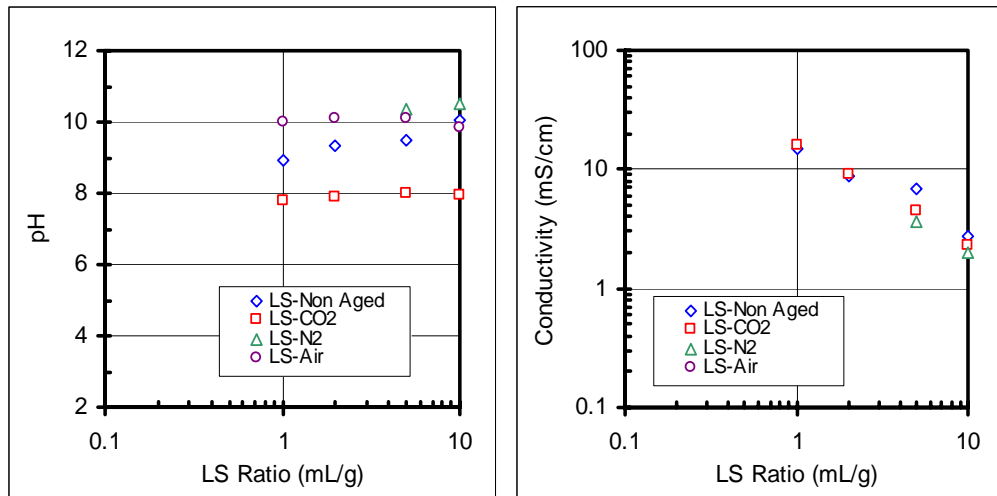


Figure 6.6. pH and Conductivity of BA batch testing as a function of LS Ratio.

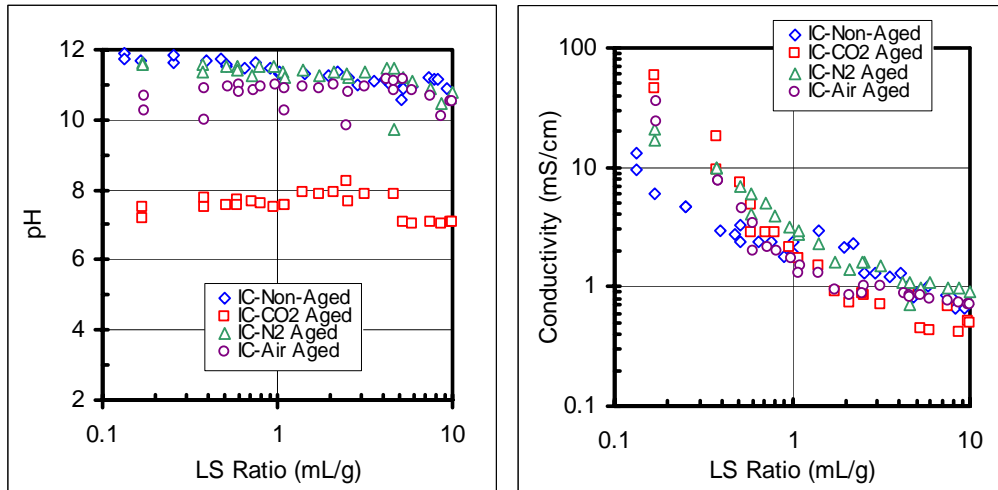


Figure 6.7. pH and conductivity of all BA cases IC column testing as a function of LS Ratio.

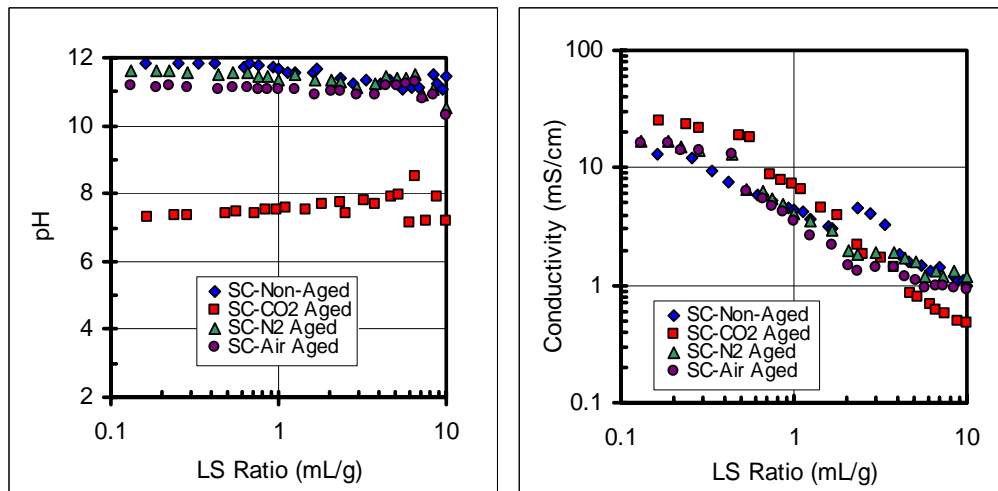


Figure 6.8. pH and conductivity of all BA cases SC column testing as a function of LS Ratio.

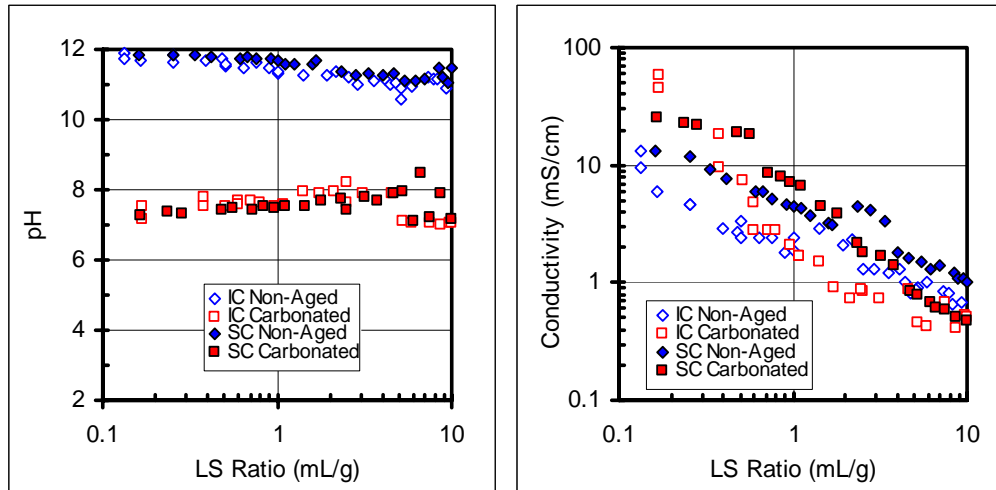


Figure 6.9. pH and conductivity of non-aged and carbonated BA column testing as a function of LS Ratio.

Major constituents

Ca, Cl and Na were the species considered representative of major constituents and species with high-solubility behavior. All elements showed a good agreement between column and batch testing based on a concentration and cumulative release. Ca release was very gradual, as can be observed in Figure 6.10. There was not a significant difference between release from different aging techniques, and the batch and column testing for both the non-aged and the carbonated material are in agreement.

Cl concentration as a function of LS ratio is displayed in Figure 6.11. The release as a function of LS ratio shows an initial higher release of Cl from the batch testing than from column testing. Release from the carbonated material is higher than for the non-aged material at low LS ratios, but at higher LS ratios (10 mL/g), the release from the carbonated material is almost an order of magnitude lower than from non-aged material. The release from batch and column testing is in agreement when compared on a cumulative basis.

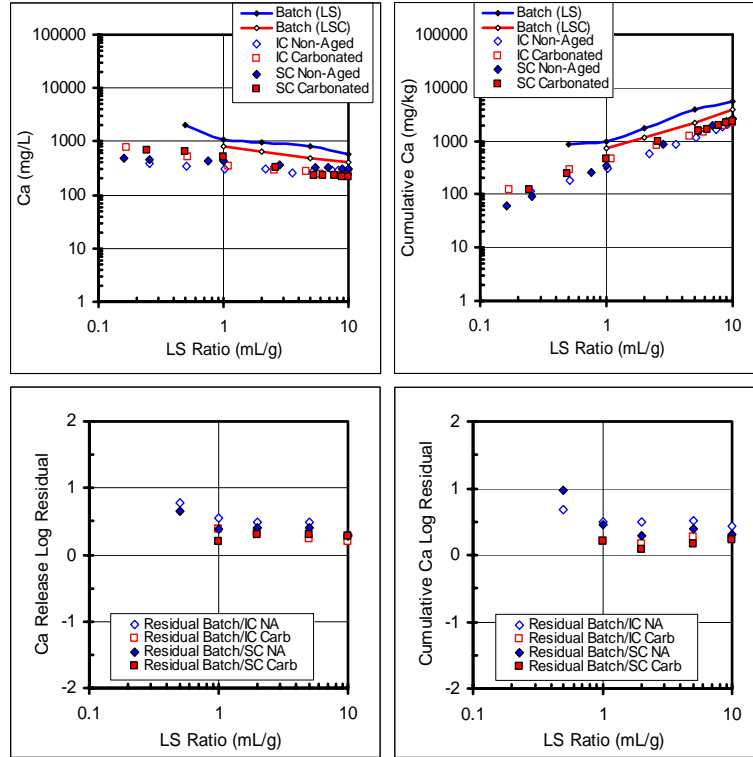


Figure 6.10. Ca release from BA as a function of LS Ratio.

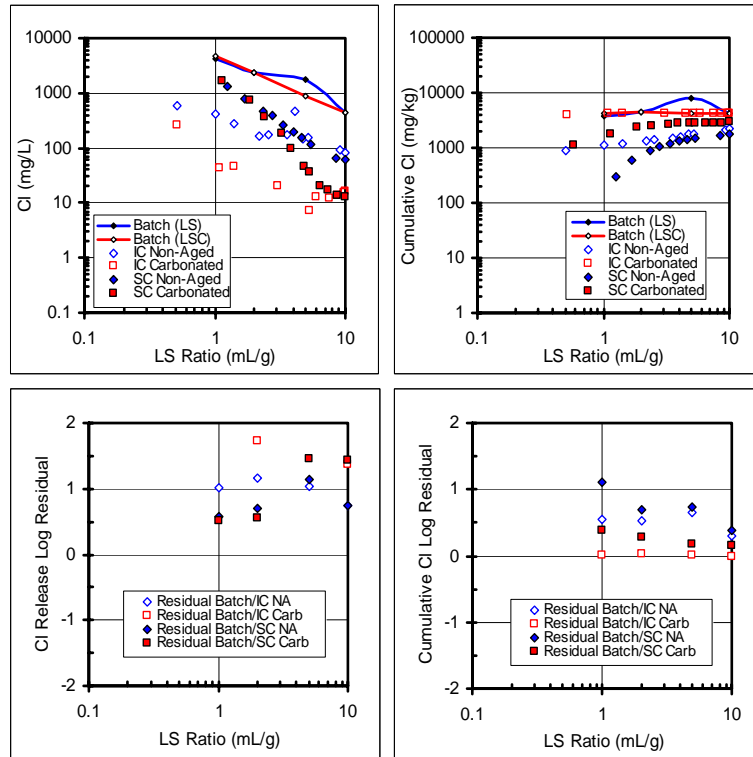


Figure 6.11. Cl release from BA as a function of LS Ratio.

Batch testing overestimates the column leaching concentrations of Na as a function of LS ratio. However, when comparing the cumulative release, the results are very consistent between both tests. The Na release from IC columns decreases faster than from the SC columns, but release from SC at higher LS ratios is higher for both non-aged and carbonated material than it is from IC columns. Carbonation of samples does not have a noticeable effect on sodium release as it does on calcium release (Figure 6.12).

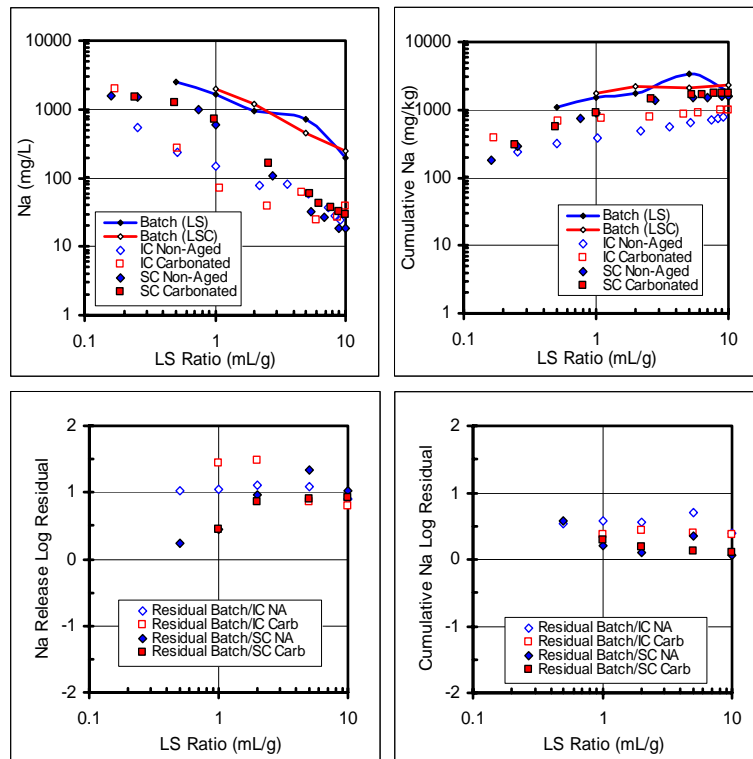


Figure 6.12. Na release from BA as a function of LS Ratio.

Minor constituents

Ba, Cd, Cu, Pb and Zn were considered the minor constituents, including species representative of pH-dependent behavior. The release of constituents from batch testing as a function of pH seemed to be in good agreement with the release of constituents from

column testing for most of the elements. In most cases, batch testing was a conservative estimate of column testing, as can be seen in Appendix B. For most of the cases there was no real effect of the different column flow regimes in the release of constituents.

For Ba, the column release from non-aged material as a function of pH varied widely (0.01-2 mg/L) as the Ba species were being washed out of the column, whereas for the carbonated material the variation was within a more defined concentration range (0.03-0.1 mg/L). No significant effect of column regime is observed in the release of Ba. On a cumulative basis, the release from non-aged bottom ash was slightly higher than from carbonated material (Figure 6.13). The Ba release from the non-aged material in batch testing is in general agreement with other studies (IAWG et al. 1997), where it has been found that the leachability of Ba shows a decrease above pH values of 12.

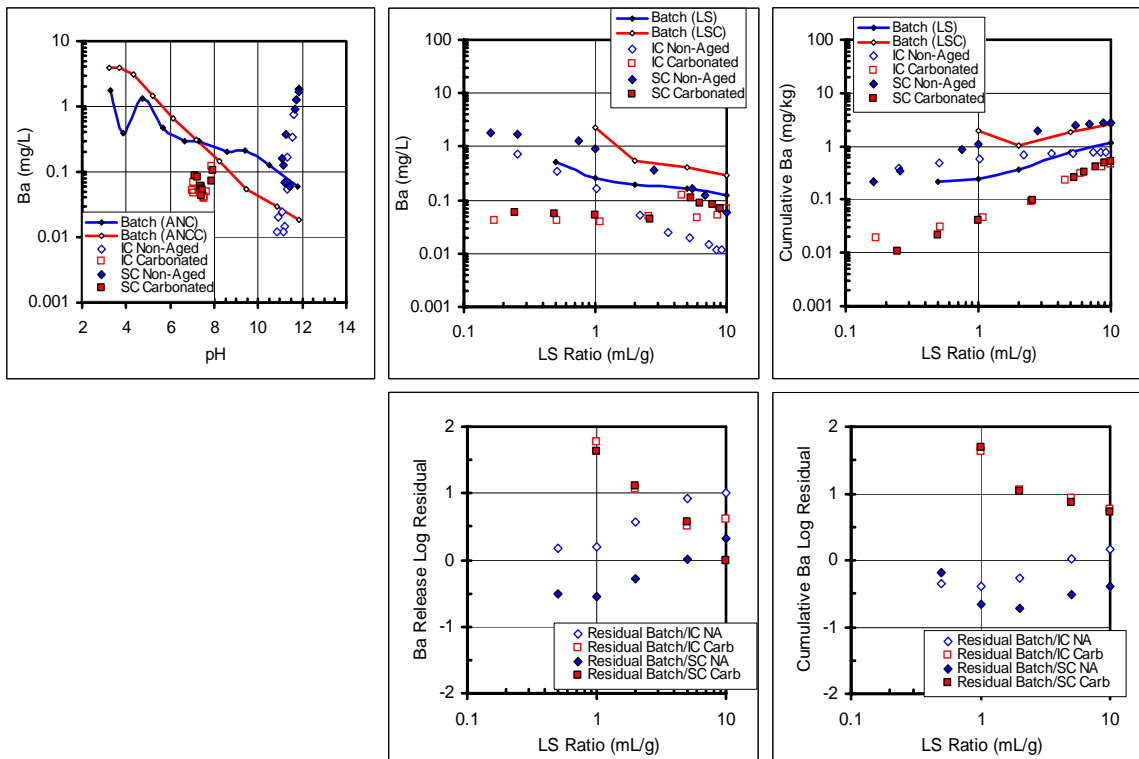


Figure 6.13. Ba release from BA as a function of pH and LS Ratio.

Cd release (Figure 6.14) shows typical behavior of a certain class (type C) of bottom ash as a function of pH, and is consistent with previous research (IAWG et al. 1997; Meima et al. 1998; Meima et al. 1999). Under batch conditions, the release from non-aged material as a function of pH is higher than the release from carbonated material, and as a function of LS ratio, there is not a significant difference between non-aged and carbonated material. For column testing, the release is higher for the non-aged material, and this difference is more significant at low LS ratios.

For Cu (Figure 6.15), the release from non-aged material was significantly higher at low pH values, but after a pH of 6, there is no significant difference in the release of Cu from non-aged material and carbonated material. This is in agreement with previous studies (IAWG et al. 1997; Meima et al. 1998; Meima et al. 1999; Meima et al. 2002). Also, there is no significant difference in the release from batch and column testing, as can be observed in the cumulative release of this constituent.

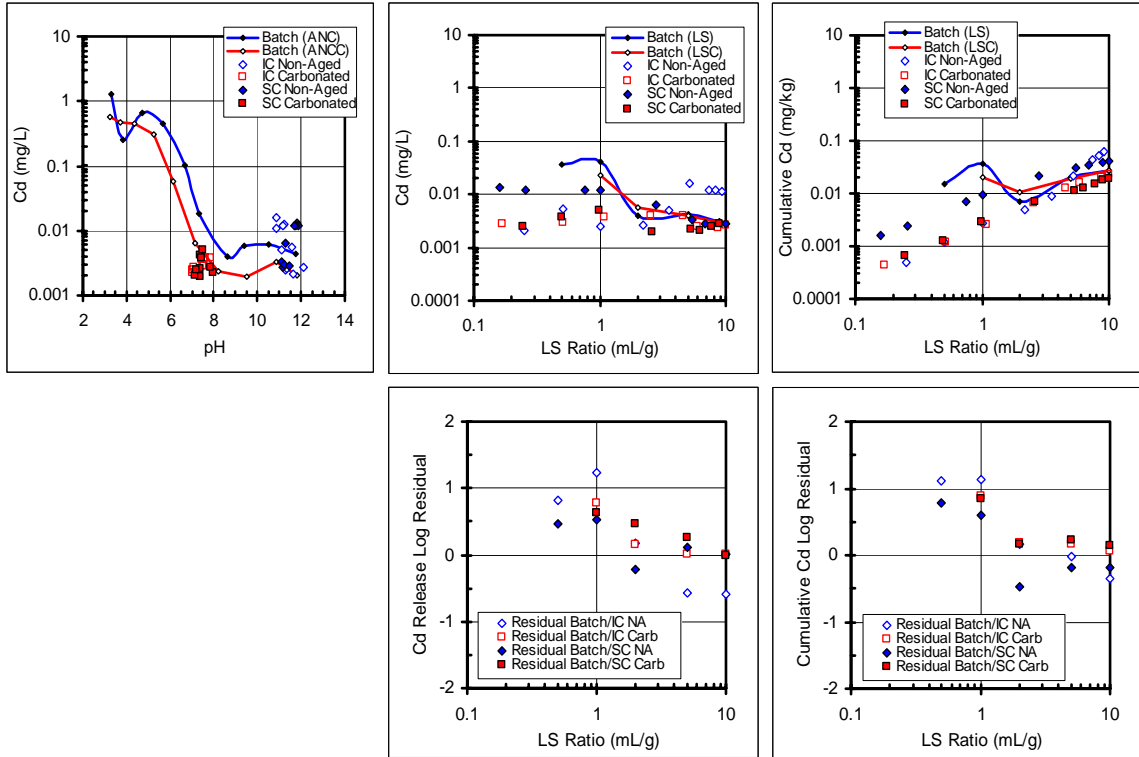


Figure 6.14. Cd release from BA as a function of pH and LS Ratio.

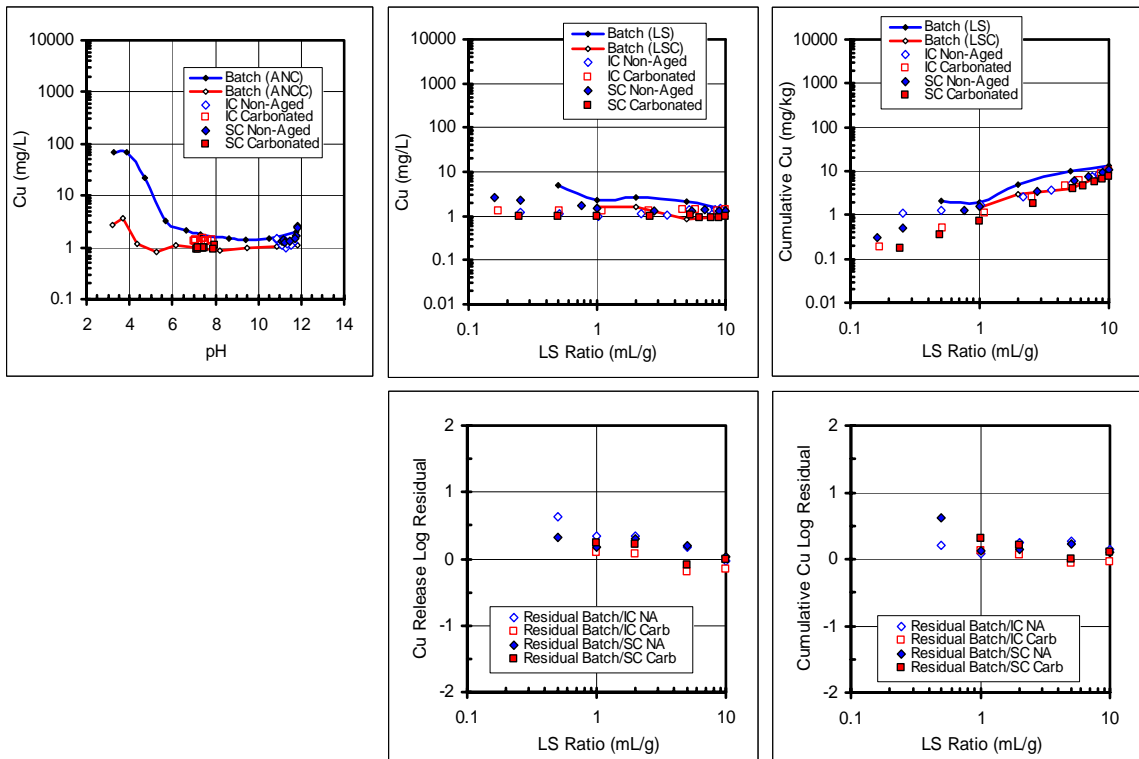


Figure 6.15. Cu release from BA as a function of pH and LS Ratio.

Pb exhibits typical pH-dependent behavior that has been observed previously (IAWG et al. 1997; Meima et al. 1998; Meima et al. 1999) (Figure 6.16). The concentration of Pb from the IC samples varies from 0.01 to 1 mg/L, while the concentration of Pb from the SC samples is more constant around 0.005-0.01 mg/L. The release from carbonated material is more than an order of magnitude smaller than from the non-aged material, as can be seen both from batch and column testing results in a cumulative basis. This is in agreement with several bottom ash studies (IAWG et al. 1997; Meima et al. 1999; Freyssinet et al. 2002).

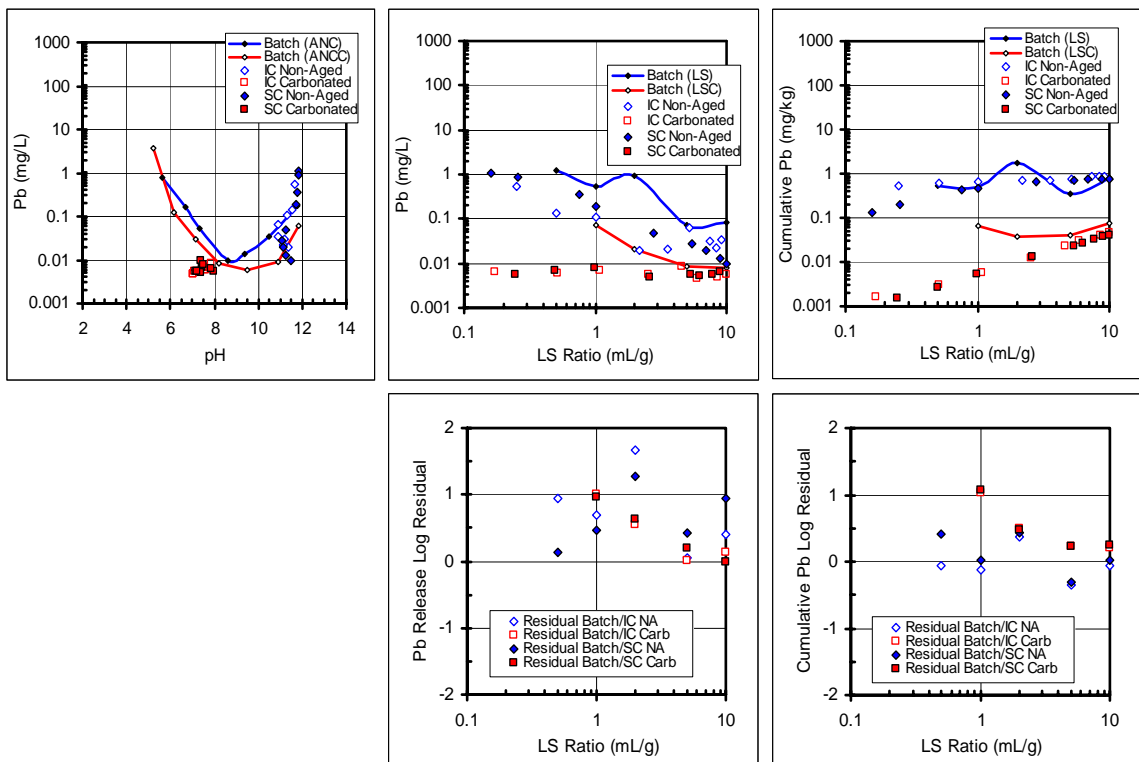


Figure 6.16. Pb release from BA as a function of pH and LS Ratio.

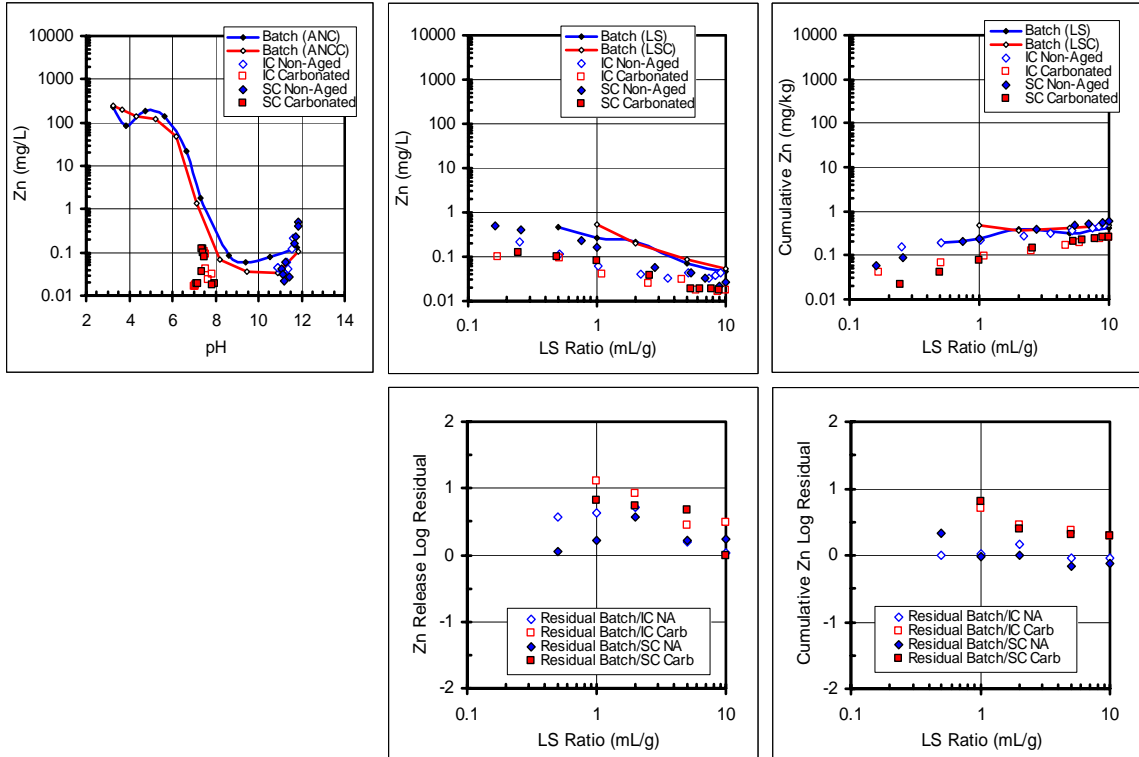


Figure 6.17. Zn release from BA as a function of pH and LS Ratio.

Zn release shows typical pH-dependent behavior observed previously (IAWG et al. 1997; Meima et al. 1998; Meima et al. 1999) (Figure 6.17). Under batch conditions, there is no significant difference in the release from non-aged and carbonated materials as a function of pH and LS ratio. For column testing, the release of Zn is slightly higher for the non-aged material at low LS ratios, but this difference is not significant at higher LS ratios.

Geochemical speciation modeling results

The latest versions of geochemical speciation modeling software LeachXS, 1.0.4.0 and 1.0.4.1, were used to obtain the results presented in this research. The solubility prediction results were based on batch results of release as a function of pH (SR002). Using the chemical speciation wizard, and after a couple of solubility

prediction iterations to get a better fit, the minerals potentially controlling solubility were selected based on their saturation indices (*SI*), chosen in the range of -1 to 1. Table 6.4 shows the solubility controlling minerals for both aging conditions. Mineral formulas are shown in Appendix D.

Si values were not available for the samples, and were initially assumed based on similar bottom ash previous experiments that have been entered into the LeachXS database (MSWI BA Austria). Assumed values for Si are included in Table 6.3.

Table 6.3. Si initial assumptions for BA.

pH	Si
3.28	2.5×10^{-2}
4.72	5.0×10^{-3}
5.65	1.9×10^{-3}
7.32	4.0×10^{-4}
9.40	6.0×10^{-5}
11.77	7.3×10^{-5}

Table 6.4. Solubility controlling minerals for BA.

Element	Non-aged BA	Carbonated BA
Al	Hercynite	Al(OH) ₃ , Laumontite Wairakite
Ba	Ba(SCr)O ₄ (96% SO ₄), Ba(SCr)O ₄ (77% SO ₄), BaSrSO ₄ (50% Ba), BaCrO ₄	Ba(SCr)O ₄ (96% SO ₄), BaSrSO ₄ (50% Ba)
Ca	Gypsum, Calcite, Wollastonite, CaMoO ₄ (c), P-Wollastonite, CSH_ECN, alpha-TCP, CaCu ₄ (PO ₄) ₃ OH, OCP, Ca ₂ Zn(PO ₄) ₂ , Ca ₃ Zn ₂ (PO ₄) ₃ OH, Tyuyamunite	Wairakite, CSH_ECN, alpha- TCP, Ca ₂ Cd(PO ₄) ₂ , CaMoO ₄ (c), Ca ₂ Pb ₂ O(PO ₄) ₂ , Ca ₃ (VO ₄) ₂
Cd	Cd(OH) ₂ , CdSiO ₃ , Otavite	Ca ₂ Cd(PO ₄) ₂
Cr	Ba(SCr)O ₄ (96% SO ₄), Ba(SCr)O ₄ (77% SO ₄), BaCrO ₄ , PbCrO ₄ , SrCrO ₄ , CuCrO ₄	Ba(SCr)O ₄ (77% SO ₄), PbCrO ₄
Cu	CuCrO ₄ , Tsumebite, CaCu ₄ (PO ₄) ₃ OH	Dioptase
Fe	Hercynite, Fe ₂ (MoO ₄) ₃	Fe ₃ (OH) ₈ , Fe_Vanadate, FeAsO ₄ ·2H ₂ O
Mg	Brucite	Sepiolite
Mn	Rhodochrosite, Bixbyite, Hausmannite	Rhodochrosite, Manganite
Mo	CaMoO ₄ (c), Fe ₂ (MoO ₄) ₃	CaMoO ₄ (c)
Ni	NiCO ₃ , Ni(OH) ₂	Bunsenite
Pb	PbCrO ₄ , Anglesite, Tsumebite, Pb ₂ O ₃ , Pb ₃ (VO ₄) ₂	PbCrO ₄ , Pb ₃ (VO ₄) ₂ , Ca ₂ Pb ₂ O(PO ₄) ₂ , Pb ₂ V ₂ O ₇
P	alpha-TCP, CaCu ₄ (PO ₄) ₃ OH, OCP, Ca ₂ Zn(PO ₄) ₂ , Tsumebite, Ca ₃ Zn ₂ (PO ₄) ₃ OH	alpha-TCP, Ca ₂ Cd(PO ₄) ₂ , Ca ₂ Pb ₂ O(PO ₄) ₂
SO ₄	Ba(SCr)O ₄ (96% SO ₄), Ba(SCr)O ₄ (77% SO ₄) BaSrSO ₄ (50% Ba), Gypsum, Anglesite	Ba(SCr)O ₄ (77% SO ₄), BaSrSO ₄ (50% Ba)
Sr	BaSrSO ₄ (50% Ba), Strontianite, SrCrO ₄	BaSrSO ₄ (50% Ba), Strontianite
V	Pb ₃ (VO ₄) ₂ , Tyuyamunite, Carnotite, V ₂ O ₅	Pb ₃ (VO ₄) ₂ , Pb ₂ V ₂ O ₇ , V ₂ O ₅ , Ca ₃ (VO ₄) ₂ , Fe_Vanadate
Zn	Willemite, Ca ₃ Zn ₂ (PO ₄) ₃ OH Ca ₂ Zn(PO ₄) ₂	Willemite, Zincite, ZnSiO ₃

The carbonated prediction shown in Table 6.4 is the result of using the carbonated material as a starting point. However, in the case where accelerated aging is not possible as part of the decision-making process, it is also of interest to predict the solubility behavior of the aged material based on the non-aged material. This was done by iteratively changing the following parameters: 1) increasing carbonate value in the system from an initial value of 35,000 mg/kg for the non-aged material to 70,000 mg/kg for the carbonated material prediction, 2) adding or removing the solubility controlling minerals so that the minerals in the carbonated prediction from non-aged data would be the same as in the carbonated prediction from carbonated data, 3) increasing availability values for Al and Pb, 4) decreasing availability values for Cd, Cu, Fe, Ni, and SO₄ (with these changes being within 20% of the original value), 5) increasing the DOC concentrations by an order of magnitude, 6) changing the SHA value from 8×10^{-4} to 1×10^{-4} kg/kg, and 7) changing the HFO value from 9×10^{-4} to 8×10^{-4} kg/kg. Another change for all prediction cases was the decrease of the ettringite parameters in ORCHESTRA by 30 orders of magnitude to hinder ettringite precipitation.

Ca, Cd, Cu, Pb and Zn were selected because they were representative of major constituents and constituents with pH-dependent behavior. In each graph, the measured batch data is presented for non-aged and carbonated material, as well as the prediction from the non-aged material to both non-aged and carbonated conditions, and the prediction from the carbonated condition. Discrepancies between predicted and measured data are presented as residuals. These residuals were calculated as previously explained in Chapter 3, and are the logarithm of the ratio of predicted to measured data. A residual of zero means the values are equal, positive values mean the predicted data are

higher than the measured data, and negative values mean the predicted data are lower than the measured data.

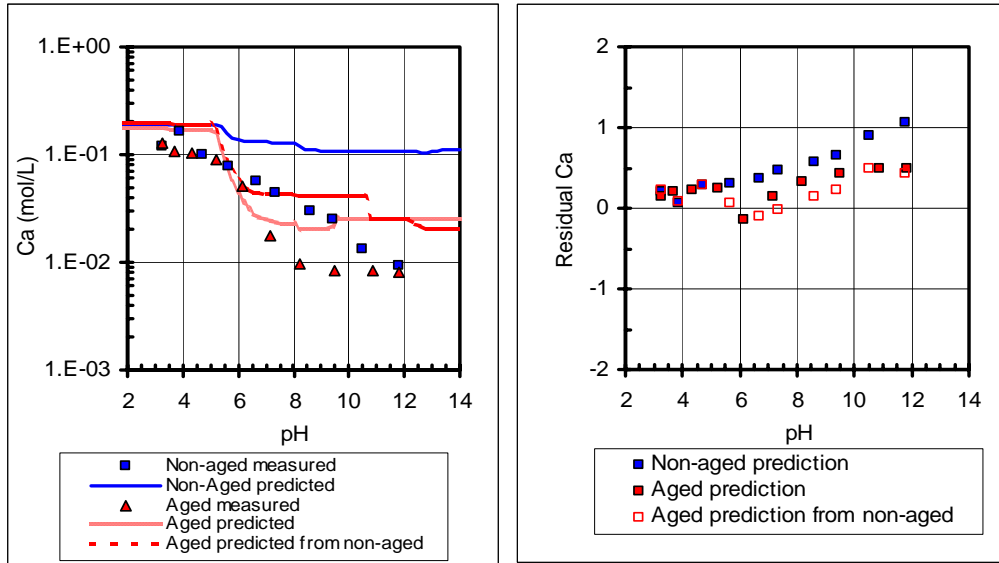


Figure 6.18. Ca prediction from BA as a function of pH.

For Ca, the prediction for both non-aged and carbonated material is in agreement with measured data (Figure 6.18). The predicted solubility for the carbonated material based on non-aged material is lower than the prediction for the non-aged material itself above a pH value of 5, but it is not the same as the carbonated prediction. Above a pH of 11, the predicted solubility for the carbonated material based on non-aged material and the prediction for the carbonated material are the same. The species controlling the solubility of Ca are mainly Calcite and to a lesser extent, Wollastonite for the non-aged material, and Ca MoO_4 for the carbonated material.

In the case of Cd, there is a significant difference between prediction of non-aged and carbonated material, despite the fact that the measured data are not very different (Figure 6.19). The difference between the prediction for the carbonated material based

on non-aged data and the prediction based on carbonated data is only noticeable between pH 6 and 9. Prediction from the carbonated data more accurately reproduces the measured data. The species controlling solubility for the non-aged material are mainly $\text{Cd}(\text{OH})_2$ and Otavite for the non-aged material, and $\text{Ca}_2\text{Cd}(\text{PO}_4)_2$ for the carbonated material. POM and HFO have a smaller effect on the Cd solubility for both aging conditions. Previous studies (Meima et al. 1999) have shown otavite as a major solubility controlling species, as well as amorphous $\text{Cd}(\text{OH})_2$, which confirms the minerals selected for the non-aged material. Carbonation results in the formation of new minerals, and that might explain the different minerals controlling the solubility for the carbonated case.

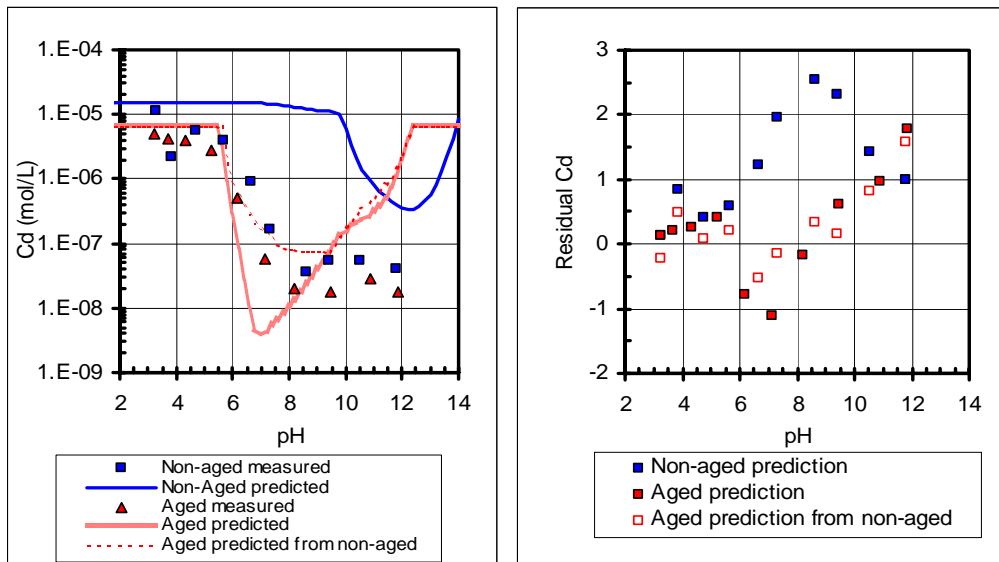


Figure 6.19. Cd prediction from BA as a function of pH.

For Cu, there is a significant difference between prediction of non-aged and carbonated material, despite the fact that the measured data are not very different, except at pH values below 6 (Figure 6.20). There is no difference between the prediction for the carbonated material based on non-aged data and the prediction for the carbonated data.

The solubility controlling species is $\text{CaCu}_4(\text{PO}_4)_3\text{OH}$ for the non-aged material and the HFO for the carbonated case. HFO also has a smaller effect on the solubility prediction for the non-aged condition. POM-bound Cu has a small role on the solubility behavior for both conditions. A previous study (Meima et al. 1999) showed Tenorite as the main species controlling Cu solubility in bottom ash tested at different weathering stages. Tenorite was initially selected as a mineral in the iteration process, but did not lead to similar results as the measured data.

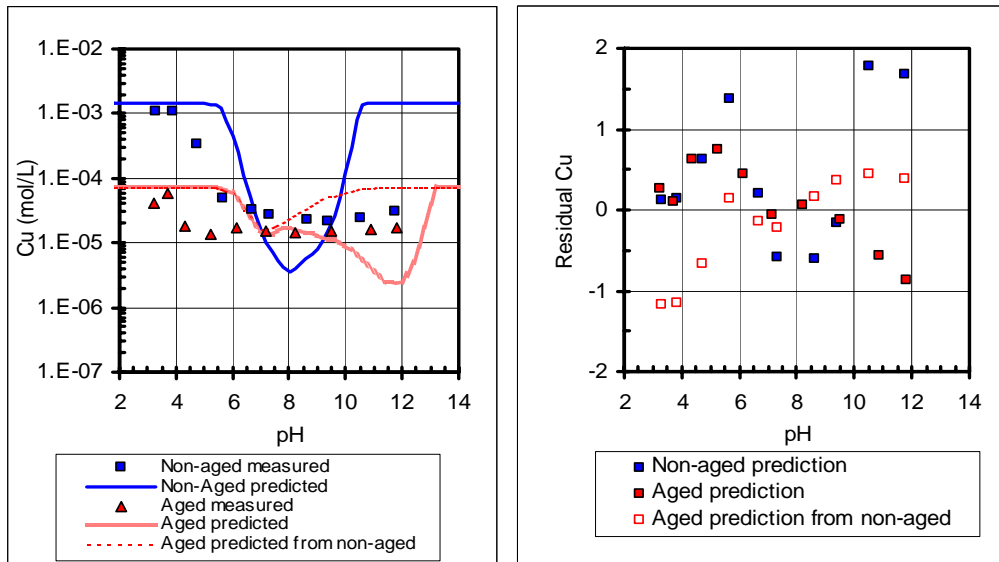


Figure 6.20. Cu prediction from BA as a function of pH.

The Pb prediction of solubility behavior for carbonated material based on carbonated data is not as accurate as the prediction of solubility behavior for carbonated material based on non-aged data (Figure 6.21). However, the predicted solubility values between pH 8 and 11 are between 1 and 2 orders of magnitude lower than the measured data. The solubility controlling species are Tsumebite and $\text{Pb}_3(\text{VO}_4)_2$ for the non-aged material, and $\text{Ca}_2\text{Pb}_2\text{O}(\text{PO}_4)_2$ for the carbonated material. HFO and POM have a strong

role on the solubility of Pb for both aging conditions. Some of the minerals selected are in agreement with previous modeling on bottom ash (Meima et al. 1999), including Anglesite and PO_4 -minerals.

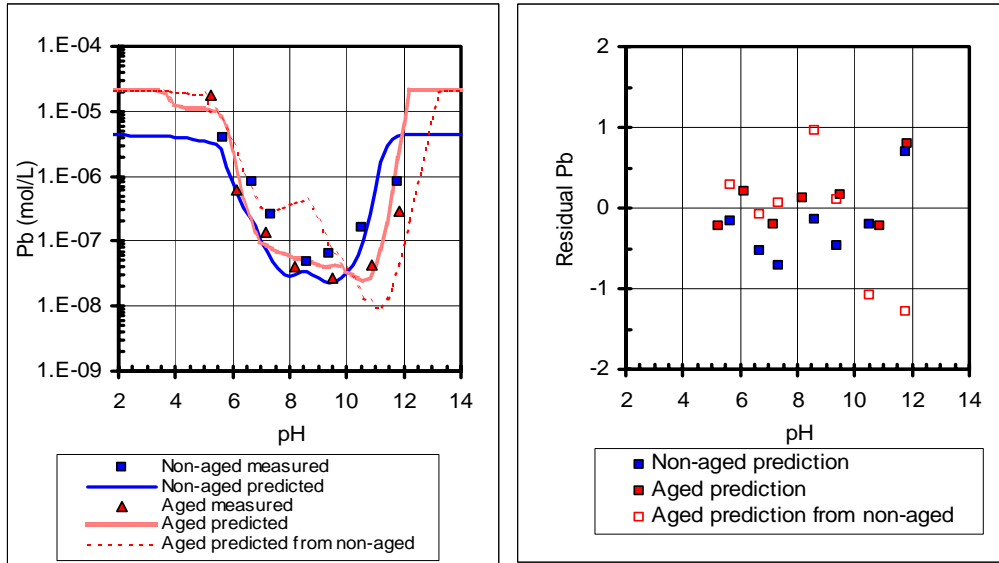


Figure 6.21. Pb prediction from BA as a function of pH.

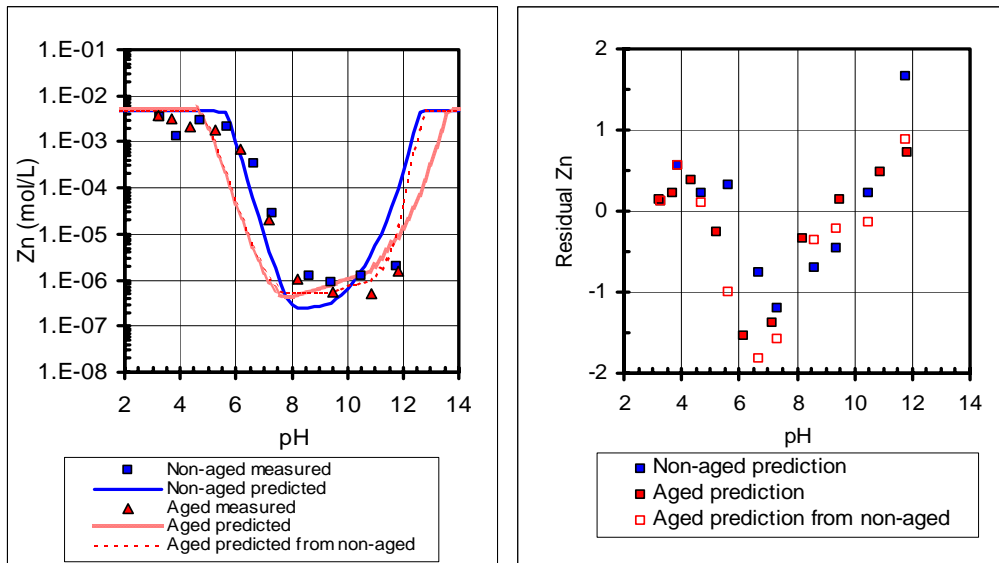


Figure 6.22. Zn prediction from BA as a function of pH.

For Zn, the solubility prediction is slightly higher for the predictions based on non-aged data, but both predictions accurately describe the solubility behavior above pH

values of 10 and below 5 (Figure 6.22). The species controlling the solubility of Zn are Willemite for the non-aged prediction, and ZnSiO_3 and Zincite for the carbonated material. POM-bound Zn has a smaller contribution to the solubility behavior. Willemite, Zincite, and ZnSiO_3 have all been considered as the species controlling the solubility of Zn in bottom ash in previous modeling studies (Meima et al. 1999).

From the presented constituents, Ca, Pb and Zn predicted solubilities are mostly in agreement with measured data (most of the residual values are within one order of magnitude); for the rest of the constituents, the residual values are more scattered and above one order of magnitude. The predictions obtained for the carbonated material based on non-aged measurements are also in agreement with the predictions based on carbonated data. Also, although the prediction and measured solubilities are not exactly the same for non-aged and carbonated materials, the predicted solubility behavior was in agreement with the behavior of the measured data for all cases.

Uncertainties in this prediction were previously discussed in Chapter 2, 4 and 5, and include mainly the lack of a complete sample analysis (including Si values), as well as the assumptions of Si, CO_3 and SHA for modeling purposes. As mentioned previously, these results are preliminary, and the additional measured data (especially Si) will be critical for long-term prediction.

Conclusions

Results indicate that there is no major difference between the non-aged and the material aged under a 100% Air, 100% N_2 and 20% CO_2 -80% N_2 atmospheres in terms of pH and conductivity, as well as release of constituents in column testing. Only non-aged

and carbonated bottom ash were considered. The effect of carbonation in the bottom ash can be observed by the decrease of pH, from about 11 to 7, of the samples resulting from batch and column testing.

When analyzing the release of constituents, results indicate that in most cases, there is good agreement between batch and column testing, and that there is not a significant difference between testing under continuously saturated or intermittent unsaturated flow. The only disagreement between batch and column testing was found for Ba, where the release was higher for the carbonated material at pH values below 7, and lower for pH values above that, and although the release from non-aged material was higher than the release from carbonated material under column testing, the release from batch testing was higher for the carbonated material.

Results show that highly soluble species, such as Cl and Na, are released faster in intermittent unsaturated columns, as shown by both the release of this constituents and conductivity values. This faster release might be due to the presence of preferential flow paths existing in the columns running down flow with intermittent unsaturated flow. At LS ratios above 5 mL/g there is no significant difference in the pH and conductivity values, as well as constituent release, between the different types of column flow regimes.

The effect of carbonation can be observed in the lower cumulative release of all species when compared to the release from non-aged material. However, in the case of Ba and Mg, the release was higher from the carbonated material.

Preliminary modeling results were obtained for the non-aged material based on the non-aged data, and for the carbonated material based from non-aged and carbonated

data. Solubility prediction results for the non-aged material were reasonable for most elements, as were the solubility predictions for the carbonated material, with residual values within one order of magnitude. The solubility predictions for the carbonated case based on non-aged measurements are mostly in agreement with the predictions based on carbonated measured data. However, for some elements (Cd, SO₄) the residual values show discrepancies of over 2 orders of magnitude. These disagreements have the potential to be improved with better Si and DOC or CO₃ estimation. These modeling results provide a strong foundation for long-term prediction of constituent release as the speciation software continues to be developed.

References

- ASTM (1992). Standard Test Method for Laboratory Determination of Water (Moisture) Content of Soil and Rock - D 2216-92. Philadelphia, PA.
- ASTM (1998). Standard Test Method for Carbon Black-Pellet Size Distribution - D1511-98. Philadelphia, PA.
- Freyssinet, P., P. Piantone, M. Azaroual, Y. Itard, B. Clozel-Leloup, D. Guyonnet and J. C. Baubron (2002). "Chemical changes and leachate mass balance of municipal solid waste bottom ash submitted to weathering." Waste Management **22**: 159-172.
- Garrabrants, A. C. and D. S. Kosson (2005). Leaching processes and evaluation tests for inorganic constituent release from cement-based matrices. Stabilization and solidification of hazardous, radioactive and mixed waste. R. Spence and C. Shi. Boca Raton, CRC Press: 229-280.
- Griffiths, C. T., Krstulovich, J.M. (2002). Utilization of Recycled Materials in Illinois Highway Construction, Federal Highway Administration: 27.
- IAWG, A. J. Chandler, T. T. Eighmy, J. Hartlen, O. Hjelmar, D. S. Kosson, S. E. Sawell, H. A. van der Sloot and J. Vehlow (1997). Municipal Solid Waste Incinerator Residues. Studies in Environmental Science **67**. Elsevier. New York.
- Kosson, D. S., H. A. van der Sloot, F. Sanchez and A. C. Garrabrants (2002). "An integrated framework for evaluating leaching in waste management and utilization of secondary materials." Environmental Engineering Science **19**(3): 159-204.
- Meima, J. A. and R. N. J. Comans (1998). "Application of surface complexation/precipitation modeling to contaminant leaching from weathered municipal solid waste incinerator bottom ash." Environmental Science & Technology **32**(5): 688-693.
- Meima, J. A. and R. N. J. Comans (1999). "The leaching of trace elements from municipal solid waste incinerator bottom ash at different stages of weathering." Applied Geochemistry **14**(2): 159-171.
- Meima, J. A., R. D. van der Weijden, T. T. Eighmy and R. N. J. Comans (2002). "Carbonation process in municipal solid waste incinerator bottom ash and their effect on the leaching of copper and molybdenum." Applied Geochemistry **17**: 1503-1513.
- Piantone, P., F. Bodéan and L. Chatelet-Snidaro (2004). "Mineralogical study of secondary mineral phases from weathered MSWI bottom ash: implications for the modelling and trapping of heavy metals." Applied Geochemistry **19**: 1891-1904.
- Polettini, A. and R. Pomi (2004). "The leaching behavior of incinerator bottom ash as affected by accelerated ageing." Journal of Hazardous Materials **113**(1-3): 209-215.

van der Sloot, H. A., D. Hoede, D. J. F. Cresswell and J. R. Barton (2001). "Leaching behaviour of synthetic aggregates." Waste Management **21**(3): 221-228.

van der Sloot, H. A., A. van Zomeren, P. Seignette, J. J. Dijkstra, R. N. J. Comans, H. Meeussen, D. S. Kosson and O. Hjelm (2003). Evaluation of Environmental Aspects of Alternative Materials Using an Integrated Approach Assisted by a Database/Expert System. Advances in Waste Management and Recycling.

Vipulanandan, C. and M. Basheer (1998). Recycled materials for embankment construction. Recycled Materials in Geotechnical Applications: Proceedings of sessions sponsored by the Soil Properties Committee of the Geo-Institute of the ASCE in conjunction with the ASCE National Convention, co-sponsored by the CIGMAT, Boston, Massachusetts.

CHAPTER VII

SUMMARY AND CONCLUSIONS

Summary of Results

Chapter 1 presented an overview of the significance of this research. It introduced the importance of adequate testing conditions that can account for the different conditions that a material will be subjected to while in use. These conditions include aging due to exposure to the environment (e.g., carbonation) and intermittent wetting. It also presented a summary of waste materials that have been used for highway and construction applications, and an overview of batch and column leaching tests that have been developed previously to account for the release of constituents at different pHs and LS ratios. Finally, this chapter introduced the potential ability of geochemical speciation modeling software to predict the solubility and the release of constituents in the long-term based on short equilibrium batch tests.

Chapter 2 presented a review of modeling techniques and introduced LeachXS, the software used in the solubility prediction of constituent release in this research. It included an empirical calculation of aqueous-solid equilibrium, adjusted to a thermodynamic activity basis from conductivity and ionic strength correlations. It also presented an overview of the theoretical background of LeachXS and presents the uncertainties that must be accounted for when using this software in this research project, such as ionic strength considerations and incomplete chemical analysis data.

Chapter 3 focused on column testing, particularly in studying the differences between saturated continuous up flow columns that have been widely studied and unsaturated intermittent down flow columns that attempt to simulate more realistic field conditions. Construction debris was the selected granular material for these tests. Two different types of unsaturated intermittent down flow were used. It was found that there is no significant difference between the two types of intermittent unsaturated flow. Furthermore, the difference between the two types of intermittent unsaturated flow and continuously saturated flow is the faster release of salts during the intermittent unsaturated flow. However, this difference was not observed above LS ratios of 2 mL/g.

Chapter 4 investigated batch leaching tests as predictors of potential field conditions by comparing batch results to column tests. Batch testing was performed as a function of pH and LS ratio. The results were compared to the release of constituents from intermittent unsaturated flow columns and continuously saturated flow columns. These tests were compared for two different types of coal fly ash, and an aluminum recycling residue. It was found that for most cases, there is good agreement between the results obtained from batch testing and column testing. Exceptions were Al, Fe and K, for which batch testing underpredicted column release. However, on a cumulative mass release basis, the results from batch and column tests were mostly in good agreement at higher LS ratios (10 mL/g). These higher LS ratios represent long-term release. Preliminary geochemical speciation modeling results for ARR suggested further Si analysis is required to improve solubility prediction of constituents, as well as long-term release prediction.

Chapter 5 introduced the concept of carbonation and its effects on constituent leaching. Laboratory formulated concrete (LFC) was produced using a previously tested recipe. Concrete was tested under “non-aged” and carbonated conditions. Carbonation took place for 30 days at a constant temperature of 35 °C. The effects of carbonation were observed in lower conductivity values, lower pH values, and lower release of some pH-dependent species, such as Cd, Cu, Pb and Zn. However, for As, the release was higher for the carbonated material than for the non-aged material. It was found that the conditions used in this research mainly promote surface carbonation, which has an impact on material used for column testing, where the external surface of the particles exerts greater control over leaching, than when particles are further size reduced for batch testing. Geochemical speciation modeling software LeachXS was used to model constituent release from LFC. A solubility prediction based on pH values was obtained for the non-aged material and aged material, and also for the aged material based on the non-aged data, taking into account the carbonation effects by adjusting simulation parameters, such as constituent availability and DOC. Si and CO₃ were not measured on the samples, so their concentrations were assumed initially based on values reported by others and then treated as adjustable parameters until a proper fit was found for most of the measured species. There are several uncertainties in this methodology, given that Si and CO₃ are main species in the material, and that Si is a necessary species for the modeling software to be able to do a long-term prediction.

Chapter 6 introduced other types of aging conditions and their effects on constituent release from a MSWI bottom ash. The material was aged under 3 different atmospheres: CO₂-enriched, N₂-enriched and air. The aging was also carried out at 35 °C

over 30 days. It was found that there was no significant difference between the air, N₂-enriched, and non-aged material. For this reason, results are presented only for the non-aged and the carbonated material. The effects of carbonation were observed in lower pH and conductivity values, and in lower release of some pH-dependent species, such as Cd, Cu, Pb, Zn. However, Ba release was higher in the carbonated sample. BA constituent release was also modeled using LeachXS. The approach to modeling aged and non-aged samples was the same as for LFC. Again, concentrations of Si and CO₃ were assumed to obtain a better prediction.

Primary Conclusions

When secondary materials are used in highway construction applications, many applications result in as intermittent infiltration due to precipitation events. In addition, alkaline materials may experience carbonation as a result of absorption and reaction with carbon dioxide in air or soil vapor. These environmental factors may affect the chemistry of the material and furthermore, they can have an impact on the leaching of constituents of concern from the material.

Batch leaching tests evaluating aqueous-solid equilibrium as a function of pH and LS have been recommended as an approach for characterizing leaching properties of materials because of their simplicity and they reflect intrinsic leaching properties. It is necessary, however, to validate and understand the uncertainties associated with using these batch testing approaches to estimate leaching under percolation conditions.

Column tests serve as a surrogate for field data, as these measurements result from the interaction of intrinsic leaching properties of the material with low infiltration rates, and

aid in the evaluation of release of constituent at low LS ratios, not easily achieved by batch testing. However, column tests lack the simplicity and the short testing periods of batch testing.

This dissertation provides an extensive comparison between batch testing and two types of column testing (unsaturated intermittent and continuously saturated flow conditions) for five different granular materials that have high potential for reuse in highway applications. These materials are aluminum recycling residue, MSWI bottom ash, two types of coal fly ash, construction debris and laboratory formulated concrete. The two alkaline materials (bottom ash and laboratory formulated concrete) were additionally analyzed for carbonation effects in the release of constituents.

Residual values, defined as the log of the ratio between the experimental and predicted values, were used to quantify the comparisons. The n values for these elements can be found in Appendix B. Figure 7.1 shows a graphical description of the mean values for every element analyzed, for all materials, and bars are included depicting the standard deviation for each mean value. The comparison of these two graphs shows that the average residuals obtained from the concentration as a function of LS ratio are further from zero than the average residuals from a cumulative release. Only Al is, in average, underpredicted (i.e., batch data was underpredicting column data). However, mean residual values for Cl and SO₄ show overpredictions of over one order of magnitude. Average residuals from the cumulative release as a function of LS ratio are closer to zero, and the mean value is within half an order of magnitude. Only Al and Pb are underpredicted. When considering the standard deviation, the cumulative release

residuals are still within one order of magnitude of overprediction and half an order of magnitude of underprediction.

Figure 7.2 shows the same graphical description but considering only the samples at a LS ratio of 10 mL/g. As a function of concentration, the residuals for all elements are positive (i.e., batch data overpredicts column data), and Cl and SO₄ still show overpredictions of over one order of magnitude. Also, mean residual values for Ba, Cl, SO₄ and Sr are higher than the mean residual values when considering all samples. Average residuals from the cumulative release are closer to zero and approximately at the same value than the residuals considering all samples. From the comparison of these graphs it can be concluded that the cumulative release graphs are a better way of interpreting leaching data from batch and column experiments. A complete statistical data set with the mean and standard deviation values for all residuals can be found at the end of Appendix B.

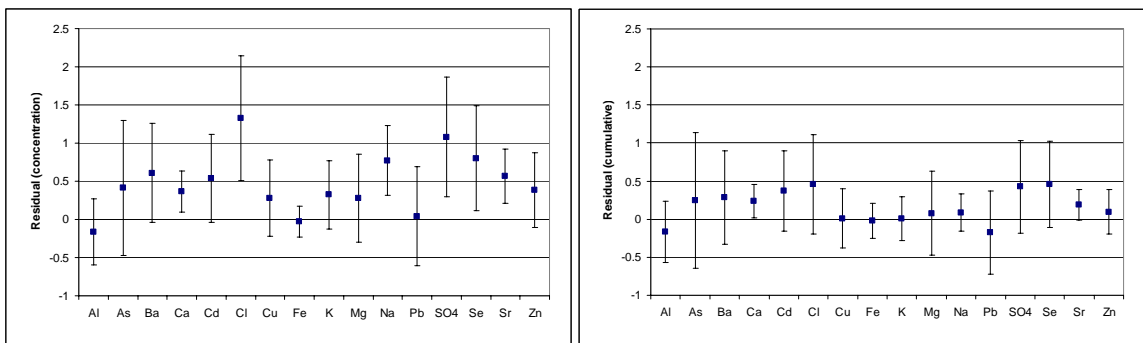


Figure 7.1. Statistical data (mean +/- 1 standard deviation) for all residual values.

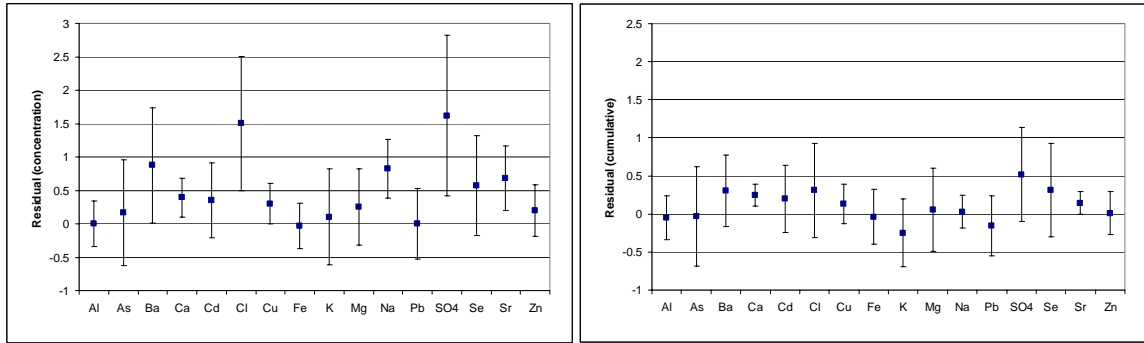


Figure 7.2. Statistical data (mean +/- 1 standard deviation) for residual values of LS 10 samples.

General conclusions are that for most cases, (i) batch testing is a conservative estimate of column testing release, (ii) carbonation reduces the release of constituents, and (iii) column flow regime has no significant effect on the release of constituents. Important exceptions to these conclusions are (i) As leaching from laboratory formulated concrete and (ii) Ba leaching from bottom ash. In both cases, carbonated samples exhibited higher release.

LeachXS, a geochemical speciation model currently under development, was used to obtain solubility predictions from batch data. In general, modeling predictions were in satisfactory agreement with experimental batch data, with experimental and predicted within +/- one order of magnitude or better. However, Cd, Cu and Pb were poorly predicted by the speciation model, with under and over predictions of at least 2 orders of magnitude. Speciation modeling could be improved with better assumptions, constraints and concentrations of some important species, such as Si and CO₃, or further sample analysis to measure these species.

Significance and applications

The significance of this research can be summarized in the answer to the question: Can one obtain, with basic sample testing, an accurate long-term prediction that will allow for the use of a material in a given site without posing a threat to the environment? In this dissertation, a comprehensive array of data is presented comparing results from batch and different types of column flow regimes for a wide range of granular materials. These data confirm that in general, batch testing is a conservative estimate of column testing results, and properly interpreted, it can be a more cost and time effective way for testing materials than column tests.

In the case where As is a constituent of potential concern in concrete materials, and carbonating conditions prevail in the potential usage application, batch testing will most likely underpredict As release and column testing may be required. This is not the case for the other materials analyzed.

In the case where column testing is necessary, this dissertation provides sufficient evidence that the continuously saturated flow conditions are equivalent to intermittent unsaturated conditions at LS ratios of 2 mL/g and higher. At low LS ratios (below 1 mL/g), the release of highly soluble species, such as Na, is significantly higher under intermittent unsaturated conditions, but this discrepancy is not relevant to the cumulative release of typical constituents of concern. This is an important observation, as it shows that the standard continuously saturated column flow case is representative, in the long term, of the more complex unsaturated intermittent field case.

The incorporation of the leaching data from all the materials analyzed in this research into the database used by geochemical speciation software LeachXS represents a

major contribution to the leaching community. Incorporation of this data into the LeachXS interface facilitates searching and retrieval of both batch and column results organized by material. These data may be used as reference comparisons for experiments on similar materials, as some other data was used to fill the information gaps for the geochemical modeling in this research, and also, the data could be used in the absence of further column experiments as a basis for long-term solubility predictions.

Future directions

Although this research presents extensive and detailed data for batch and column analysis under non-aged and carbonated conditions for a representative group of granular materials, there are some areas that need further elucidation and validation. In the few cases where batch testing failed to predict release of constituents from column testing (such as As in concrete), further mechanistic analysis is recommended. These differences between batch and column testing may be a function of the infiltration rate in the column experiments or the difference in particle size used in the two experiments. A detailed investigation on a case by case basis may suggest a testing methodology that can account for these discrepancies.

This research has shown that the effects of intermittent unsaturated infiltration, as opposed to continuously saturated flow, are minimal and have no significance in the long-term release of constituents, as observed on a cumulative mass basis. For some conceivable applications, however, there may be interest in the effect of extremely long drying periods. These research results could provide a control case for such an investigation.

Part of the value of having these research data available in the LeachXS database is the ability to use them as a basis for long-term predictions. However, these data will become even more useful when coupled with further analysis of a few important species. Si analysis is important for correct solubility prediction and long-term prediction. DOC and CO₃ values would also enhance the ability of LeachXS to successfully predict long-term release of constituents.

APPENDIX A

DEFINING CONDITIONS FOR MATERIAL CARBONATION

Introduction

The goal of this experiment is to develop a common protocol for laboratory carbonation of materials prior to leaching evaluations. The specific objectives are: 1) to determine the time necessary to obtain a stable carbonated sample, and 2) to define a standard procedure for carbonating alkali waste material samples. In order to achieve these objectives, materials more likely to experience carbonation (i.e., having alkaline pHs) were exposed to a higher temperature and different humidity levels, and were tested for carbonation degrees at different time intervals and for different particle sizes.

Materials and Methods

Materials

The materials to be carbonated were only the materials having more alkaline pHs (pH > 10). The pH was measured at a LS ratio of 10 mL/g, using deionized water.

1. Bottom Ash (Non-aged) – pH = 12
2. Construction Debris – pH = 10
3. Laboratory Formulated Concrete – pH = 13

Methods

Flow from a 100% CO₂ tank was combined with flow from a 100% air tank passed through a water-saturated sand, in order to obtain a 20% CO₂ humidified gas stream (Figure A.1). The expected 20% of CO₂ was achieved by using flow meters to combine the flow of the two streams. There were two containers for experimentation. The first one only had the humidity (RH) given by the humidified stream of gas. This was accomplished by passing the air stream through a sparger containing sand and glass wool, and filling it with water. The second container contained a beaker filled with water to provide extra humidity. The expected conditions were:

1. 20% CO₂ – 80% Air, 80% RH
2. 20% CO₂ – 80% Air, 40% RH

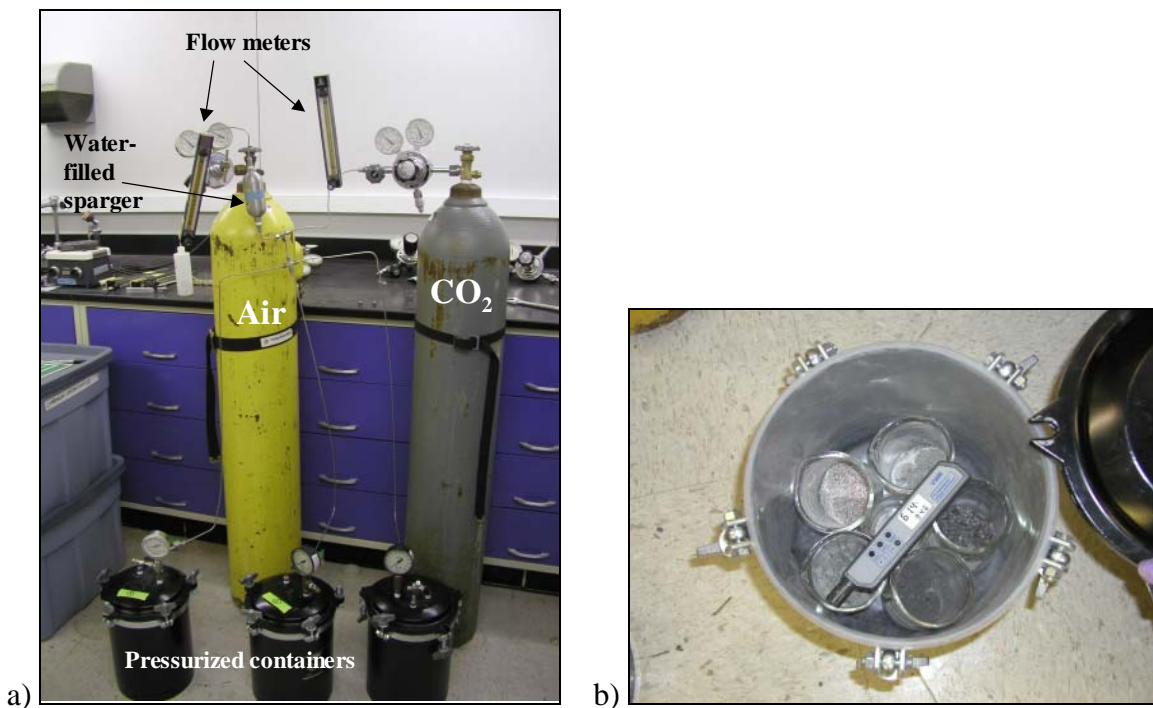


Figure A.1. Carbonation experiment: a) apparatus, b) pressurized chambers.

In order to investigate the effects of particle size in the carbonation process, two sets of samples were carbonated under each condition.

1. Particle size < 2 mm (batch testing maximum particle size)
2. Particle size < 5 mm (column testing maximum particle size)

The carbonation took place in a constant temperature room (35°C) in pressurized containers. Every day while the experiment was in progress, the humidity present in each container was measured with a hygrometer. The samples were stirred daily (by hand) to maximize the contact of all particle surfaces with the CO₂ atmosphere.

The amount of carbonation was measured at different intervals: 3, 7, 14, 21, 28, and 35 days.

For materials with a maximum particle size of 2 mm, a sample of 0.1 g was placed inside a 5 mL vial with a septa lid. A 5 mL syringe was inserted in the lid. Then, 0.1 mL of nitric acid (trace metal grade) was injected into the vial, making sure the acid covered the sample entirely. The volume displaced in the 5 mL syringe was assumed to be the CO₂ produced by the reaction (Figure A.2).

For materials with a maximum particle size of 5 mm, the procedure was similar, changing the sample size to 0.3 g, the volume of acid added to 0.3 mL, and the injection took place in a 15 mL vial.

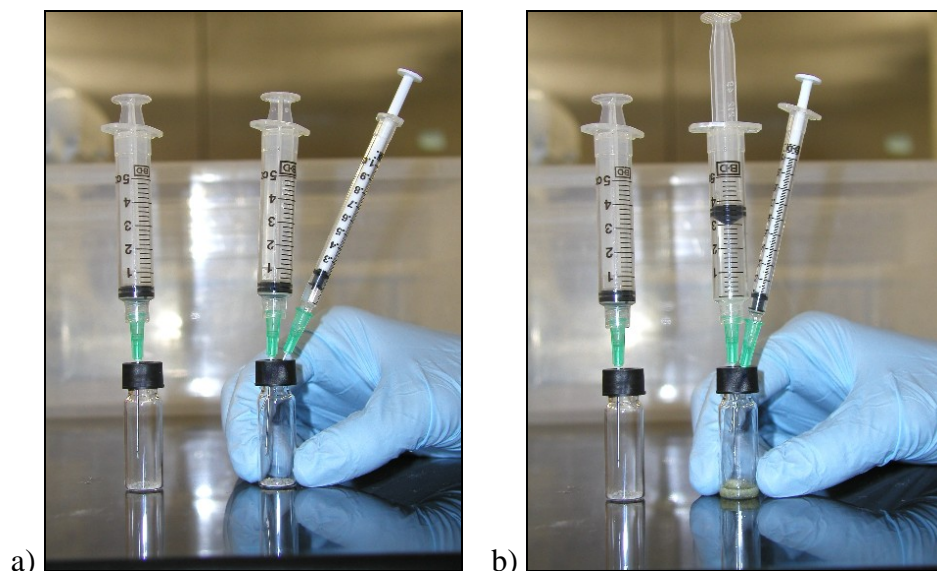


Figure A.2. Carbonation degree measurement: a) before acid injection, b) displacement after acid injection.

Results

Humidity results are shown in table 5.1. Humidity #1 represents the humidity measured in the first container, where the only humidity present was that given by the humidified air stream. Humidity #2 is the humidity measured in the container that had the beaker of water to provide extra humidity.

Results for BA carbonation are shown in Figure A.3. As would be expected, the carbonation degree of samples from the second container is higher. This is due to the fact that more humid environments help accelerate carbonation because of the higher diffusion of carbon dioxide in humid air. The effect of particle size can also be observed; the measurements are higher for smaller particle sizes due to the larger surface area. In the case of larger particle sizes, the material is not completely homogeneous, and even though up to 5 replicates were run for each sample, it was very difficult to obtain a sample that would be similar to the previous one.

Table A.1. Humidity of samples carbonation experiment

Day No.	Humidity %	
	1	2
1	18	80
3	22	84
4	32	66
5	29	69
6	28	88
7	25	84
10	11	67
11	27	72
12	16	66
13	43	85
14	39	80
17	30	80
18	21	65
19	16	62
20	26	65
21	15	91
24	11	66
25	11	65
26	11	61
27	11	66
28	11	63
31	13	84
32	11	95
33	11	86
34	11	95
35	11	94
Average	20	76
Std. Dev.	10	12

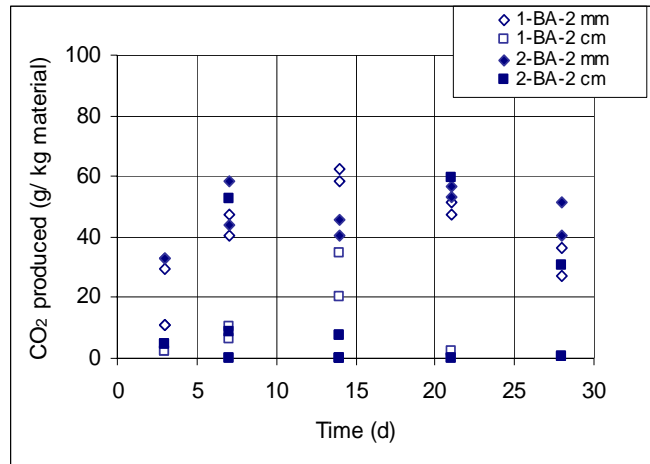


Figure A.3. Carbonation data for BA. (1-BA-2: low humidity, 2 mm; 1-BA-5: low humidity, 5 mm; 2-BA-2: high humidity, 2 mm; 2-BA-5: high humidity, 5 mm).

Extent of carbonation for LFC is shown in Figure A.4. In this material, the higher humidity results in a slight increase of carbonation in the samples. Replication is better because of the homogeneity of the material for both particle sizes. Smaller particle sizes present a higher degree of carbonation than larger ones, as would be expected.

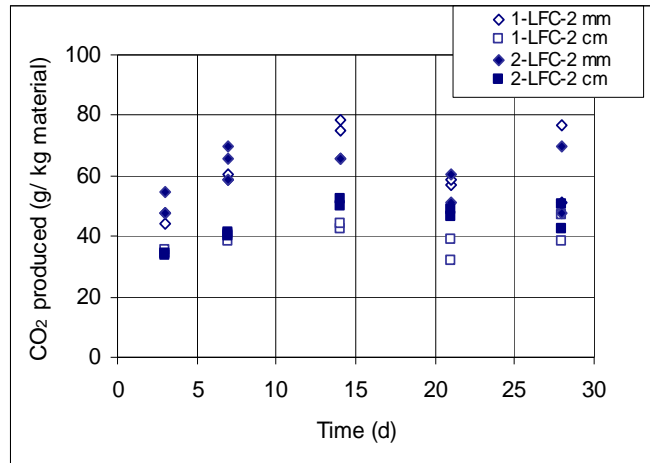


Figure A.4. Carbonation data for LFC. (1-LFC-2: low humidity, 2 mm; 1-LFC-5: low humidity, 5 mm; 2-LFC-2: high humidity, 2 mm; 2-LFC-5: high humidity, 5 mm).

Construction Debris samples only had one particle size, as all the material was crushed below 2 mm after it was received (Figure A.5). Contrary to expected, the degree of carbonation was higher in the sample subjected to a lower humidity. As in the bottom ash experiment, the lack of homogeneity in the sample could be the cause for the poor replication of results. Concrete blocks and brick mainly form construction debris, and given that the samples used for this test were very small, it was difficult to get similar samples for replication.

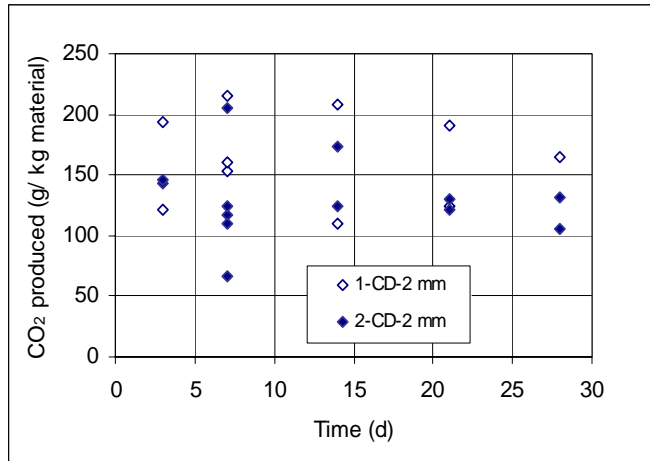


Figure A.5. Carbonation data for CD (1-CD: low humidity, and 2-CD: high humidity).

Conclusions and Recommendations

When both particle sizes are compared, smaller particles do not seem to have a higher degree of carbonation than larger particles. This might be the result of the size of sample used. Higher humidity levels show a small increase in the extent of carbonation. After 15 days, the carbonation degree reaches a high level, so it is possible to assume that a sample that has been carbonated for 15 days or more has reached full carbonation under the conditions provided in this experiment. The recommended conditions for obtaining a carbonated sample are to place the material in a pressurized container with a carbon dioxide enriched atmosphere (20% CO₂-80%N₂) for a minimum time of 15 days and with a relative humidity of at least 60%.

APPENDIX B

EXPERIMENTAL RESULTS

pH, conductivity values, and concentrations of Al, As, Ba, Ca, Cd, Cl, Cu, Fe, K, Na, Mg, Pb, Se, SO₄, Sr and Zn are presented for ARR, BA, CD, CFA #1, CFA # 2 and LFC. Results are shown for batch and column testing release as a function of pH, as a function of LS ratio, and for cumulative release as a function of LS ratio. Cumulative release (mg/kg) is calculated according to Equation B.1:

$$Cumulative = \left(\frac{\left(\frac{C_{i+1} - C_i}{2} \right)}{M_{column}} (V_{i+1} - V_i) \right) \quad (B.1)$$

where C is the concentration of the species (mg/L), V is the volume between intervals $i+1$ and i (L) and M is the total weight of the column (kg). Residuals, calculated as presented in Chapter 4, are also shown for each graph as a function of LS ratio.

Additionally, for ARR, BA and LFC, graphs comparing selected column results in terms of activity to activity from batch results are shown for species with valences of ± 1 , ± 2 and ± 3 . Figure B.1 presents a general case for the changes in the activity coefficient, as a function of ionic strength, for species with valences of ± 1 , ± 2 and ± 3 . This is a general case because the ionic strength used for this graph is not obtained from the conductivities of these particular materials and samples. The equations to obtain activity

and the activity coefficient from ionic strength, and the equation relating conductivity and ionic strength, were explained in detail in Chapter 2.

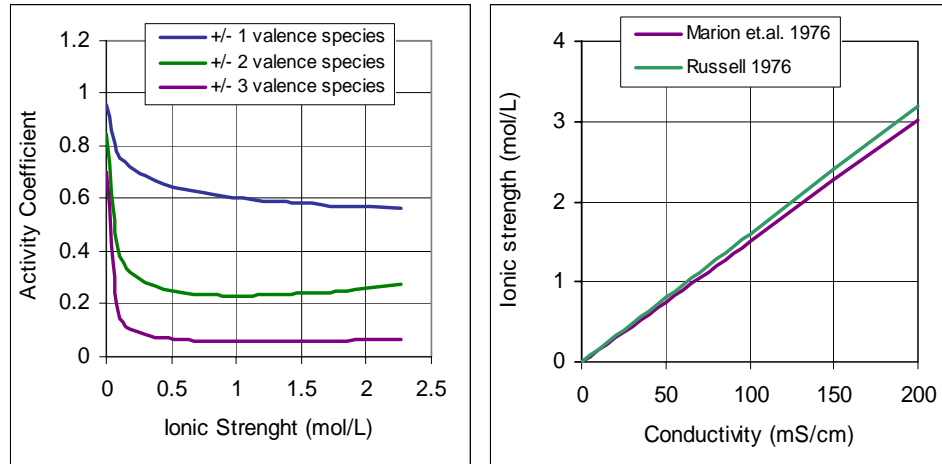


Figure B.1. Relationship between activity coefficient, ionic strength and conductivity.

Statistical data for all experimental data shown in this appendix is presented and explained at the end of this section.

Aluminum Recycling Residue

pH and conductivity data

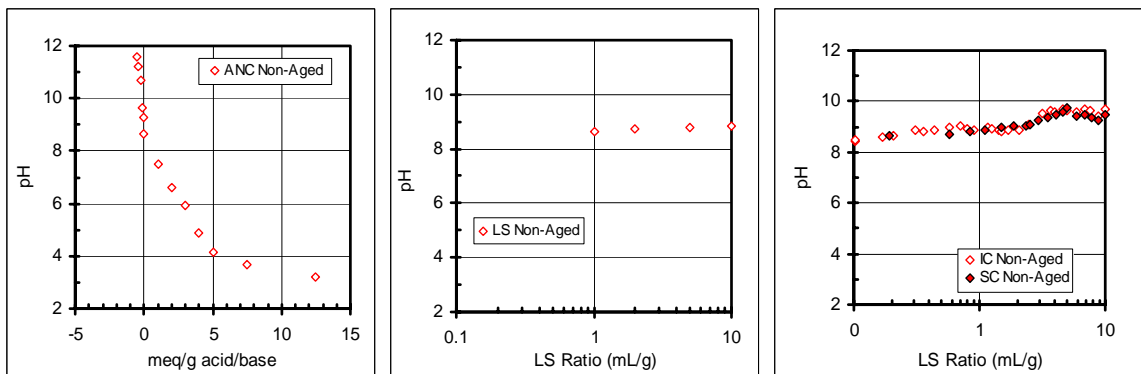


Figure B.2. pH of ARR batch and column testing.

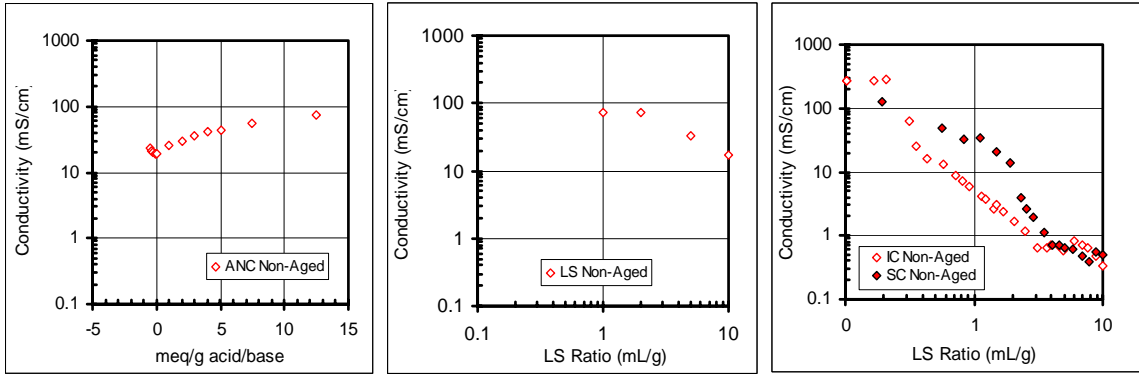


Figure B.3. Conductivity of ARR batch and column testing.

Activity and ionic strength data

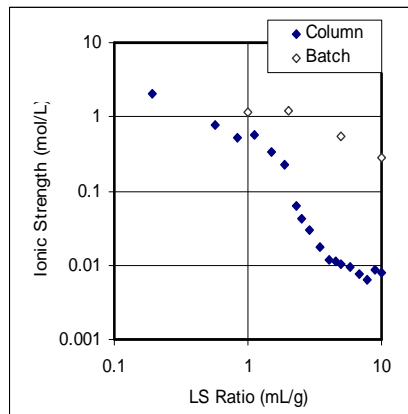


Figure B.4. Ionic strength as a function of LS Ratio for ARR.

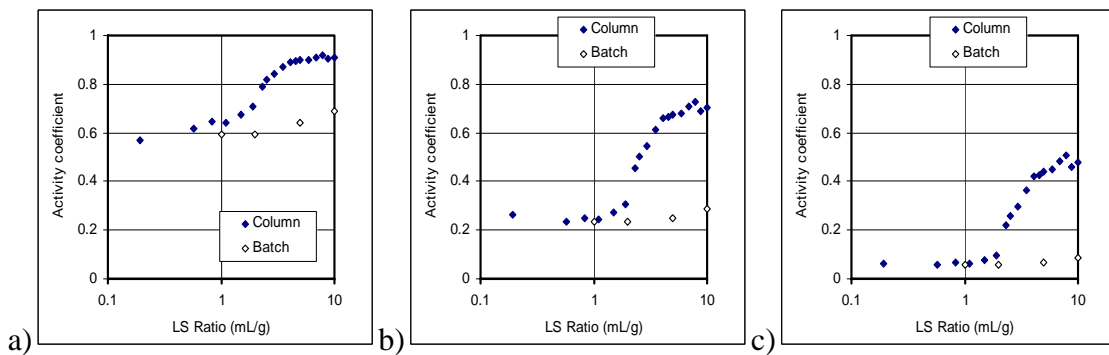


Figure B.5. Activity of a) ± 1 , b) ± 2 and c) ± 3 species for ARR (SC column data).

Elemental data

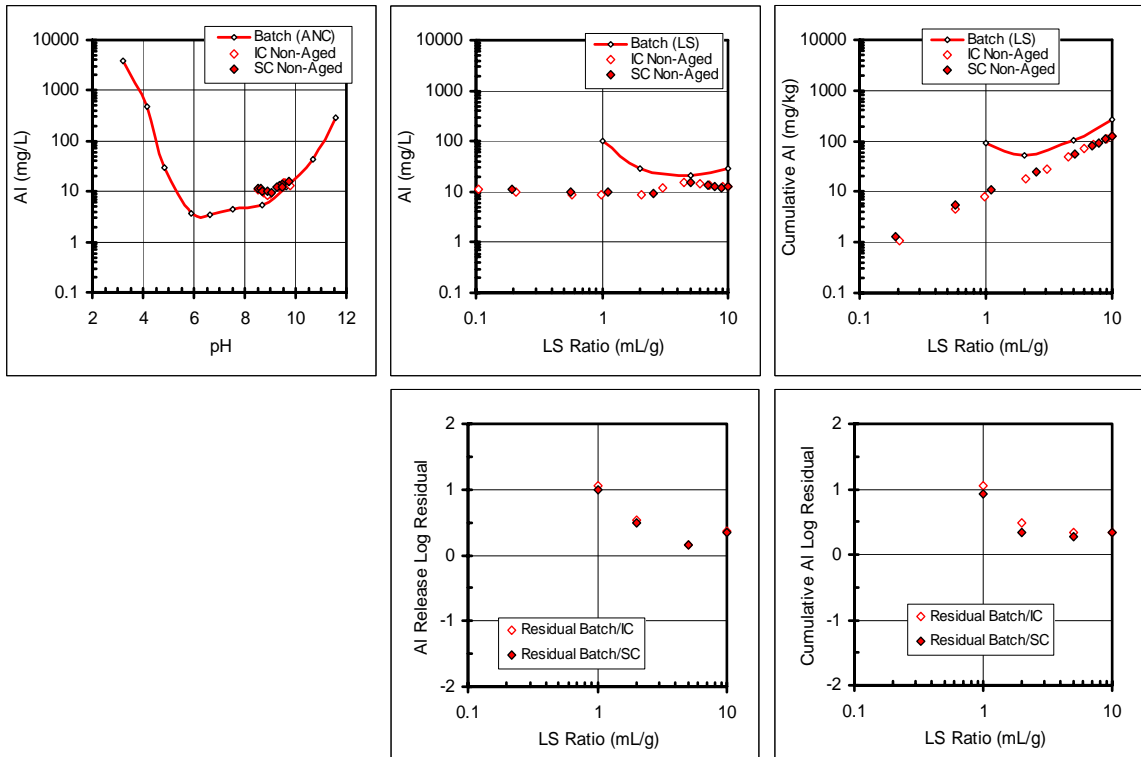


Figure B.6. Al release from ARR as a function of pH and LS ratio.

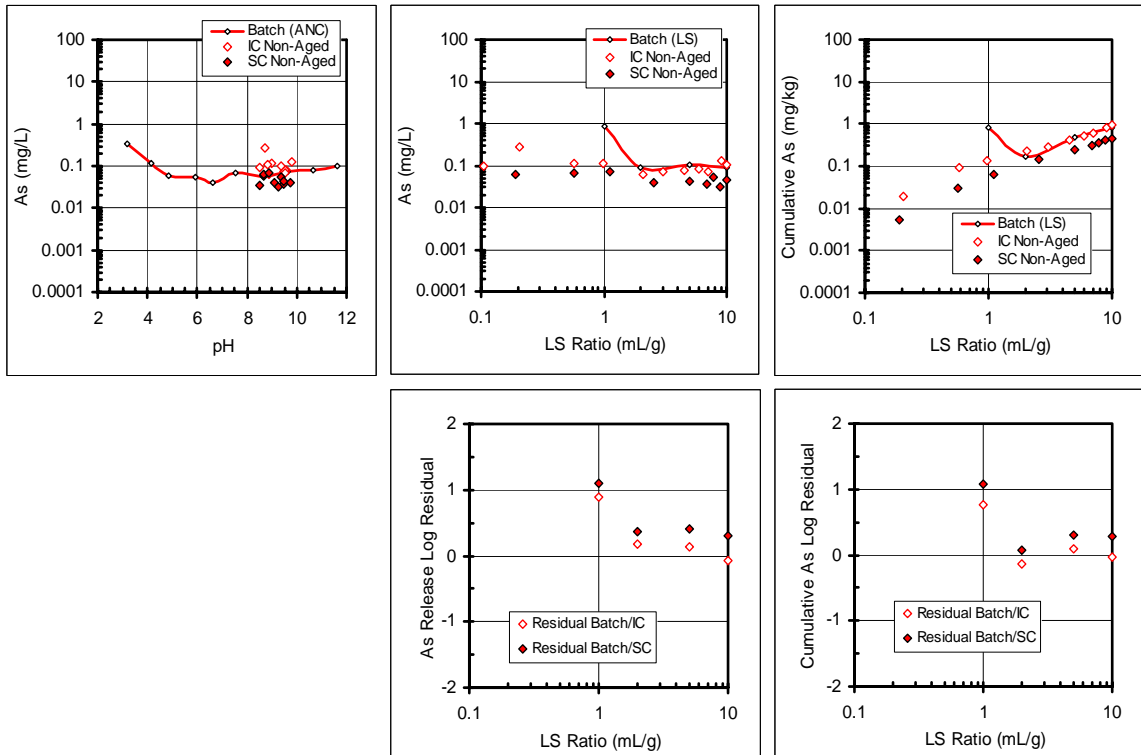


Figure B.7. As release from ARR as a function of pH and LS ratio.

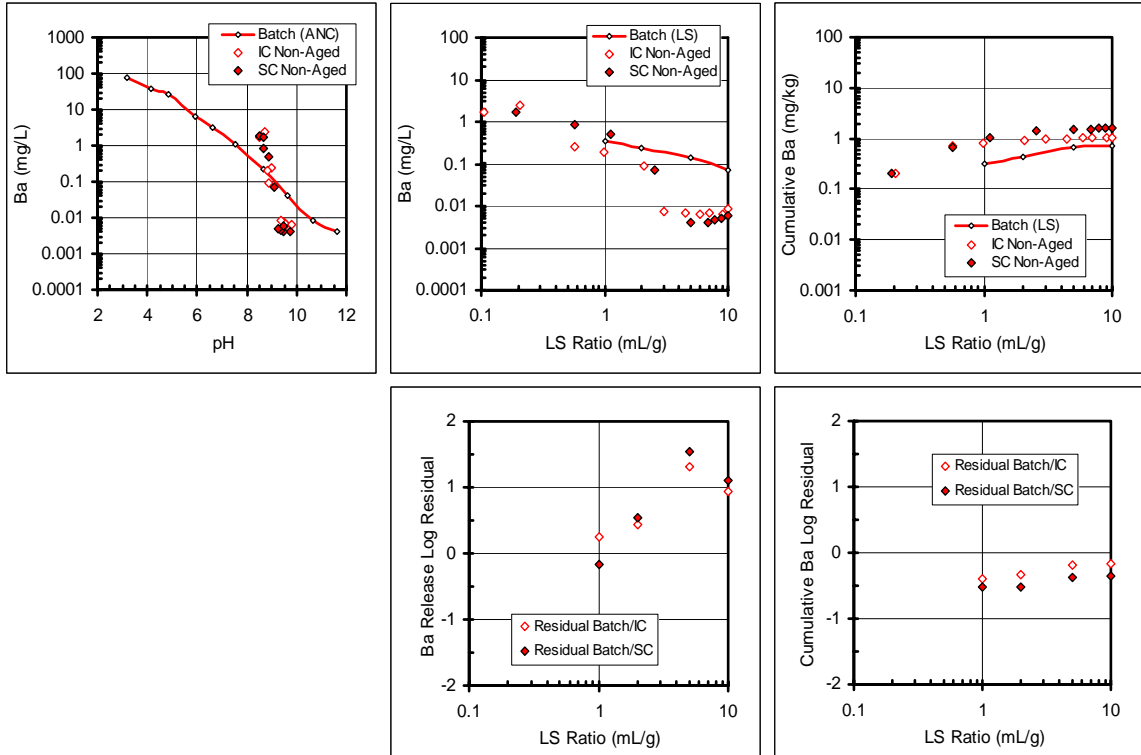


Figure B.8. Ba release from ARR as a function of pH and LS ratio.

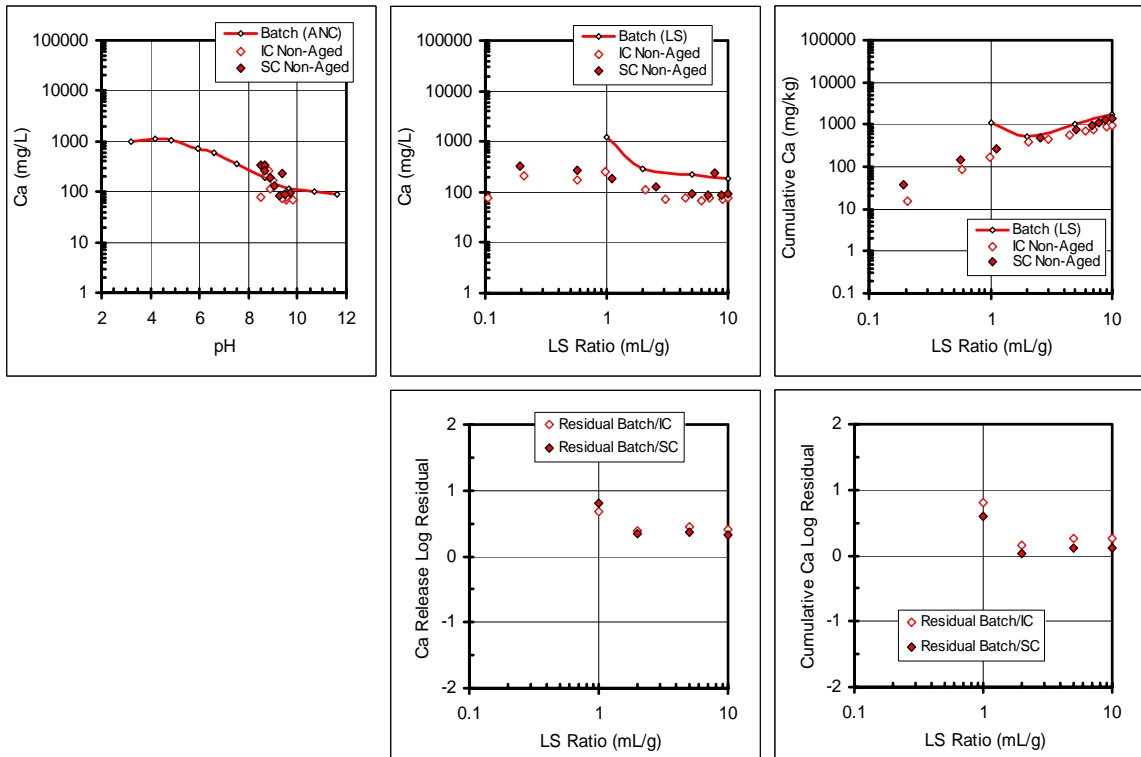


Figure B.9. Ca release from ARR as a function of pH and LS ratio

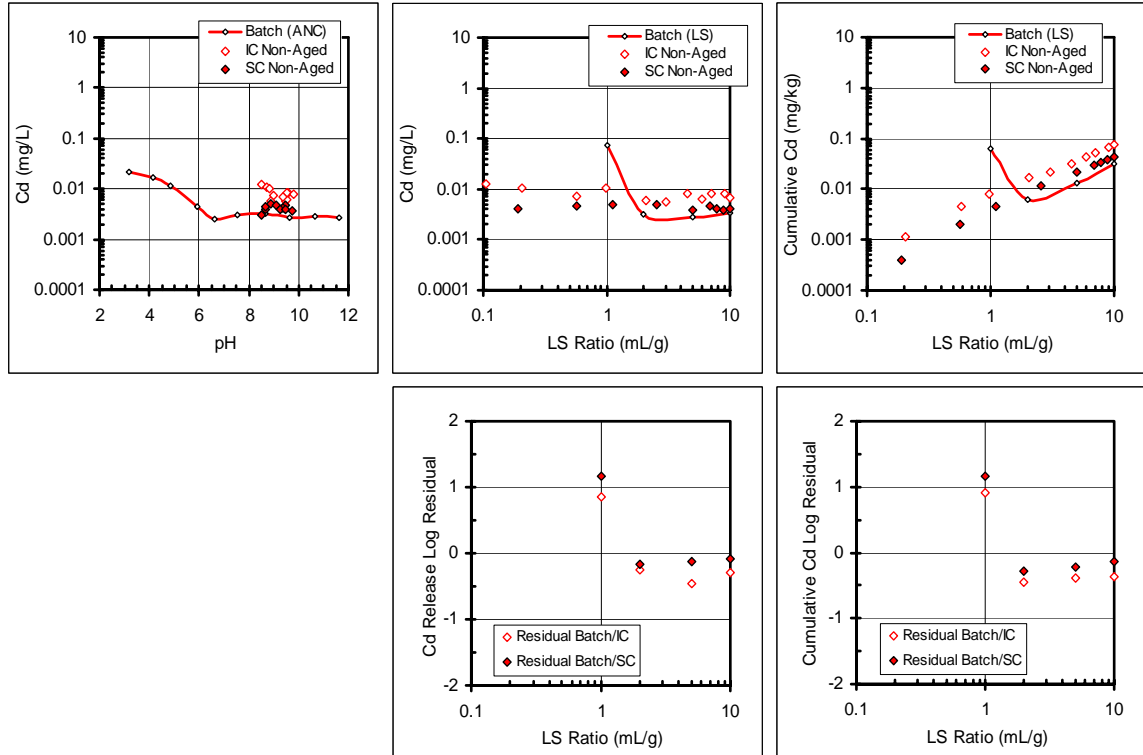


Figure B.10. Cd release from ARR as a function of pH and LS ratio.

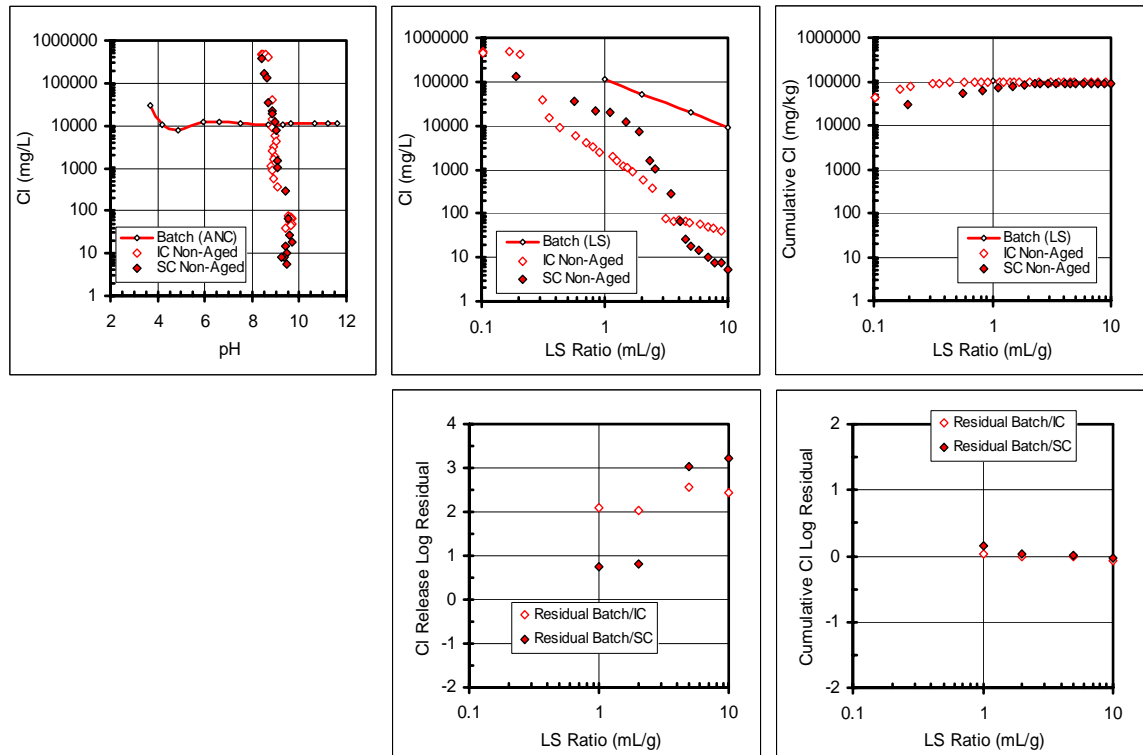


Figure B.11. Cl release from ARR as a function of pH and LS ratio.

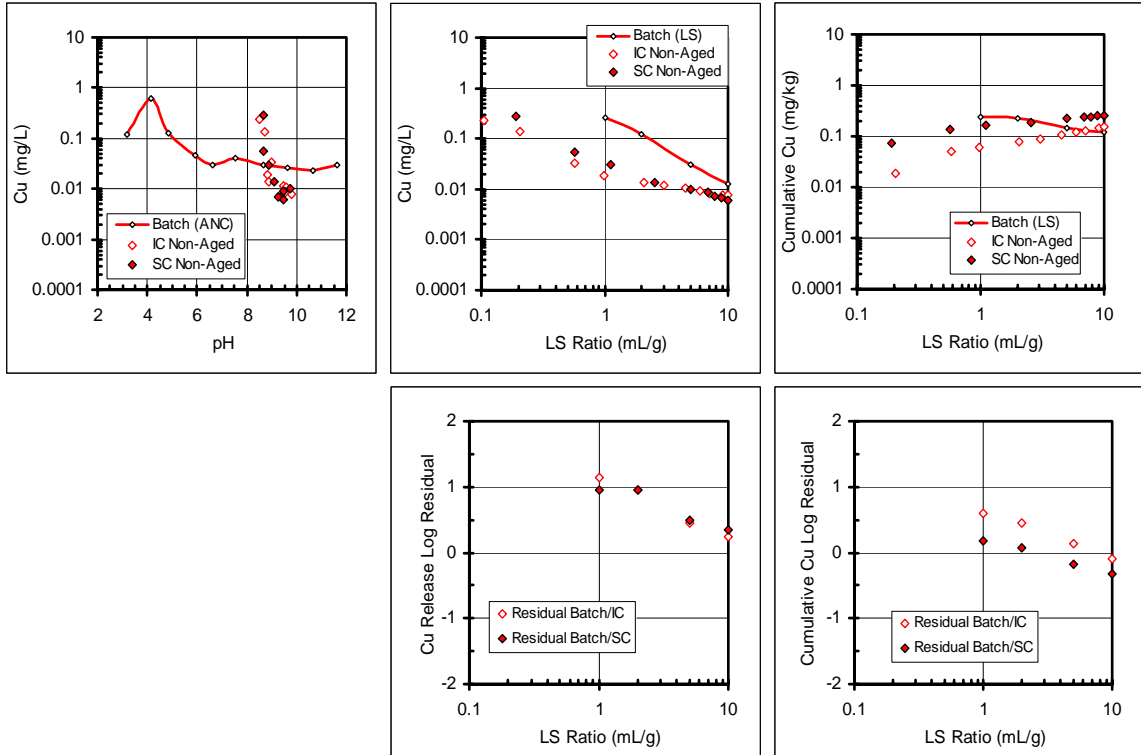


Figure B.12. Cu release from ARR as a function of pH and LS ratio.

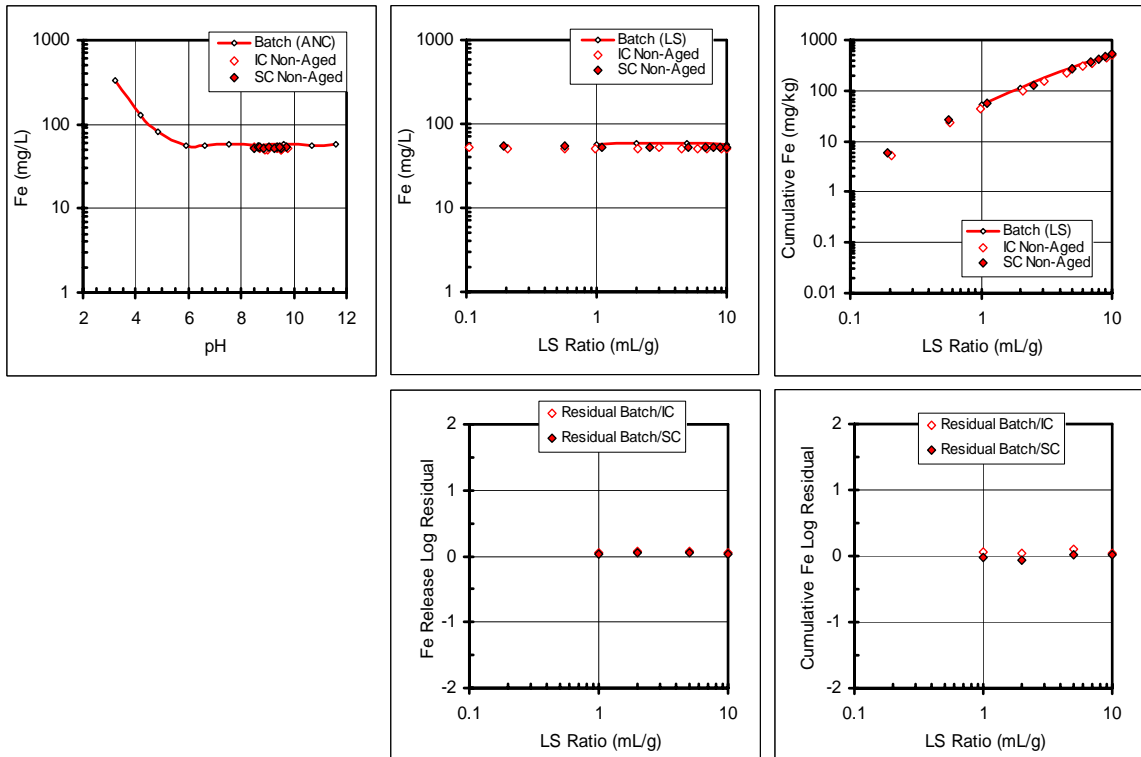


Figure B.13. Fe release from ARR as a function of pH and LS ratio.

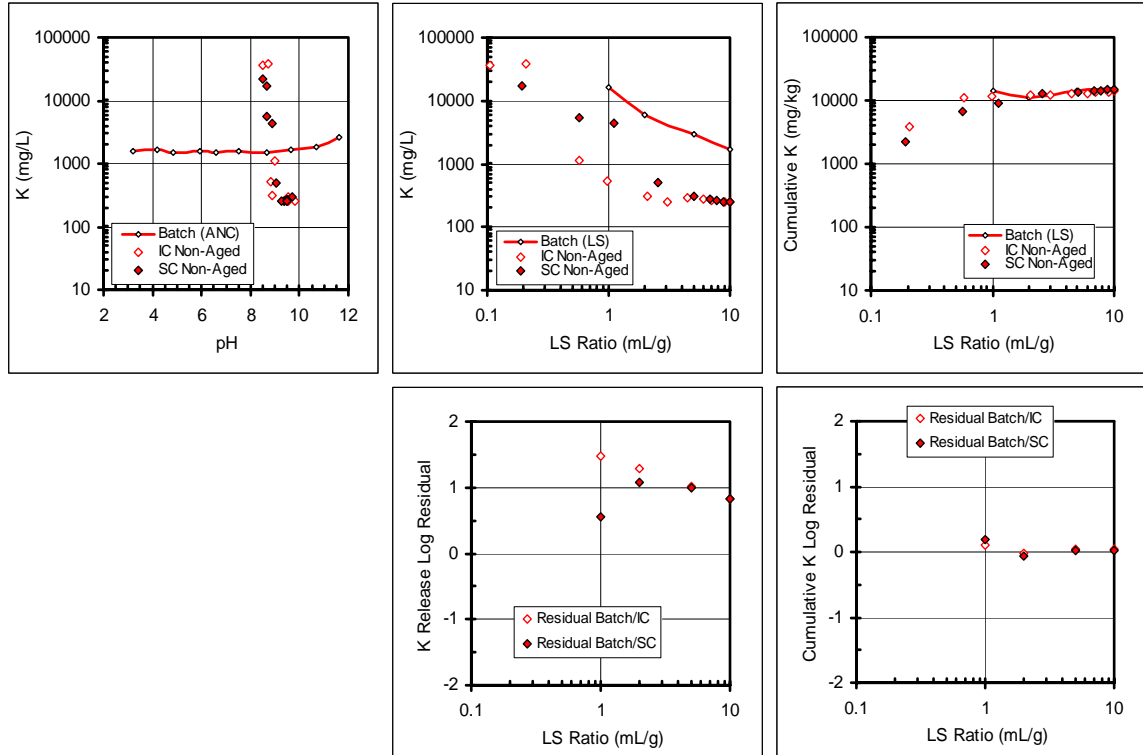


Figure B.14. K release from ARR as a function of pH and LS ratio.

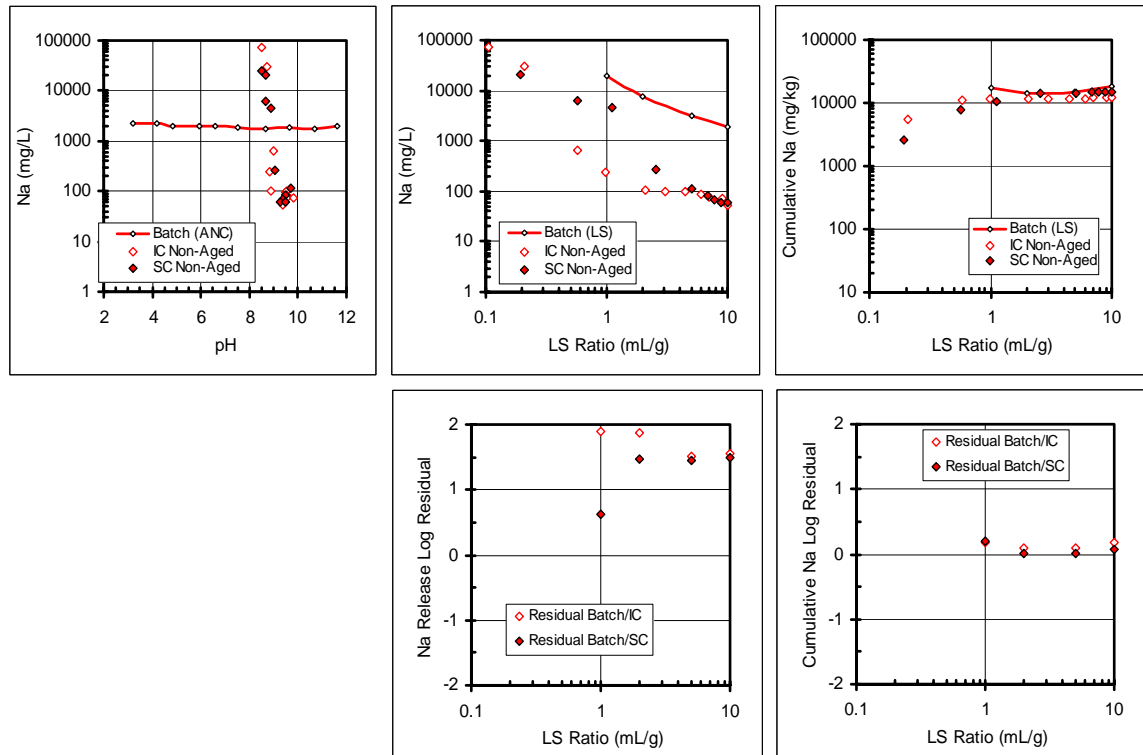


Figure B.15. Na release from ARR as a function of pH and LS ratio.

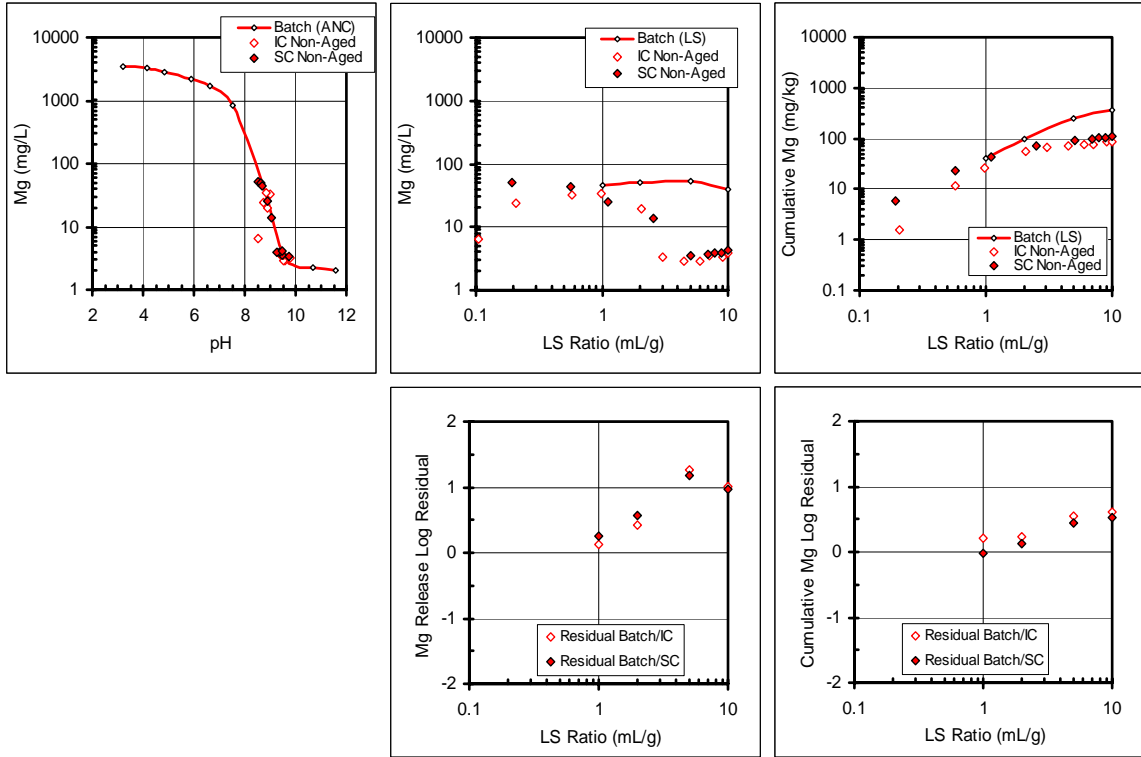


Figure B.16. Mg release from ARR as a function of pH and LS ratio.

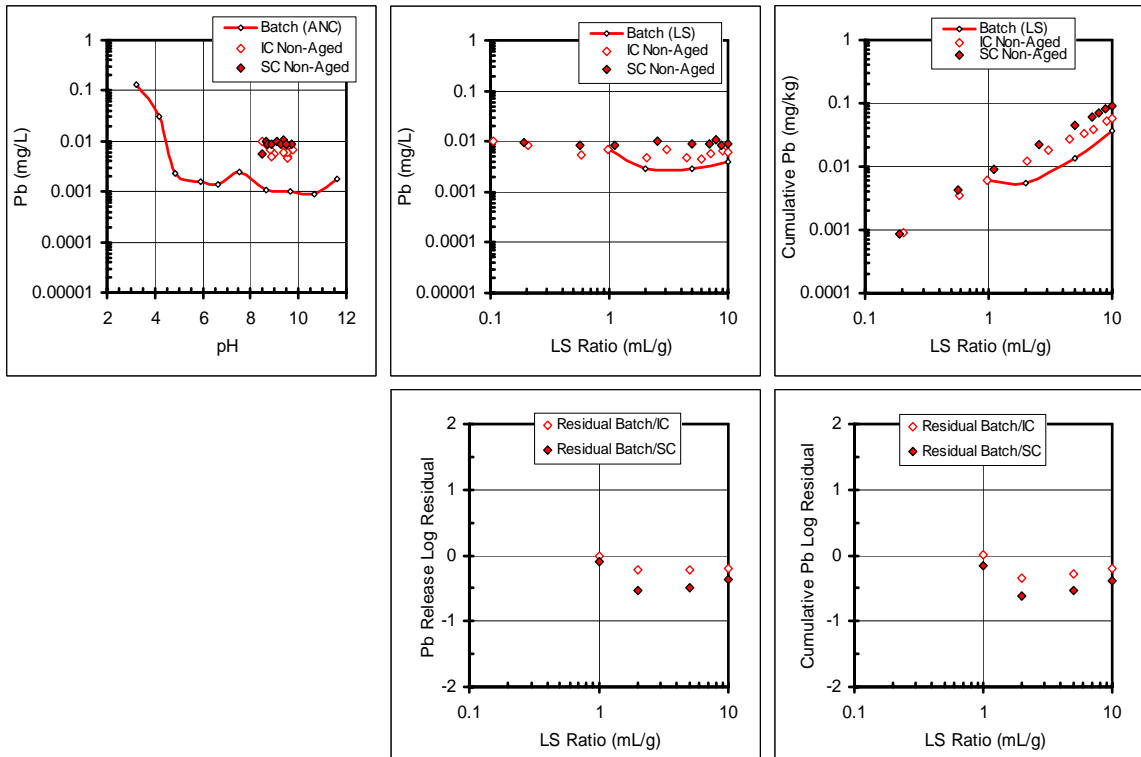


Figure B.17. Pb release from ARR as a function of pH and LS ratio.

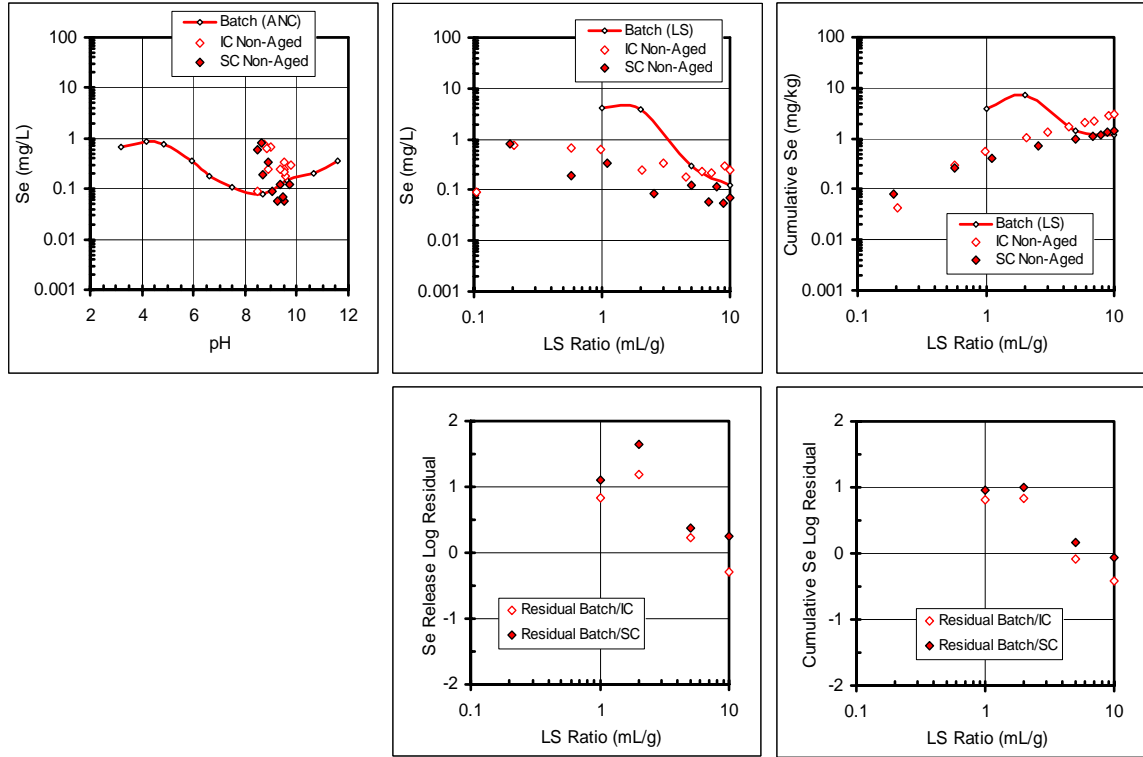


Figure B.18. Se release from ARR as a function of pH and LS ratio.

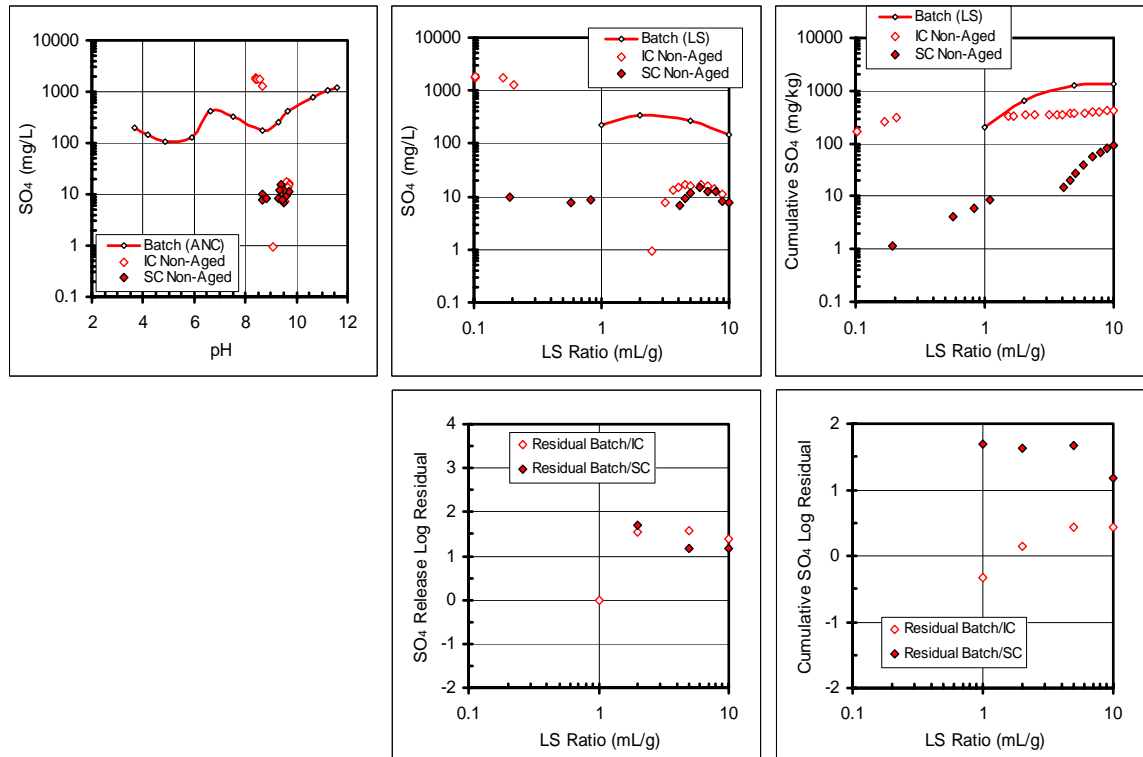


Figure B.19. SO_4 release from ARR as a function of pH and LS ratio.

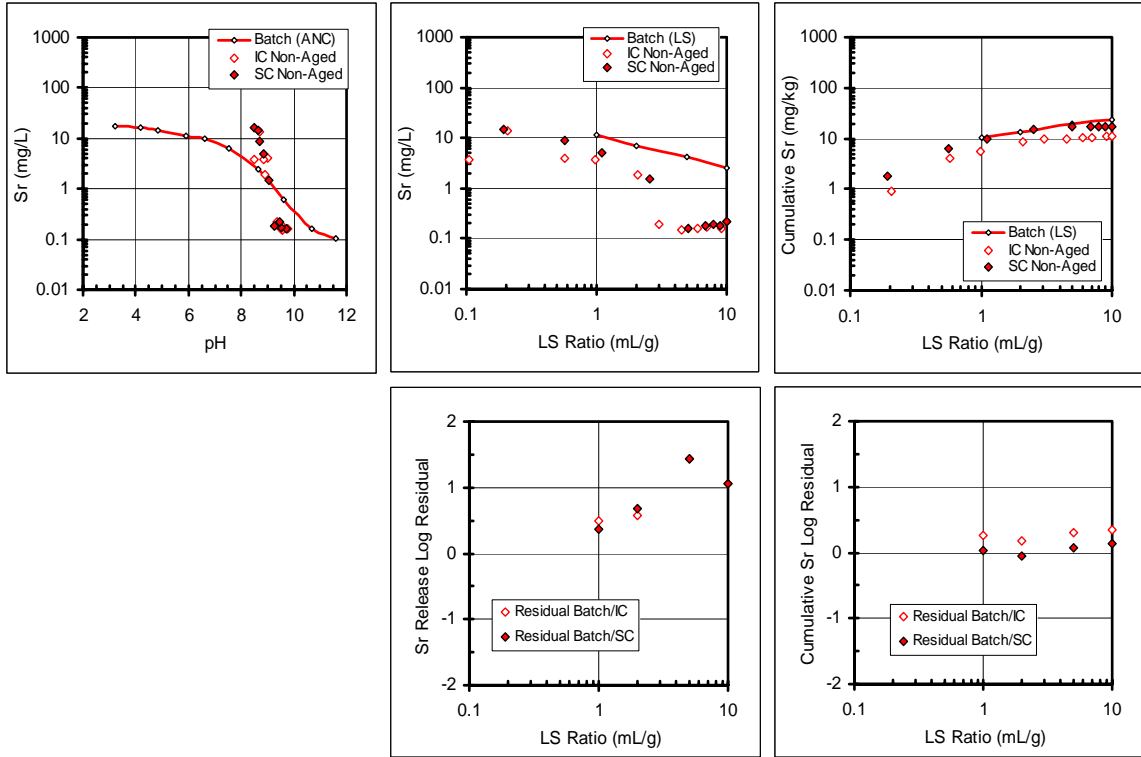


Figure B.20. Sr release from ARR as a function of pH and LS ratio.

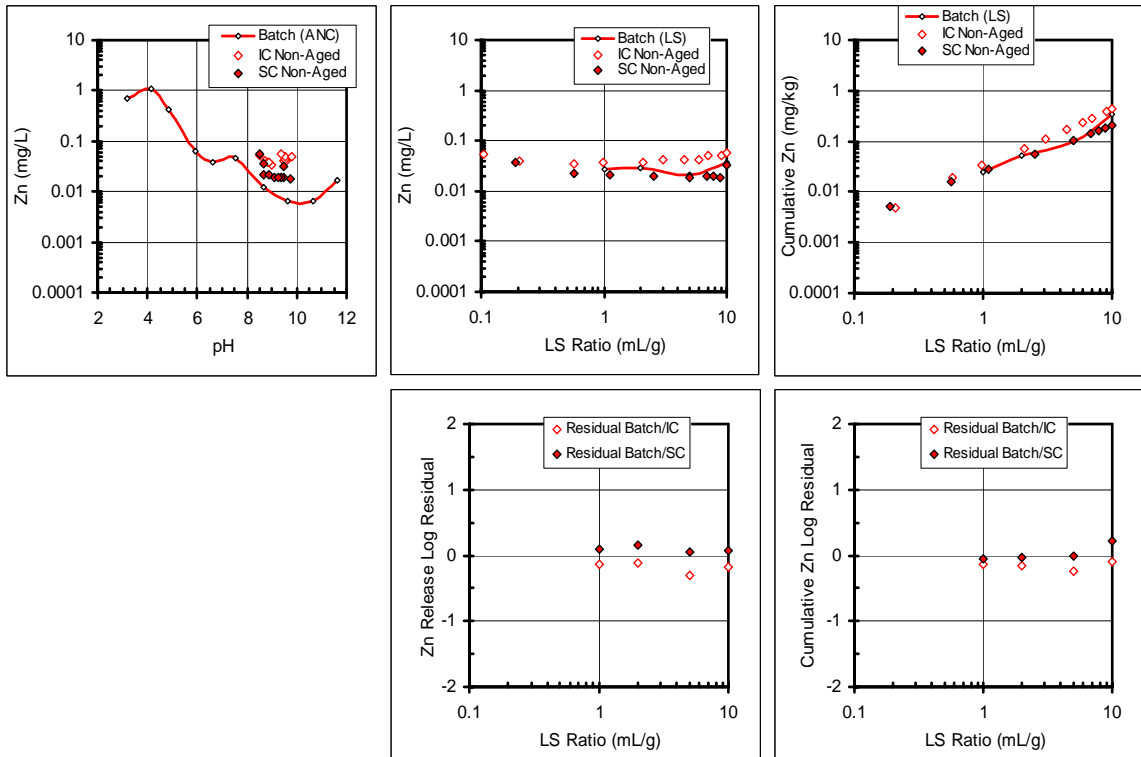


Figure B.21. Zn release from ARR as a function of pH and LS ratio.

MSWI Bottom Ash

pH and conductivity data

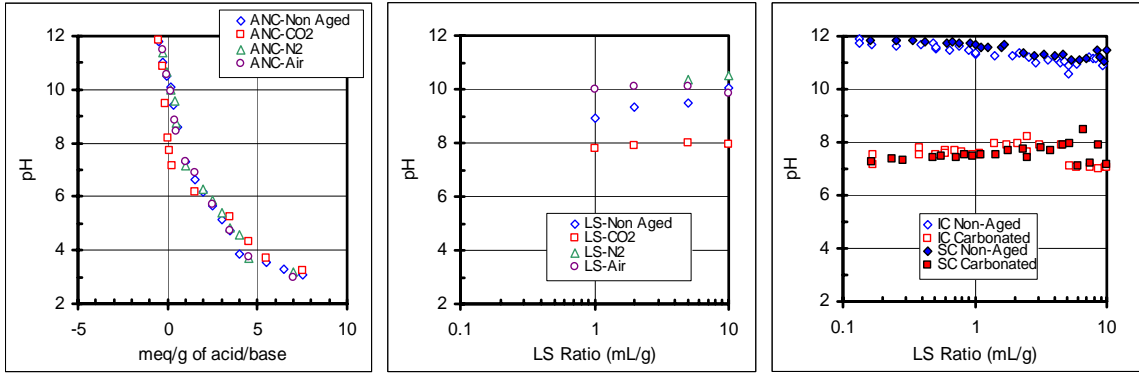


Figure B.22. pH of BA batch and column testing.

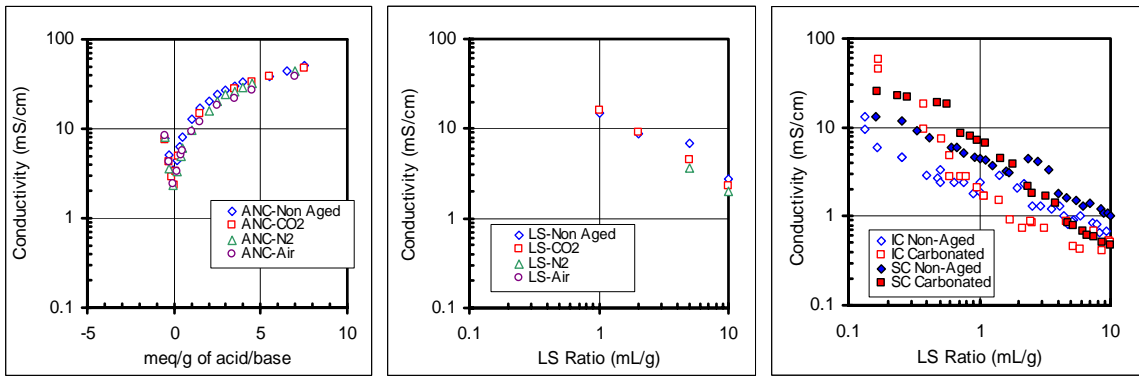


Figure B.23. Conductivity of BA batch and column testing.

Activity and ionic strength data

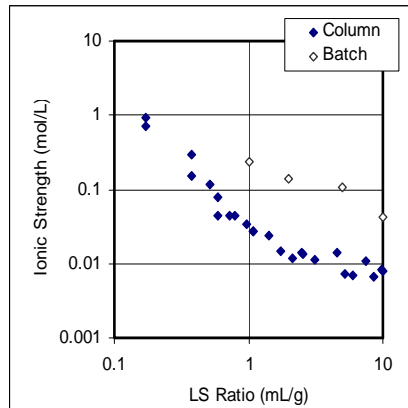


Figure B.24. Ionic strength as a function of LS Ratio for BA

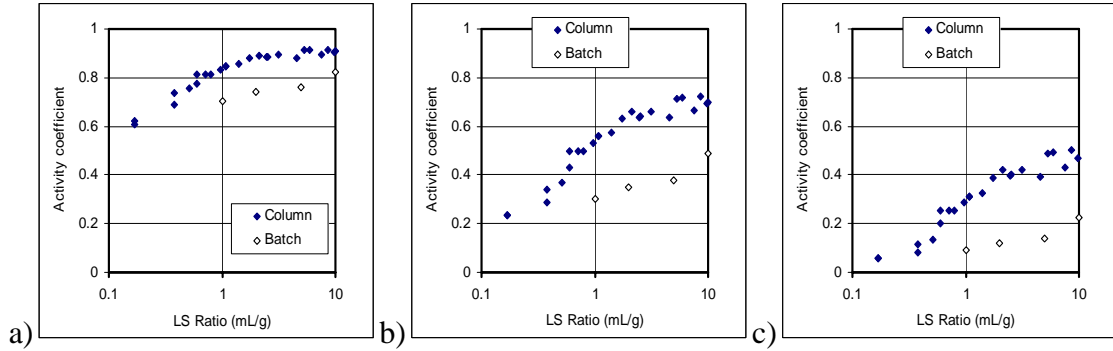


Figure B.25. Activity of a) ± 1 , b) ± 2 and c) ± 3 species for BA (SC column data).

Elemental data

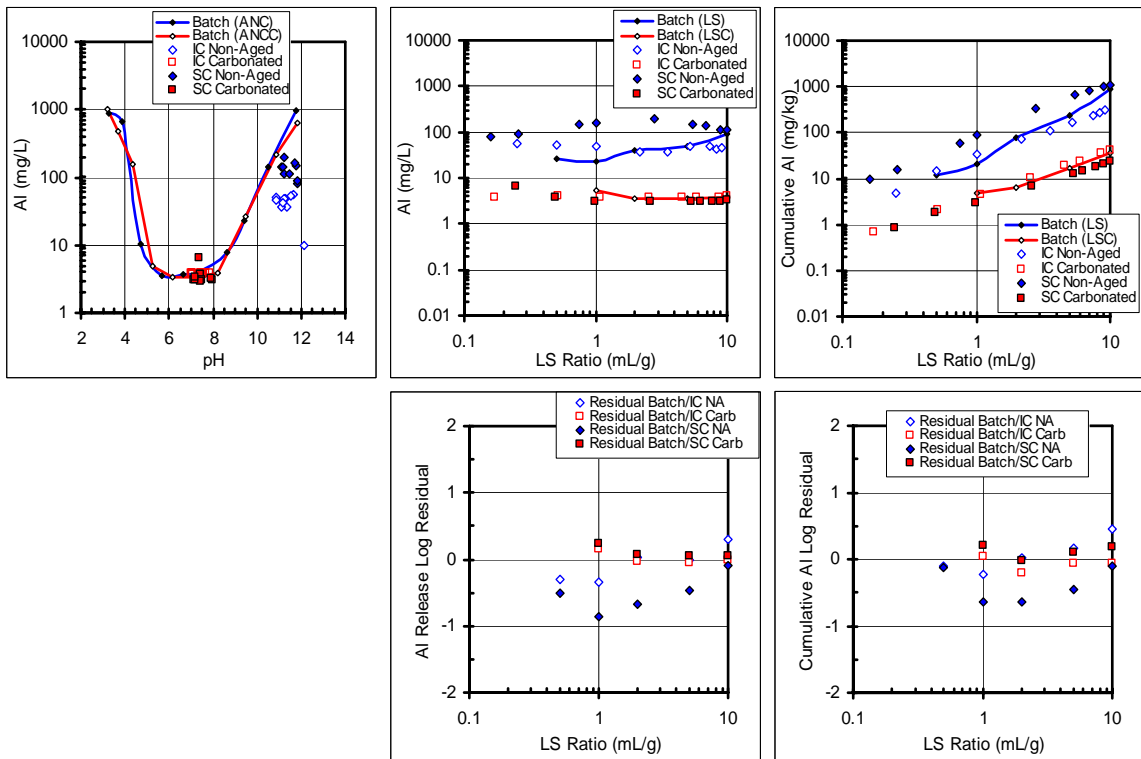


Figure B.26. Al release from BA as a function of pH and LS ratio.

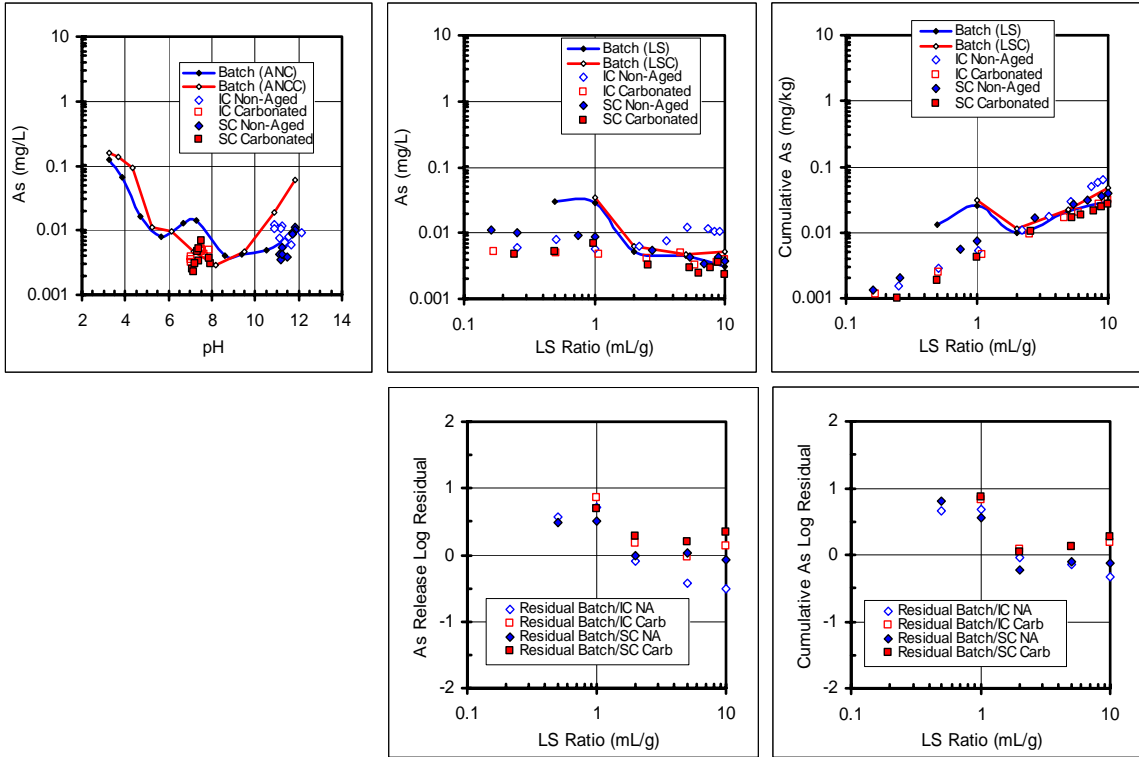


Figure B.27. As release from BA as a function of pH and LS ratio.

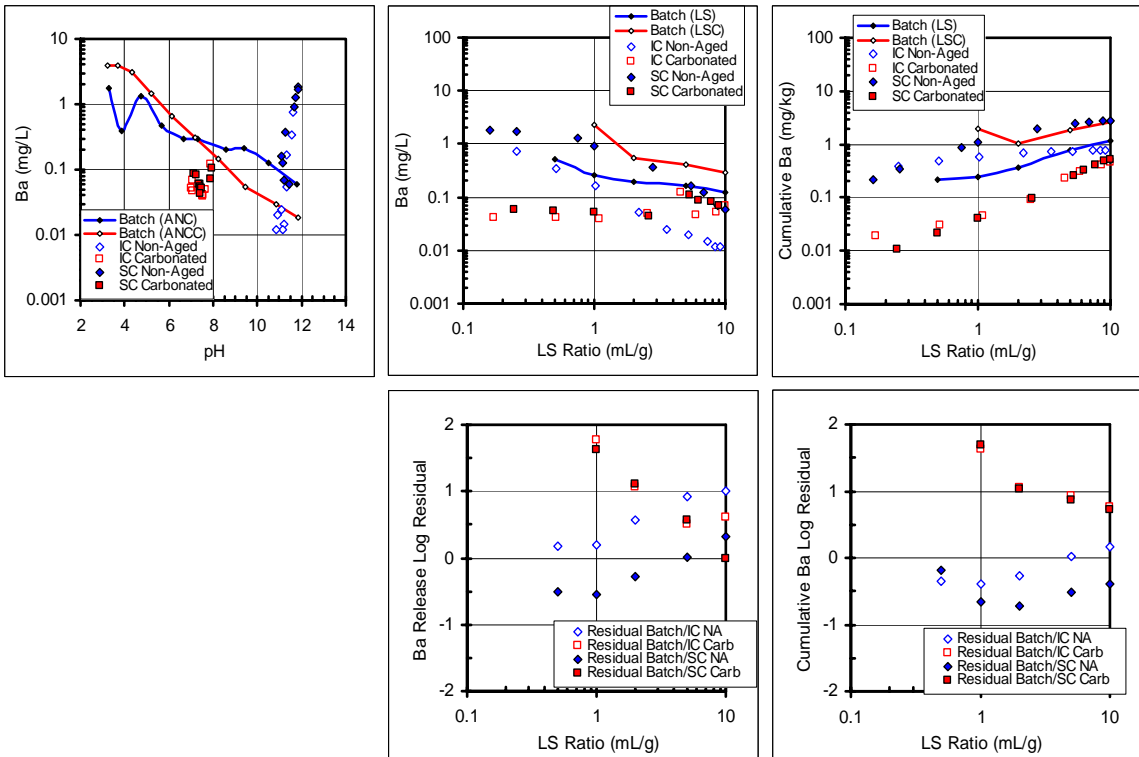


Figure B.28. Ba release from BA as a function of pH and LS ratio.

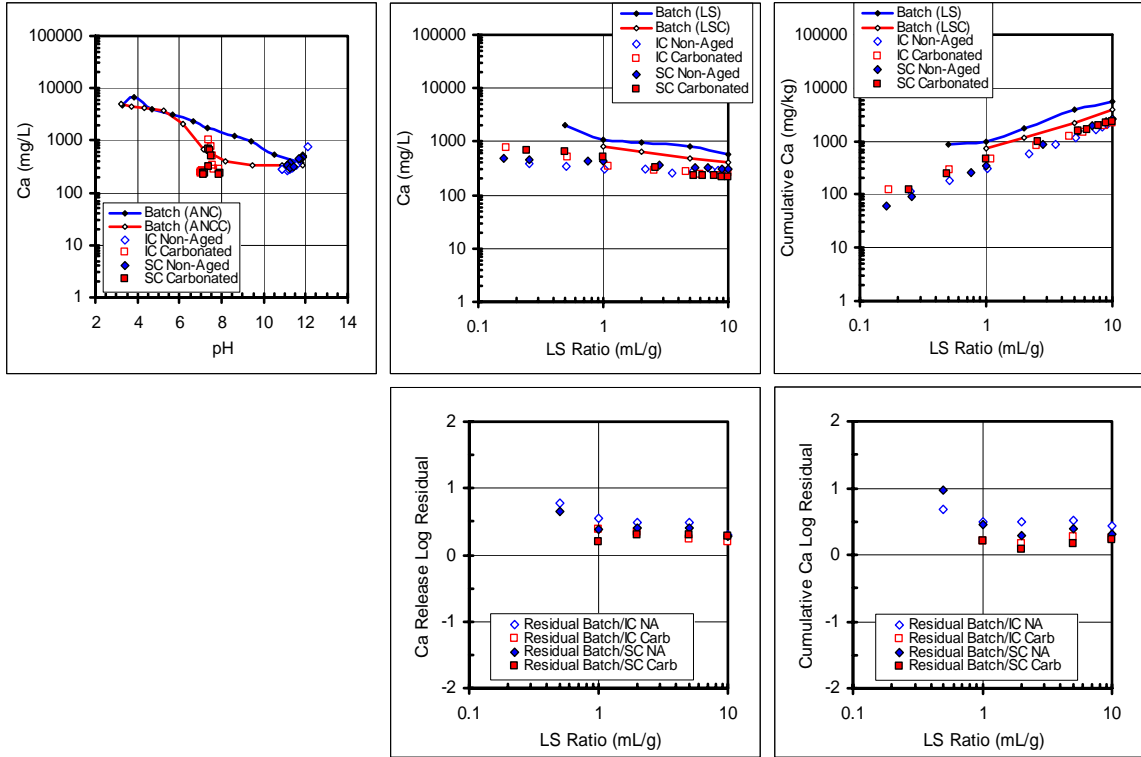


Figure B.29. Ca release from BA as a function of pH and LS ratio.

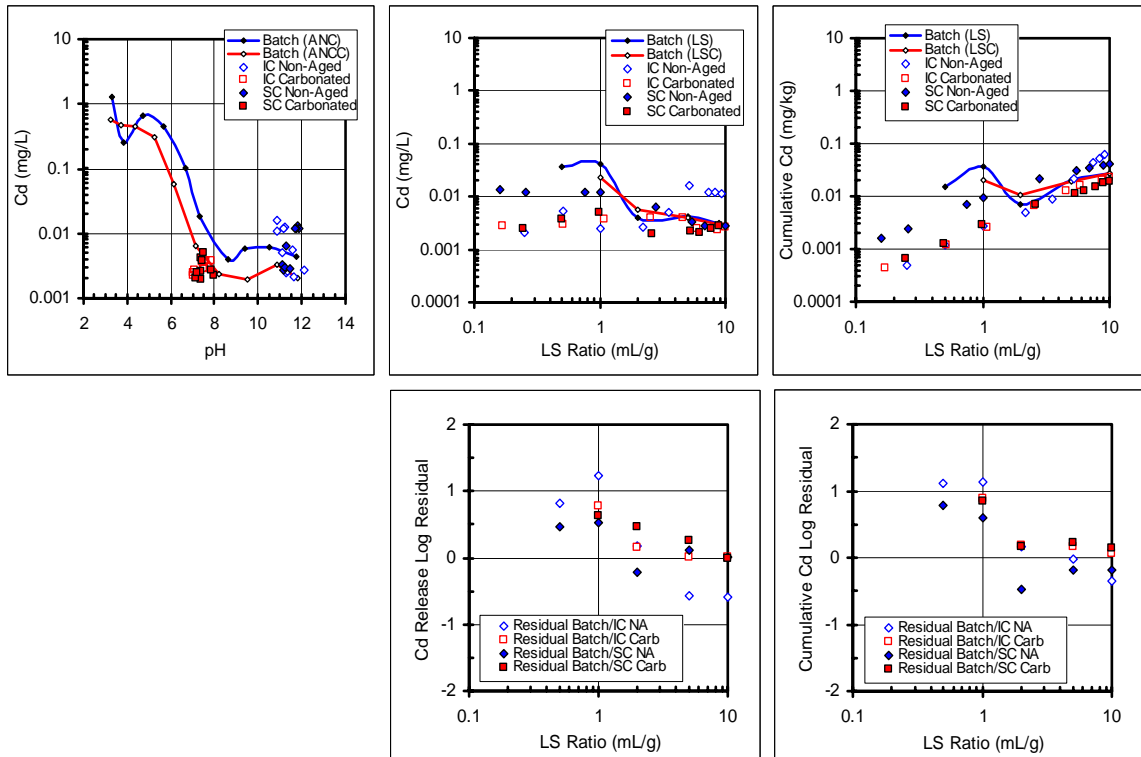


Figure B.30. Cd release from BA as a function of pH and LS ratio.

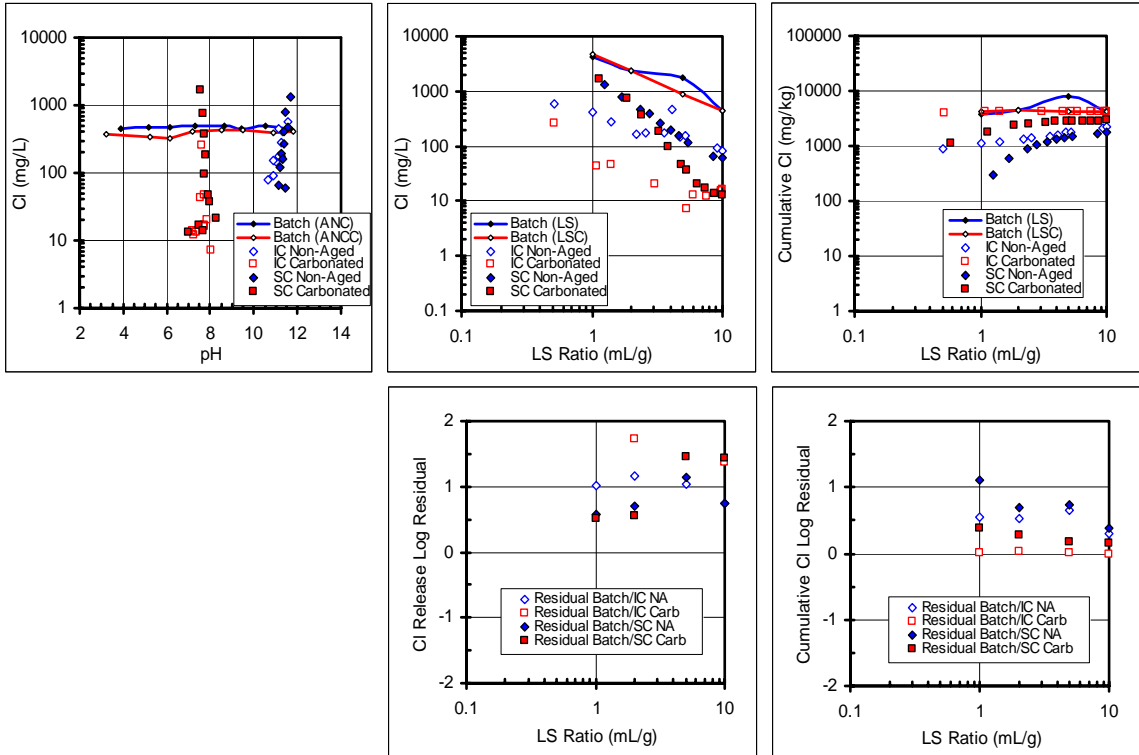


Figure B.31. Cl release from BA as a function of pH and LS ratio.

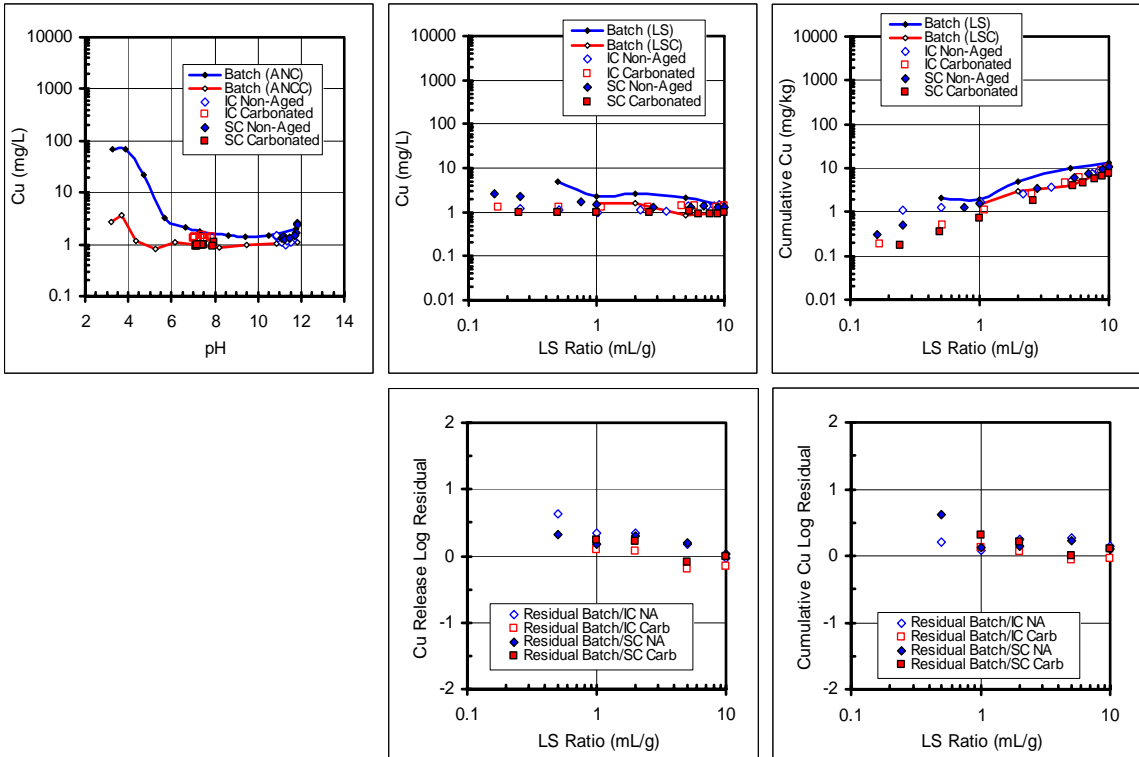


Figure B.32. Cu release from BA as a function of pH and LS ratio.

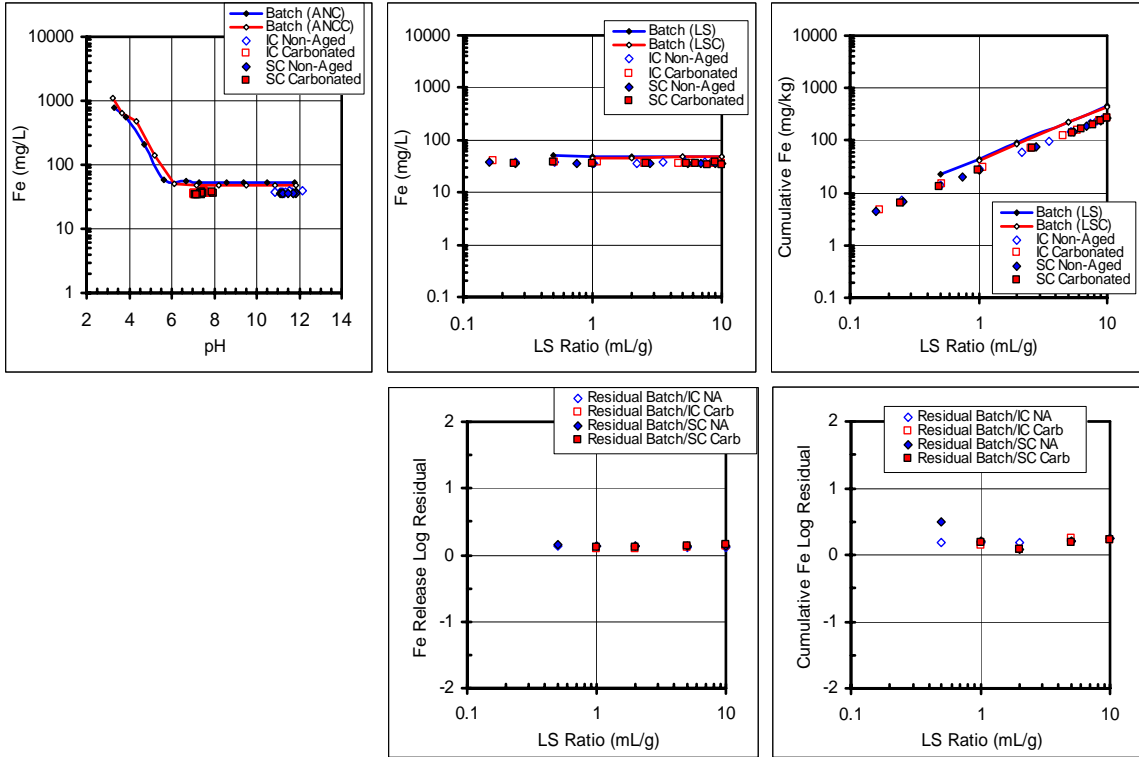


Figure B.33. Fe release from BA as a function of pH and LS ratio.

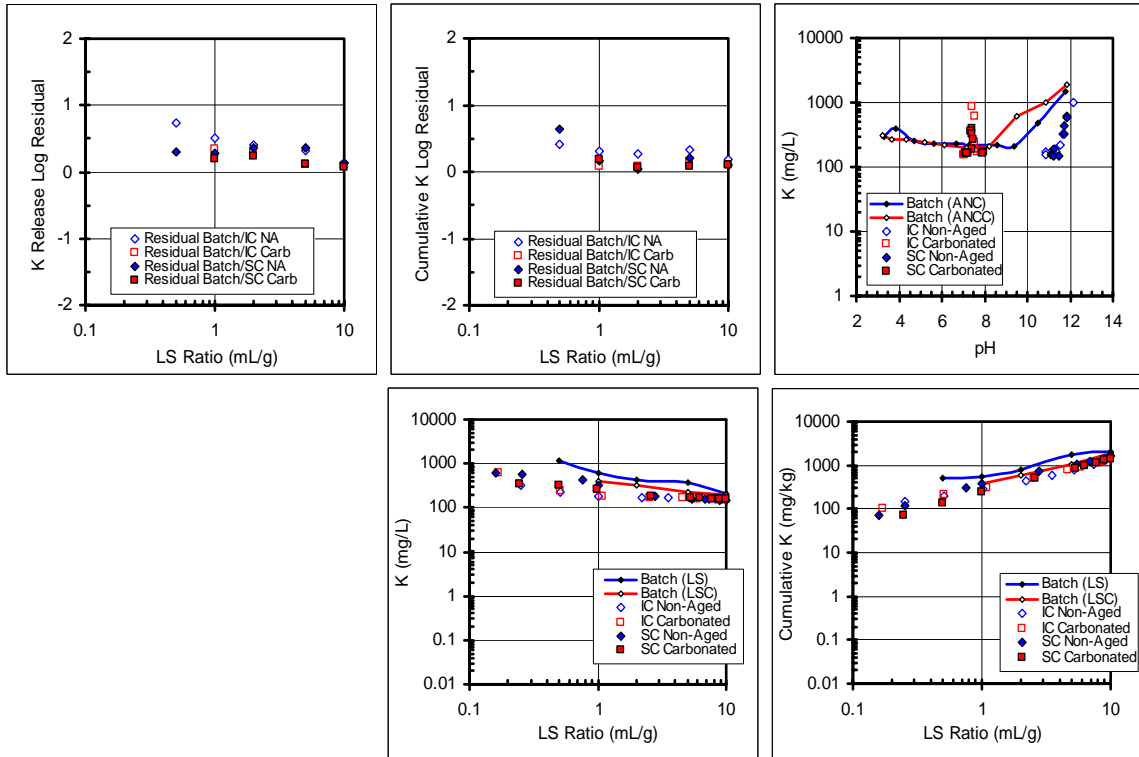


Figure B.34. K release from BA as a function of pH and LS ratio.

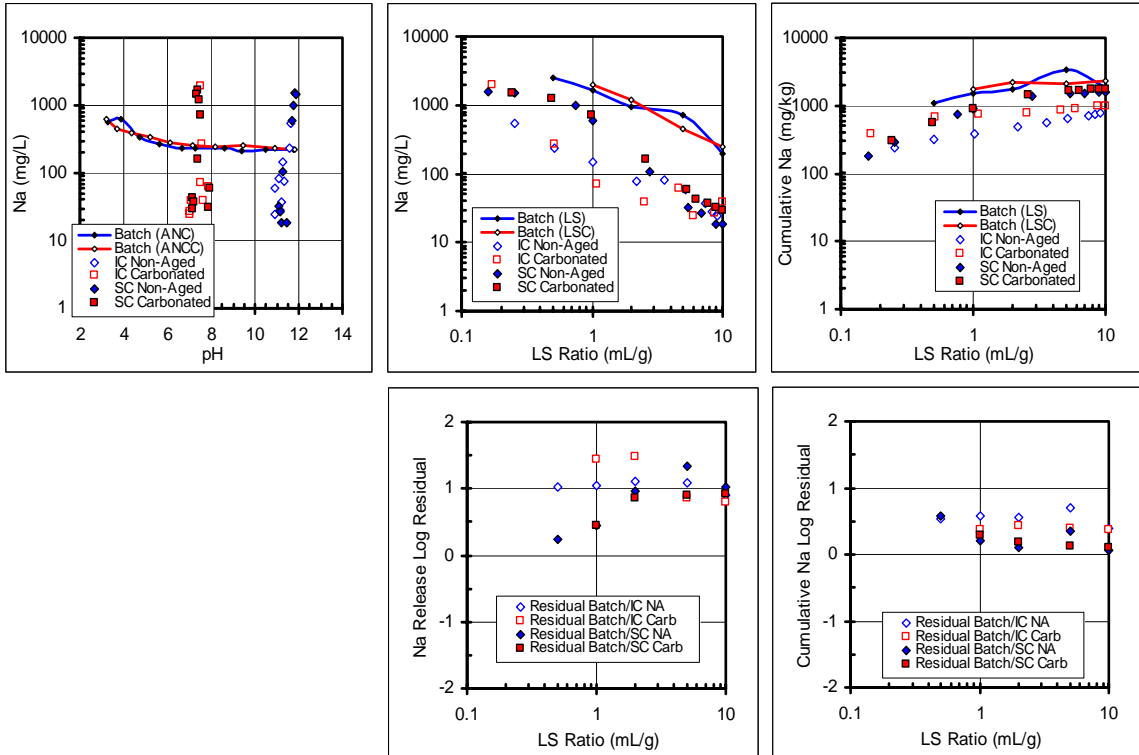


Figure B.35. Na release from BA as a function of pH and LS ratio.

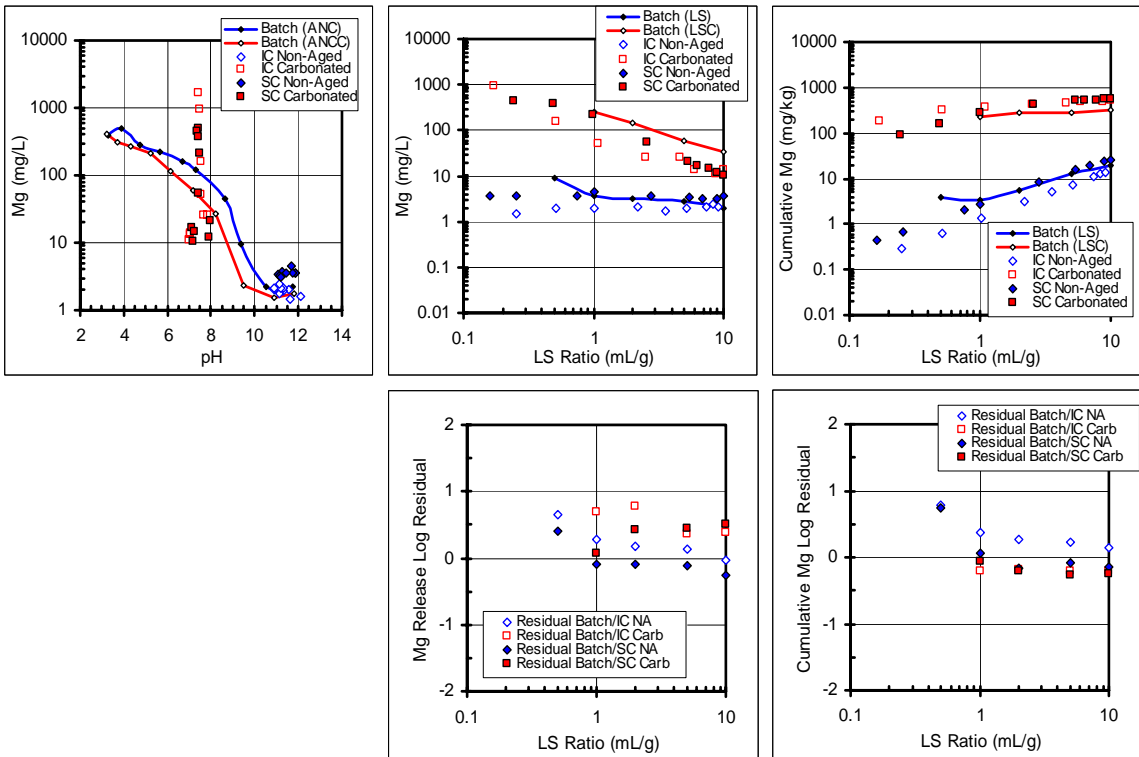


Figure B.36. Mg release from BA as a function of pH and LS ratio.

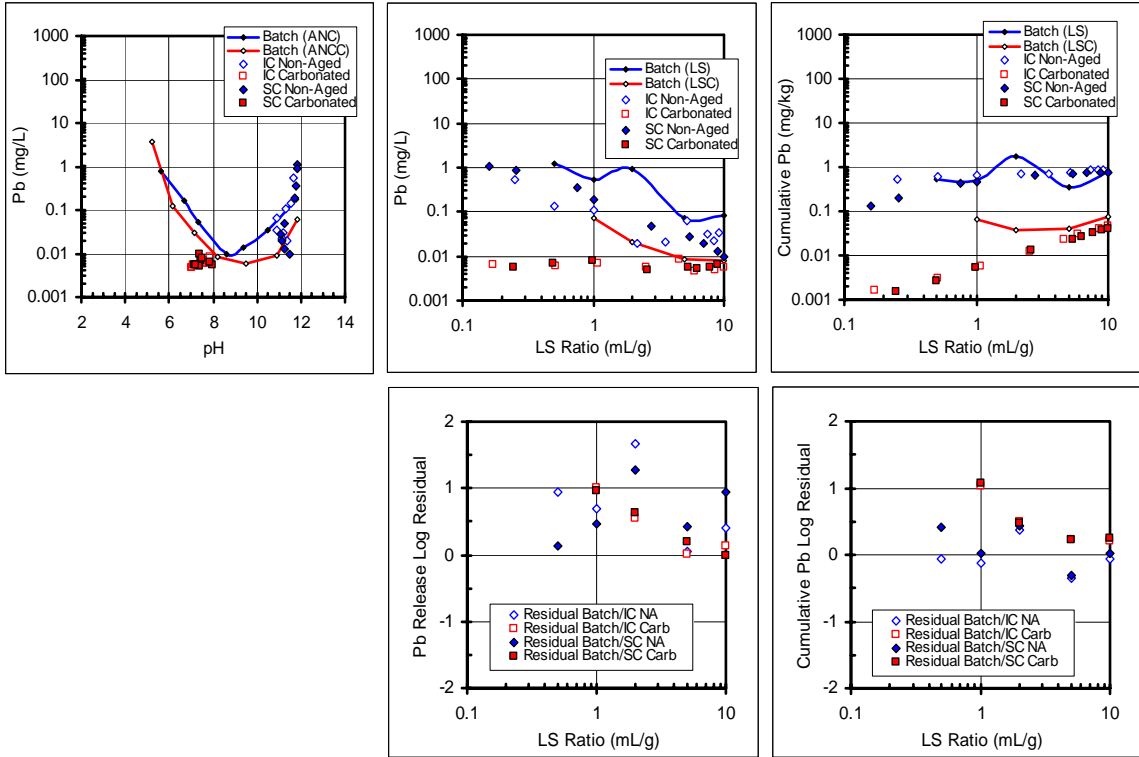


Figure B.37. Pb release from BA as a function of pH and LS ratio.

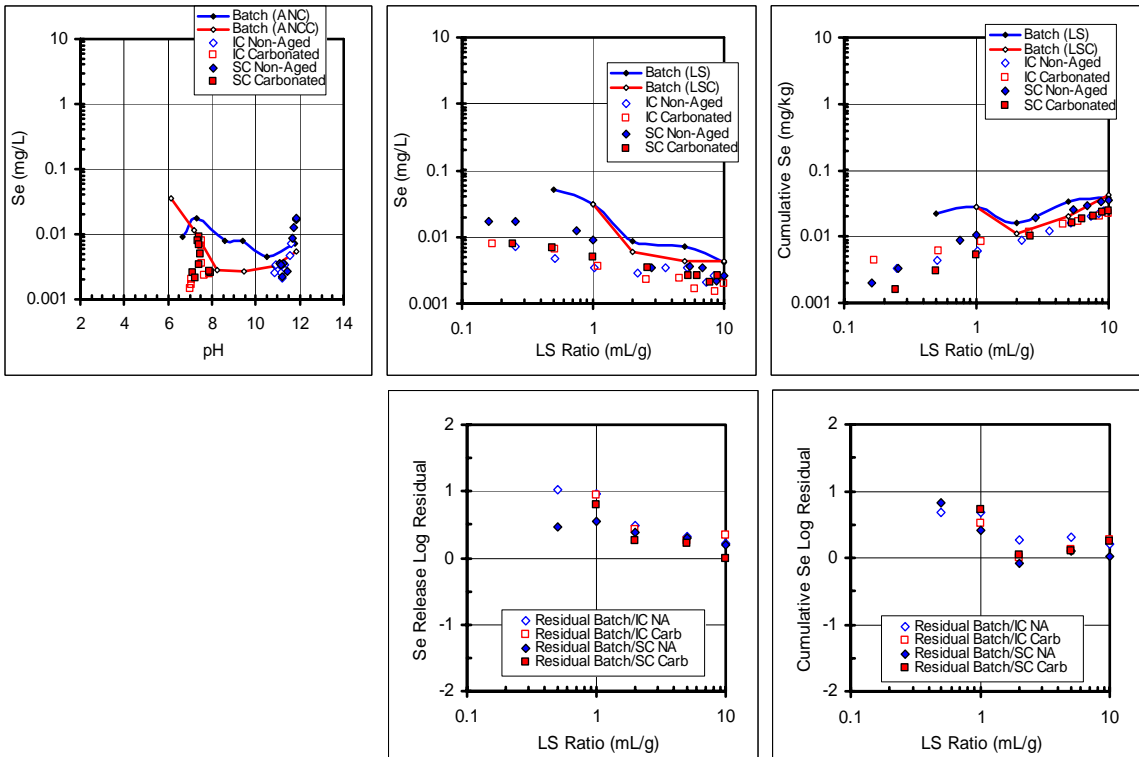


Figure B.38. Se release from BA as a function of pH and LS ratio.

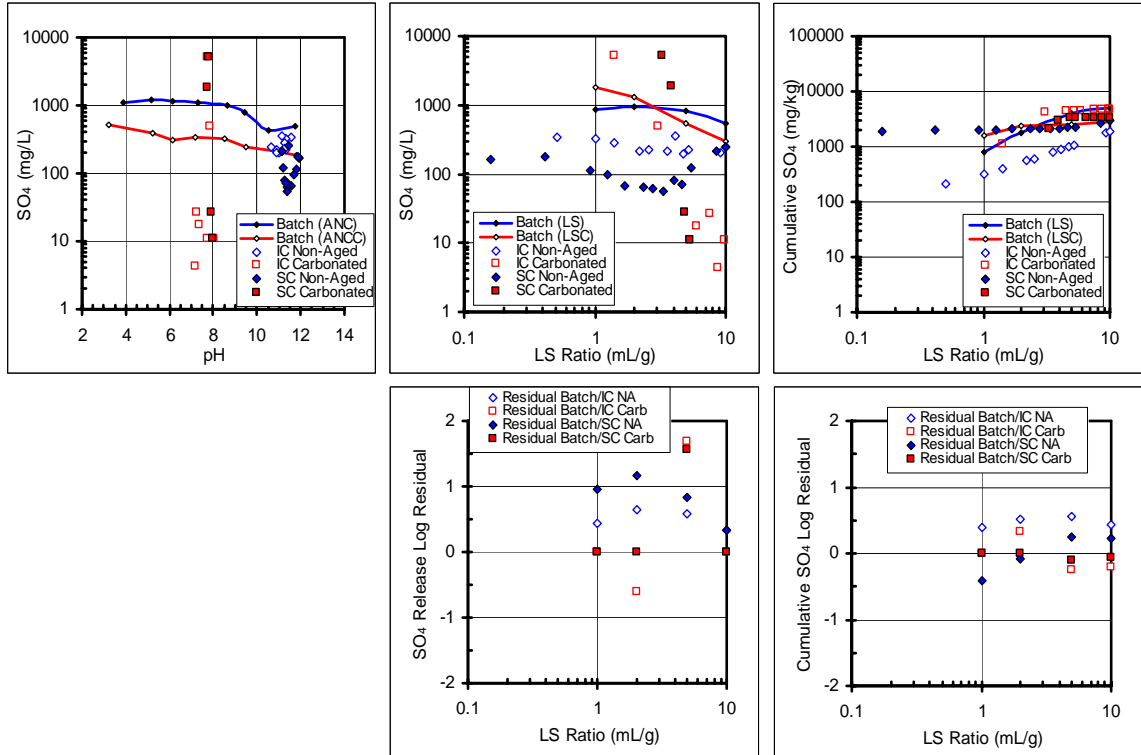


Figure B.39. SO_4 release from BA as a function of pH and LS ratio.

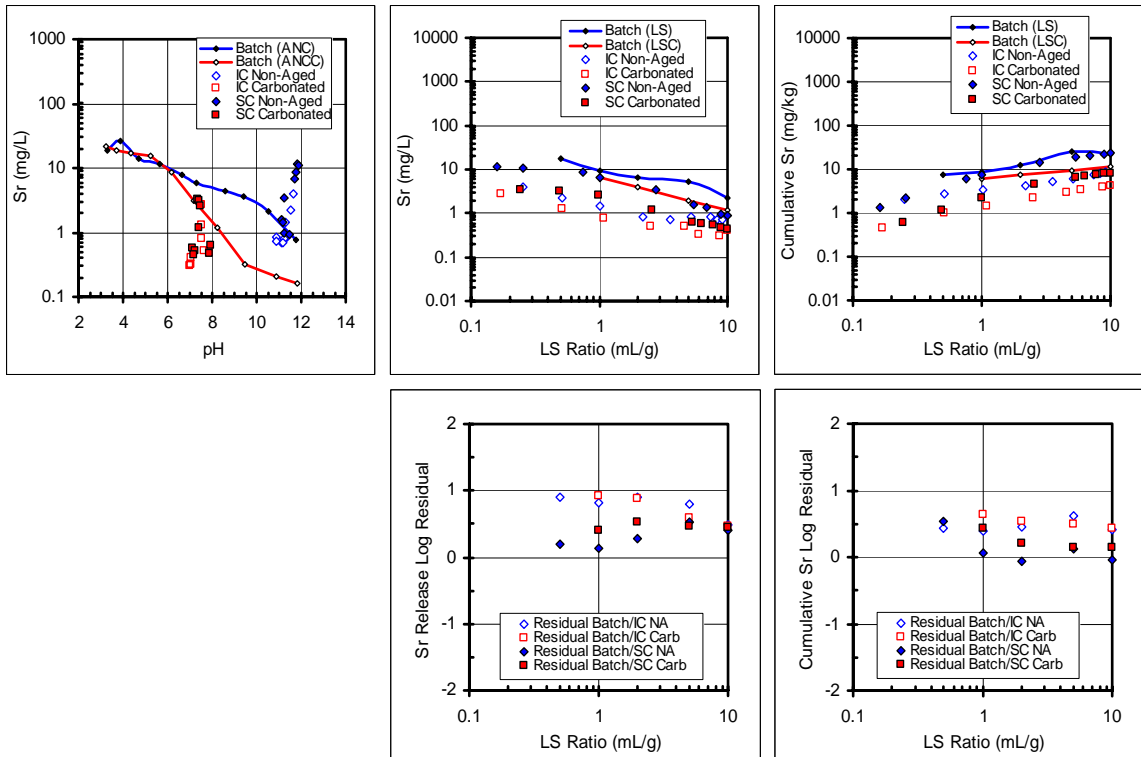


Figure B.40. Sr release from BA as a function of pH and LS ratio.

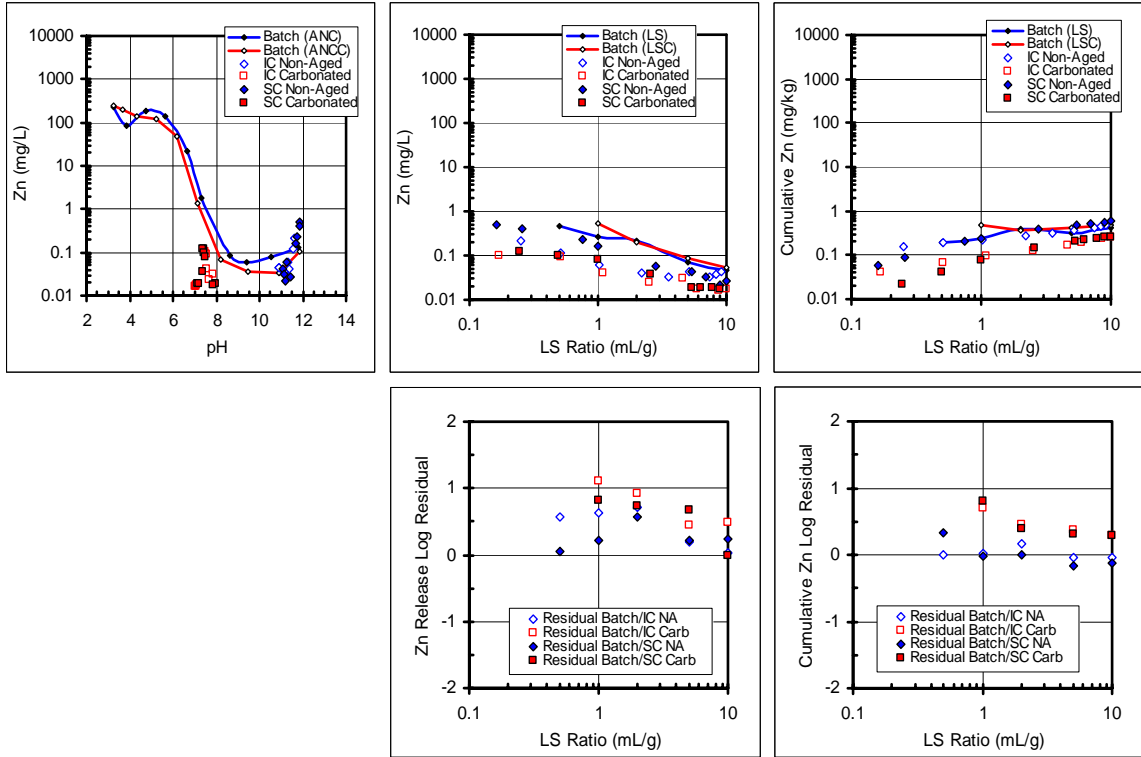


Figure B.41. Zn release from BA as a function of pH and LS ratio.

Coal Fly Ash # 1

pH and conductivity data

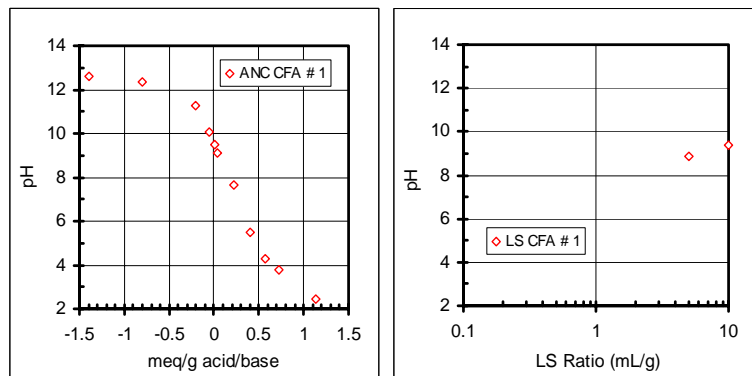


Figure B.42. pH of CFA #1 batch testing as a function of LS Ratio.

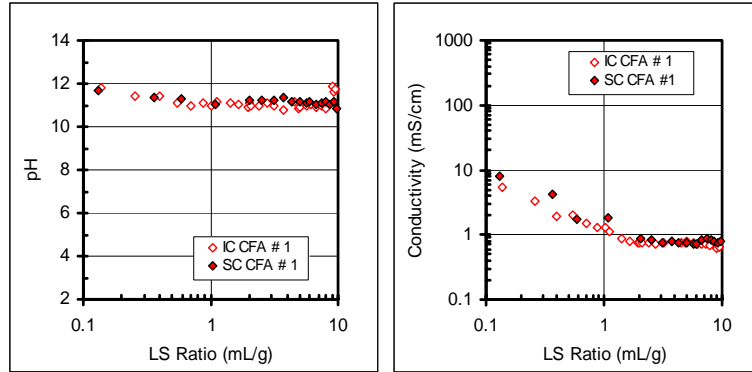


Figure B.43. pH and Conductivity of CFA #1 column testing as a function of LS Ratio.

Activity and ionic strength data

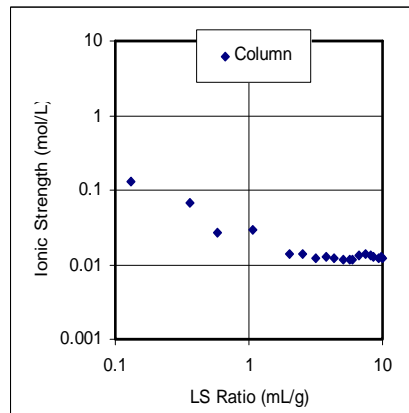


Figure B.44. Ionic strength as a function of LS Ratio for CFA #1.

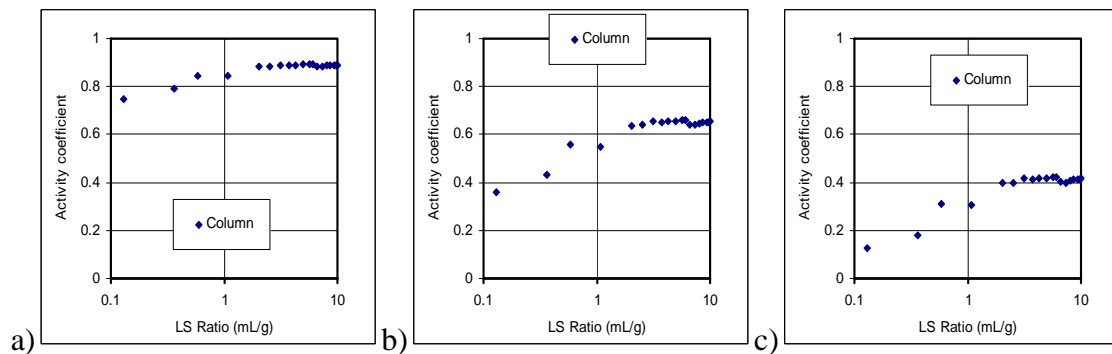


Figure B.45. Activity of a) ± 1 , b) ± 2 and c) ± 3 species for CFA #1 (SC column data).

Elemental data

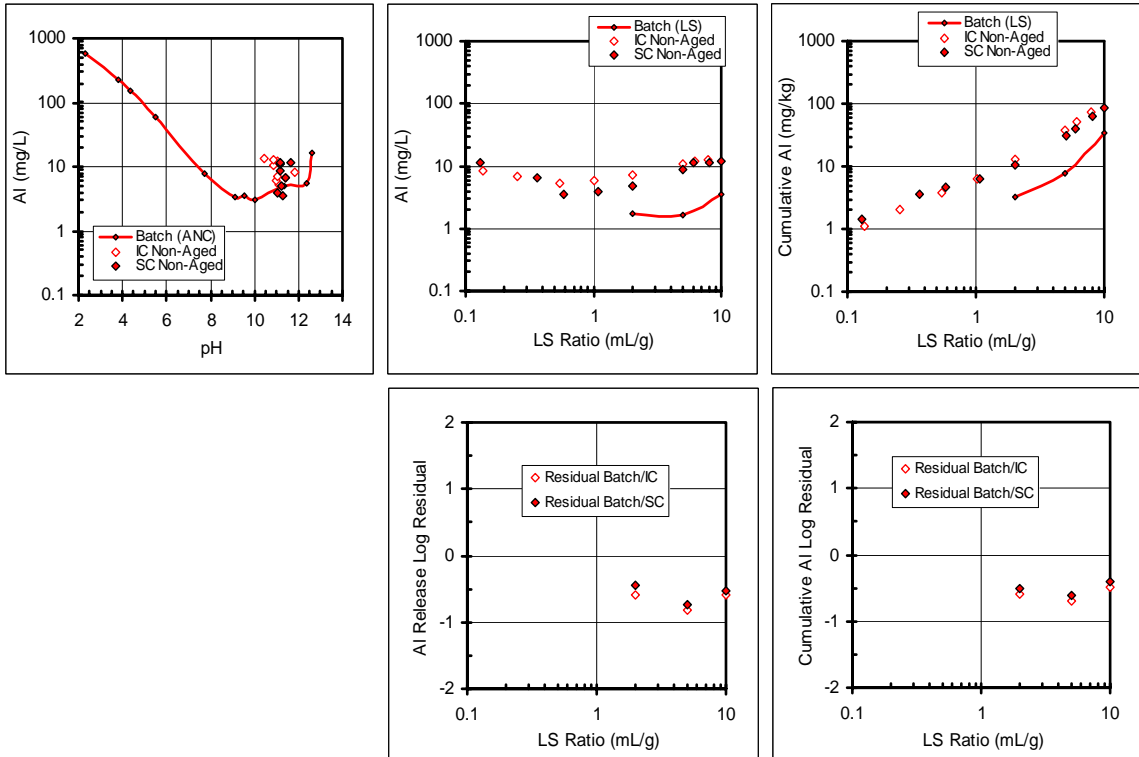


Figure B.46. AI release from CFA # 1 as a function of pH and LS ratio.

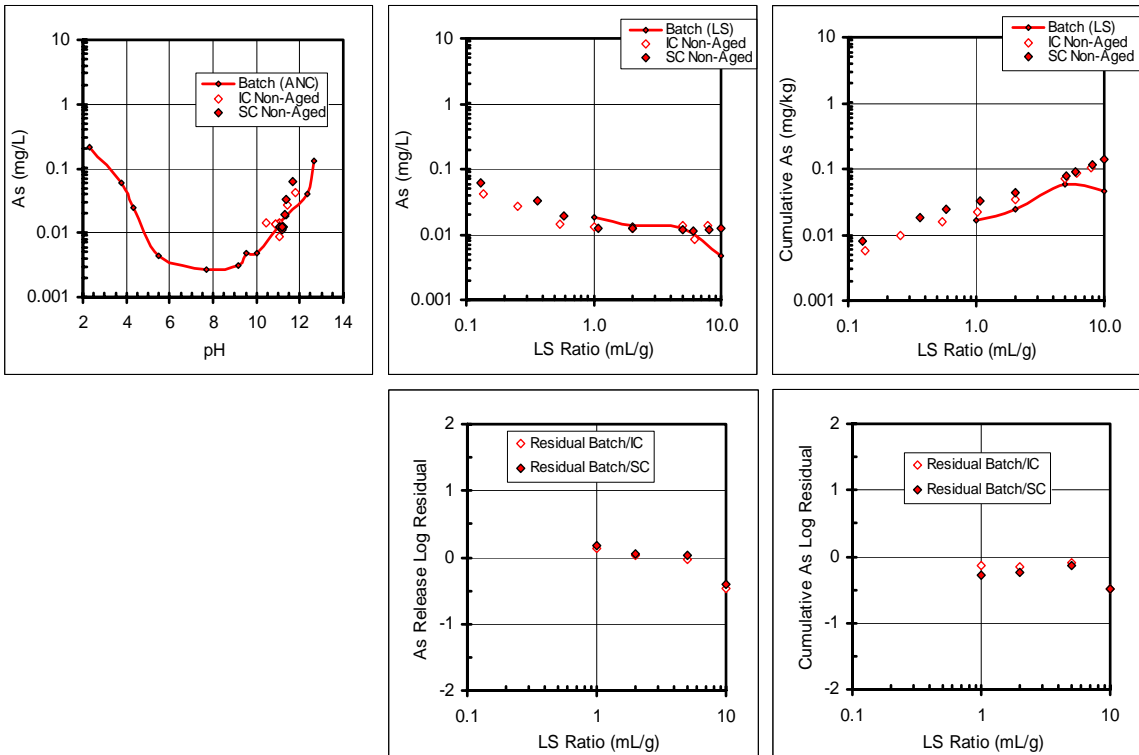


Figure B.47. As release from CFA # 1 as a function of pH and LS ratio.

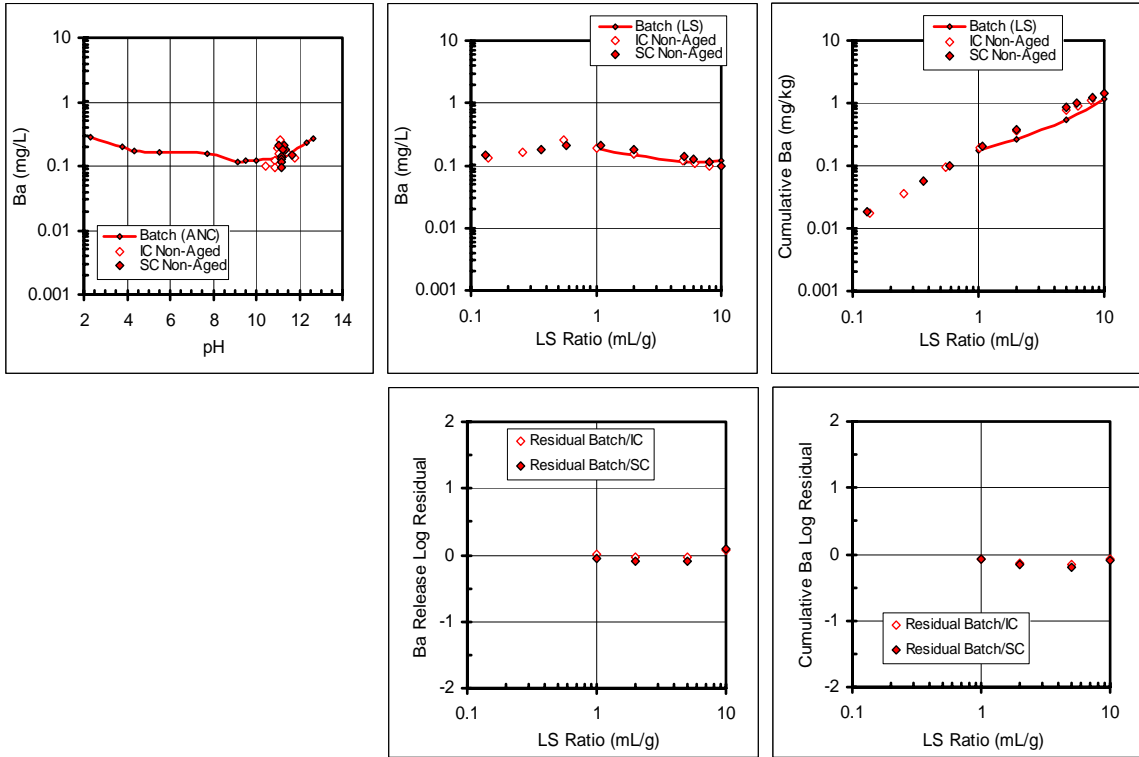


Figure B.48. Ba release from CFA # 1 as a function of pH and LS ratio.

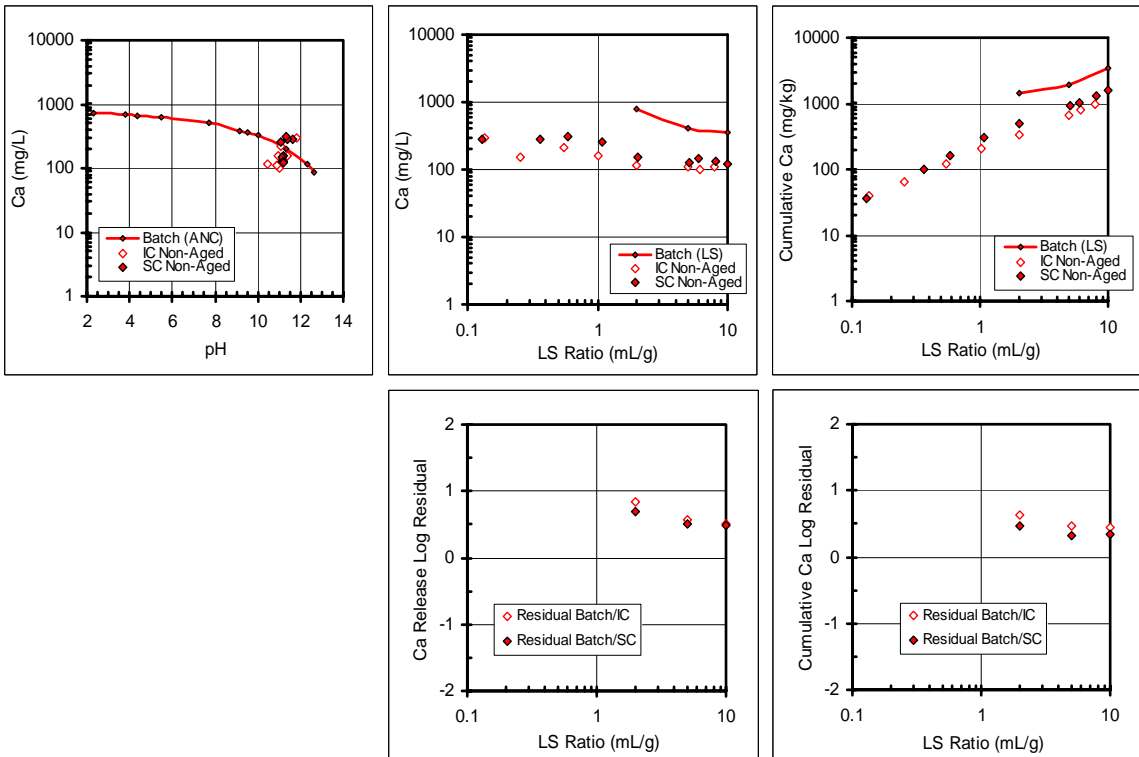


Figure B.49. Ca release from CFA # 1 as a function of pH and LS ratio.

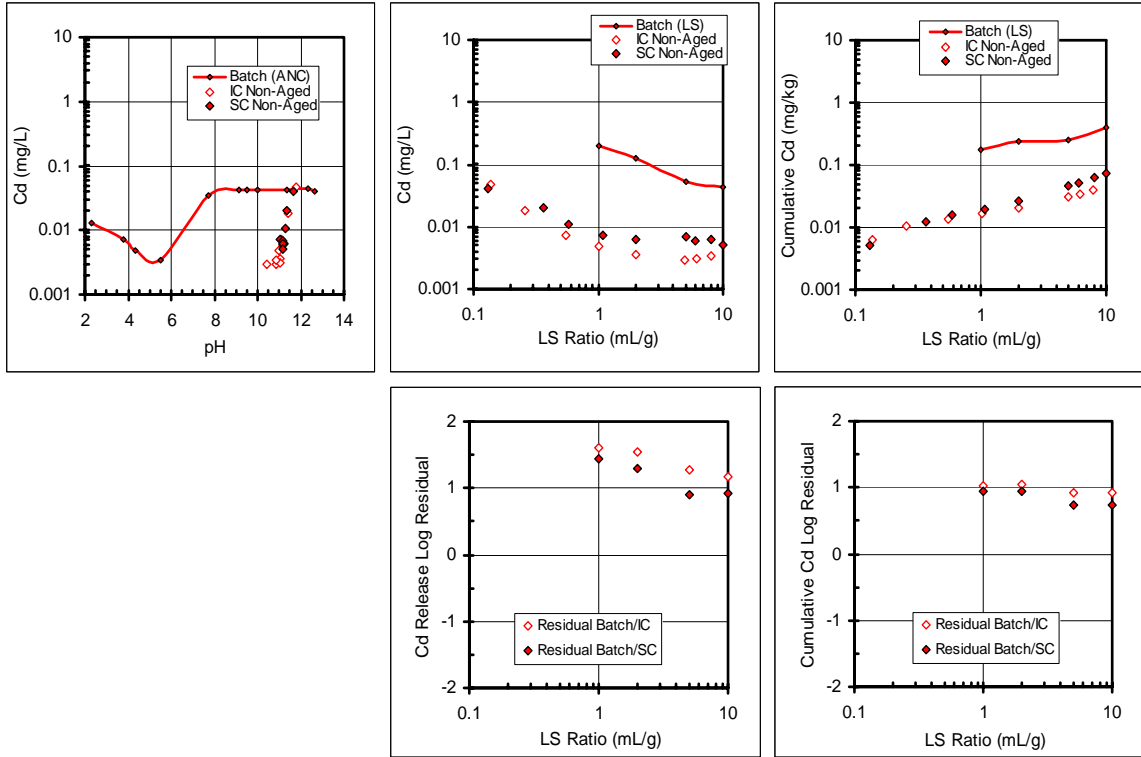


Figure B.50. Cd release from CFA # 1 as a function of pH and LS ratio.

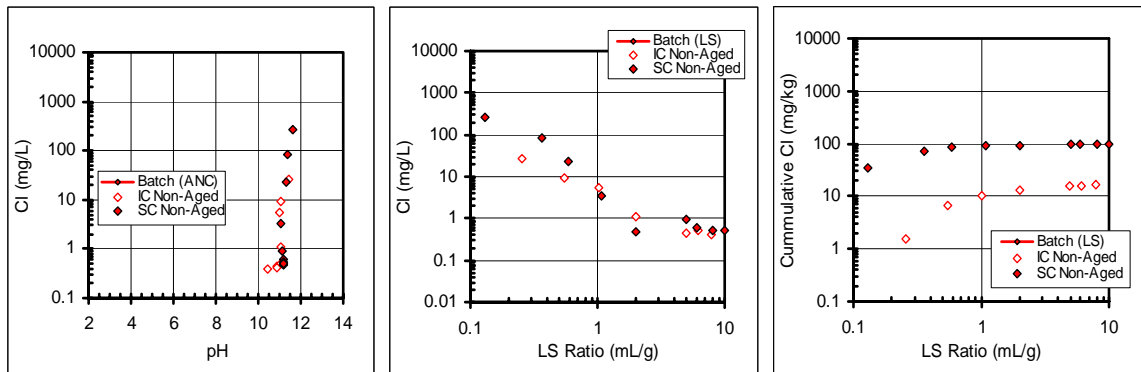


Figure B.51. Cl release from CFA # 1 as a function of pH and LS ratio (no batch data).

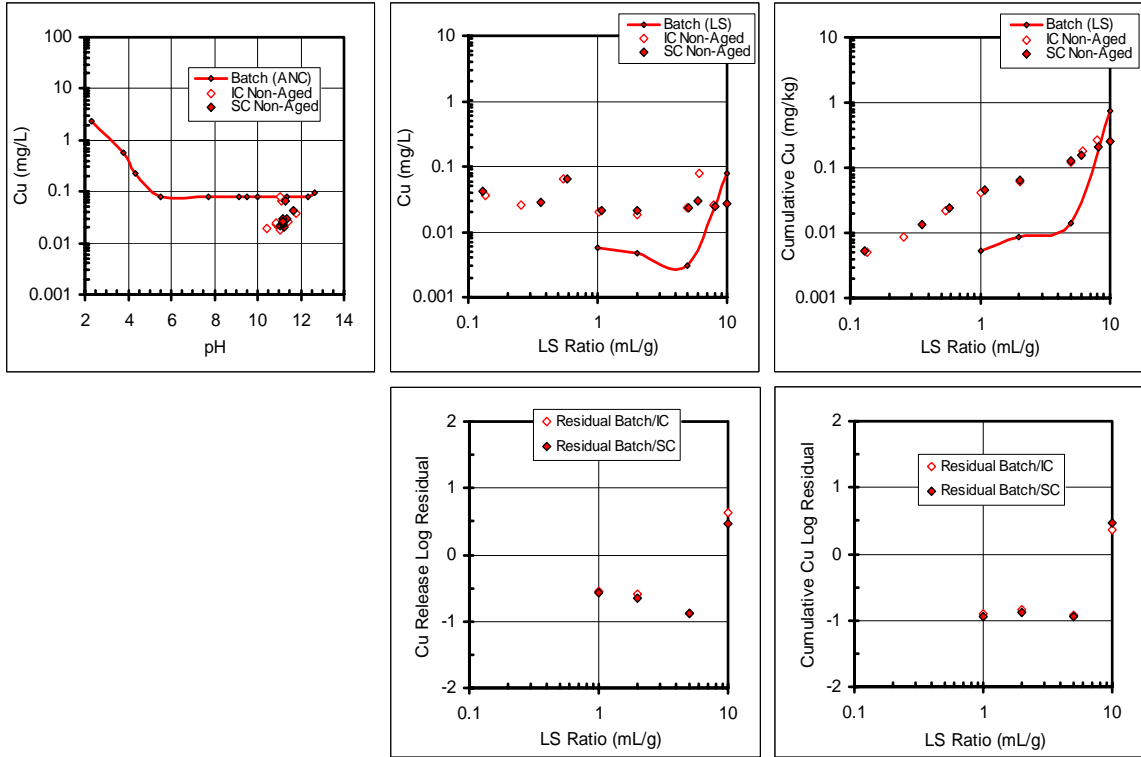


Figure B.52. Cu release from CFA # 1 as a function of pH and LS ratio.

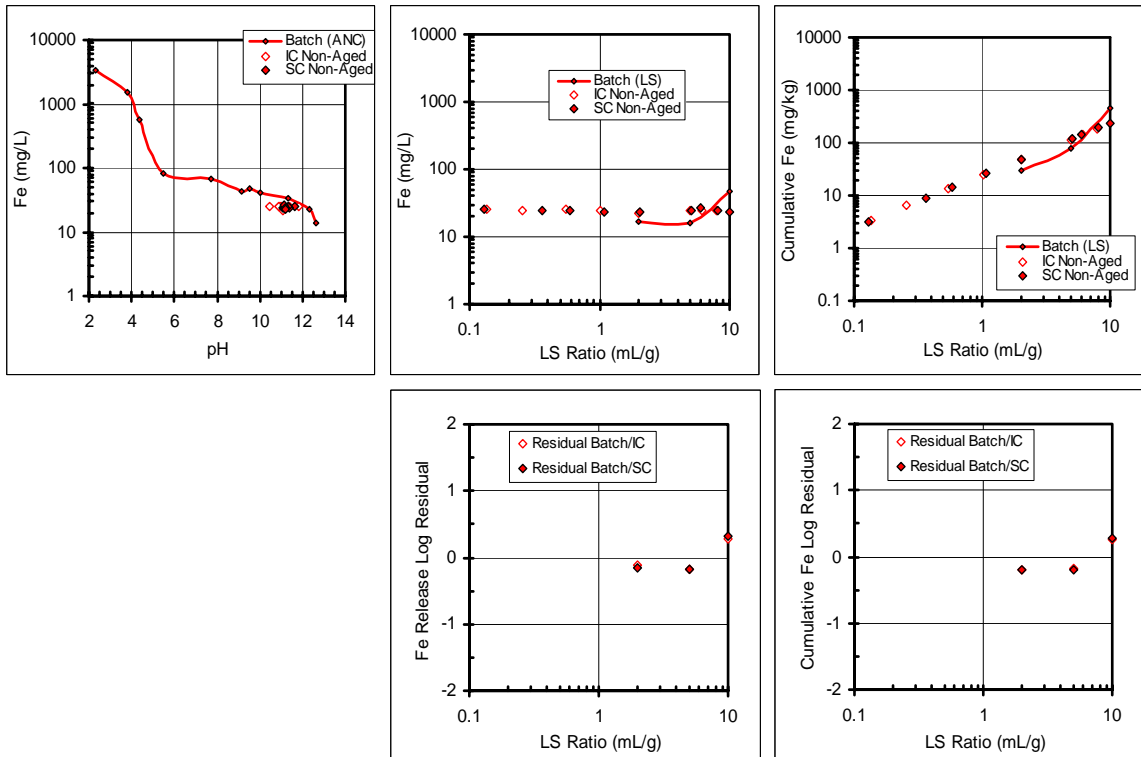


Figure B.53. Fe release from CFA # 1 as a function of pH and LS ratio.

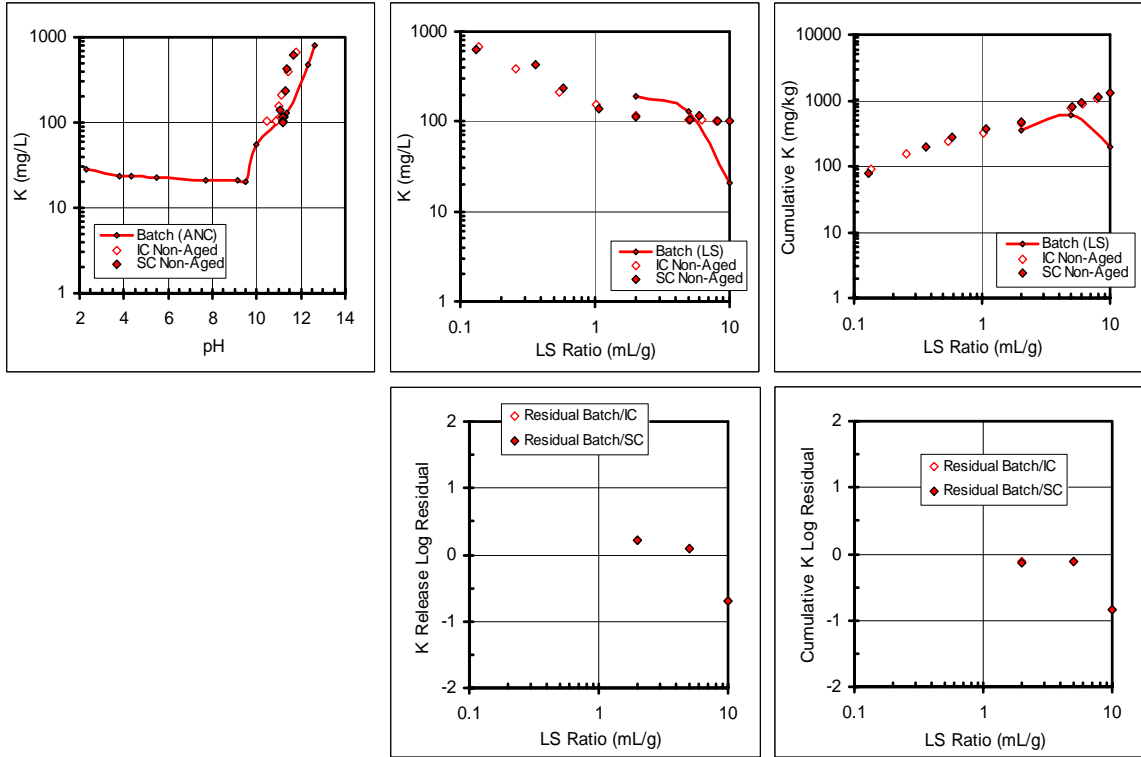


Figure B.54. K release from CFA # 1 as a function of pH and LS ratio.

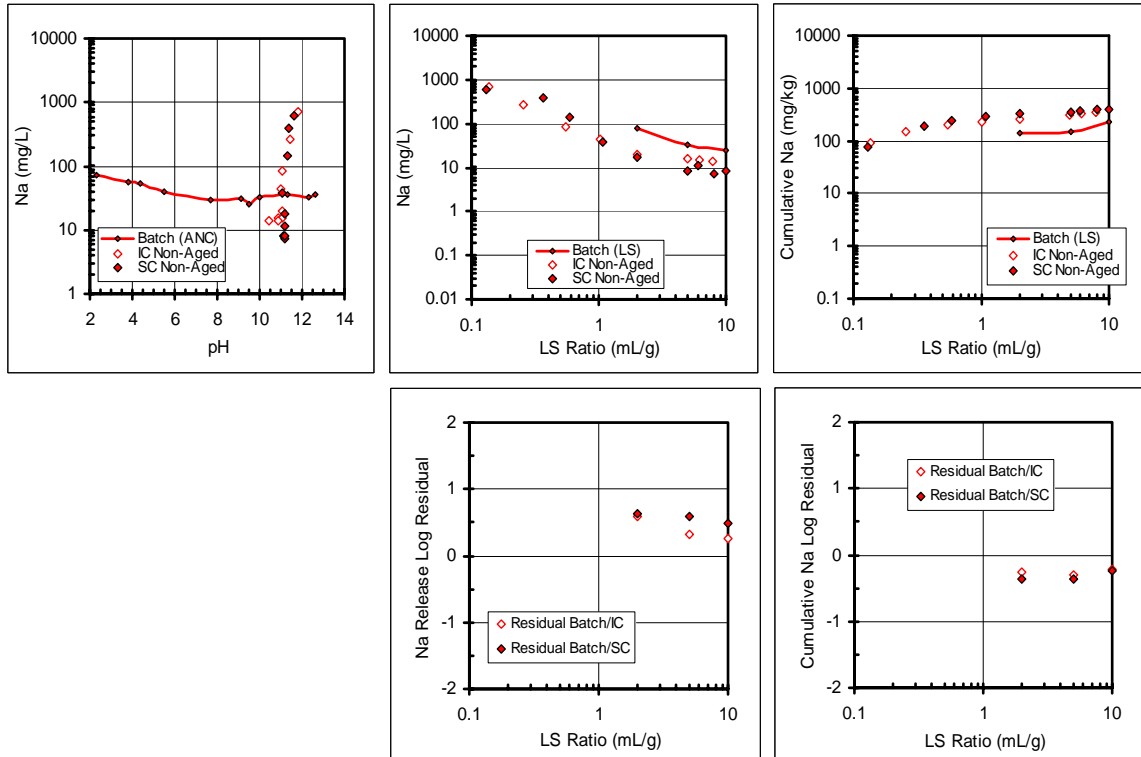


Figure B.55. Na release from CFA # 1 as a function of pH and LS ratio.

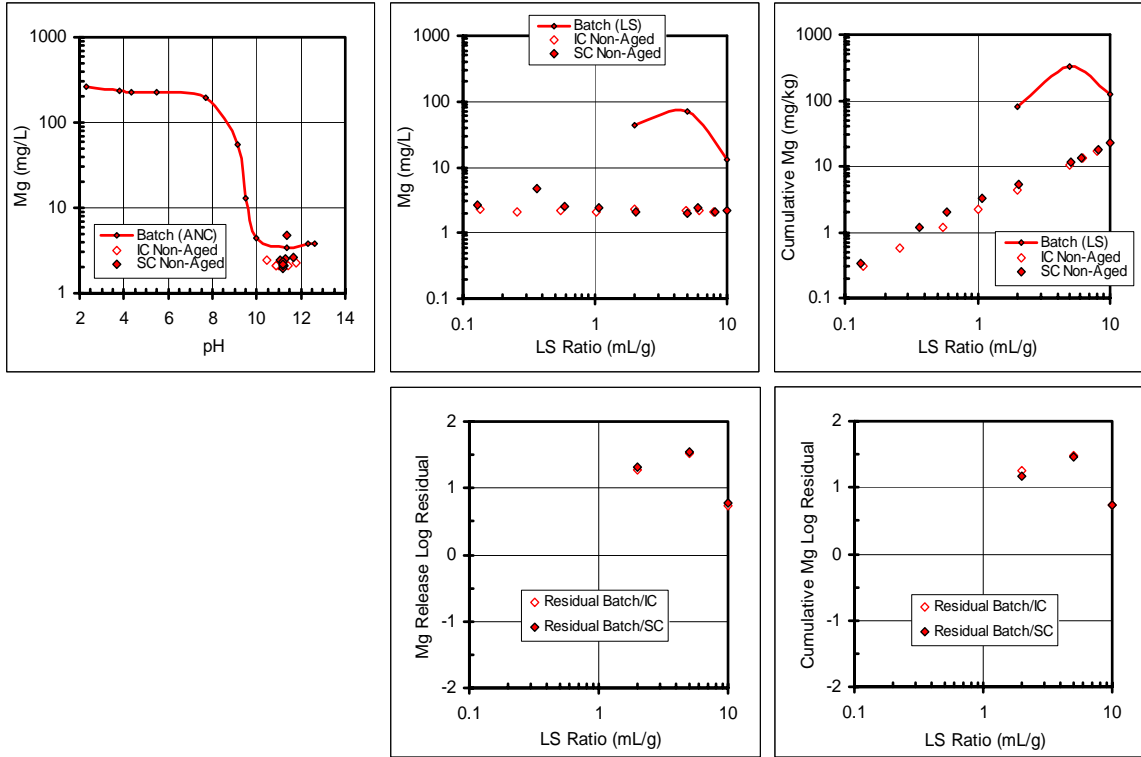


Figure B. 56. Mg release from CFA # 1 as a function of pH and LS ratio.

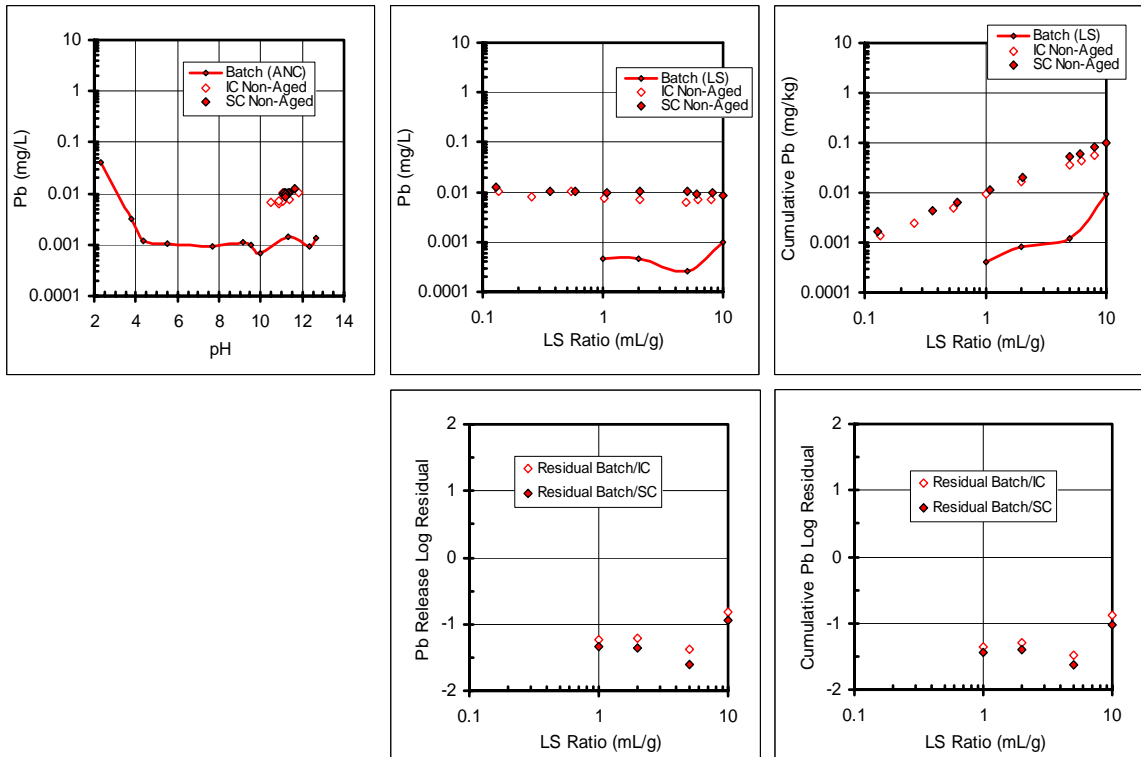


Figure B.57. Pb release from CFA # 1 as a function of pH and LS ratio.

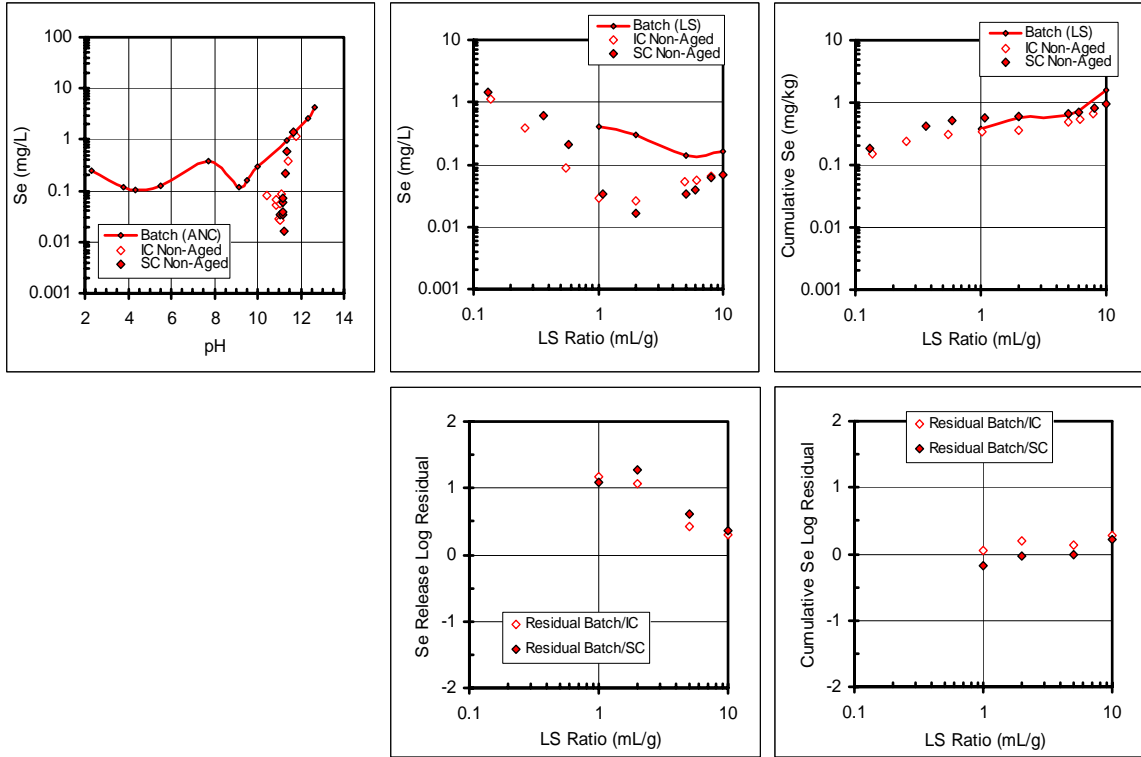


Figure B.58. Se release from CFA # 1 as a function of pH and LS ratio.

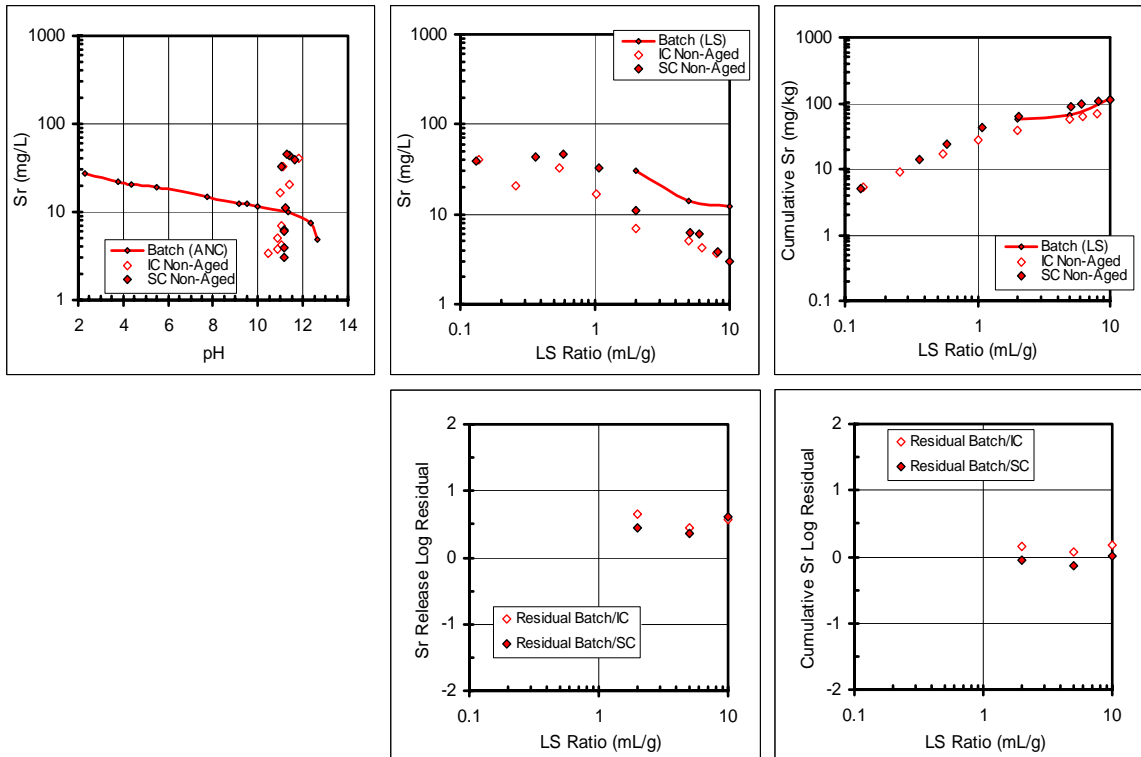


Figure B.59. Sr release from CFA # 1 as a function of pH and LS ratio.

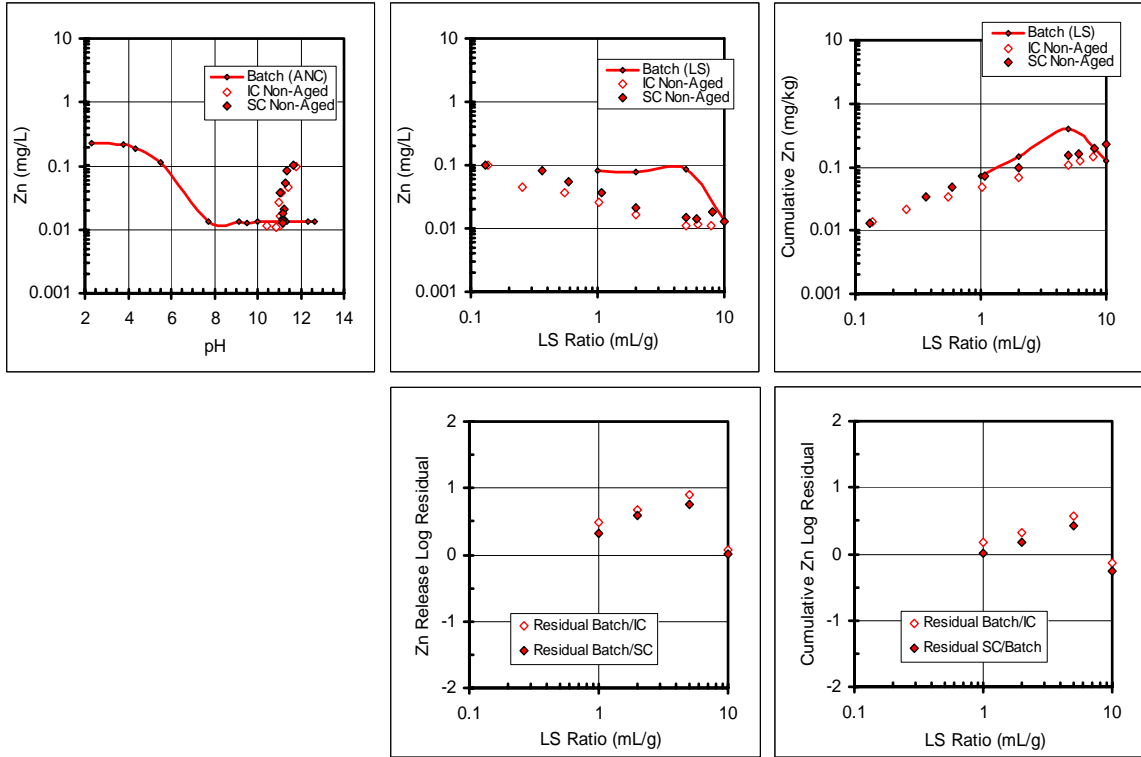


Figure B.60. Zn release from CFA # 1 as a function of pH and LS ratio.

Coal Fly Ash # 2

pH and conductivity data

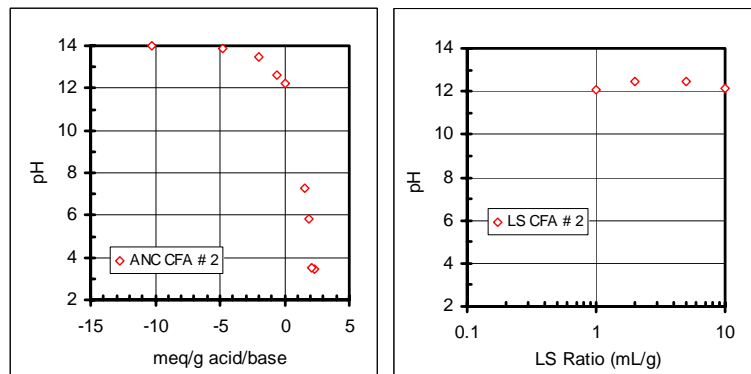


Figure B.61. pH of CFA #2 batch testing as a function of LS Ratio.

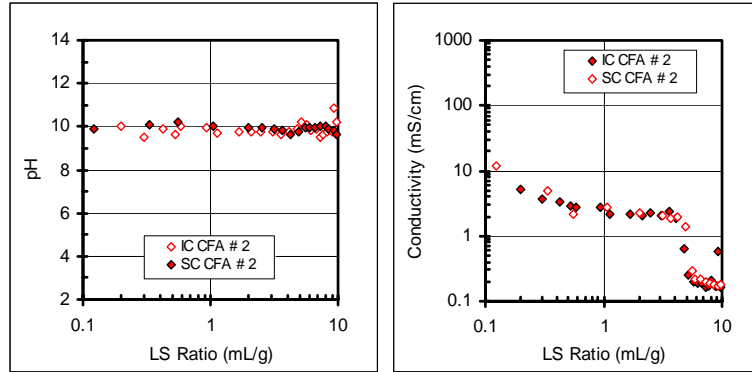


Figure B.62. pH and Conductivity of CFA #2 column testing as a function of LS Ratio.

Activity and ionic strength data

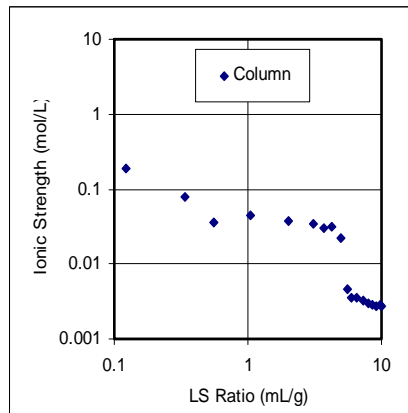


Figure B.63. Ionic strength as a function of LS Ratio for CFA #2.

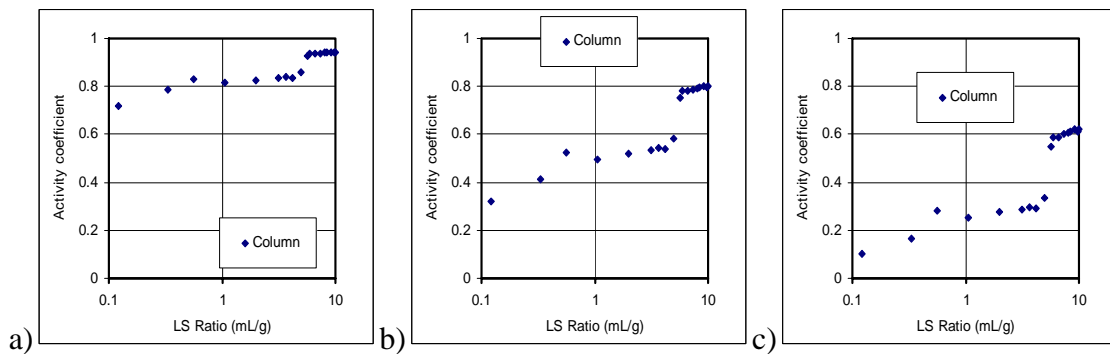


Figure B.64. Activity of a) ± 1 , b) ± 2 and c) ± 3 species for CFA #2 (SC column data).

Elemental data

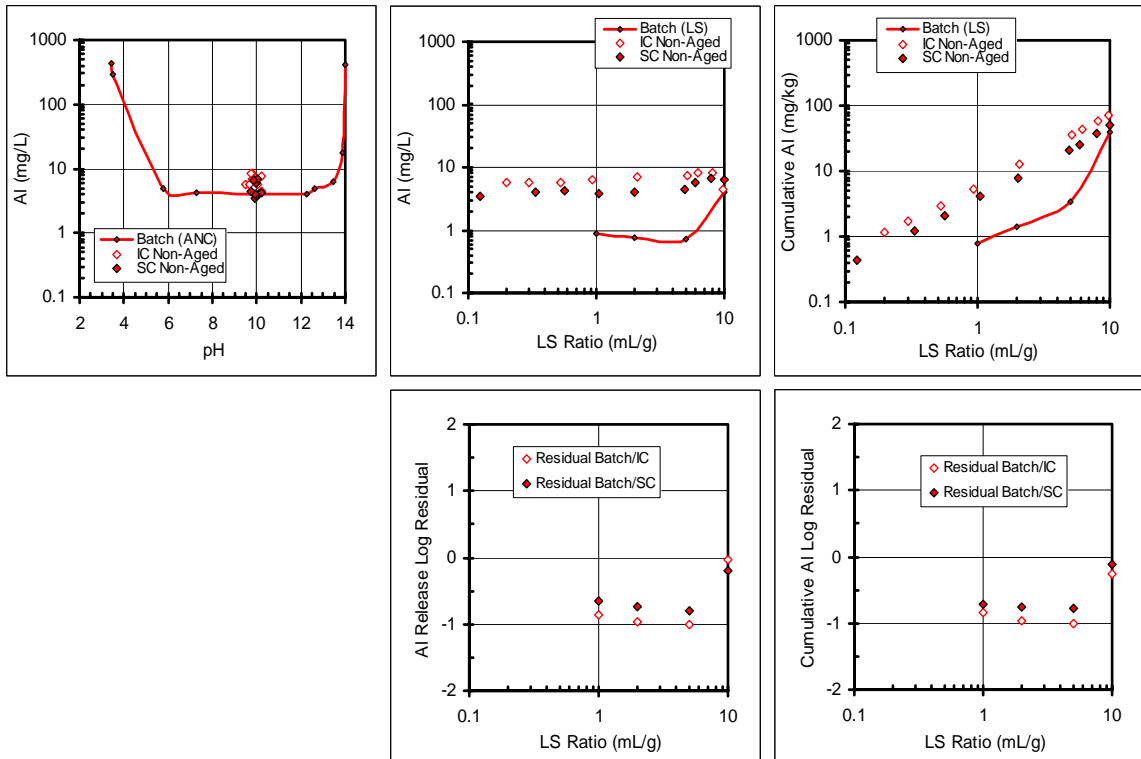


Figure B.65. Al release from CFA # 2 as a function of pH and LS ratio.

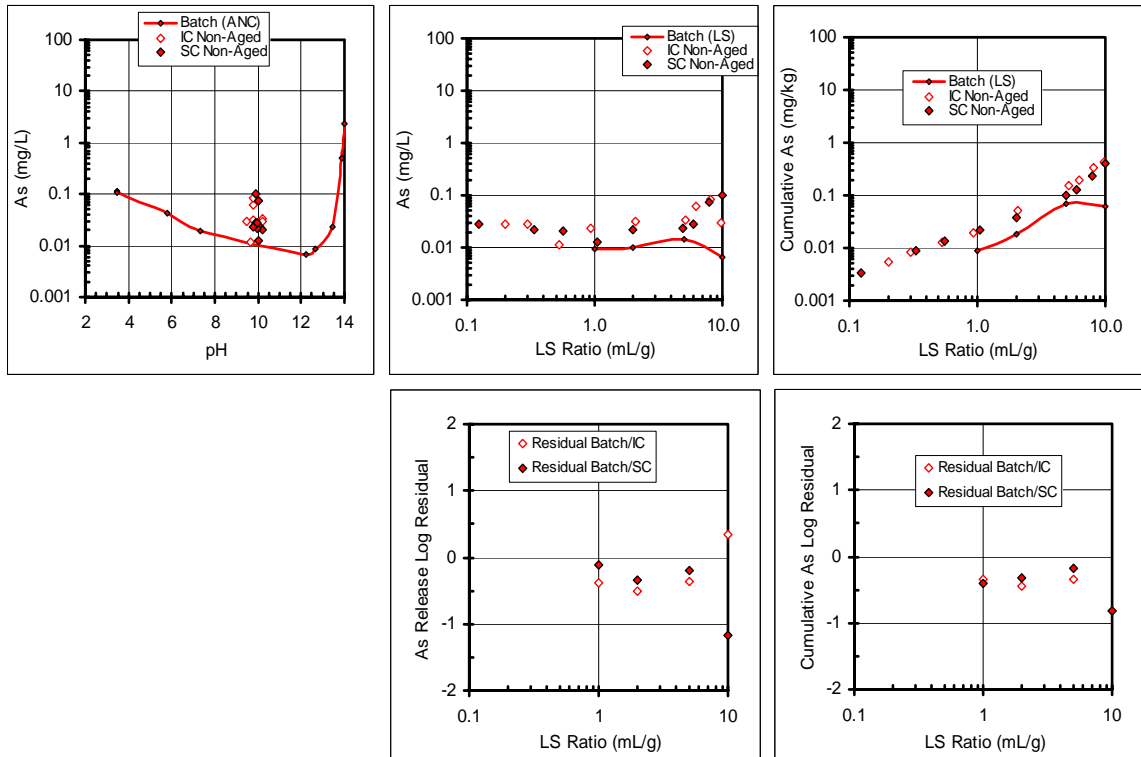


Figure B.66. As release from CFA # 2 as a function of pH and LS ratio.

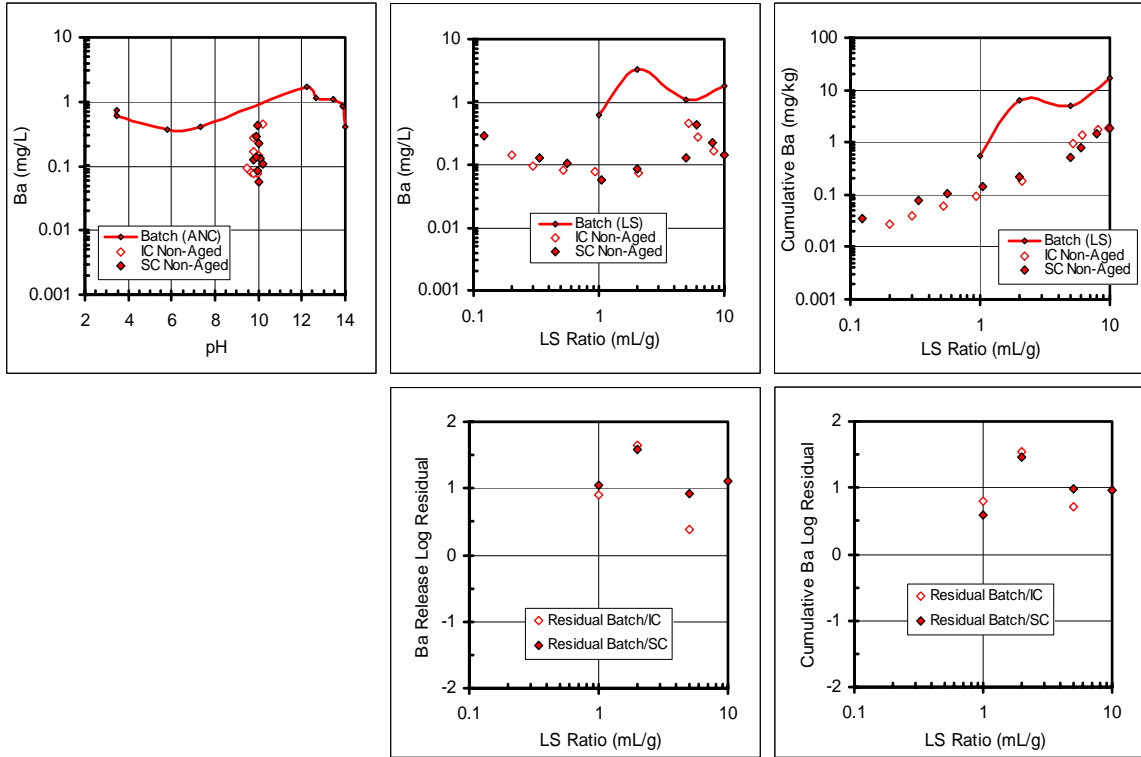


Figure B.67. Ba release from CFA # 2 as a function of pH and LS ratio.

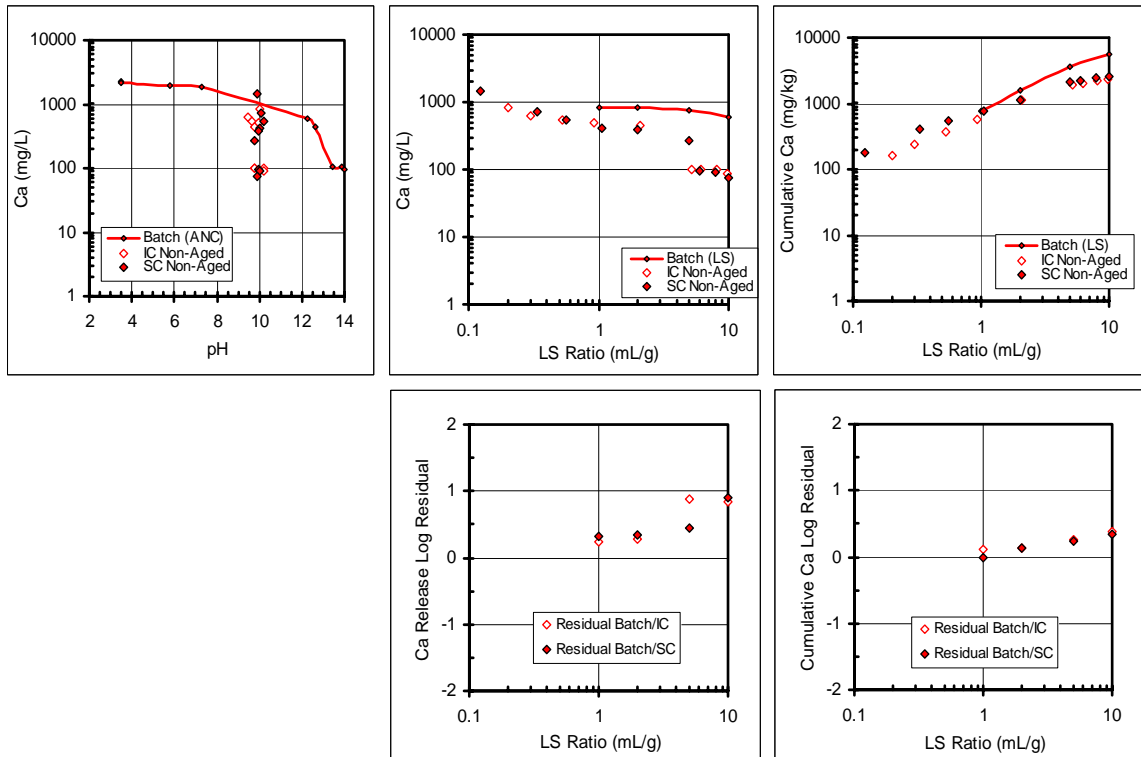


Figure B.68. Ca release from CFA # 2 as a function of pH and LS ratio.

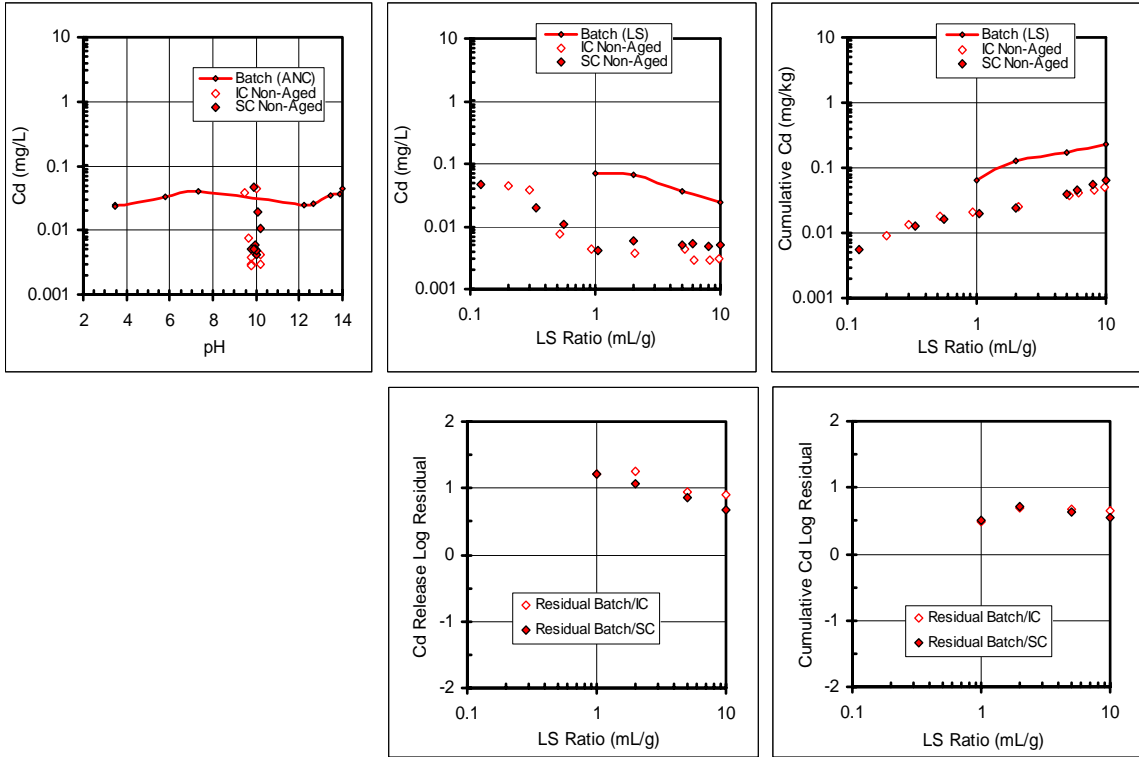


Figure B.69. Cd release from CFA # 2 as a function of pH and LS ratio.

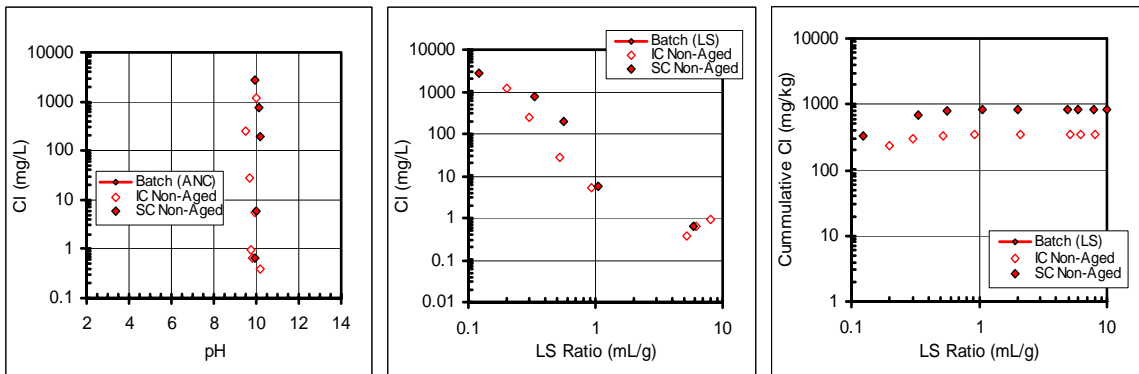


Figure B.70. Cl release from CFA # 2 as a function of pH and LS ratio (no batch data).

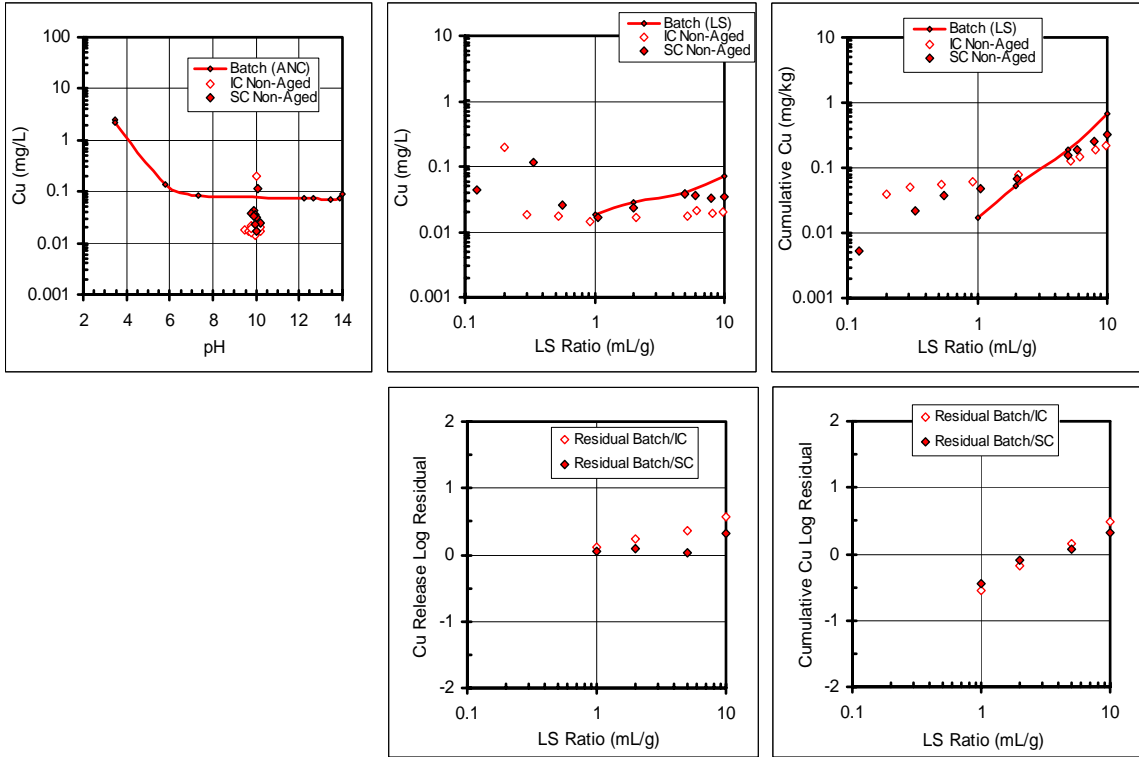


Figure B.71. Cu release from CFA # 2 as a function of pH and LS ratio.

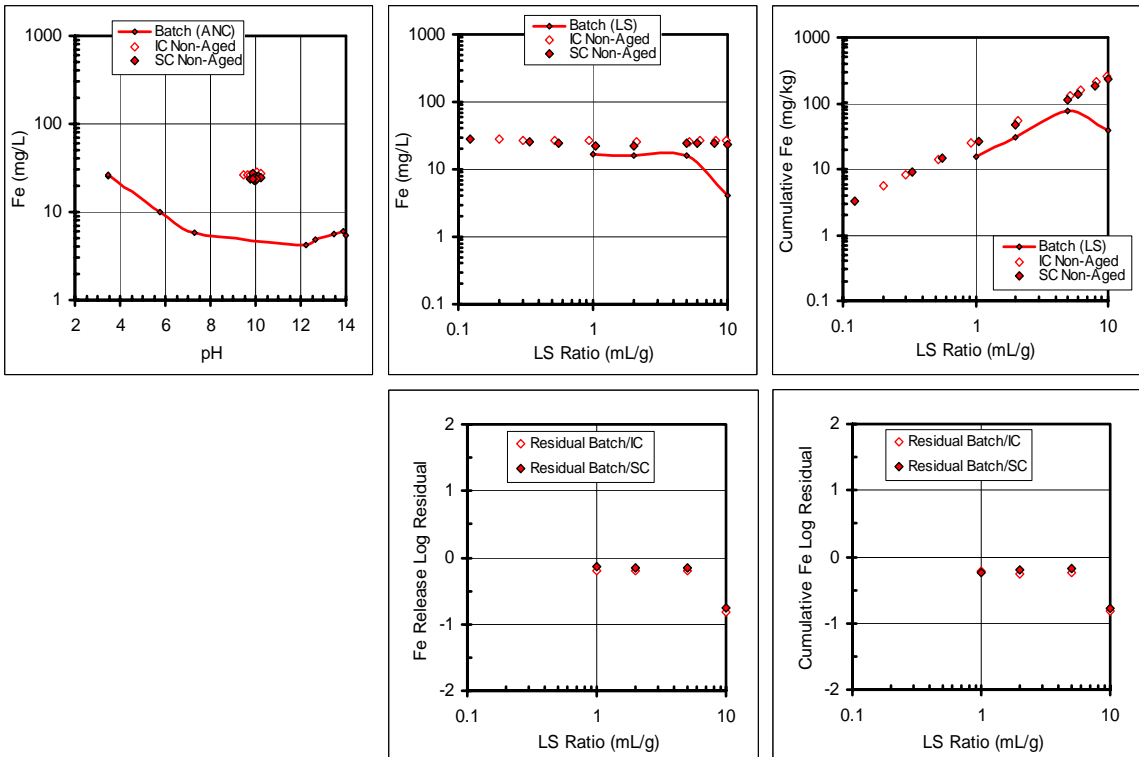


Figure B.72. Fe release from CFA # 2 as a function of pH and LS ratio.

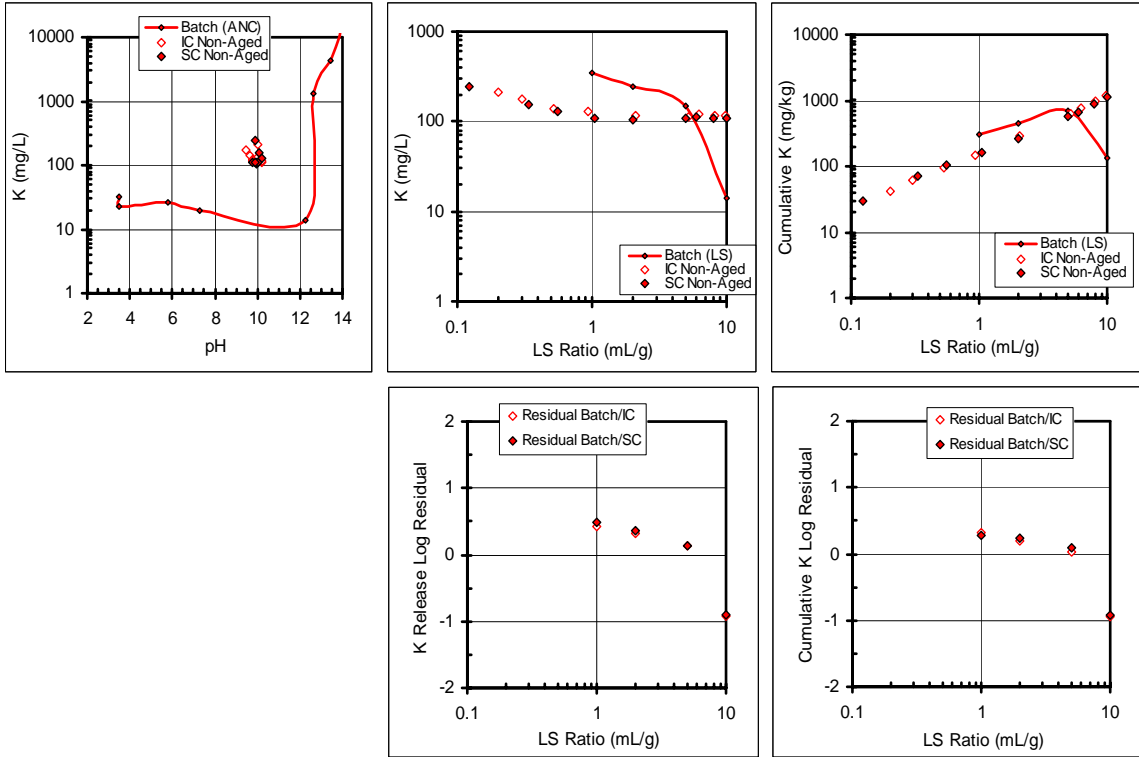


Figure B.73. K release from CFA # 2 as a function of pH and LS ratio.

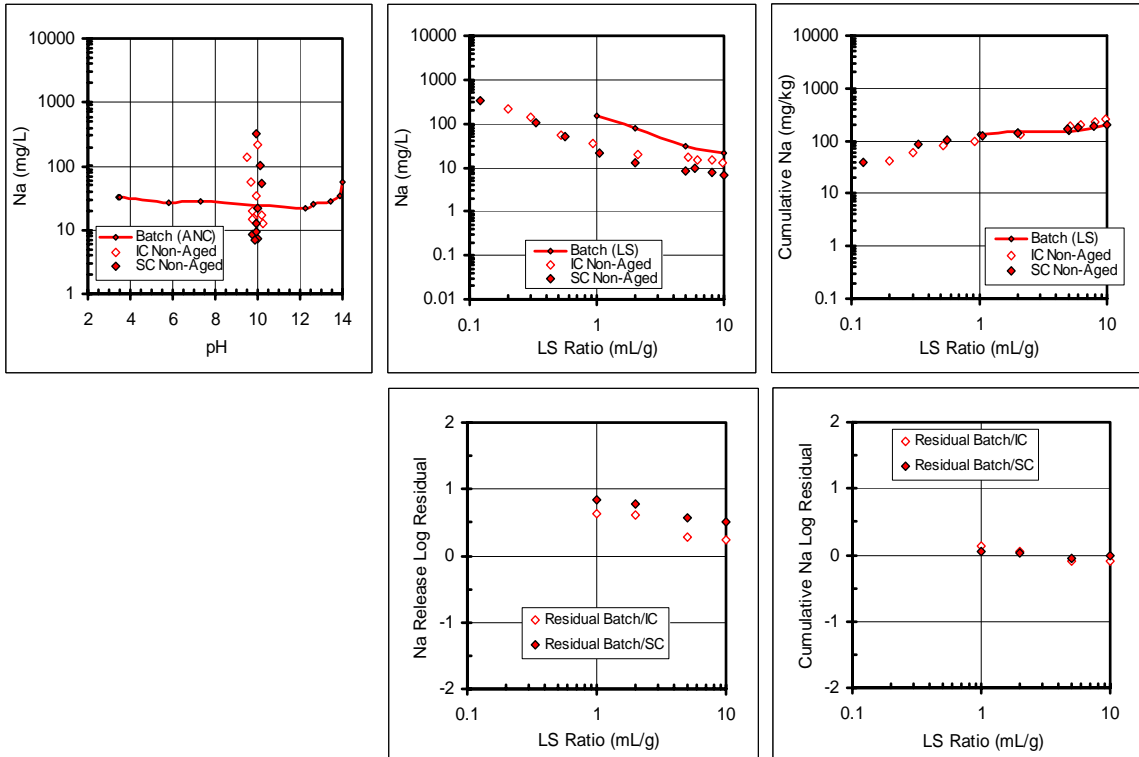


Figure B.74. Na release from CFA # 2 as a function of pH and LS ratio.

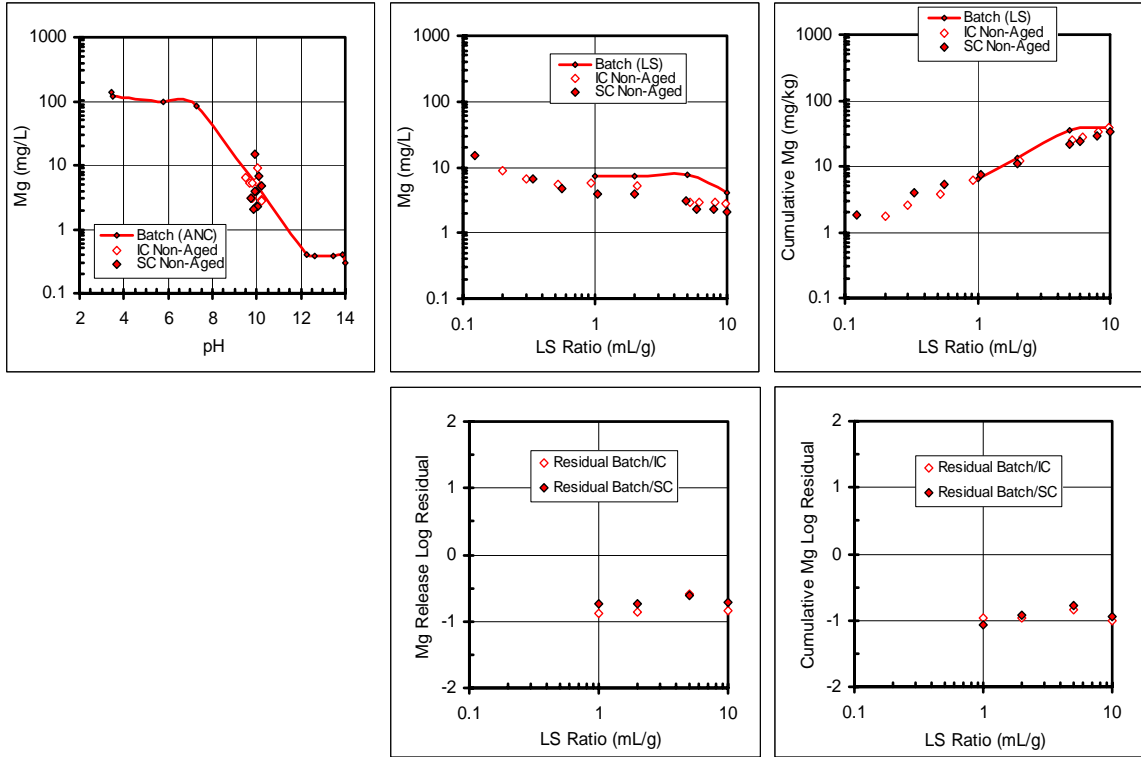


Figure B.75. Mg release from CFA # 2 as a function of pH and LS ratio.

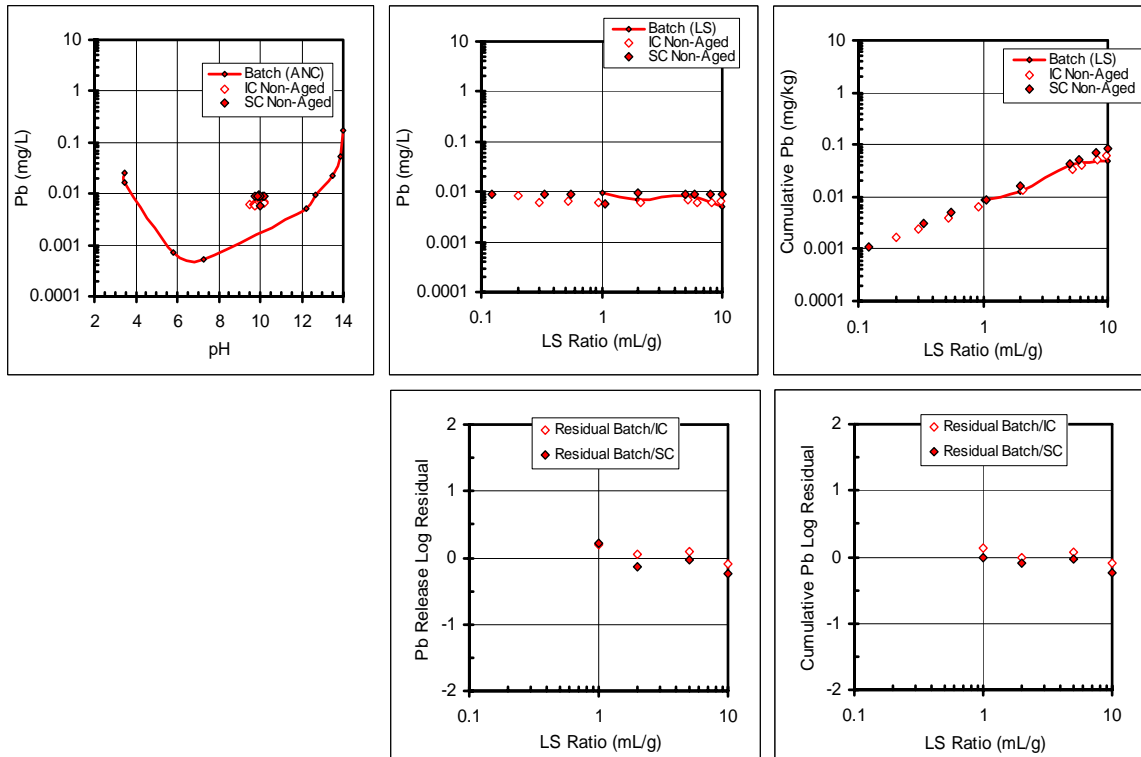


Figure B.76. Pb release from CFA # 2 as a function of pH and LS ratio.

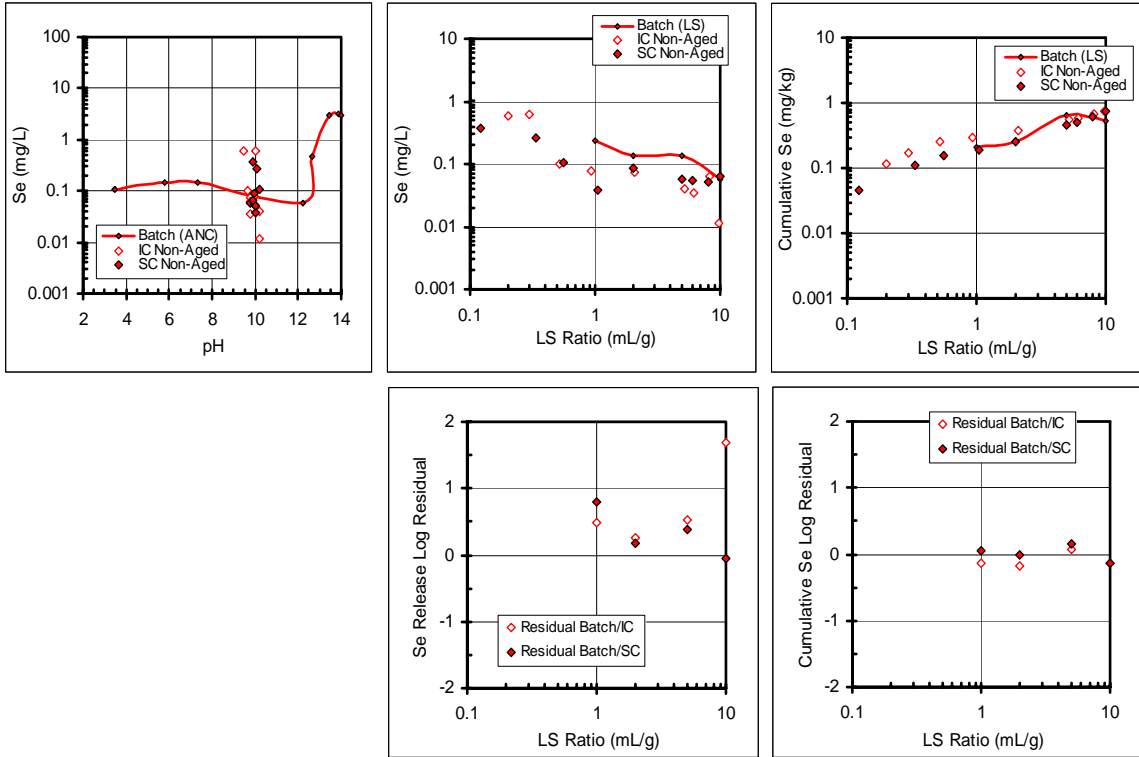


Figure B.77. Se release from CFA # 2 as a function of pH and LS ratio.

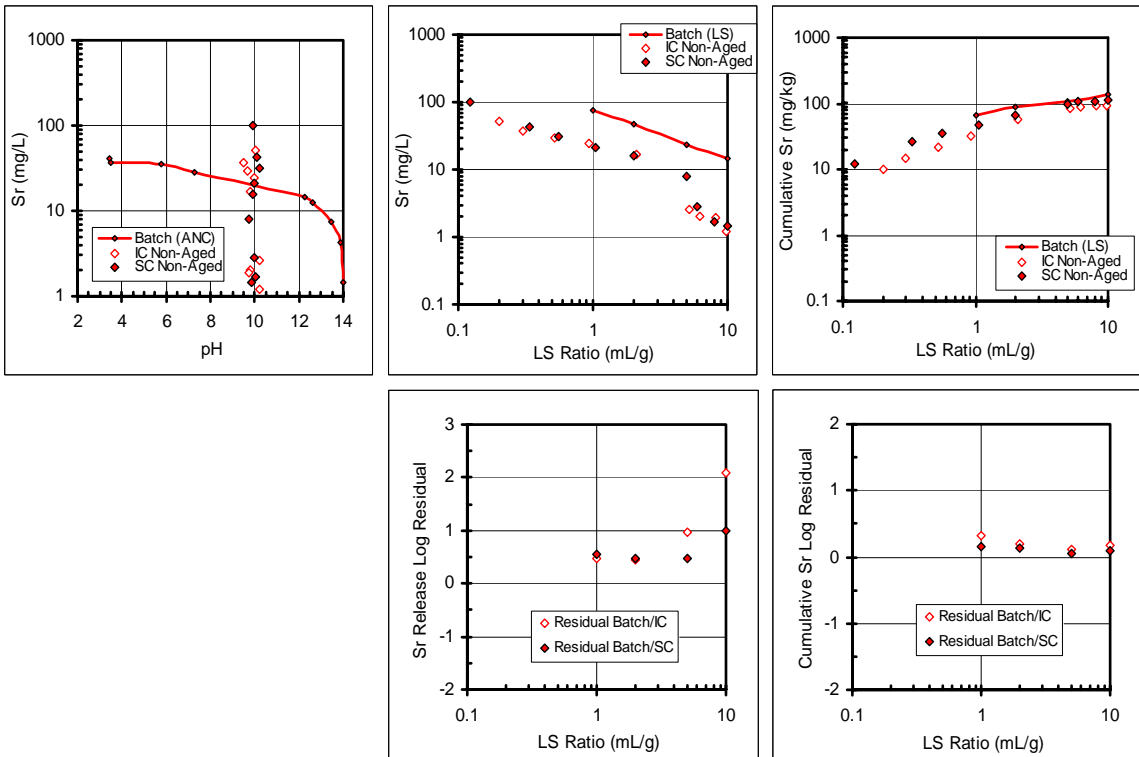


Figure B.78. Sr release from CFA # 2 as a function of pH and LS ratio.

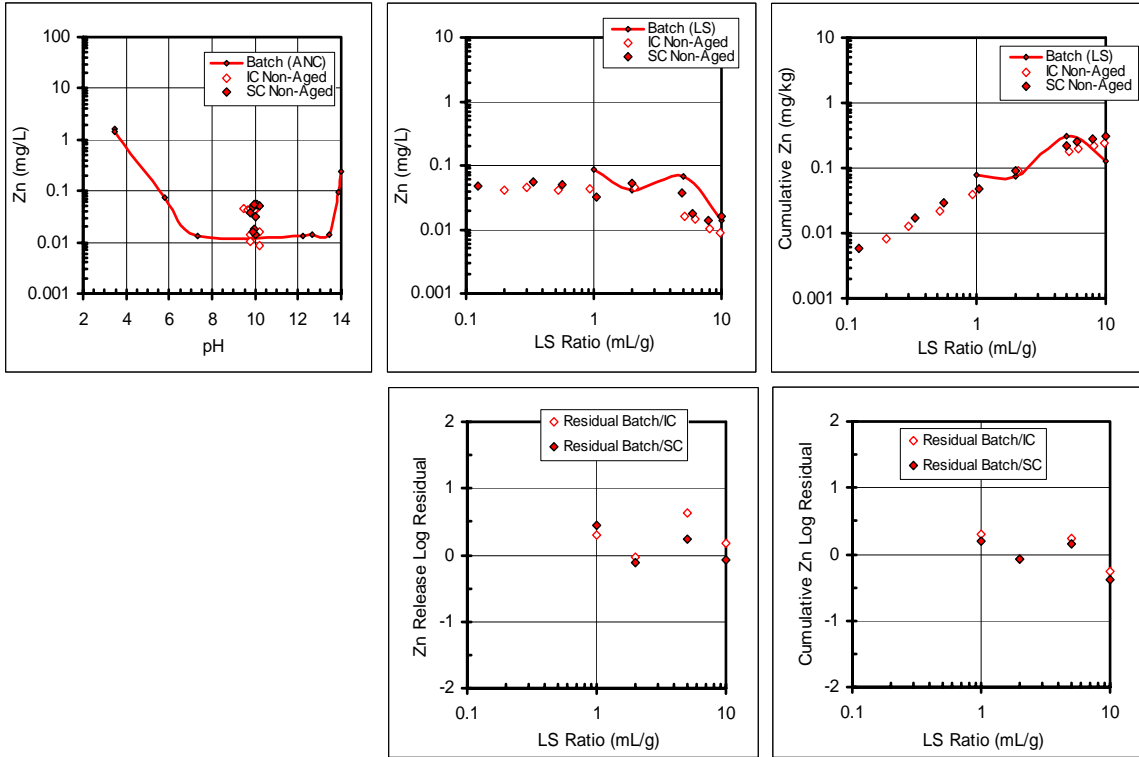


Figure B.79. Zn release from CFA # 2 as a function of pH and LS ratio.

Construction Debris

pH and conductivity data

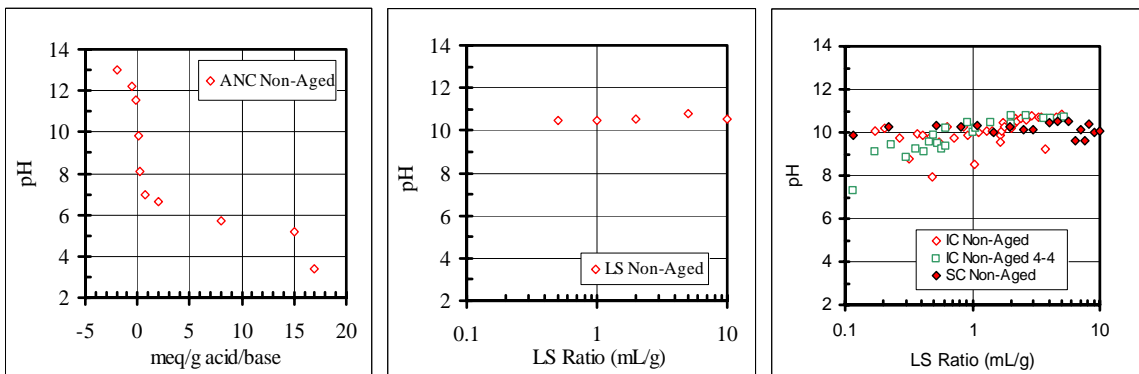


Figure B.80. pH of CD batch and column testing.

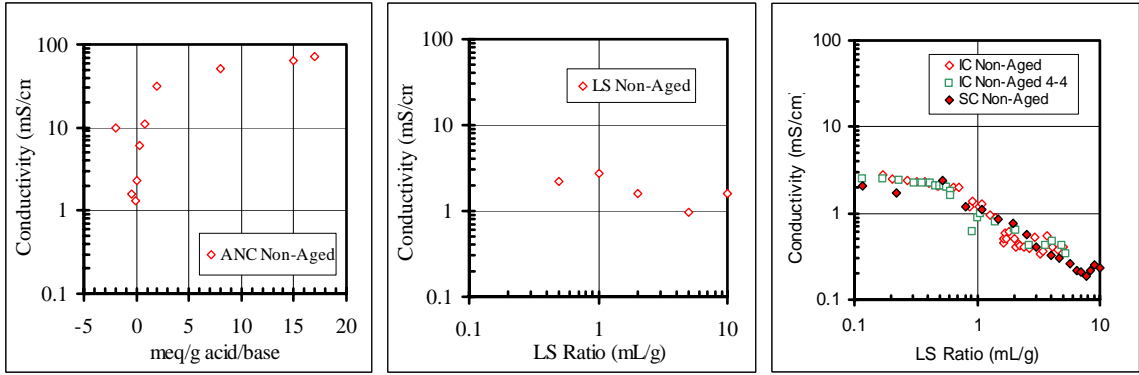


Figure B.81. Conductivity of CD batch and column testing.

Activity and ionic strength data

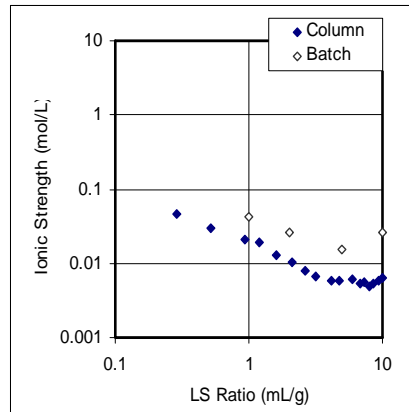


Figure B.82. Ionic strength as a function of LS Ratio for CD.

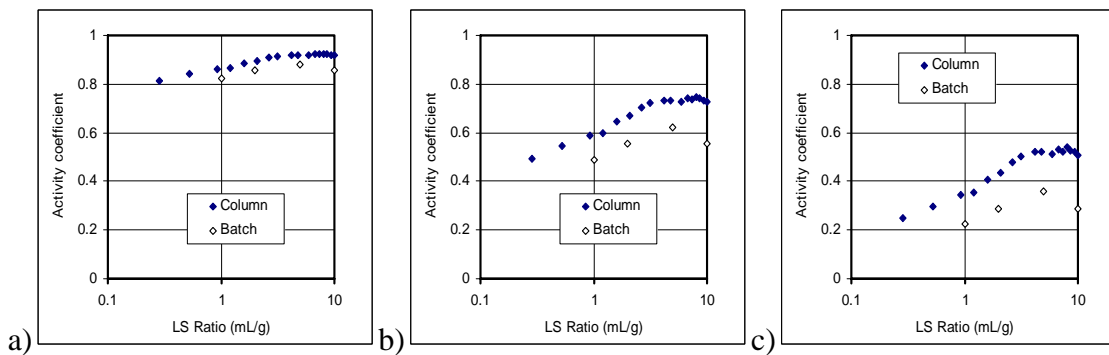


Figure B.83. Activity of a) ± 1 , b) ± 2 and c) ± 3 species for CD (SC column data).

Elemental data

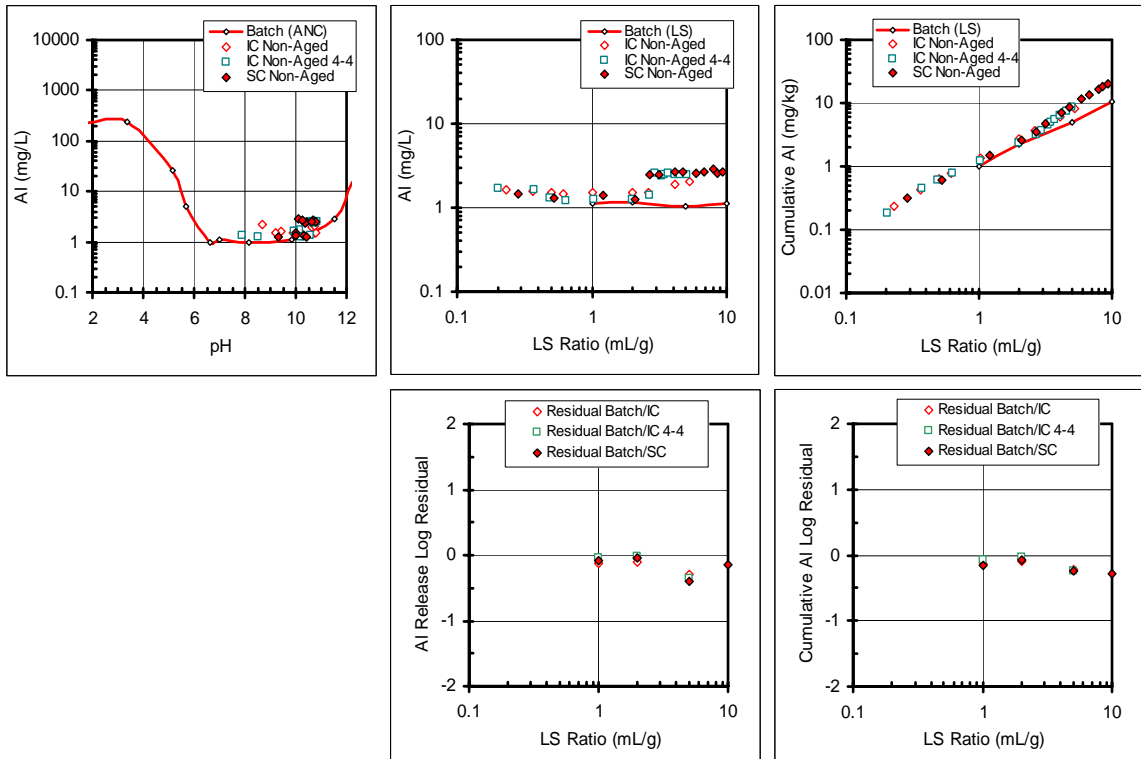


Figure B.84. Al release from CD as a function of pH and LS ratio.

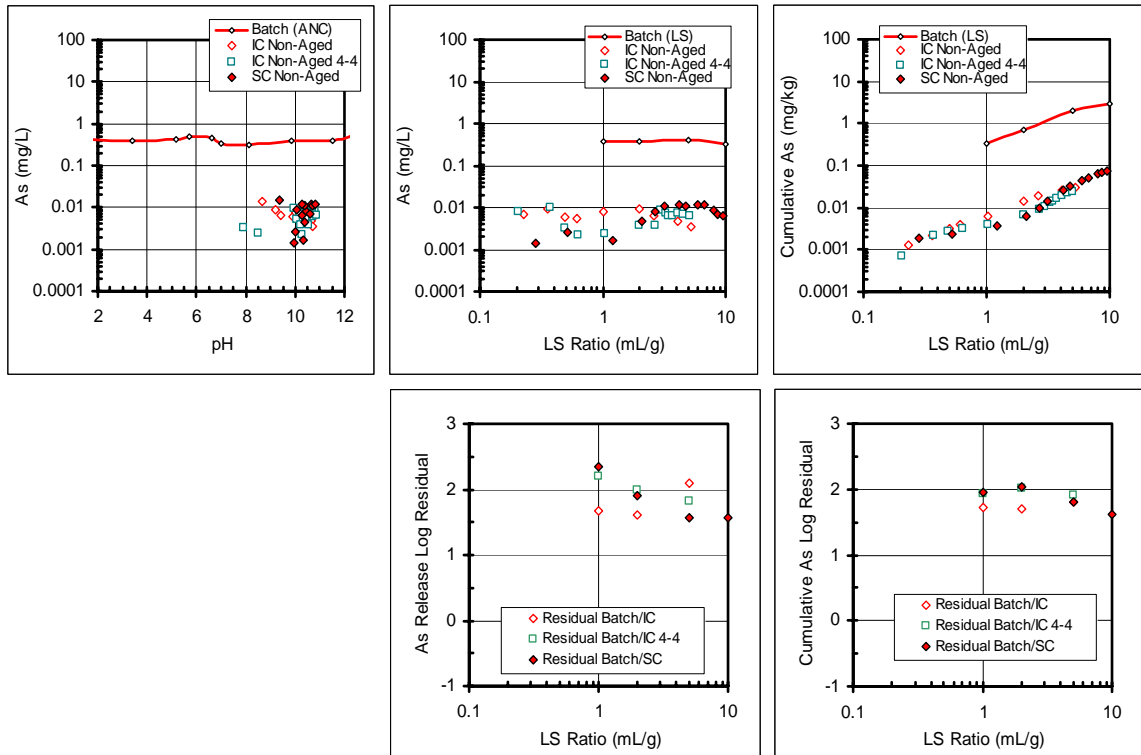


Figure B.85. As release from CD as a function of pH and LS ratio.

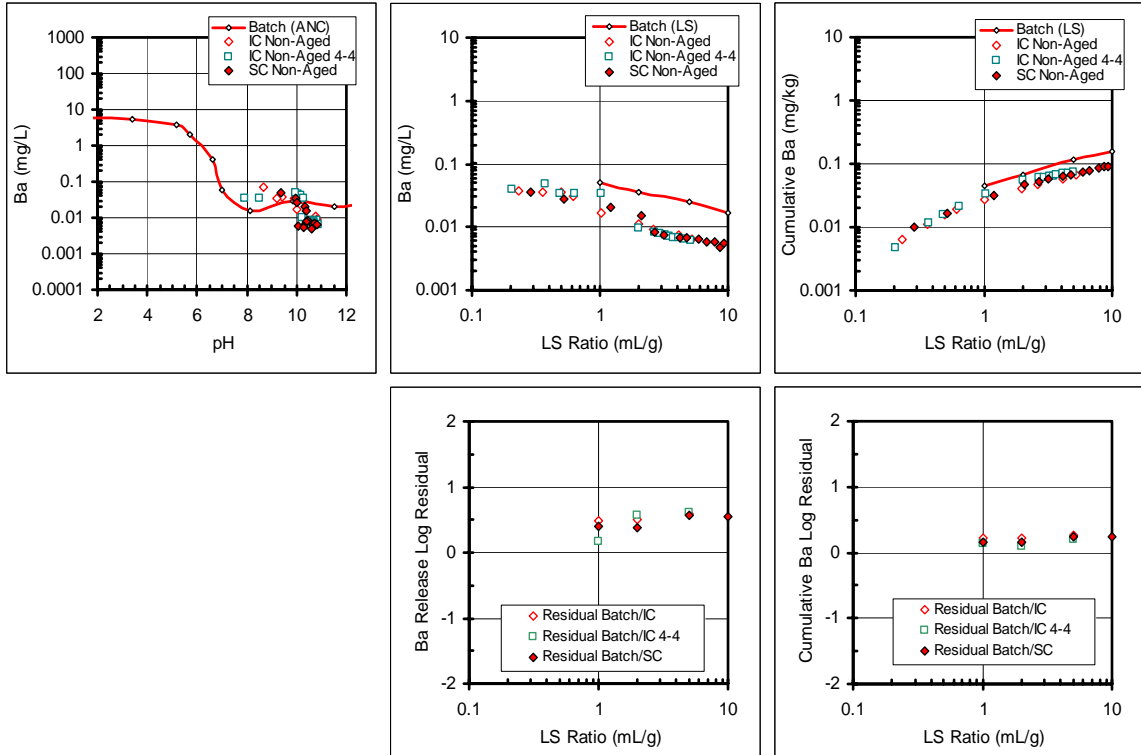


Figure B.86. Ba release from CD as a function of pH and LS ratio.

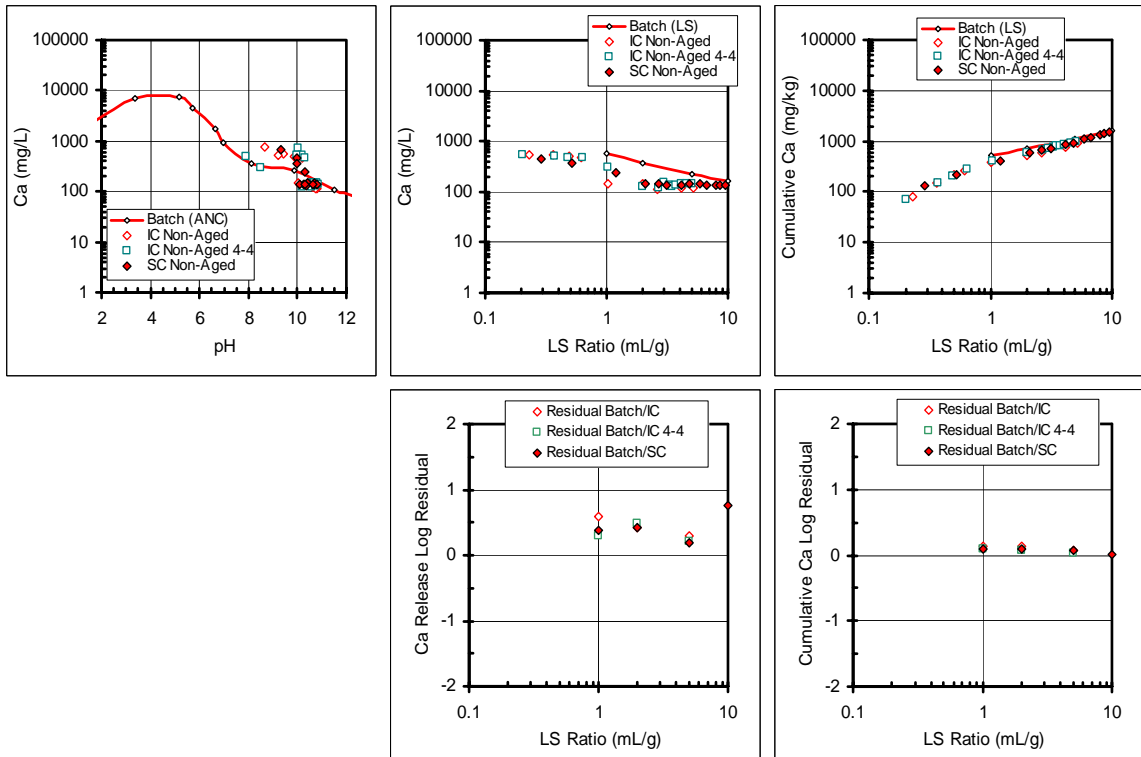


Figure B.87. Ca release from CD as a function of pH and LS ratio.

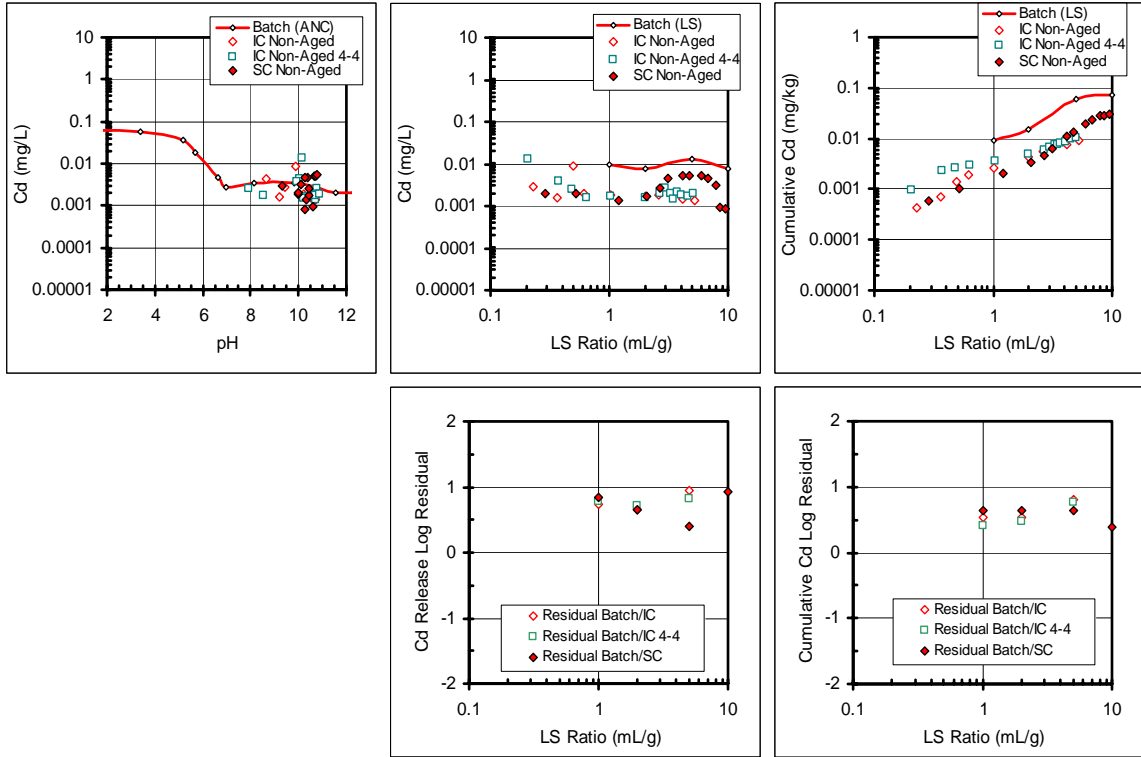


Figure B.88. Cd release from CD as a function of pH and LS ratio.

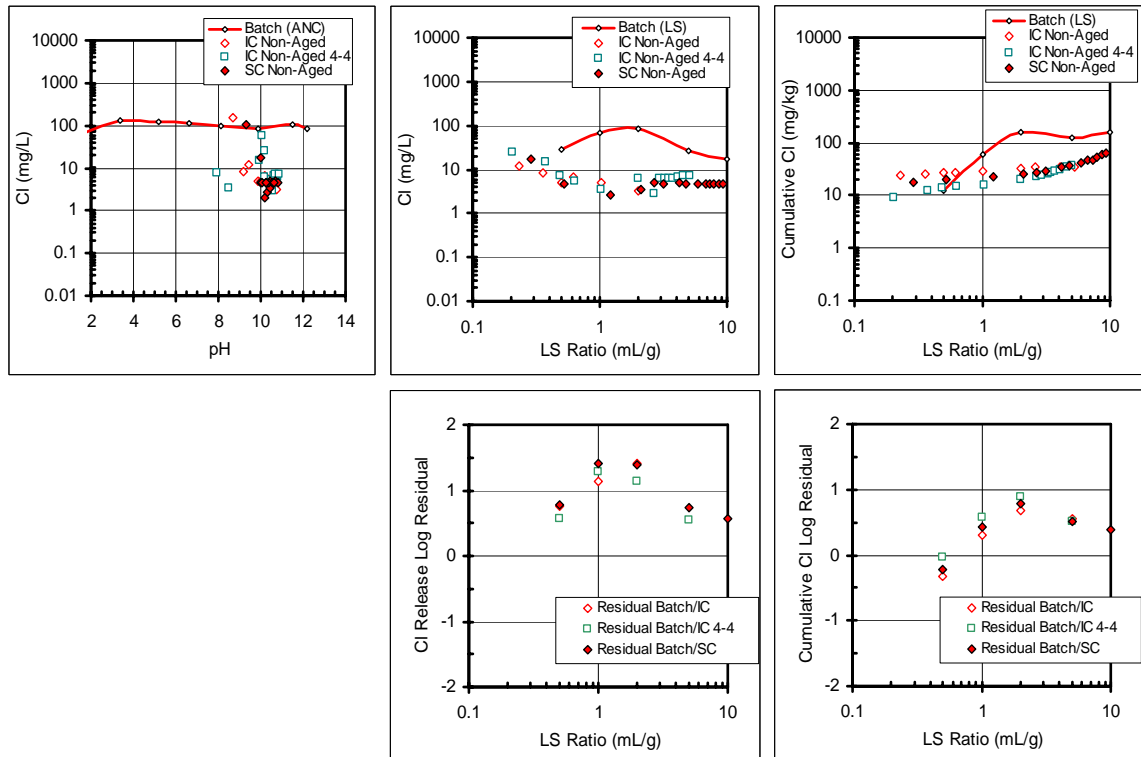


Figure B.89. Cl release from CD as a function of pH and LS ratio.

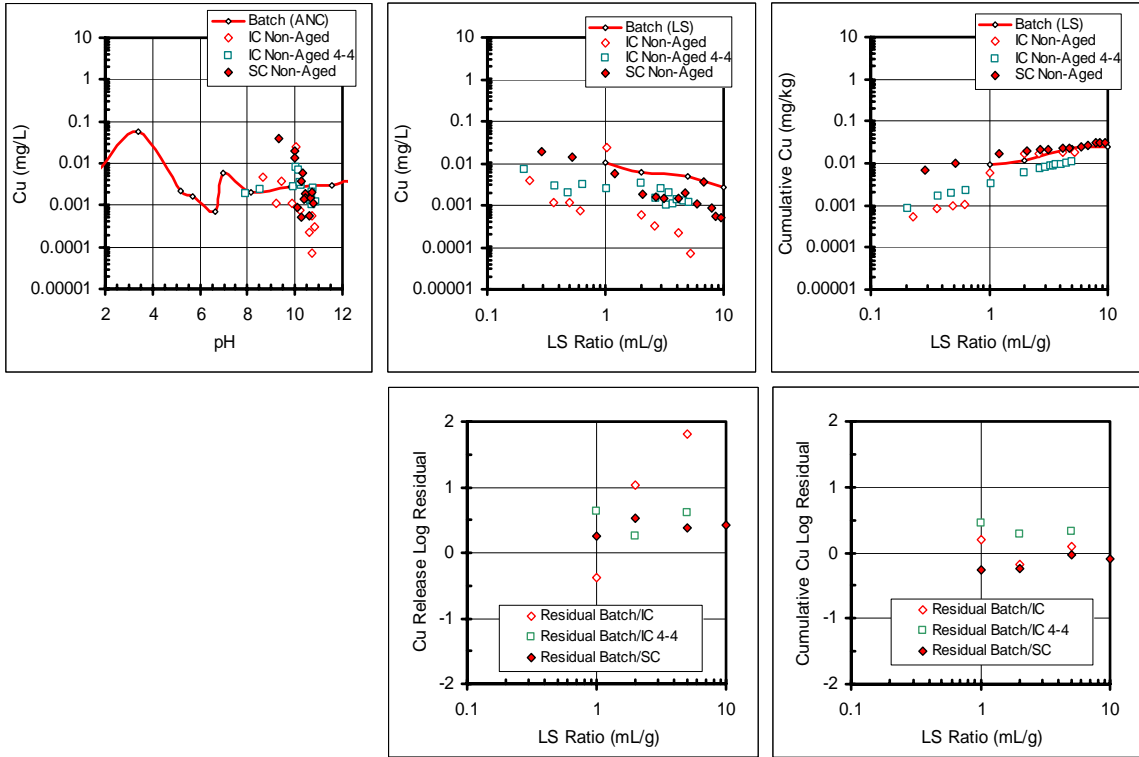


Figure B.90. Cu release from CD as a function of pH and LS ratio.

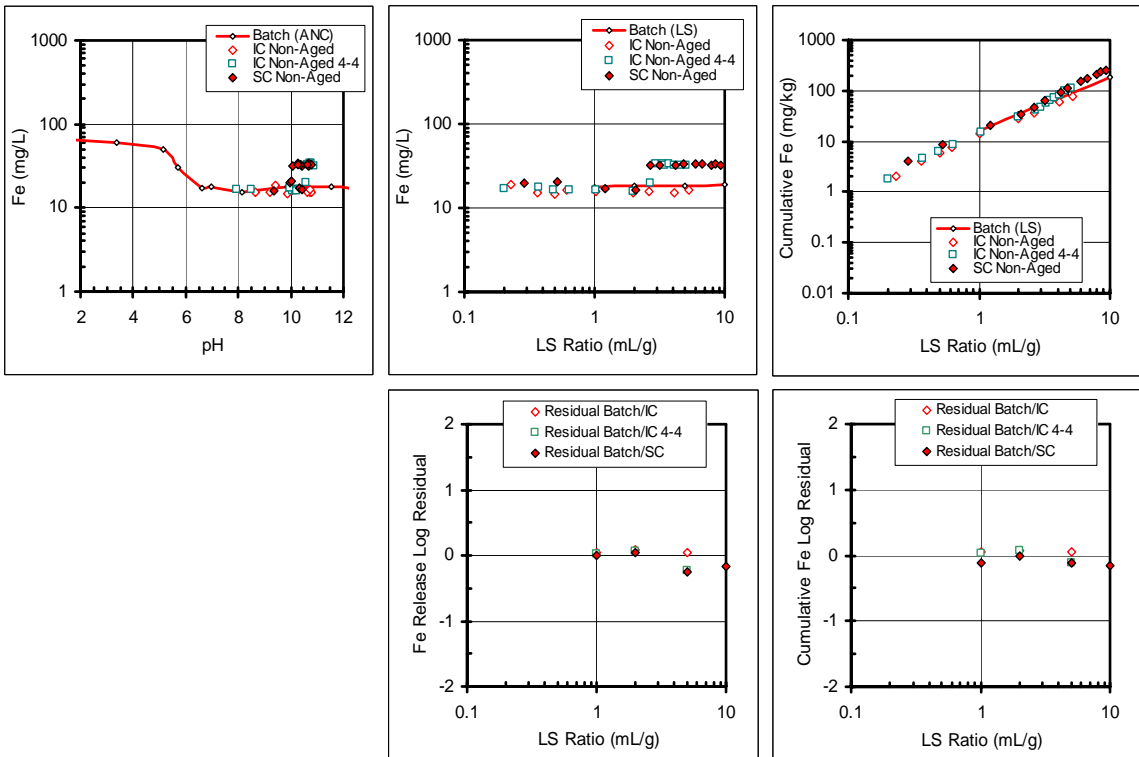


Figure B.91. Fe release from CD as a function of pH and LS ratio.

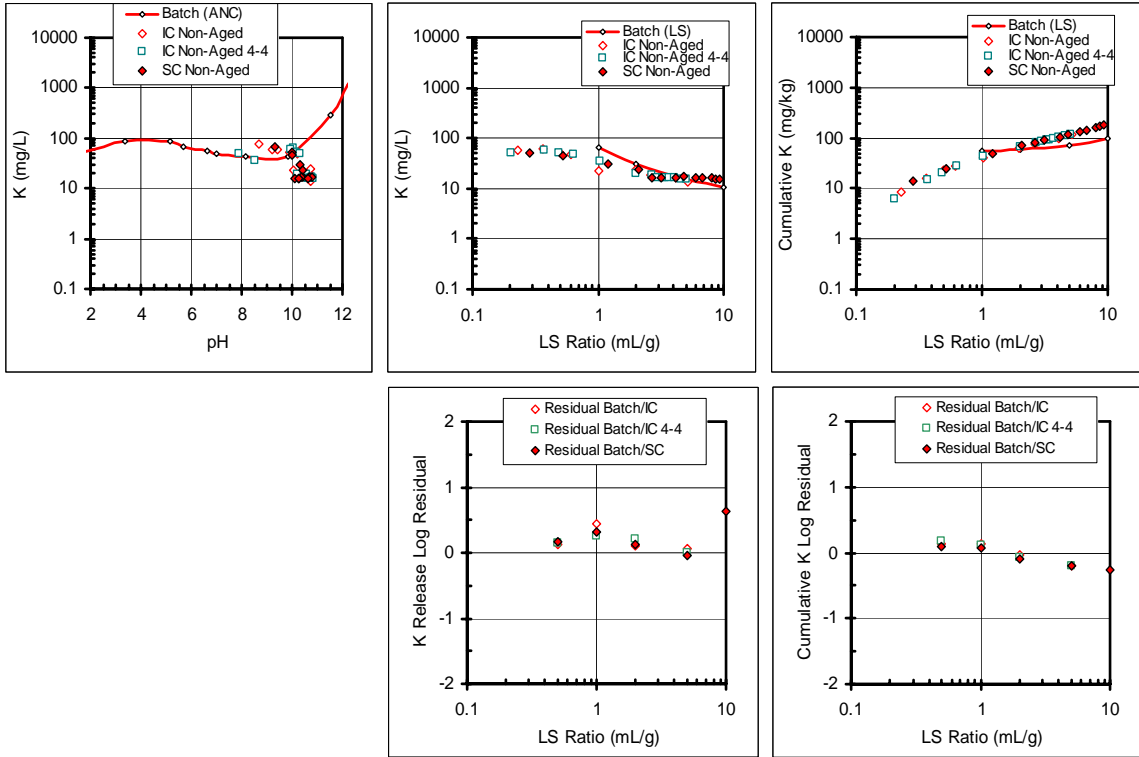


Figure B.92. K release from CD as a function of pH and LS ratio.

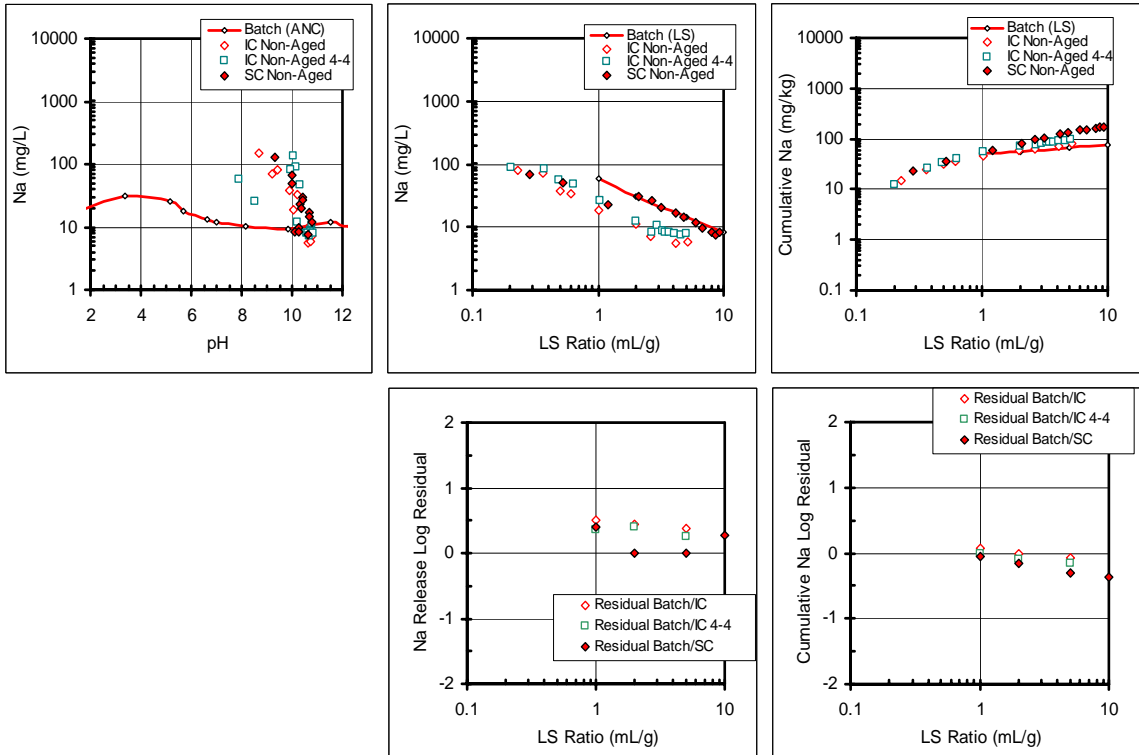


Figure B.93. Na release from CD as a function of pH and LS ratio.

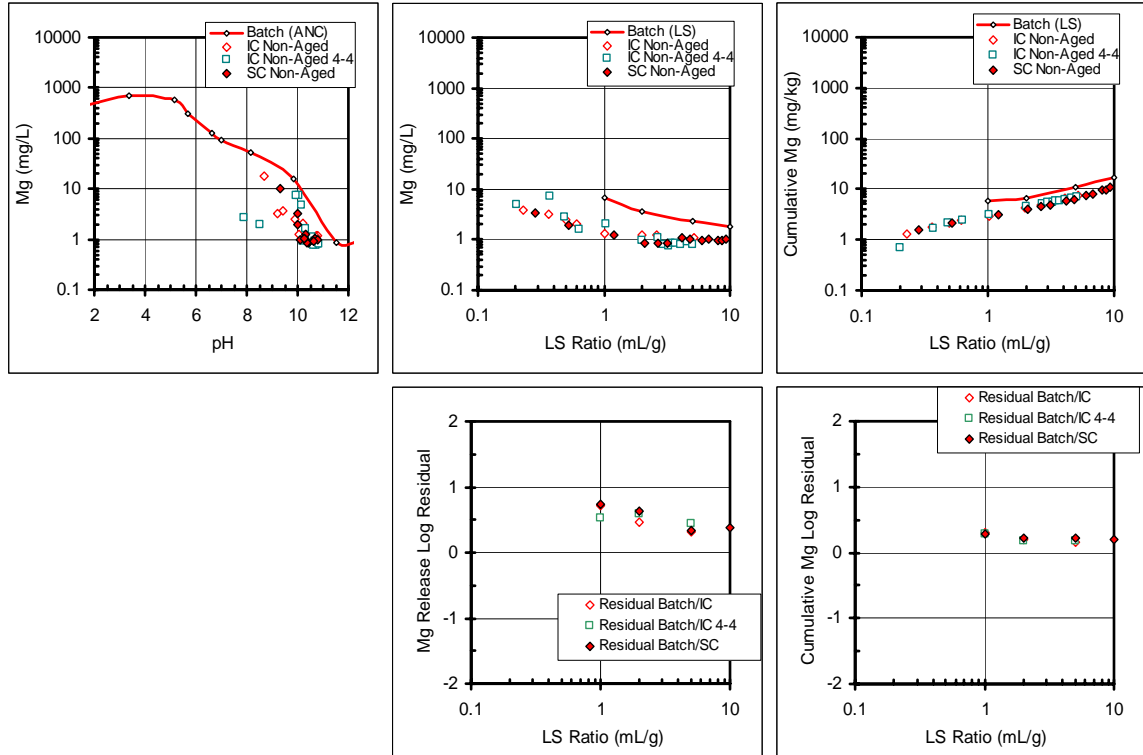


Figure B.94. Mg release from CD as a function of pH and LS ratio.

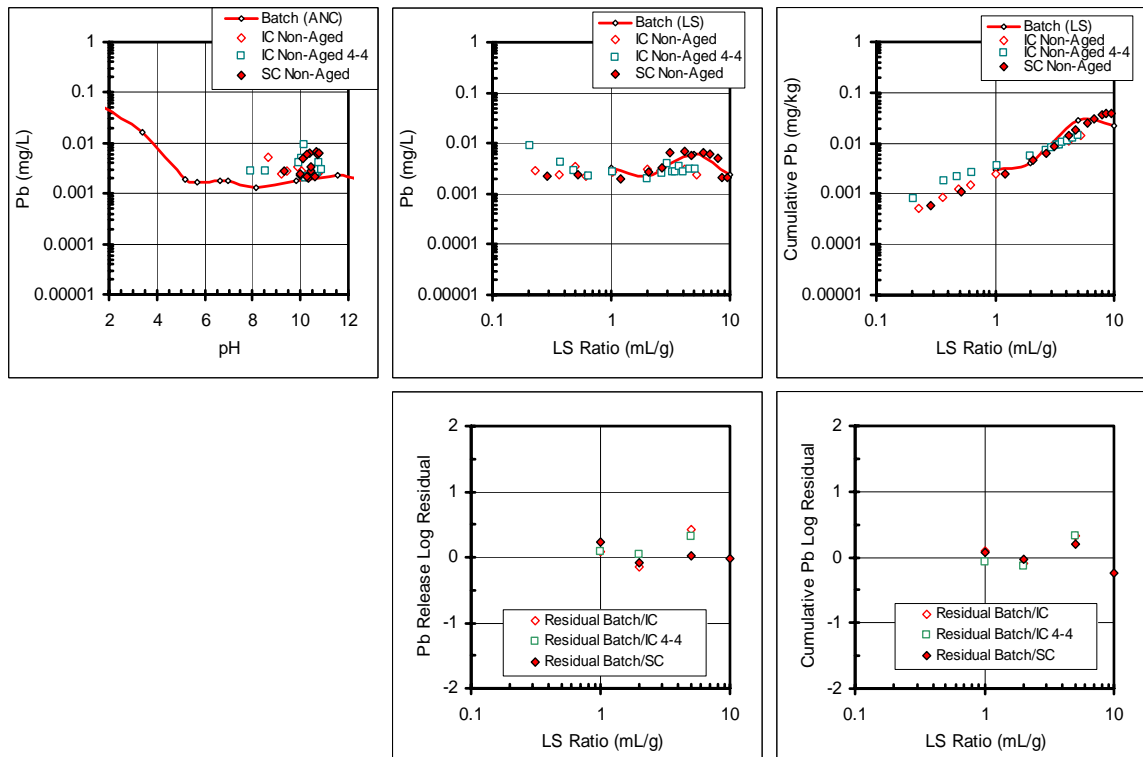


Figure B.95. Pb release from CD as a function of pH and LS ratio.

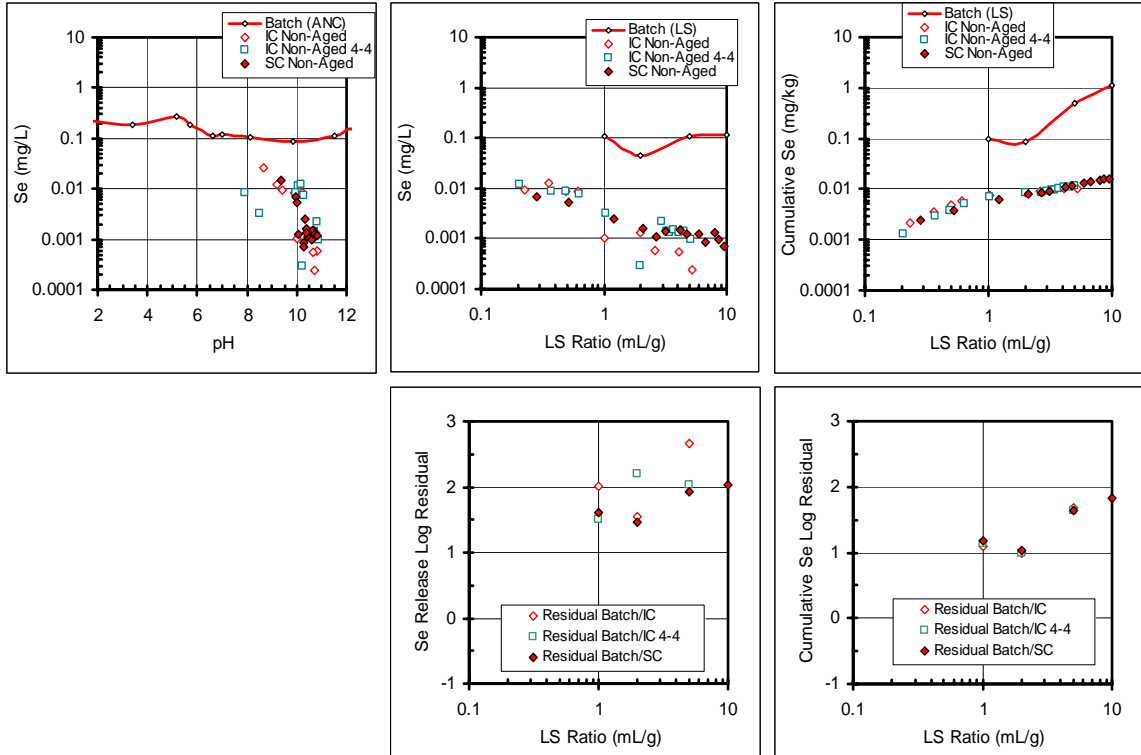


Figure B.96. Se release from CD as a function of pH and LS ratio.

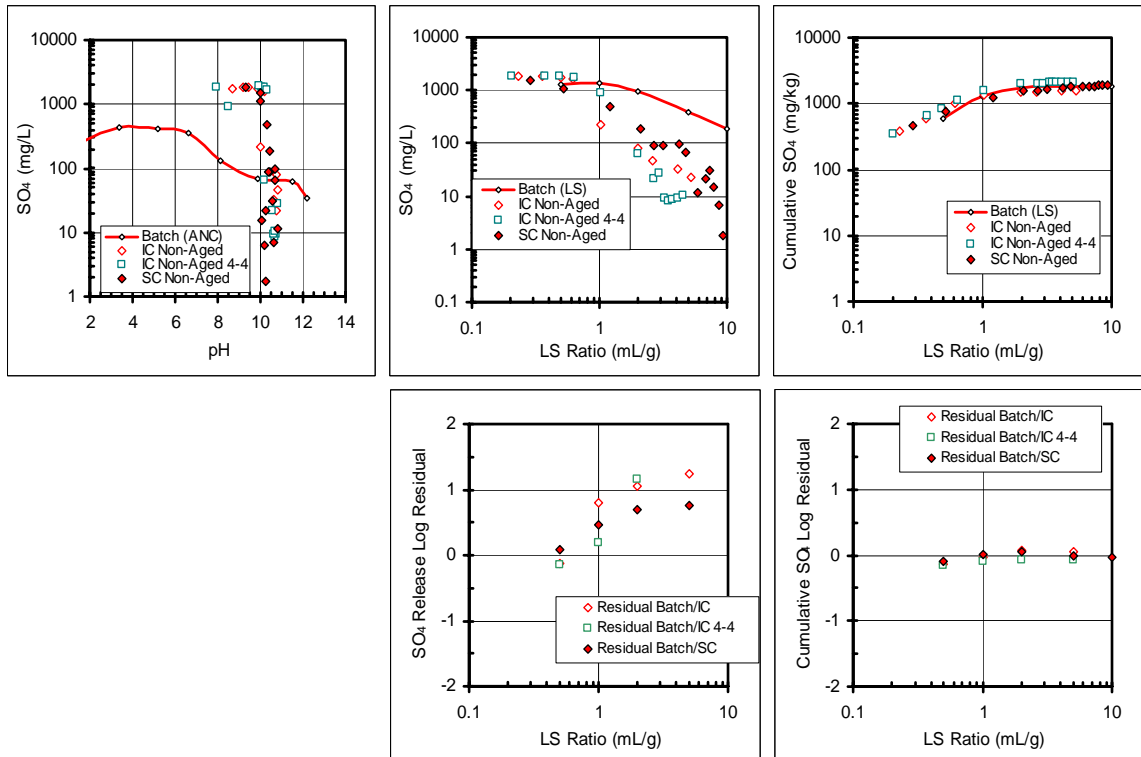


Figure B.97. SO_4 release from CD as a function of pH and LS ratio.

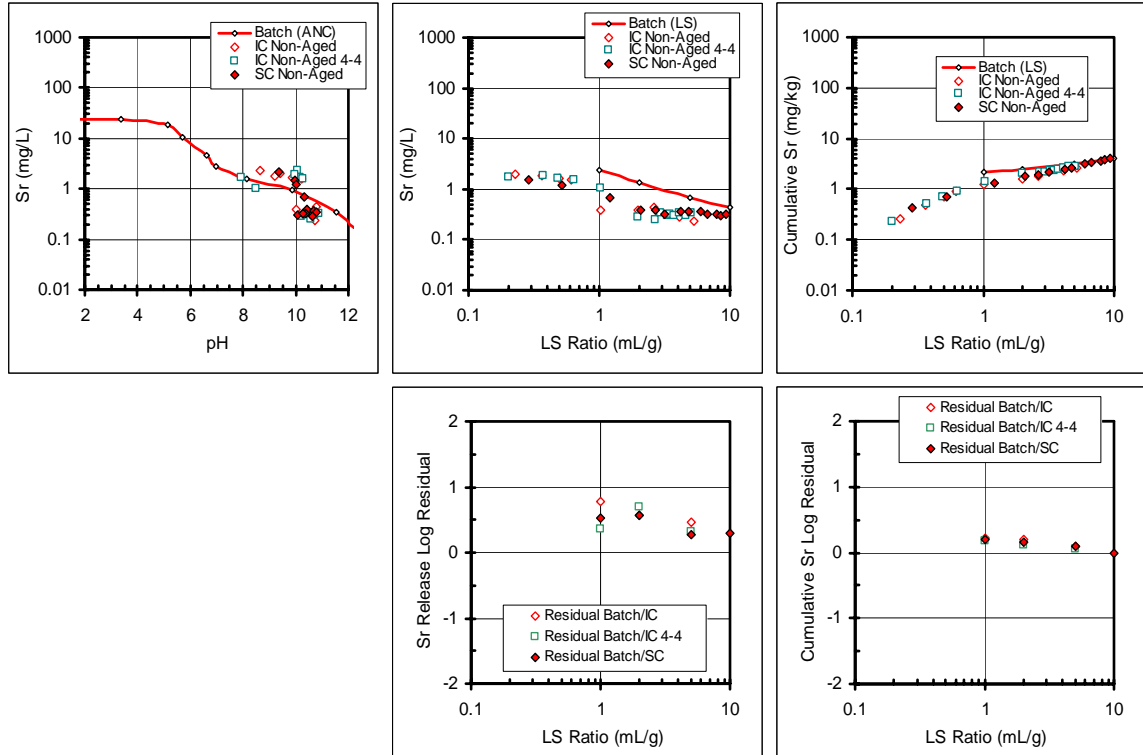


Figure B.98. Sr release from CD as a function of pH and LS ratio.

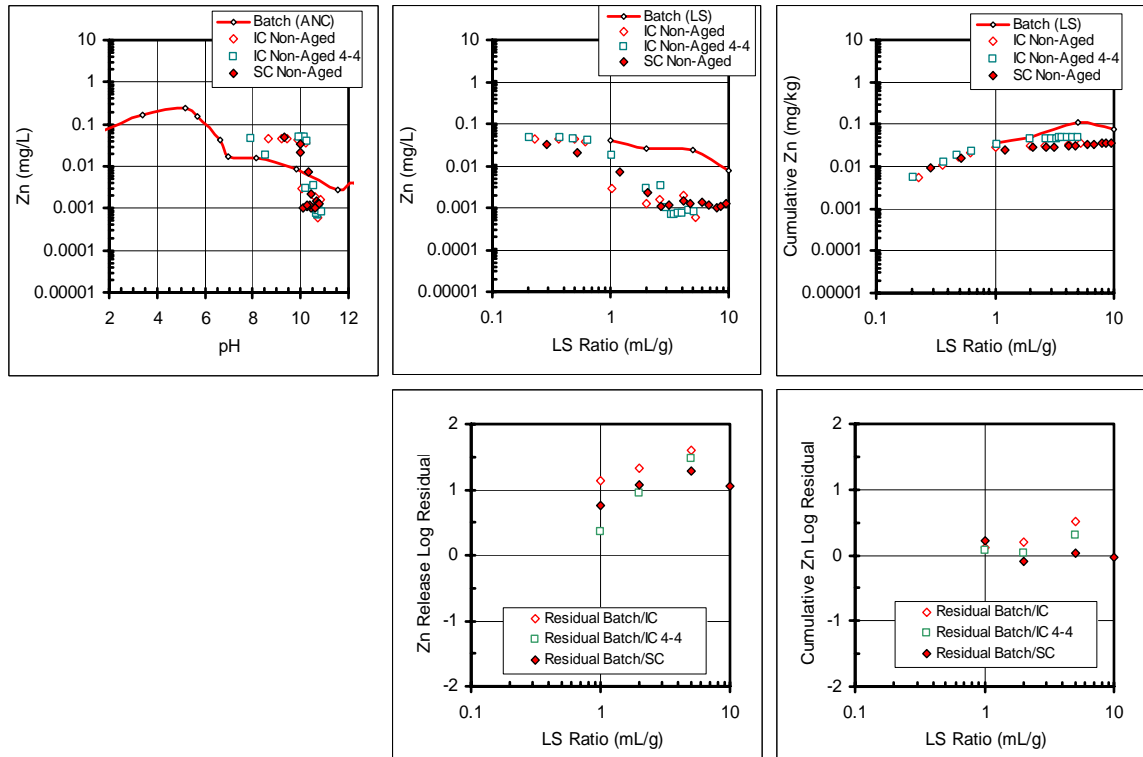


Figure B.99. Zn release from CD as a function of pH and LS ratio.

Laboratory Formulated Concrete

pH and conductivity data

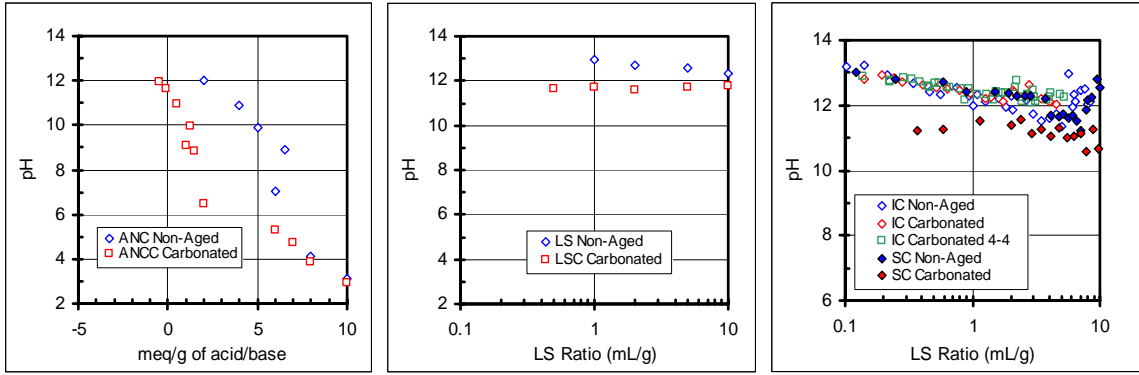


Figure B.100. pH of LFC batch and column testing.

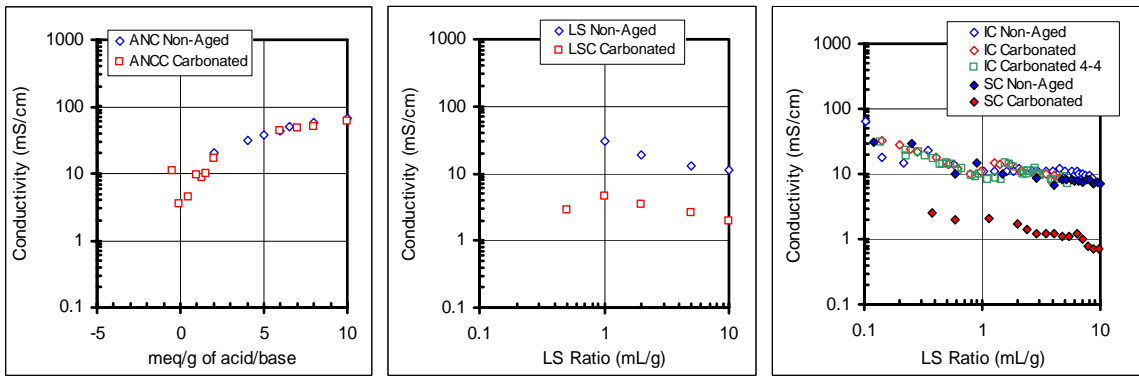


Figure B.101. Conductivity of LFC batch and column testing.

Activity and ionic strength data

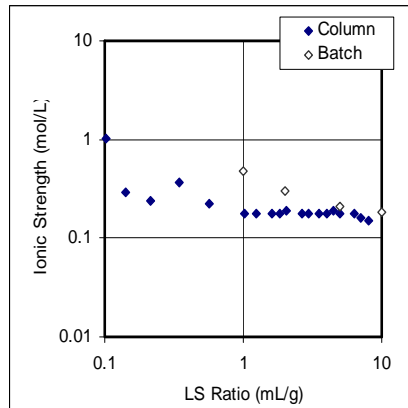


Figure B.102. Ionic strength as a function of LS Ratio for LFC.

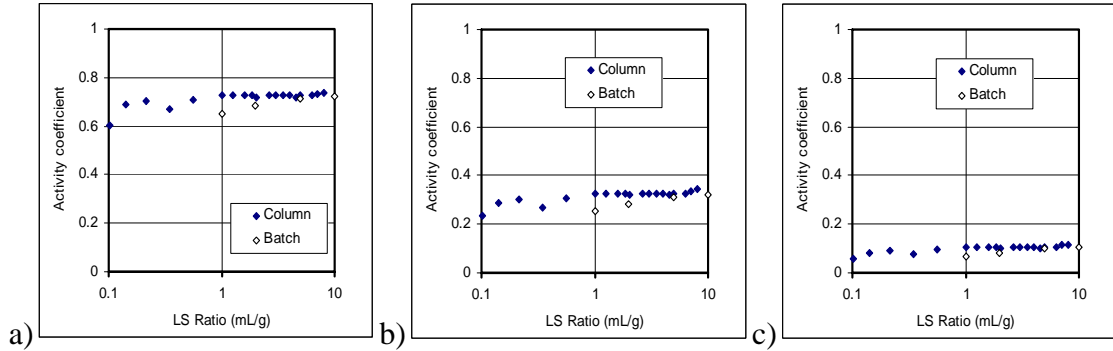


Figure B.103. Activity of a) ± 1 , b) ± 2 and c) ± 3 species for LFC (SC column data).

Elemental data

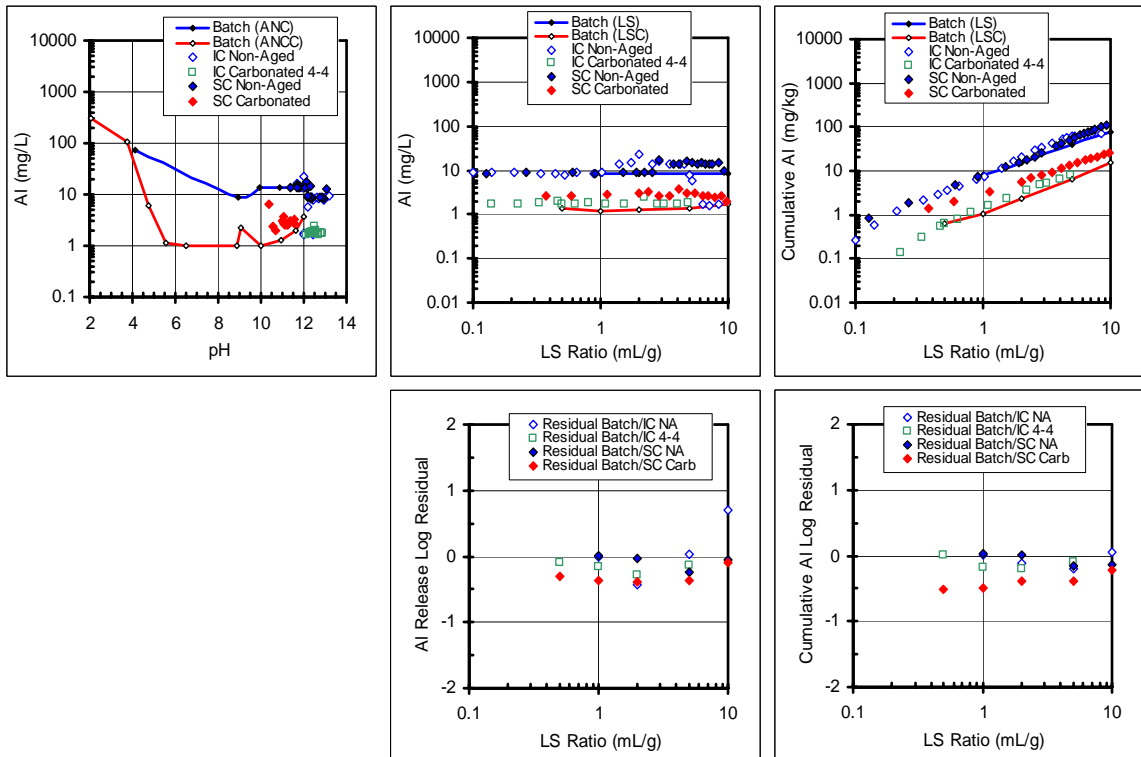


Figure B.104. Al release from LFC as a function of pH and LS ratio.

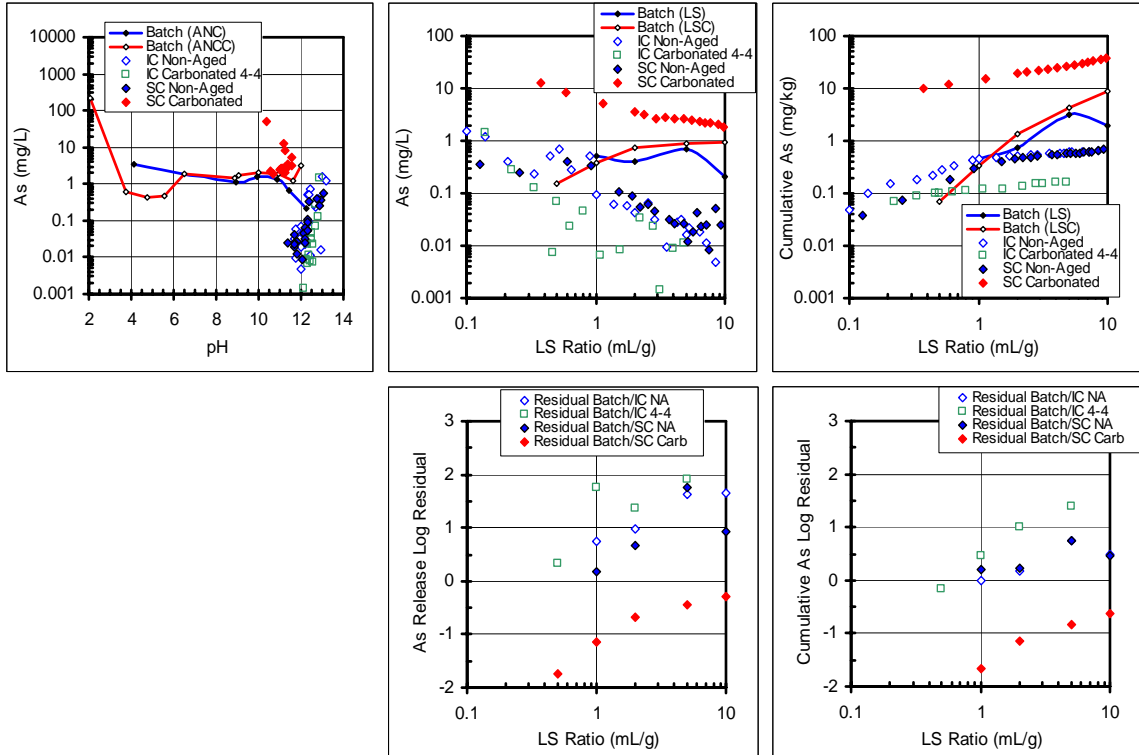


Figure B.105. As release from LFC as a function of pH and LS ratio.

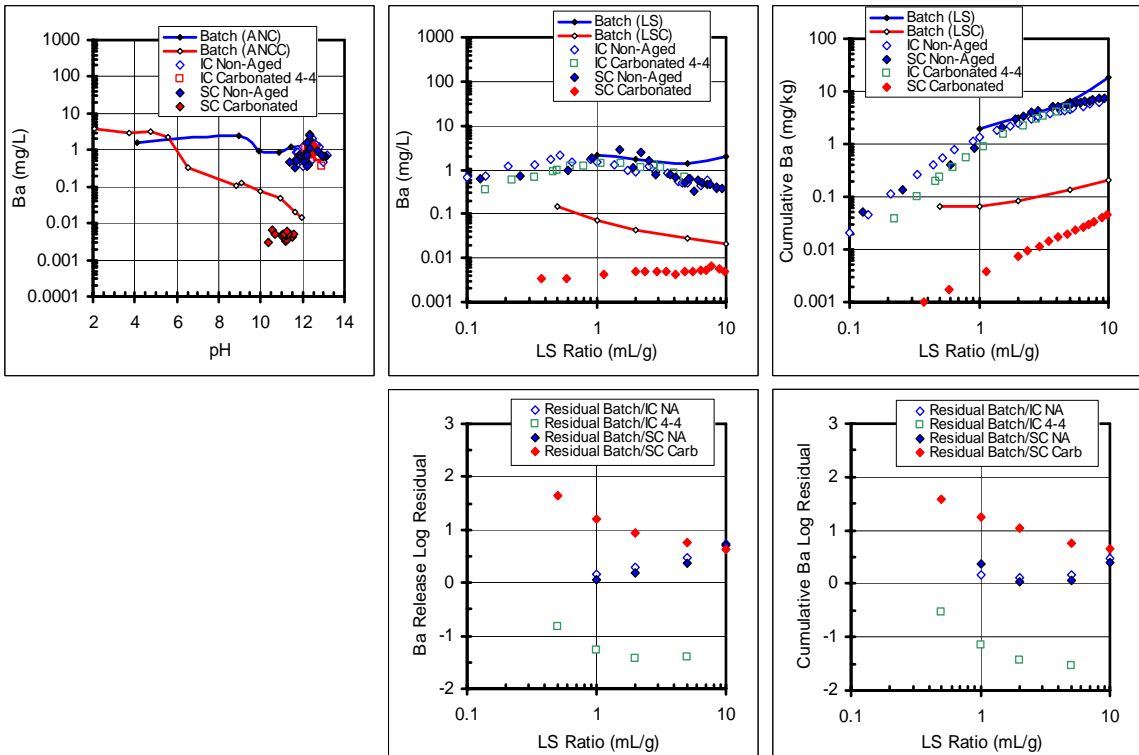


Figure B.106. Ba release from LFC as a function of pH and LS ratio.

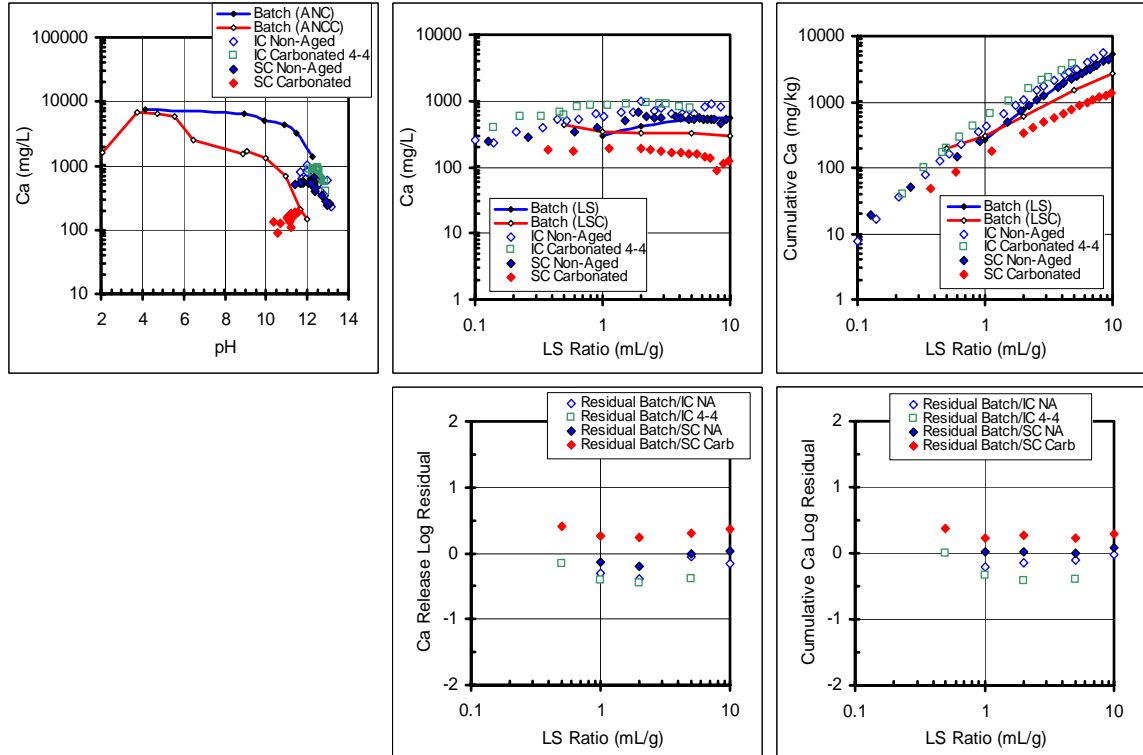


Figure B.107. Ca release from LFC as a function of pH and LS ratio.

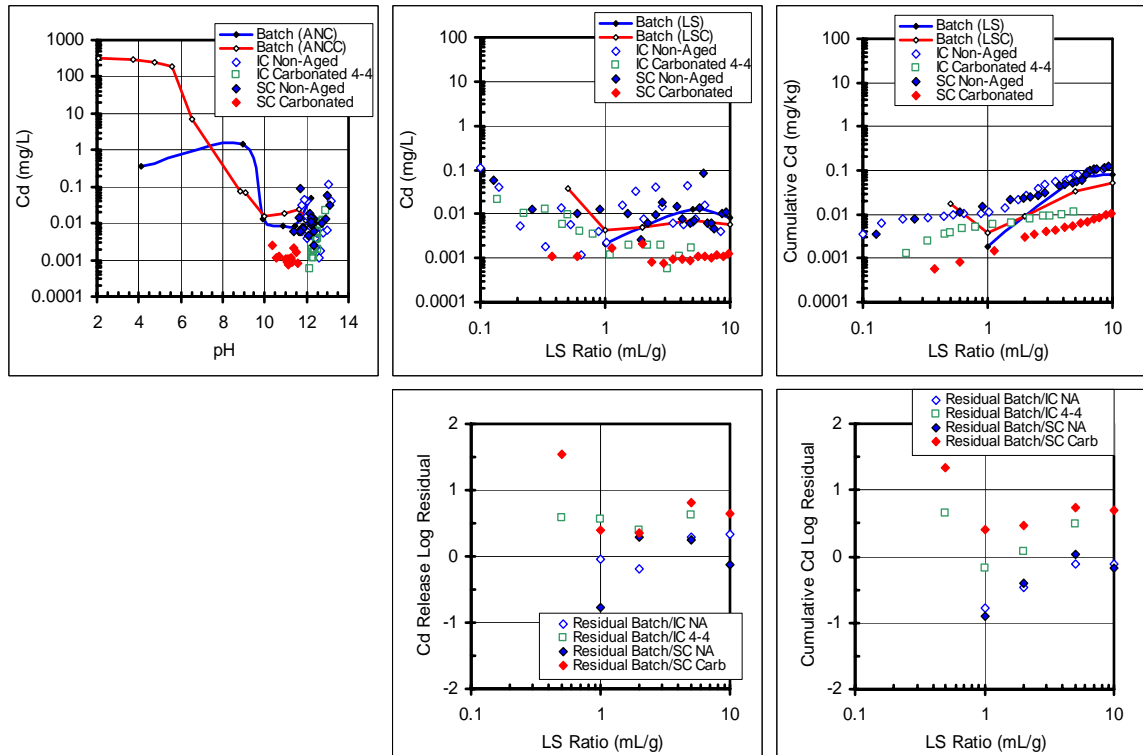


Figure B.108. Cd release from LFC as a function of pH and LS ratio.

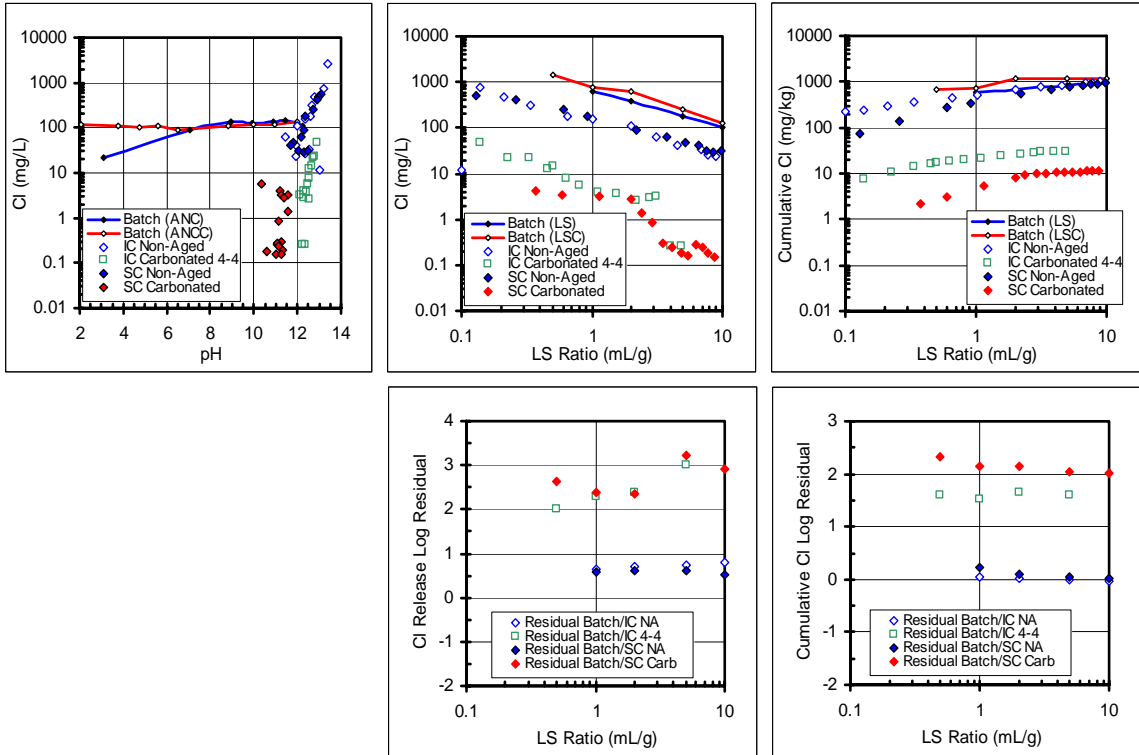


Figure B.109. Cl release from LFC as a function of pH and LS ratio.

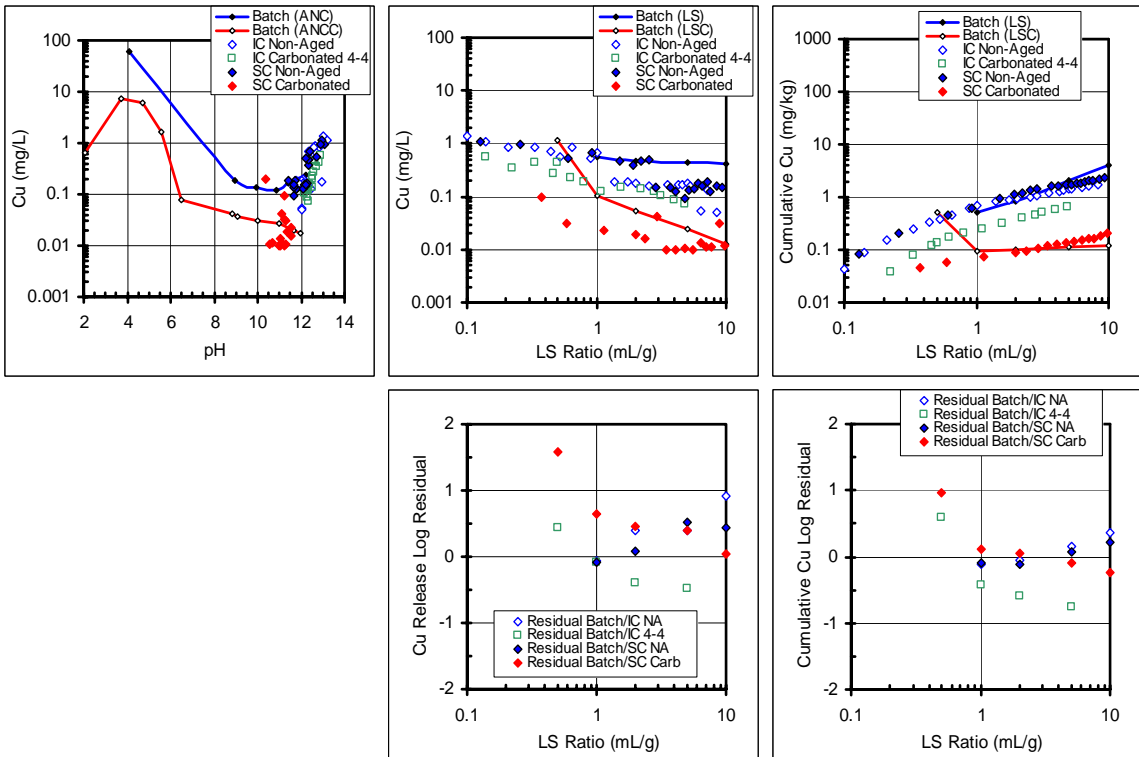


Figure B.110. Cu release from LFC as a function of pH and LS ratio.

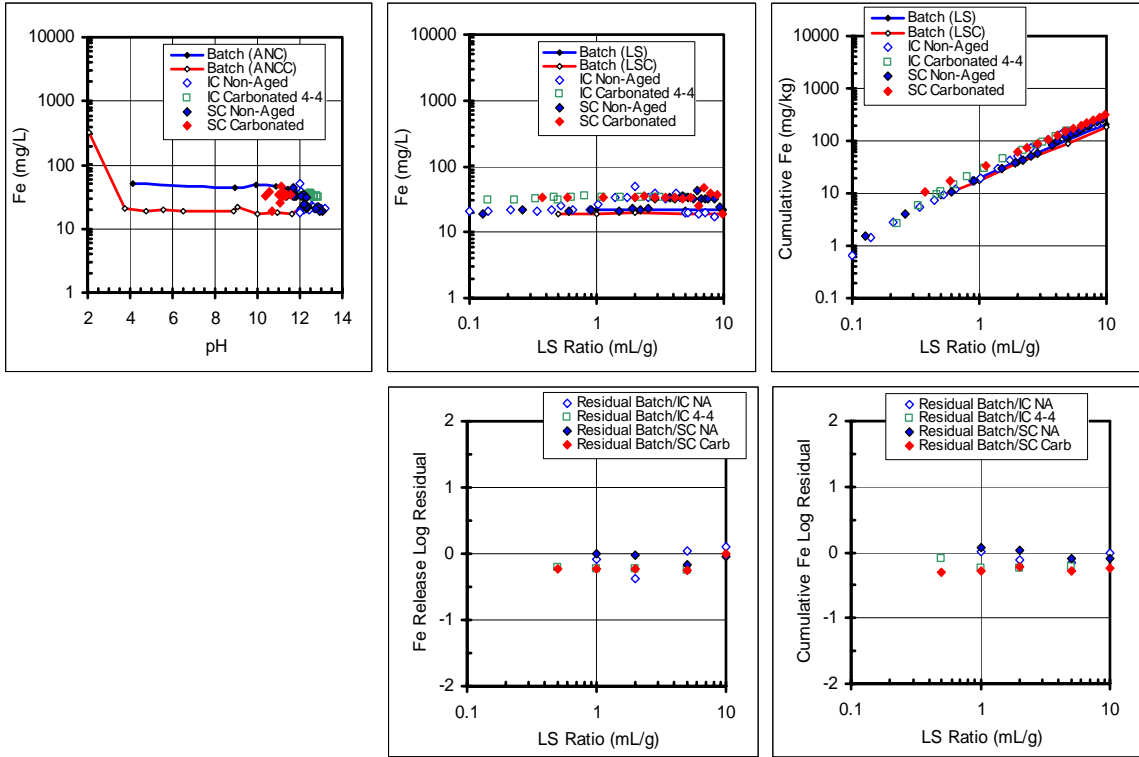


Figure B.111. Fe release from LFC as a function of pH and LS ratio.

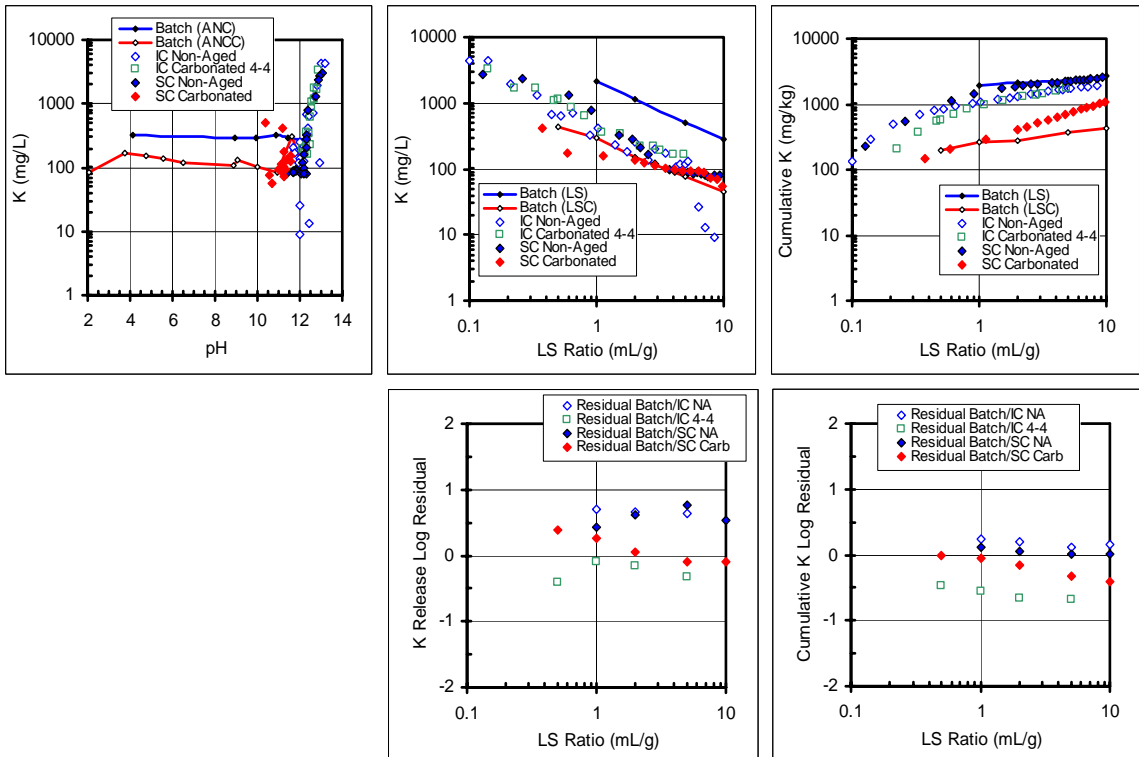


Figure B.112. K release from LFC as a function of pH and LS ratio.

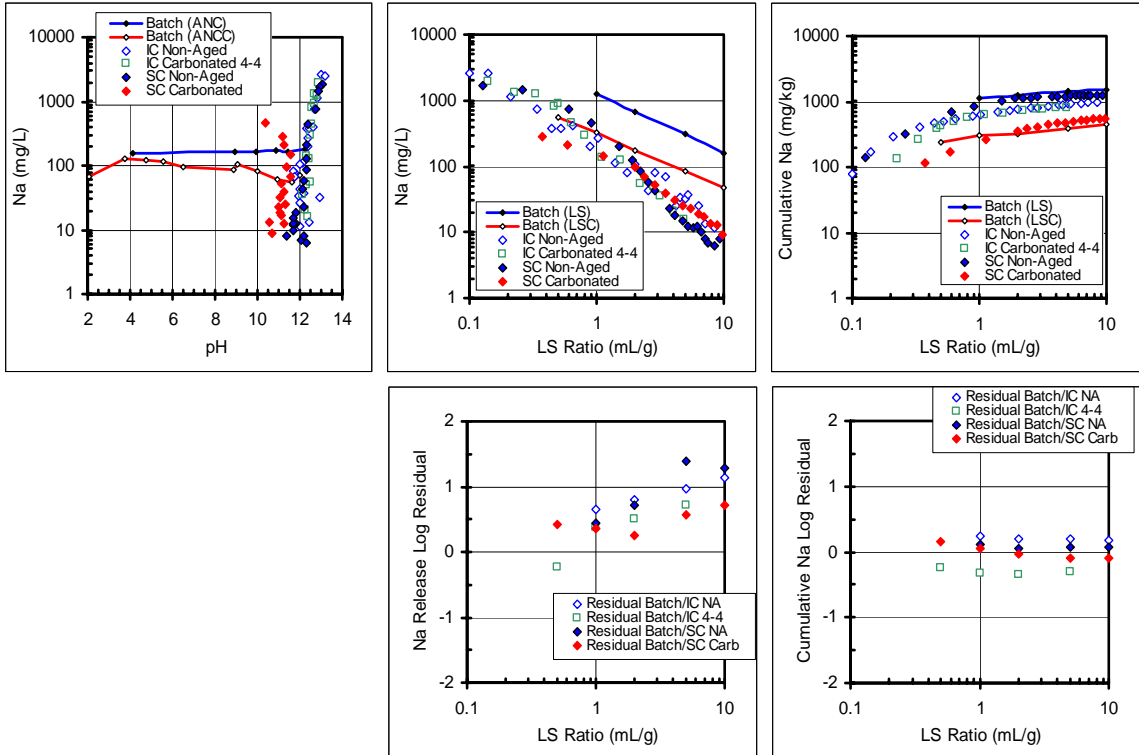


Figure B.113. Na release from LFC as a function of pH and LS ratio.

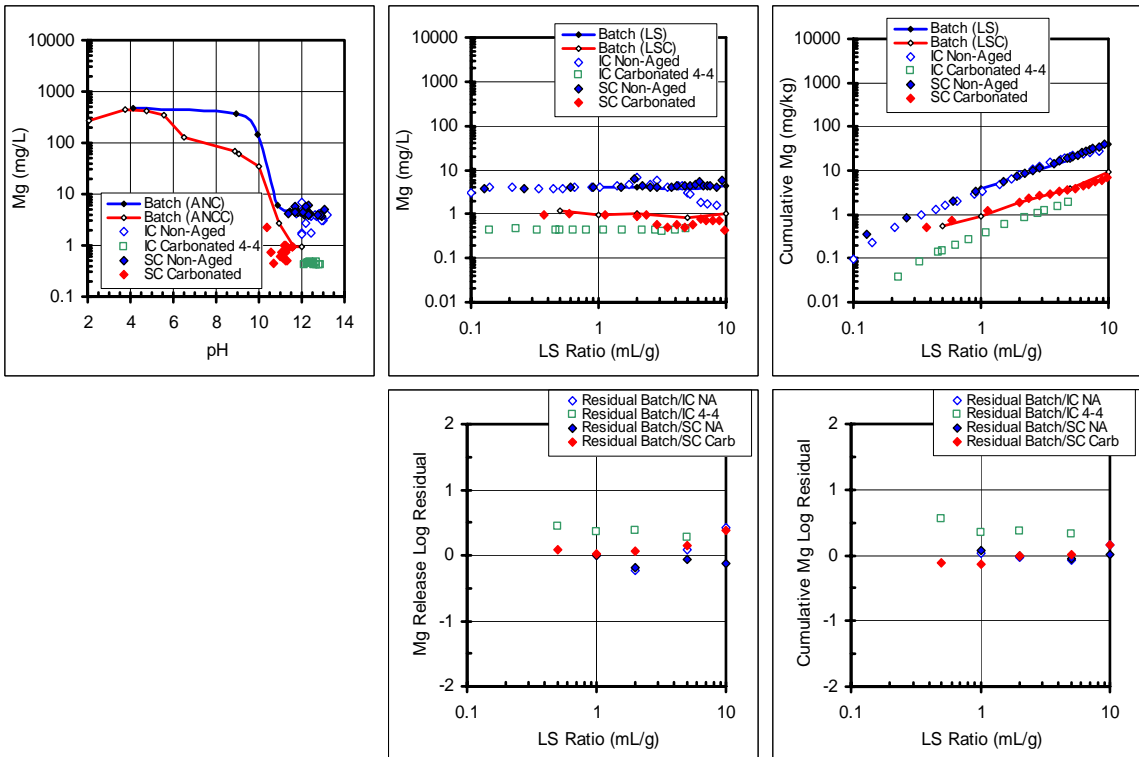


Figure B.114. Mg release from LFC as a function of pH and LS ratio.

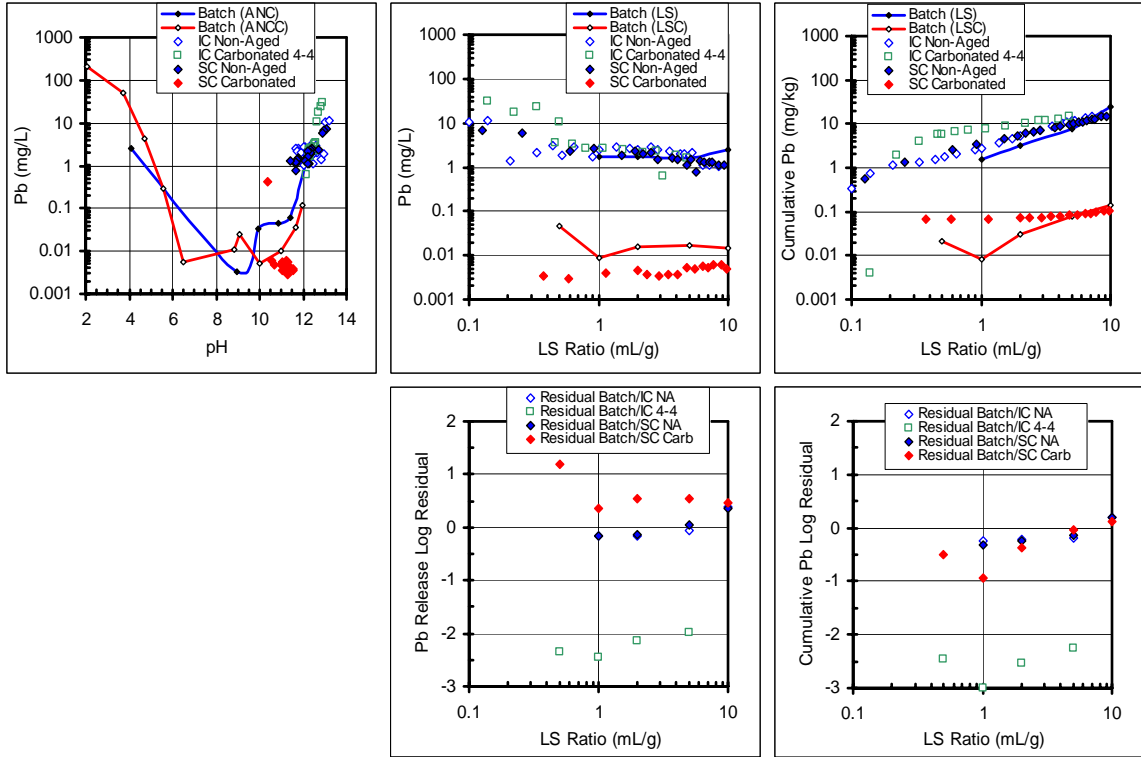


Figure B.115. Pb release from LFC as a function of pH and LS ratio.

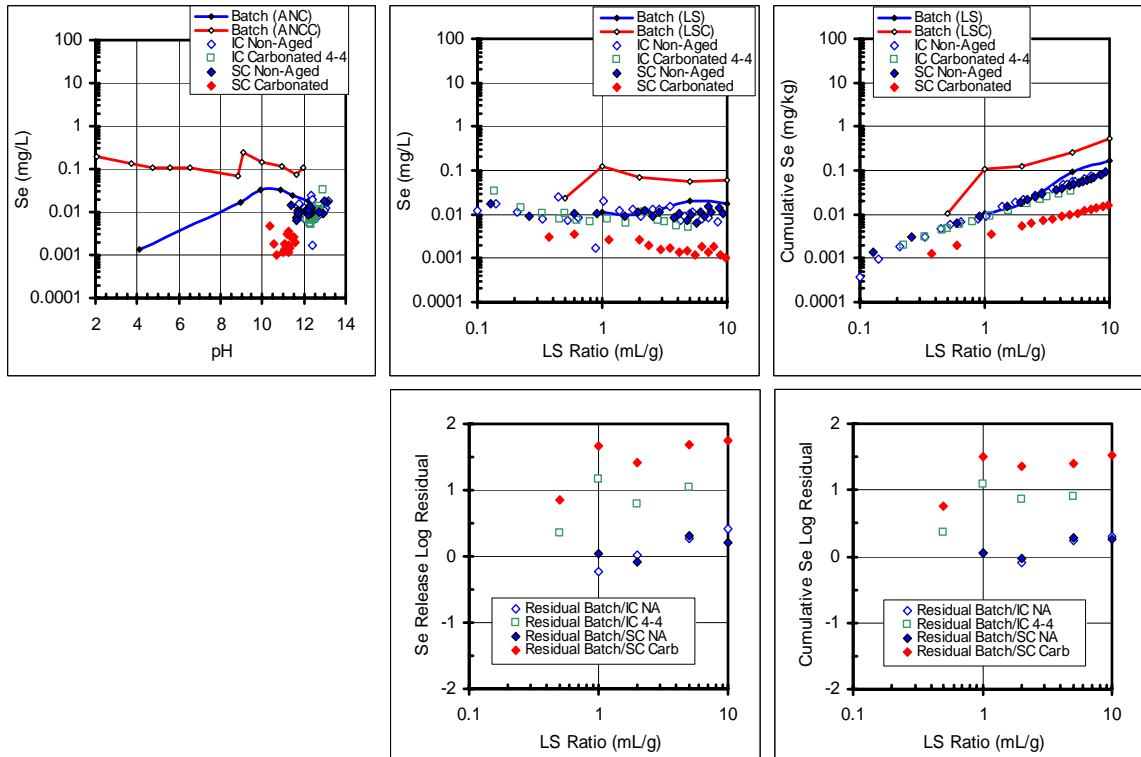


Figure B.116. Se release from LFC as a function of pH and LS ratio.

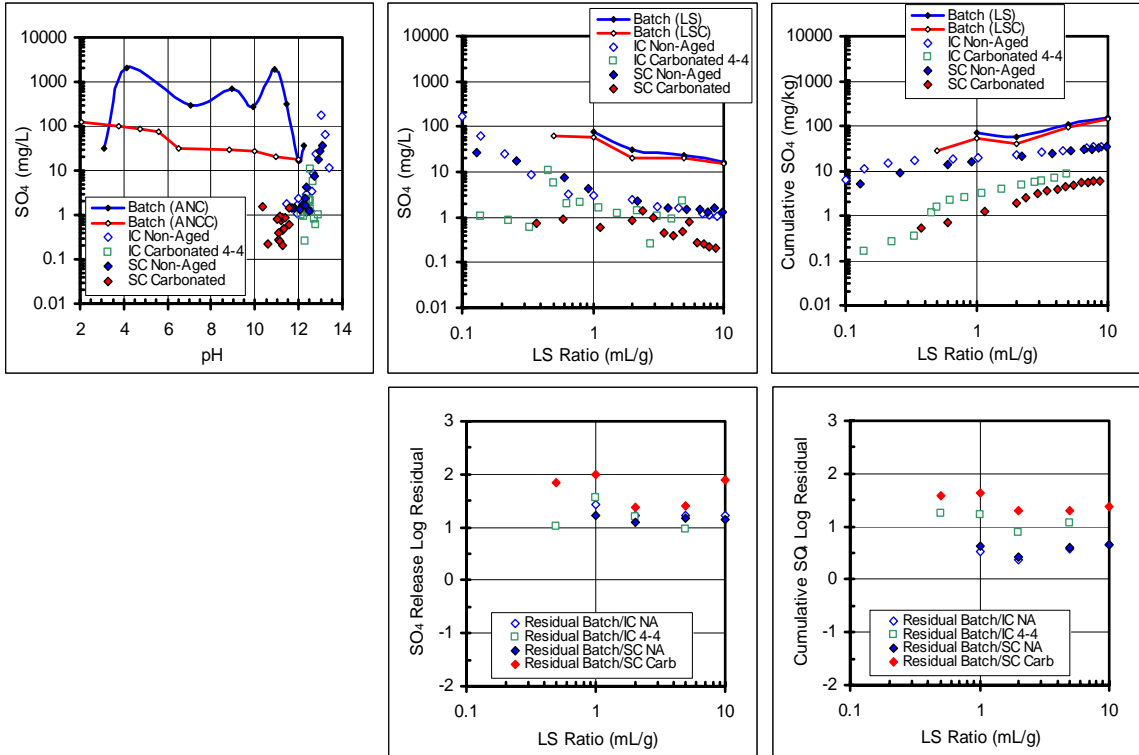


Figure B.117. SO_4 release from LFC as a function of pH and LS ratio.

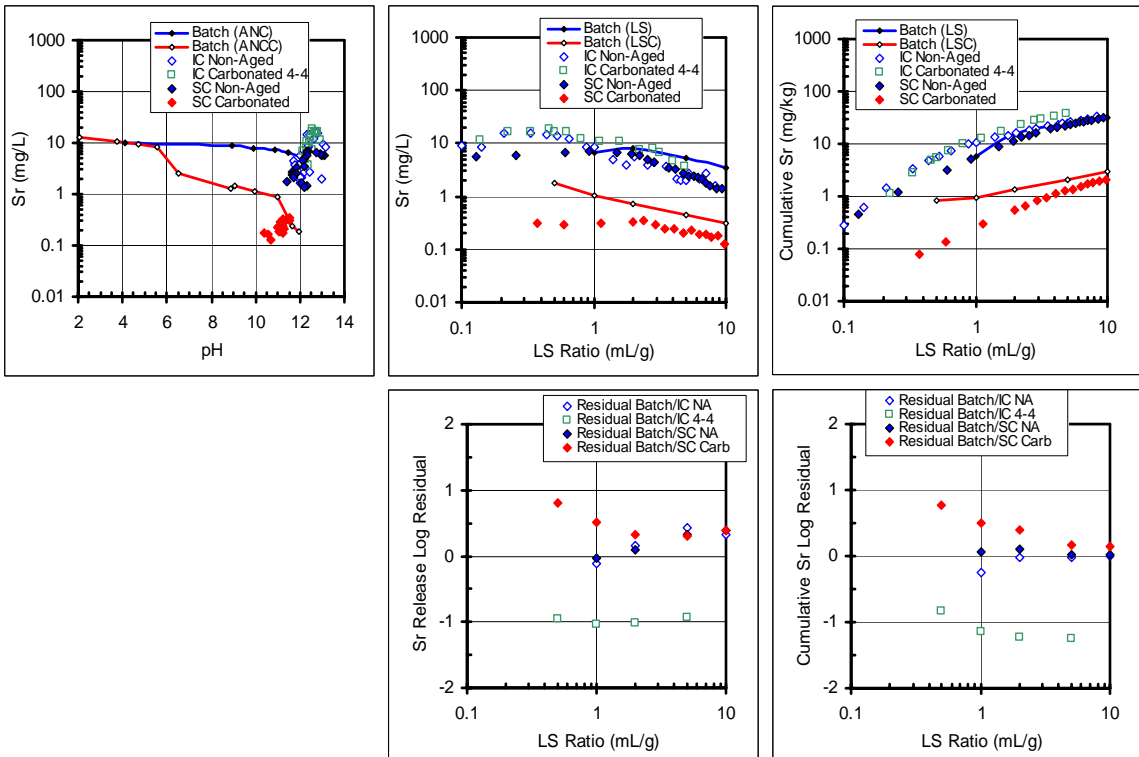


Figure B.118. Sr release from LFC as a function of pH and LS ratio.

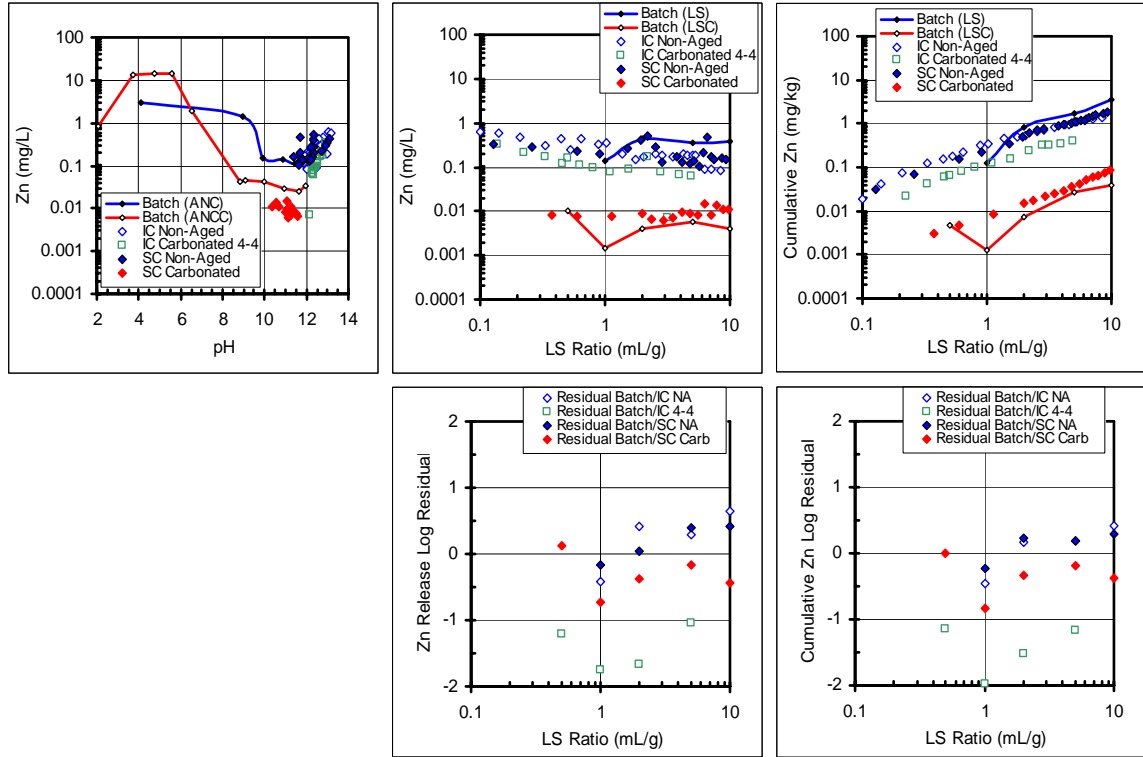


Figure B.119. Zn release from LFC as a function of pH and LS ratio.

Data interpretation

All the elemental concentration data for all materials were analyzed and are presented in this section. Table B.1. shows the sample number (n), mean and standard deviation values for all residuals calculated from the experimental data presented previously. The two types of residuals are residuals on a concentration as a function of LS ratio basis, and residuals from a cumulative release basis. Figures B.120 and B.121 show a graphical description of the mean values for every element analyzed, and bars are included depicting the standard deviation for each mean value. Figure B.120 shows data for residuals on a concentration basis, and Figure B.121 shows data for residuals calculated from cumulative release.

Table B.1. Statistical data for residual values.

Element	Concentration based residuals			Cumulative based residuals		
	Sample number (n)	Mean	Standard deviation	Sample number (n)	Mean	Standard deviation
Al	63	-0.1649	0.4334	63	-0.1616	0.4032
As	65	0.4137	0.8806	65	0.2468	0.8896
Ba	64	0.6104	0.6523	65	0.2849	0.6137
Ca	63	0.3643	0.2695	63	0.2391	0.2214
Cd	64	0.5386	0.5795	65	0.3726	0.5258
Cl	50	1.3263	0.8152	50	0.4578	0.6545
Cu	65	0.2797	0.4963	65	0.0110	0.3894
Fe	63	-0.0284	0.2023	63	-0.0199	0.2279
K	66	0.3224	0.4513	66	0.0098	0.2876
Mg	63	0.2757	0.5756	63	0.0783	0.5511
Na	63	0.7739	0.4538	63	0.0869	0.2425
Pb	64	0.0425	0.6493	65	-0.1726	0.5472
SO ₄	43	1.0811	0.7828	46	0.4246	0.6052
Se	64	0.8008	0.6891	65	0.4579	0.5699
Sr	63	0.5647	0.3540	63	0.1879	0.2024
Zn	64	0.3856	0.4919	65	0.0962	0.2898

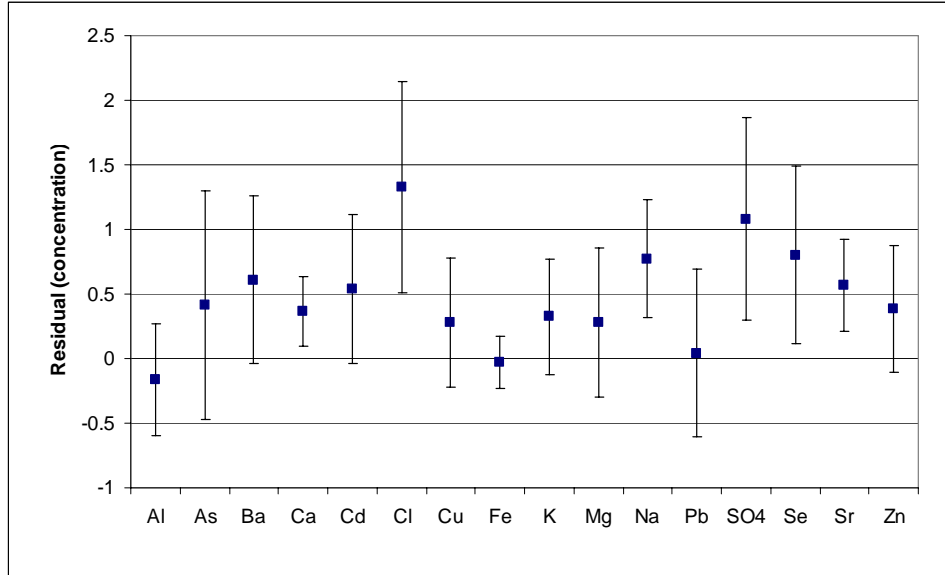


Figure B.120. Mean and standard deviation data for concentration residuals.

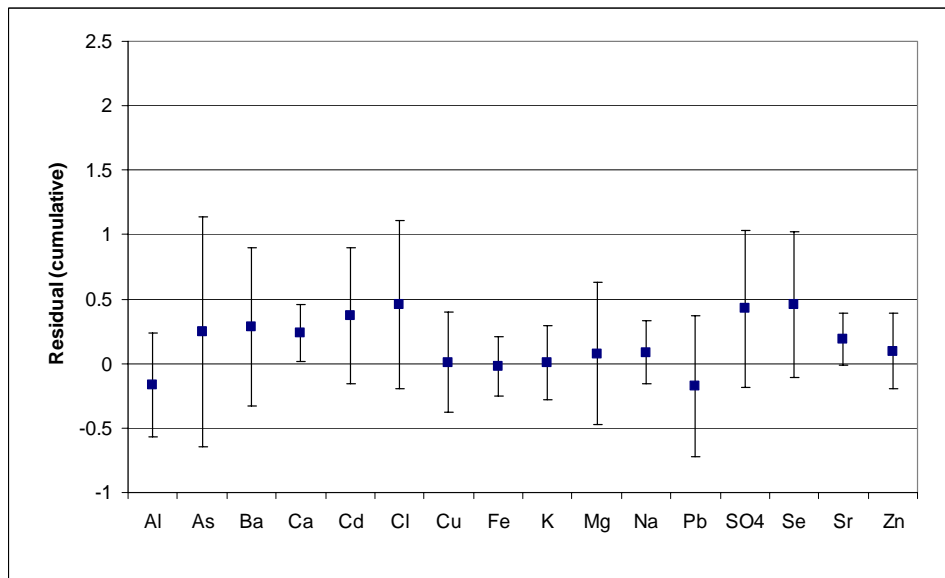


Figure B.121. Mean and standard deviation data for cumulative residuals.

Table B.2. shows the sample number (n), mean and standard deviation values for these LS ratio residuals. Figures B.122 and B.123 show the same information as Figures B.120 and B.121, but only LS 10 samples were considered for the residual calculation.

Table B.2. Statistical data for residual values of LS 10 samples.

Element	Concentration based residuals			Cumulative based residuals		
	Sample number (n)	Mean	Standard deviation	Sample number (n)	Mean	Standard deviation
Al	14	0.0028	0.3426	14	-0.0507	0.2888
As	14	0.1618	0.7918	14	-0.0295	0.6506
Ba	13	0.8764	0.8622	14	0.3010	0.4698
Ca	14	0.3912	0.2921	14	0.2469	0.1478
Cd	13	0.3481	0.5603	13	0.2011	0.4434
Cl	10	1.5010	1.0055	10	0.3098	0.6211
Cu	14	0.3017	0.3007	14	0.1284	0.2583
Fe	14	-0.0322	0.3405	14	-0.0393	0.3602
K	14	0.1042	0.7223	14	-0.2496	0.4482
Mg	14	0.2547	0.5748	14	0.0537	0.5428
Na	14	0.8259	0.4425	14	0.0304	0.2159
Pb	13	0.0017	0.5297	14	-0.1548	0.3932
SO ₄	8	1.6190	1.2007	10	0.5182	0.6184
Se	13	0.5701	0.7449	14	0.3150	0.6170
Sr	14	0.6832	0.4841	14	0.1436	0.1506
Zn	13	0.1941	0.3844	14	0.0116	0.2818

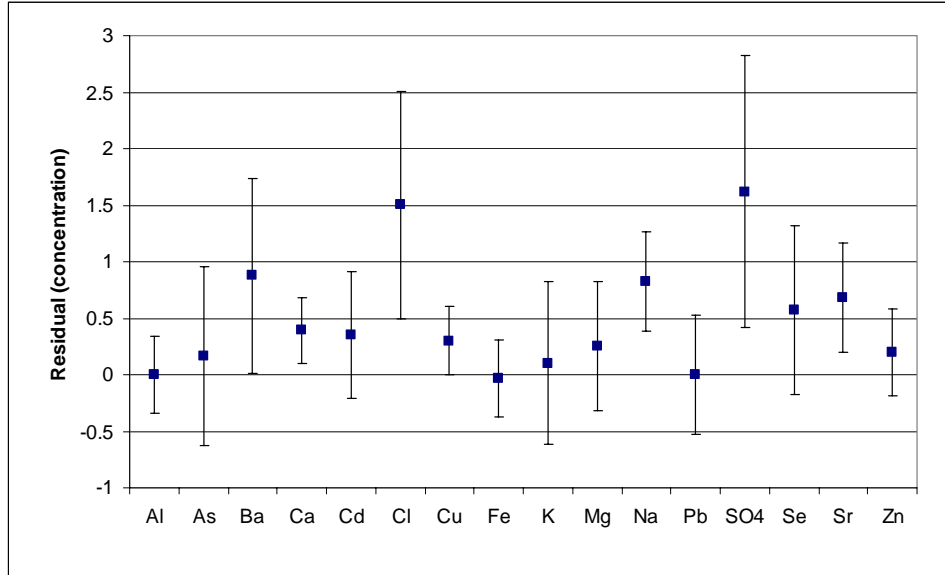


Figure B.122. Mean and standard deviation data for concentration residuals.

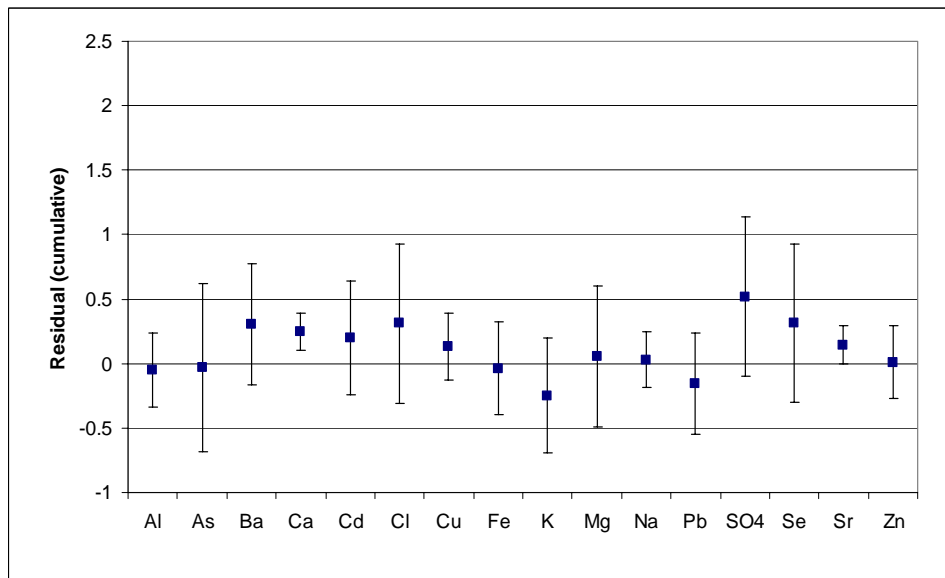


Figure B.123. Mean and standard deviation data for cumulative residuals.

APPENDIX C

GEOCHEMICAL SPECIATION MODELING RESULTS

Geochemical speciation modeling results obtained with LeachXS versions 1.0.4.0 and 1.0.4.1 are presented for ARR and non-aged and carbonated BA and LFC. These results include solubility predictions, residual values for the solubility prediction graphs, and liquid solid phase partitioning diagrams.

Figure C.1 shows 2 examples of a phase partitioning diagram. The reduced concentration at high pH values (above 11 for (b)) is controlled by ettringite. This spurious feature is characteristic to LeachXS, and is present in various diagrams throughout the appendix. It appears as a clear area because ettringite is considered a solid solution, instead of a controlling mineral. For bottom ash, ettringite presence was hindered by decreasing the ettringite parameters in ORCHESTRA by 30 orders of magnitude. This way, ettringite presence was not a problem for BA diagrams, but it can be seen in ARR and LFC diagrams. The light blue area represents the amount of species free in solution. For (a), at pH 14, the controlling species is Hausmannite, and DOC is controlling the solubility of species in solution, as indicated by the light green area. Starting at pH 13 to pH 9, POM has a smaller effect in the solubility of Mn, and below pH 8, the species is free in solution. For (b), the mineral controlling the solubility of Ba in solution at pH of 10.5 is $\text{Ba}(\text{SCr})\text{O}_4$, and then at pH of 9.5, the solubility is controlled by BaSrSO_4 .

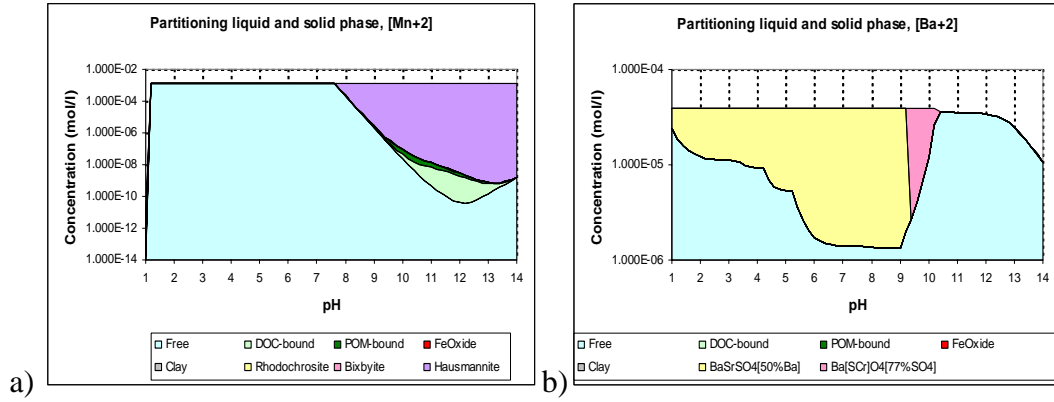


Figure C.1. Example of phase partitioning diagram.

Aluminum Recycling Residue

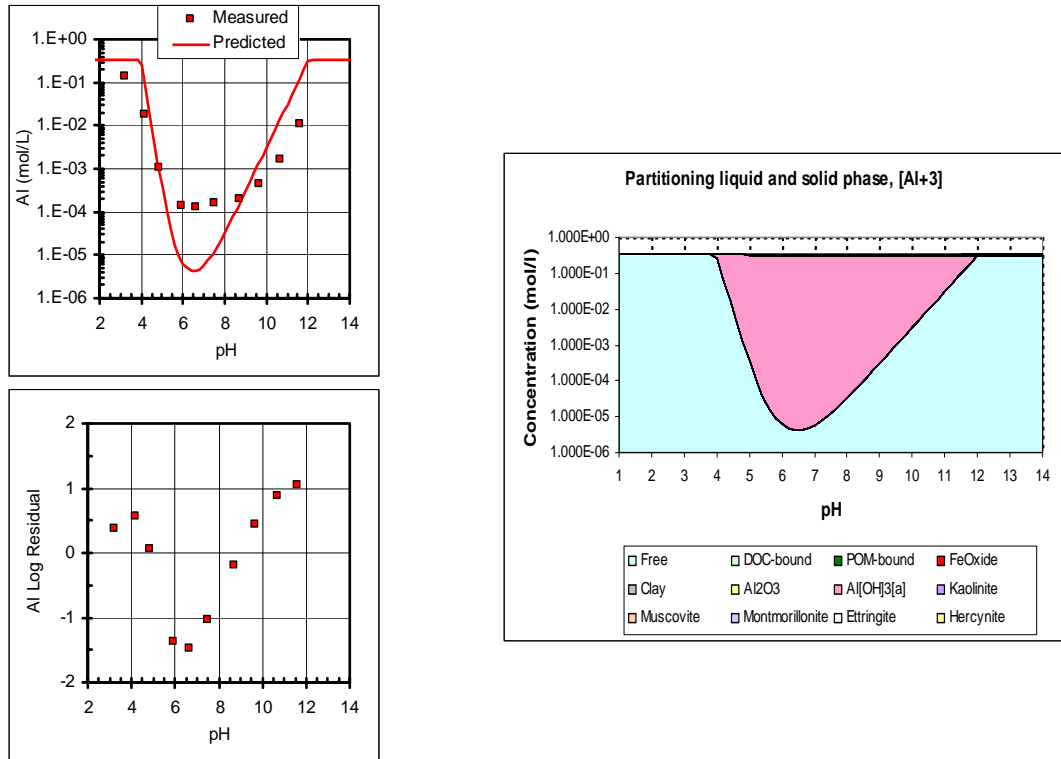


Figure C.2. Al solubility prediction and phase partitioning for ARR.

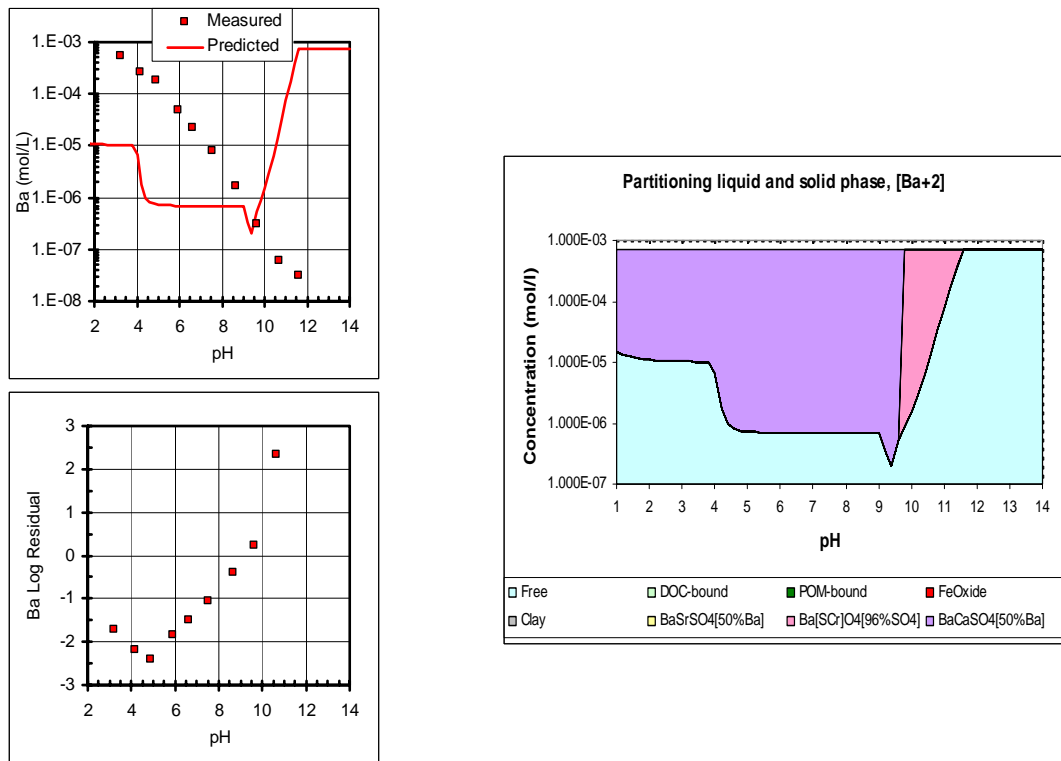


Figure C.3. Ba solubility prediction and phase partitioning for ARR.

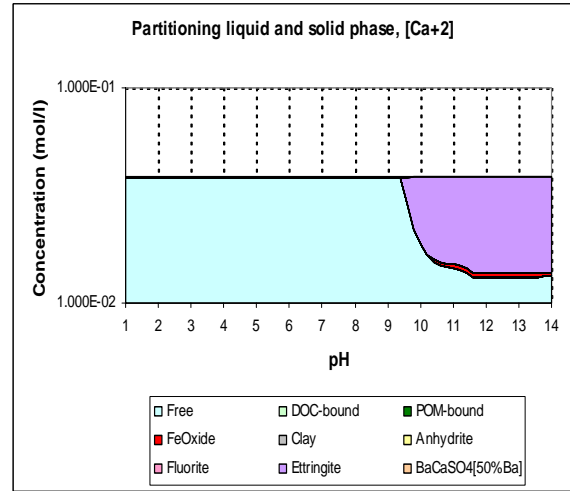
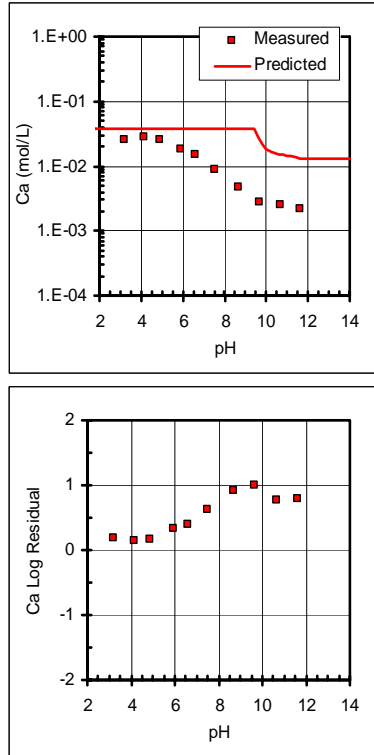


Figure C.4. Ca solubility prediction and phase partitioning for ARR.

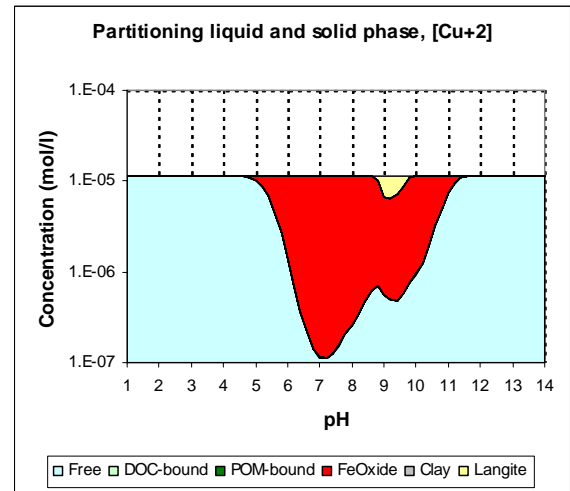
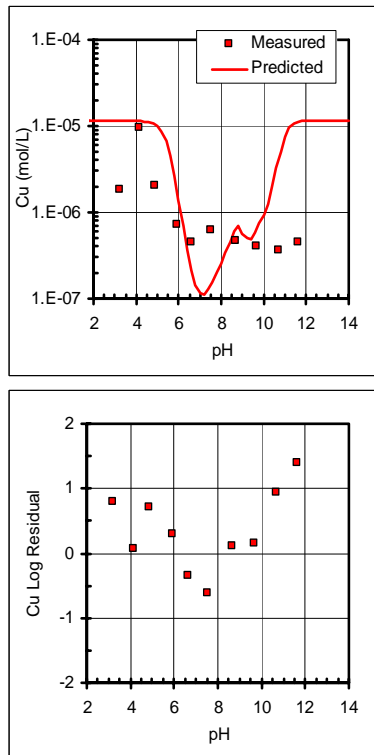


Figure C.5. Cu solubility prediction and phase partitioning for ARR.

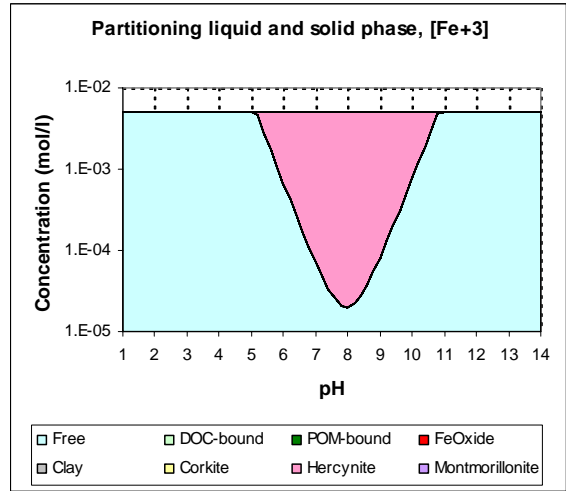
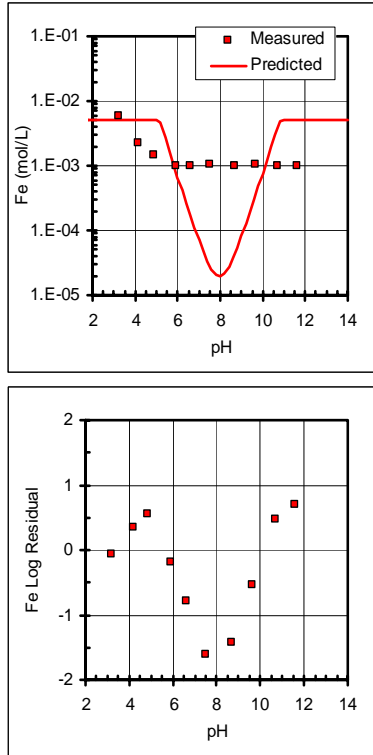


Figure C.6. Fe solubility prediction and phase partitioning for ARR.

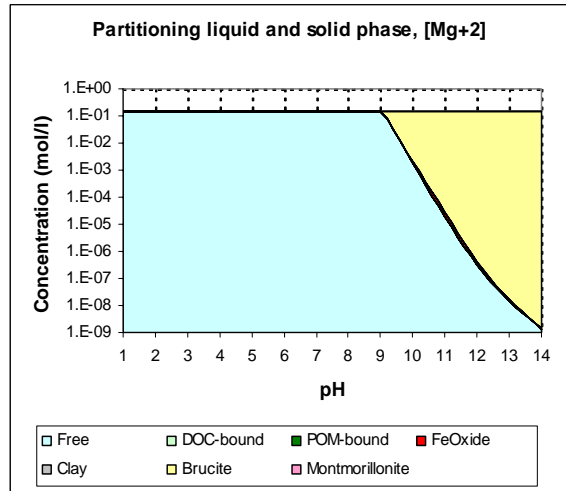
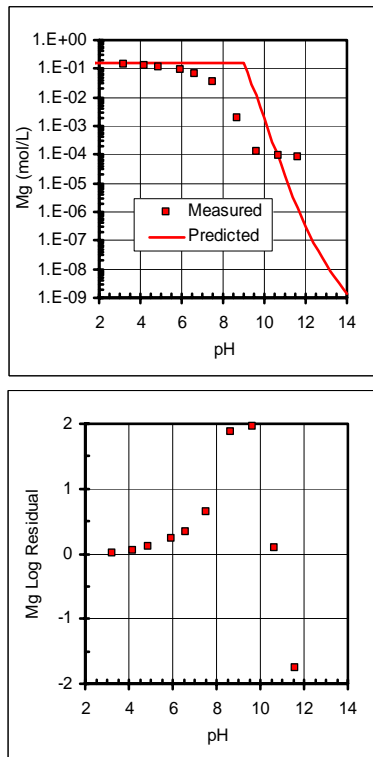


Figure C.7. Mg solubility prediction and phase partitioning for ARR.

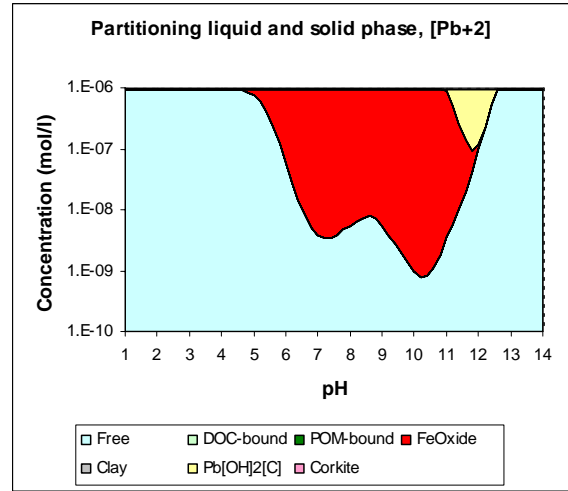
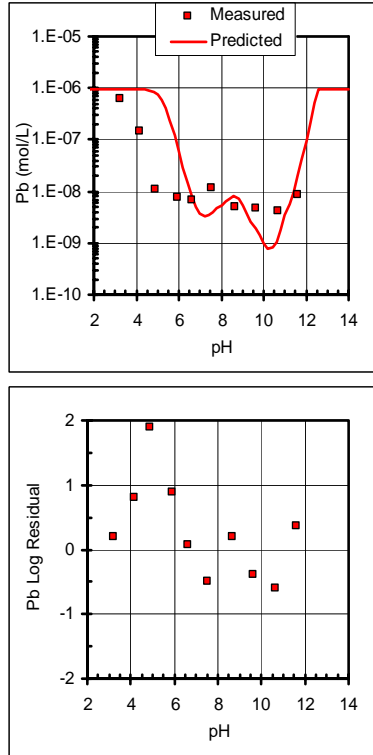


Figure C.8. Pb solubility prediction and phase partitioning for ARR.

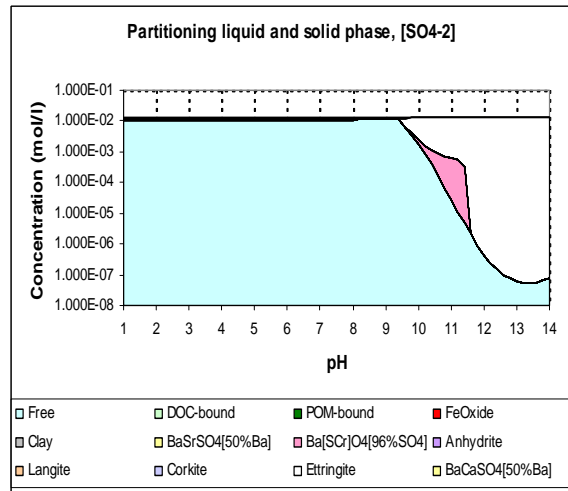
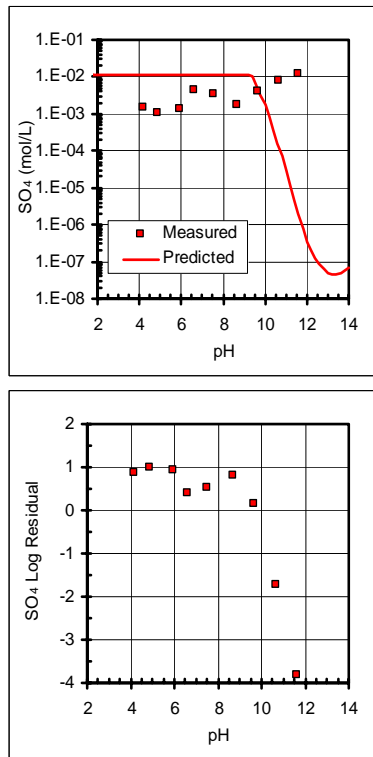


Figure C.9. SO₄ solubility prediction and phase partitioning for ARR.

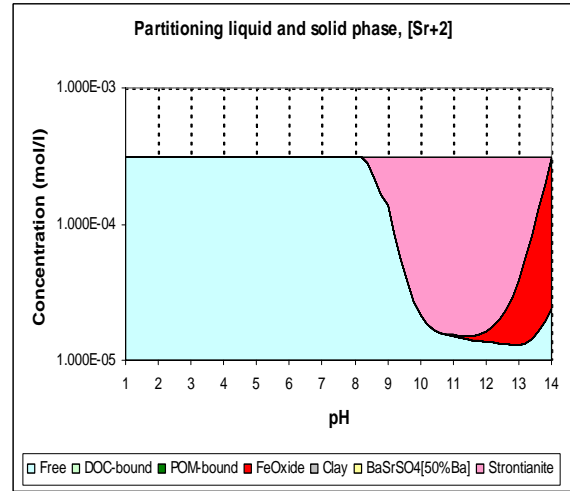
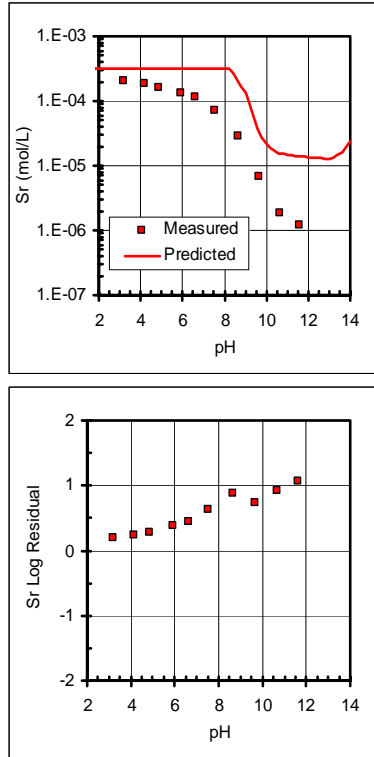


Figure C.10. Sr solubility prediction and phase partitioning for ARR.

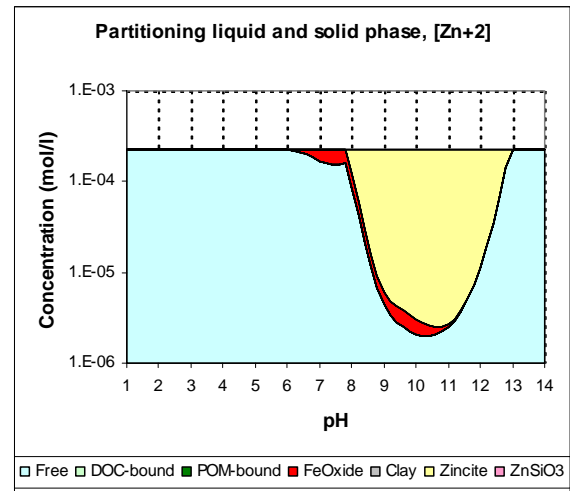
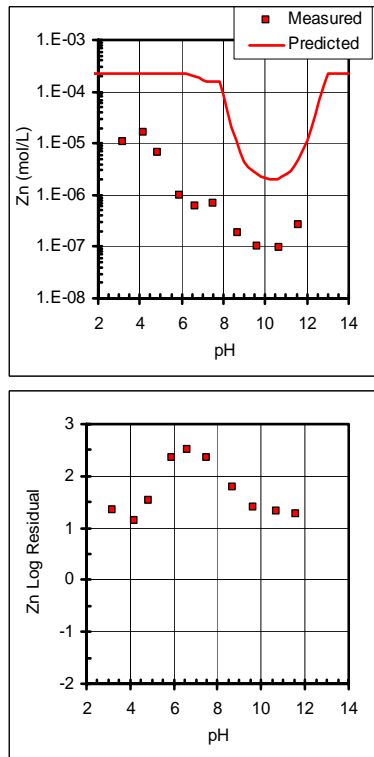


Figure C.11. Zn solubility prediction and phase partitioning for ARR.

Bottom Ash

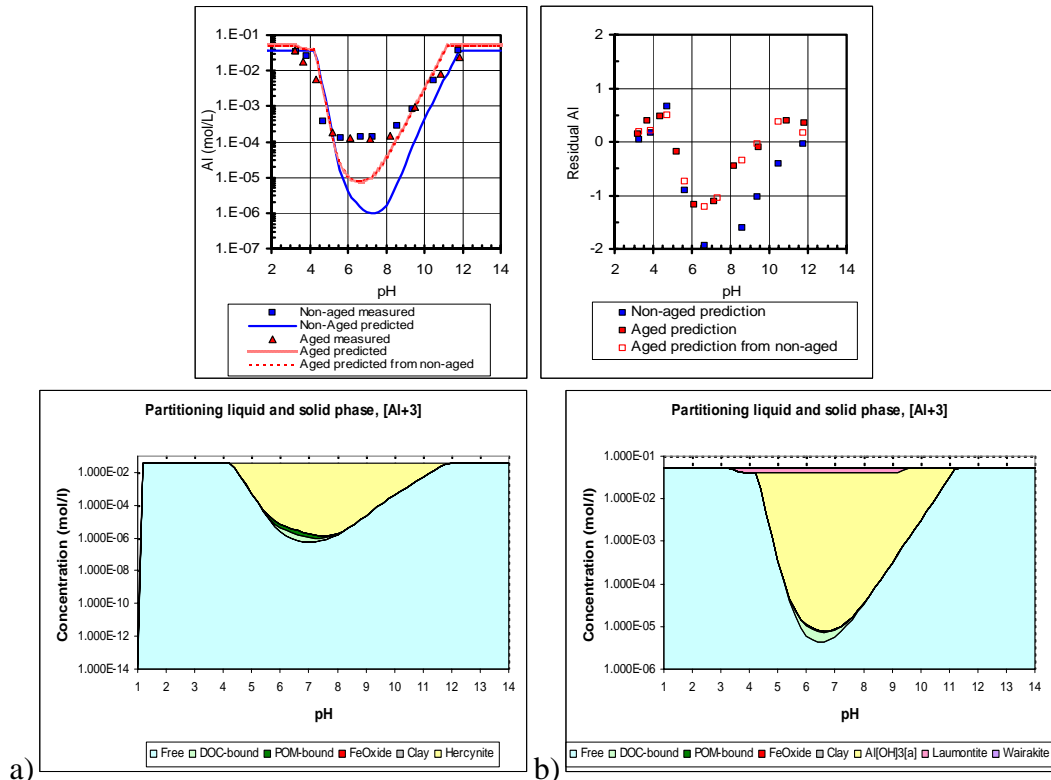


Figure C.12. Al solubility prediction and phase partitioning for BA. ((a) NA (b) Carb)

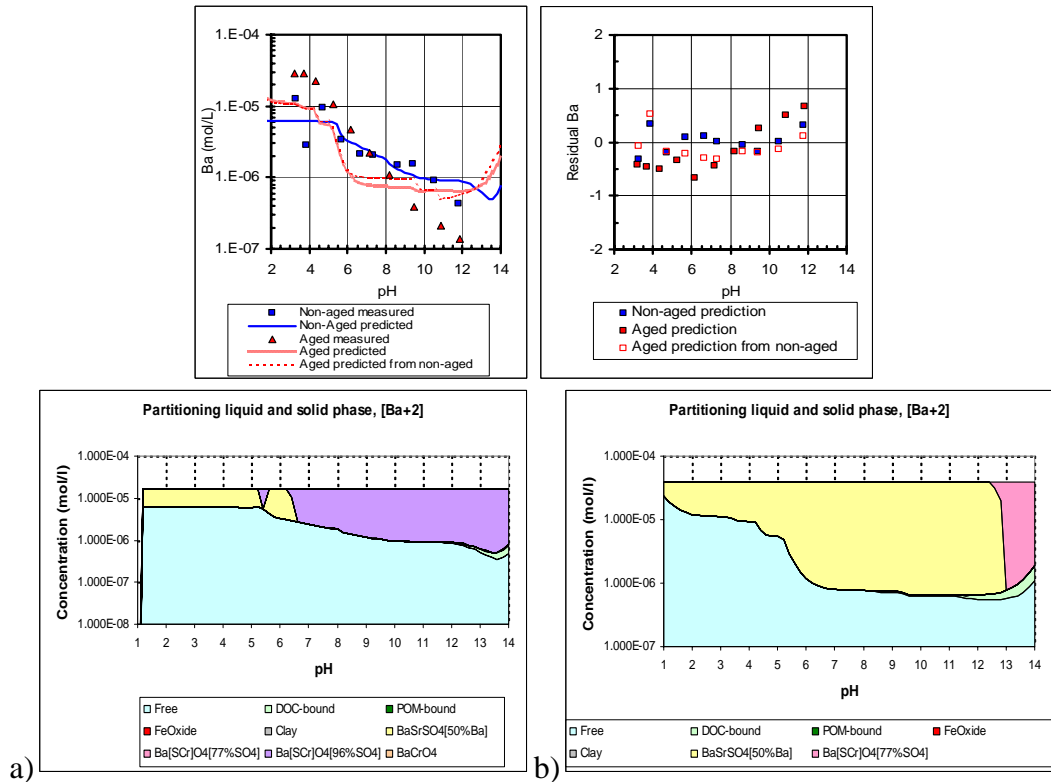


Figure C.13. Ba solubility prediction and phase partitioning for BA. ((a) NA (b) Carb)

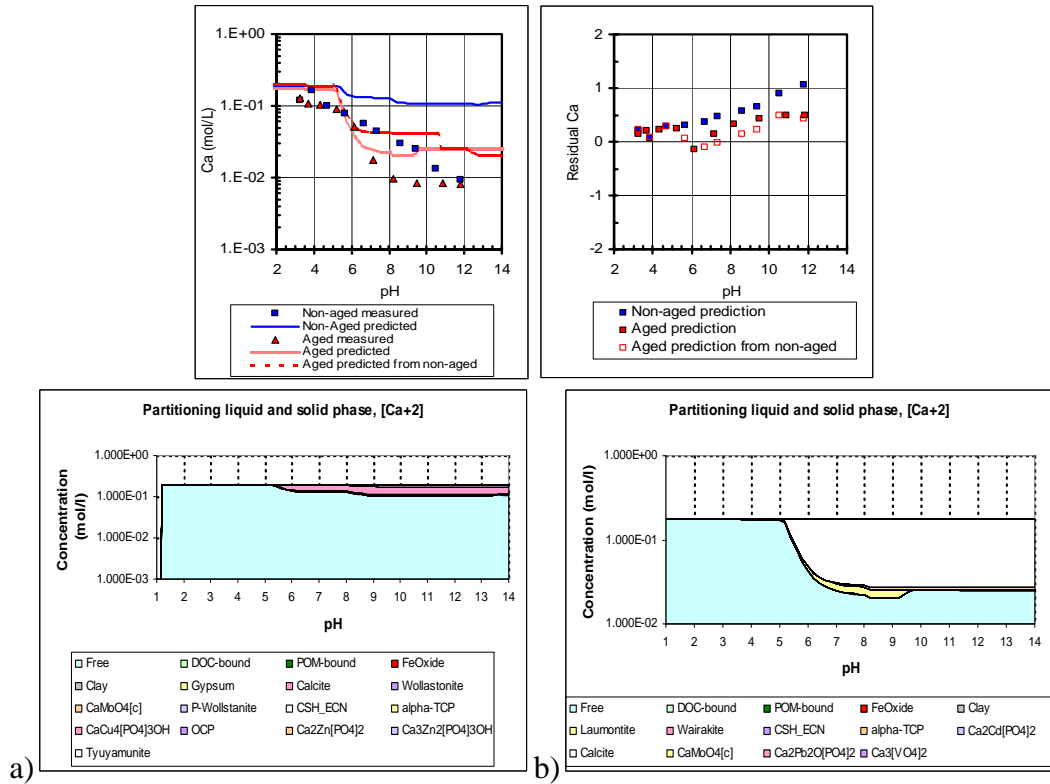


Figure C.14. Ca solubility prediction and phase partitioning for BA. ((a) NA (b) Carb)

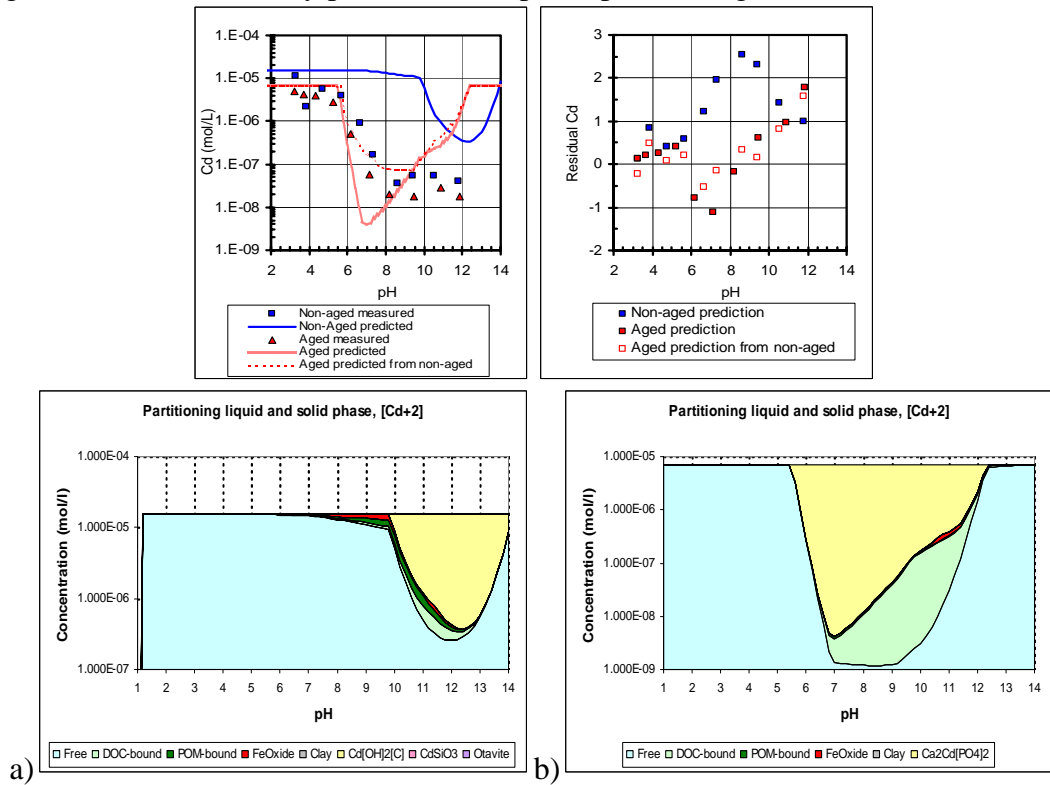


Figure C.15. Cd solubility prediction and phase partitioning for BA. ((a) NA (b) Carb)

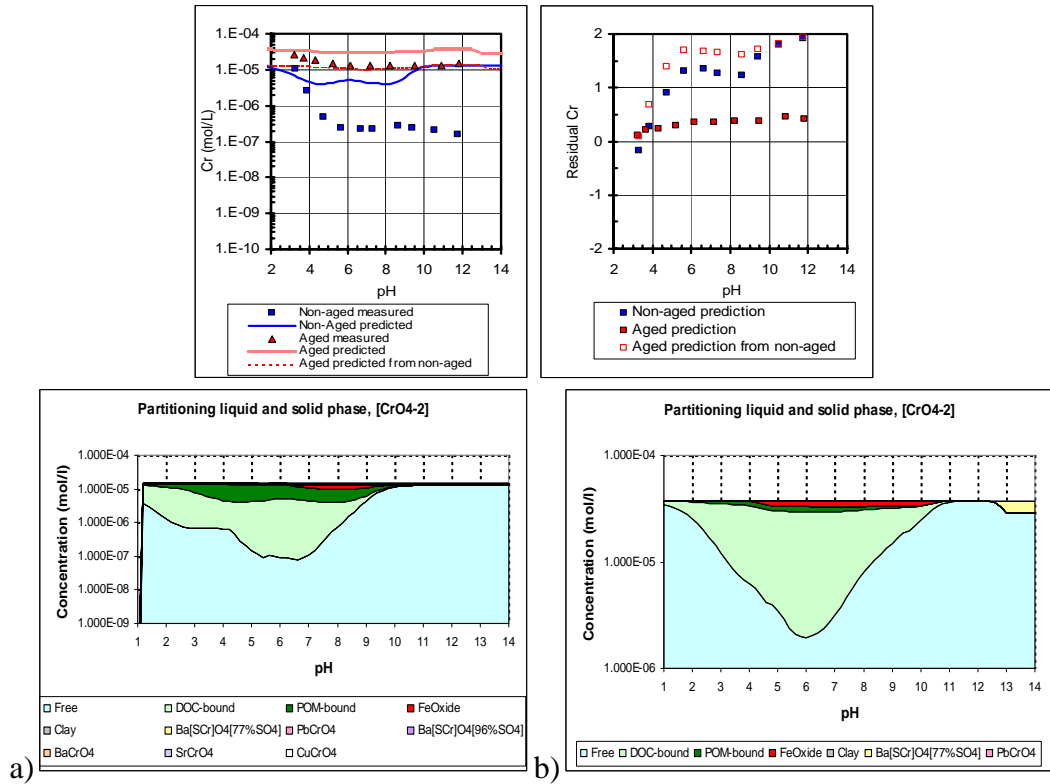


Figure C.16. Cr solubility prediction and phase partitioning for BA. ((a) NA (b) Carb)

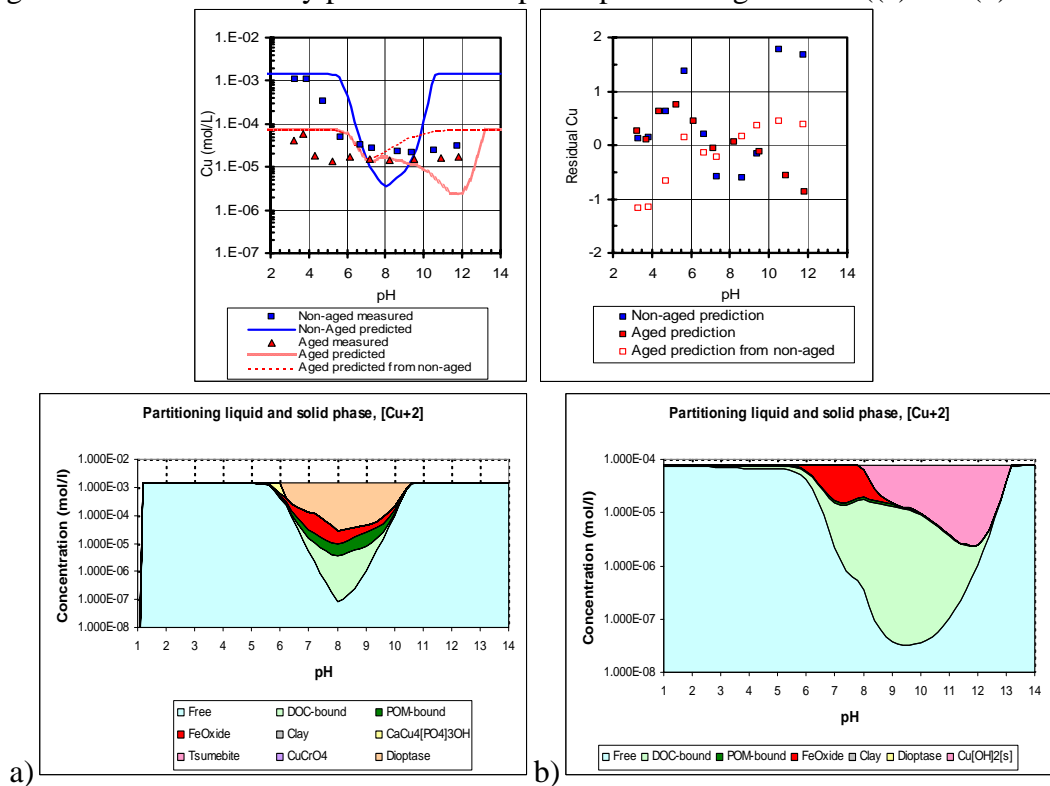


Figure C.17. Cu solubility prediction and phase partitioning for BA. ((a) NA (b) Carb)

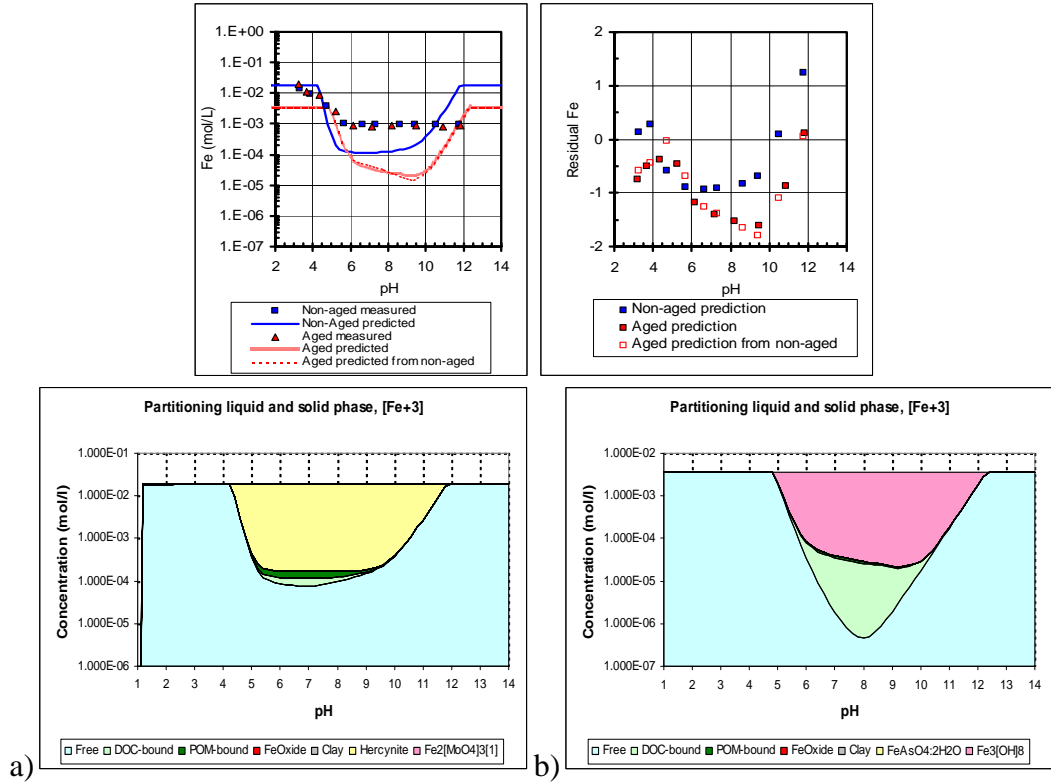


Figure C.18. Fe solubility prediction and phase partitioning for BA. ((a) NA (b) Carb)

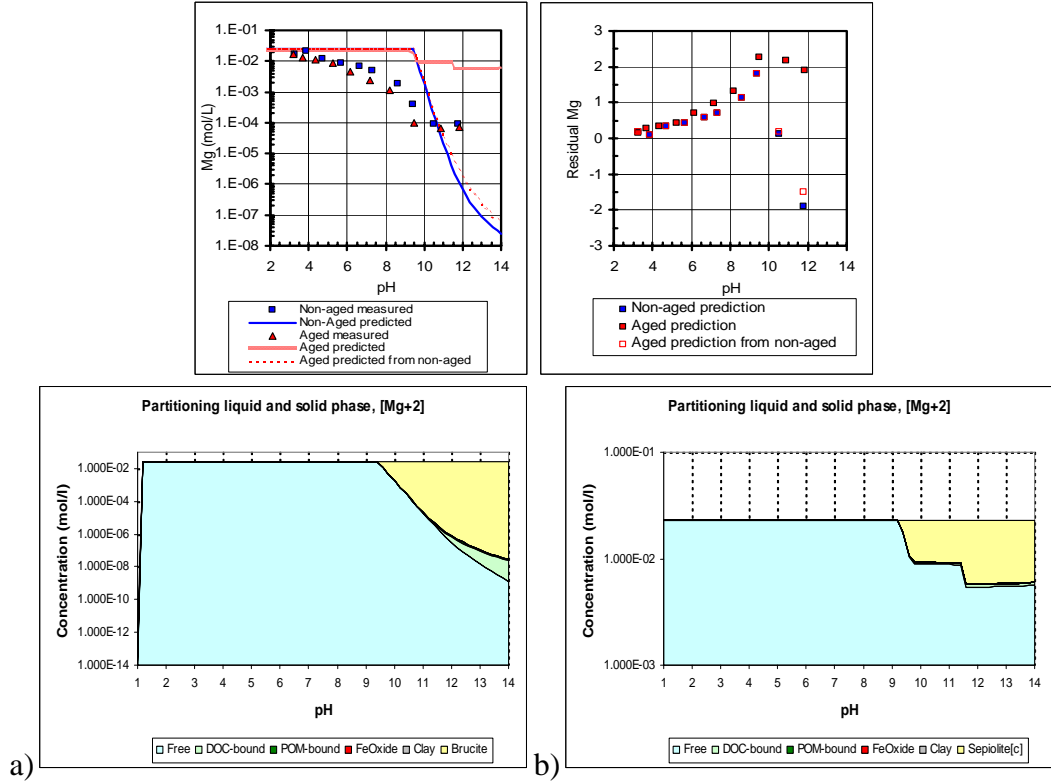


Figure C.19. Mg solubility prediction and phase partitioning for BA. ((a) NA (b) Carb)

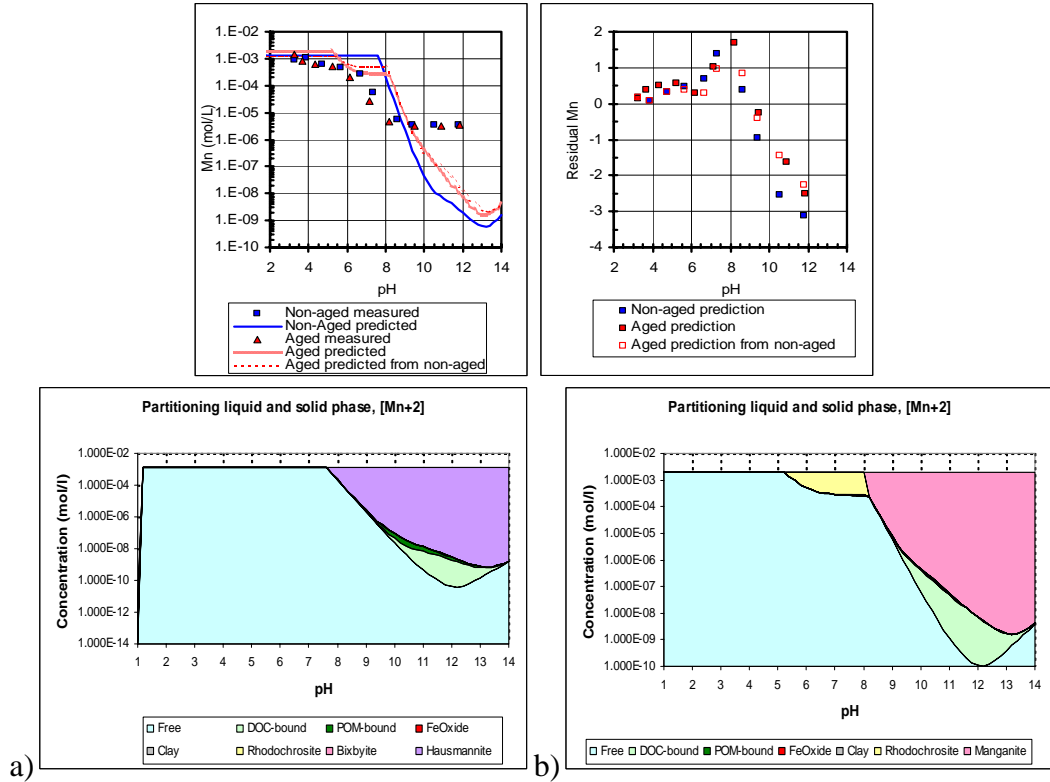


Figure C.20. Mn solubility prediction and phase partitioning for BA. ((a) NA (b) Carb)

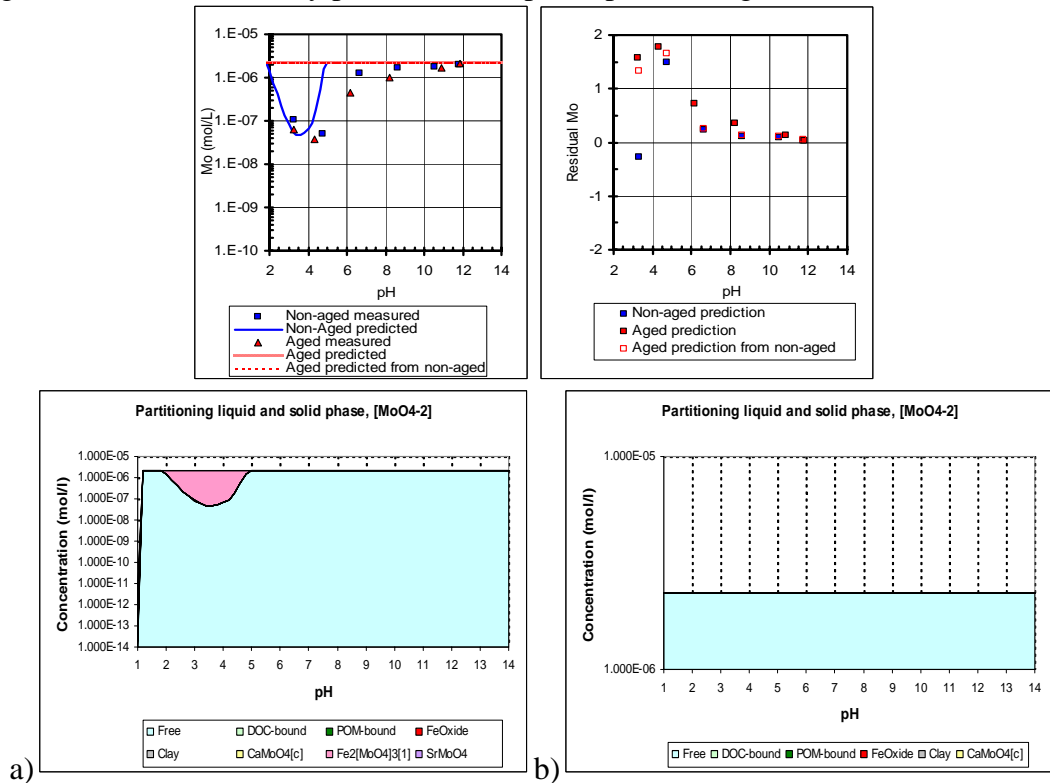


Figure C.21. Mo solubility prediction and phase partitioning for BA. ((a) NA (b) Carb)

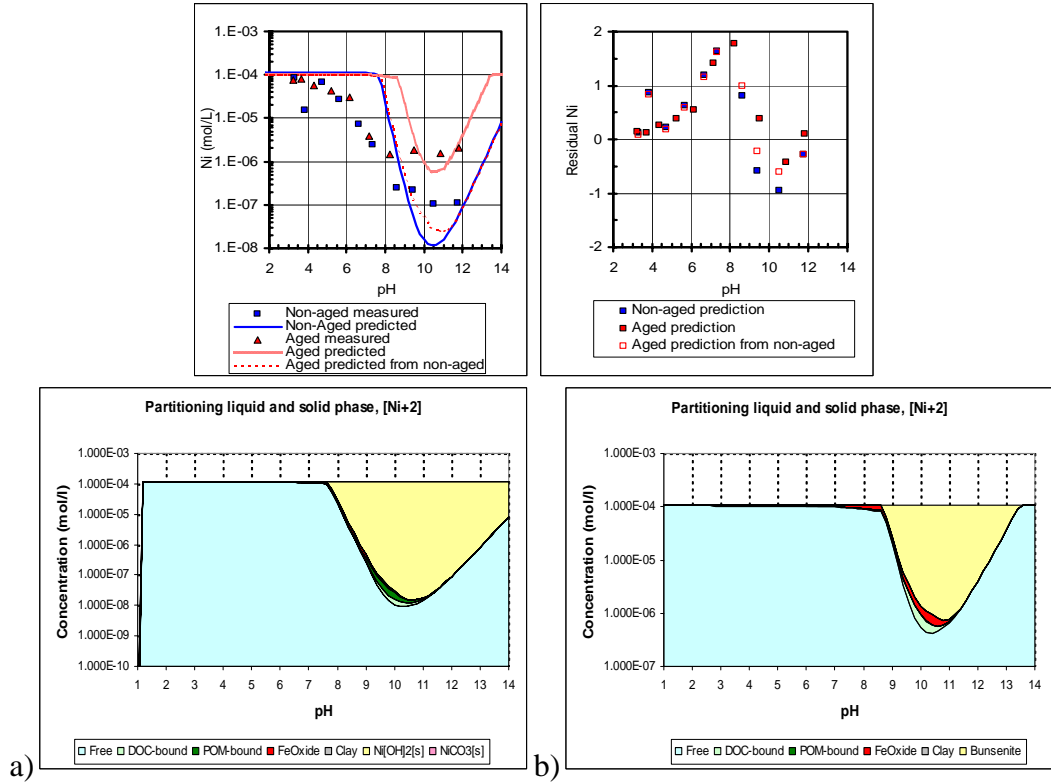


Figure C.22. Ni solubility prediction and phase partitioning for BA. ((a) NA (b) Carb)

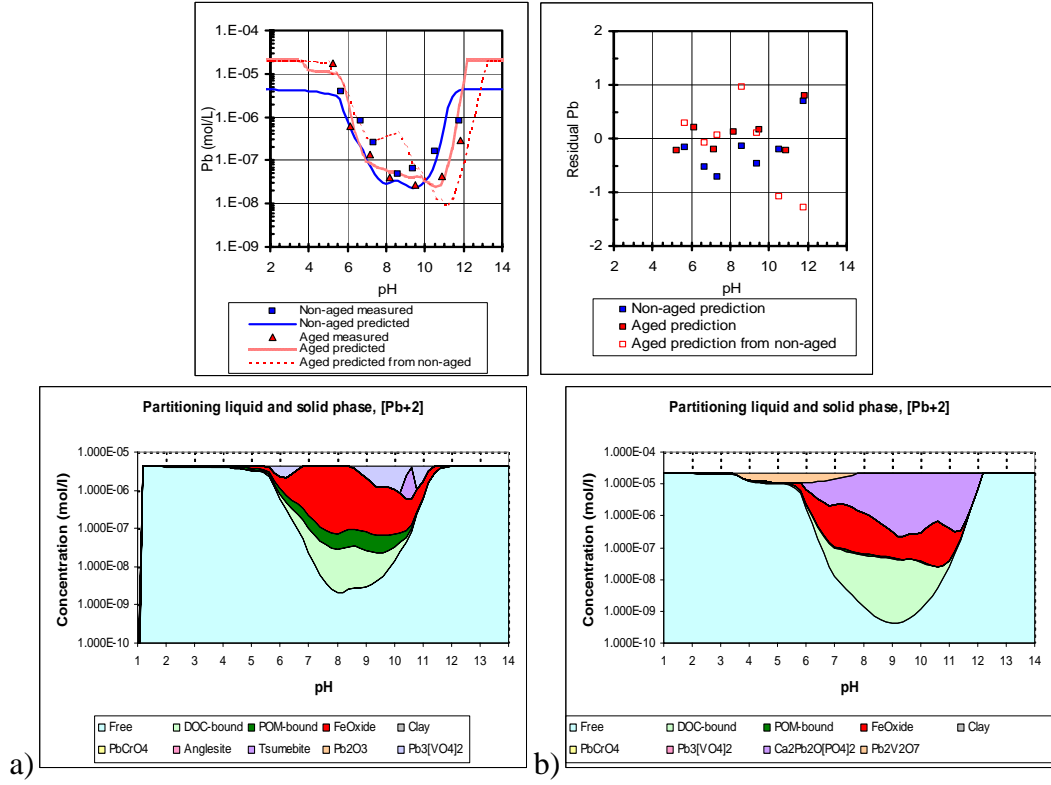


Figure C.23. Pb solubility prediction and phase partitioning for BA. ((a) NA (b) Carb)

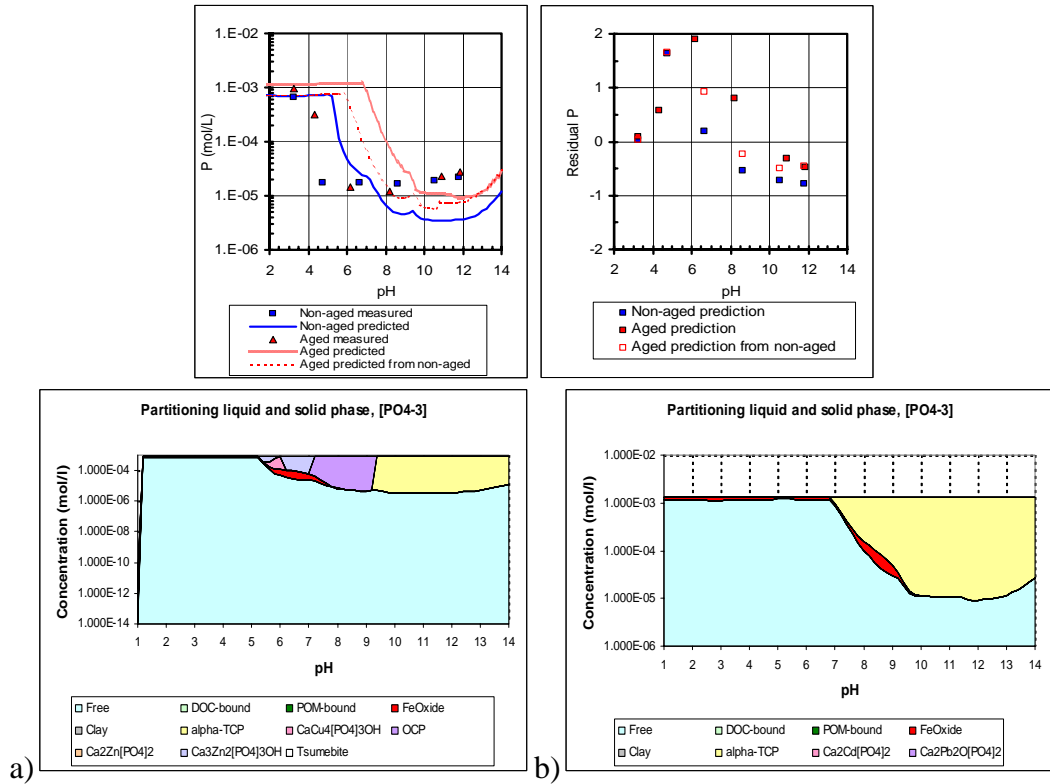


Figure C.24. P solubility prediction and phase partitioning for BA. ((a) NA (b) Carb)

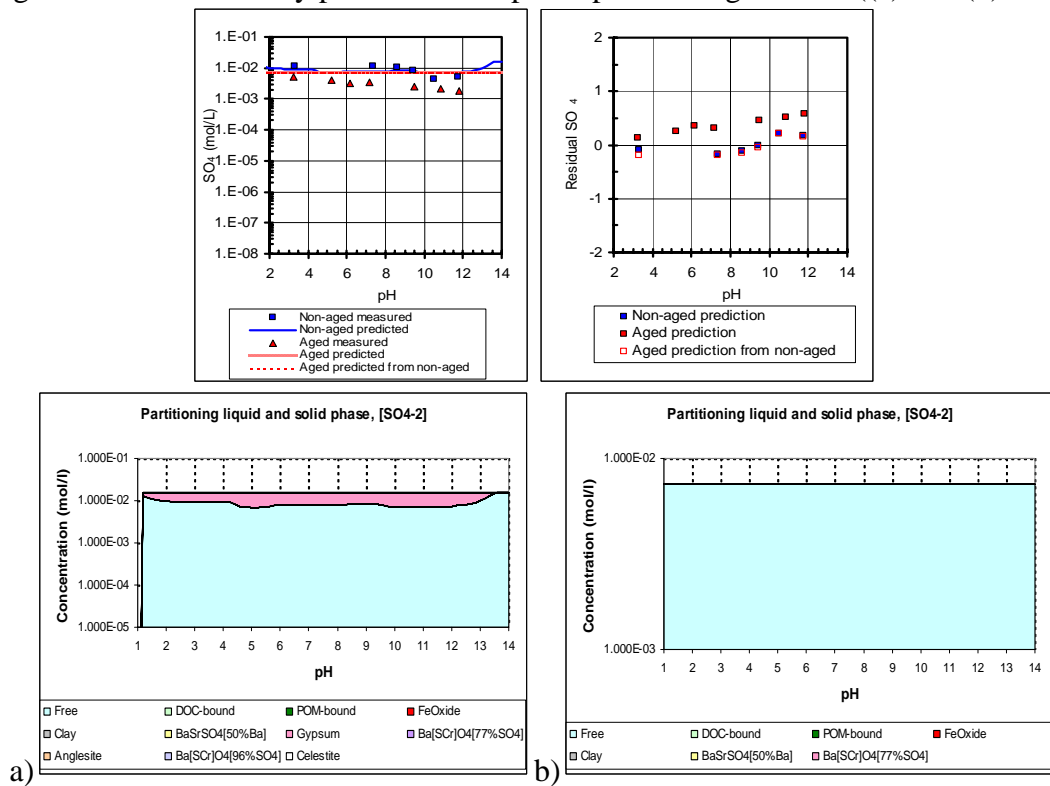


Figure C.25. SO4 solubility prediction and phase partitioning for BA. ((a) NA (b) Carb)

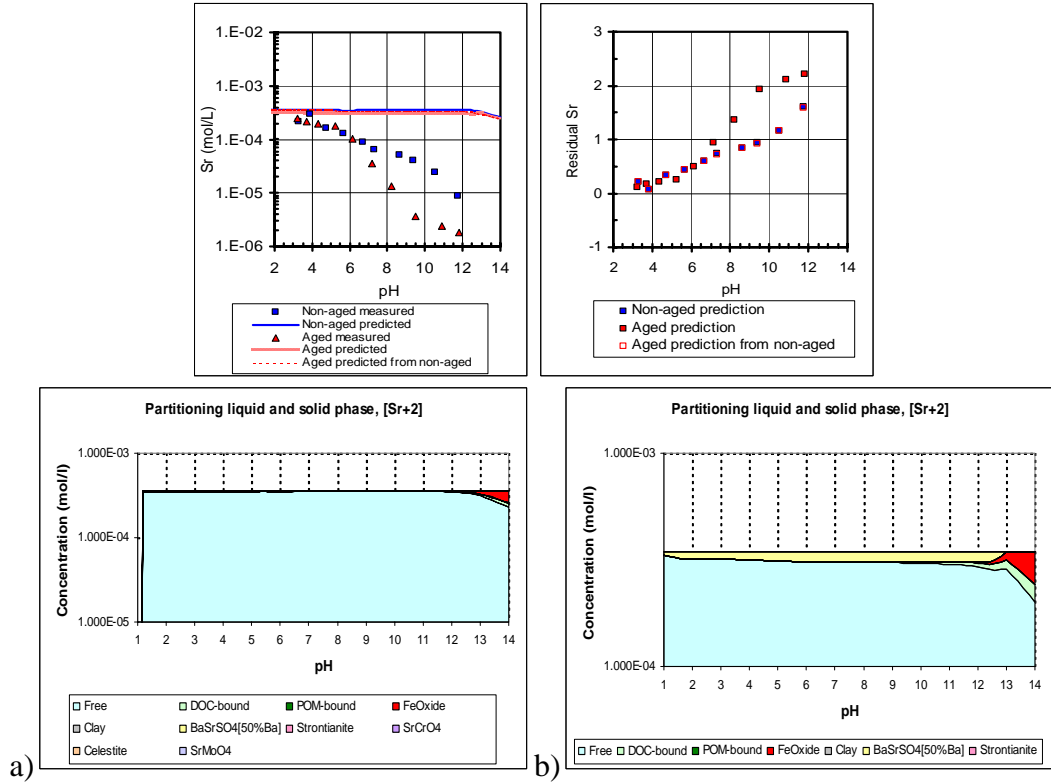


Figure C.26. Sr solubility prediction and phase partitioning for BA. ((a) NA (b) Carb)

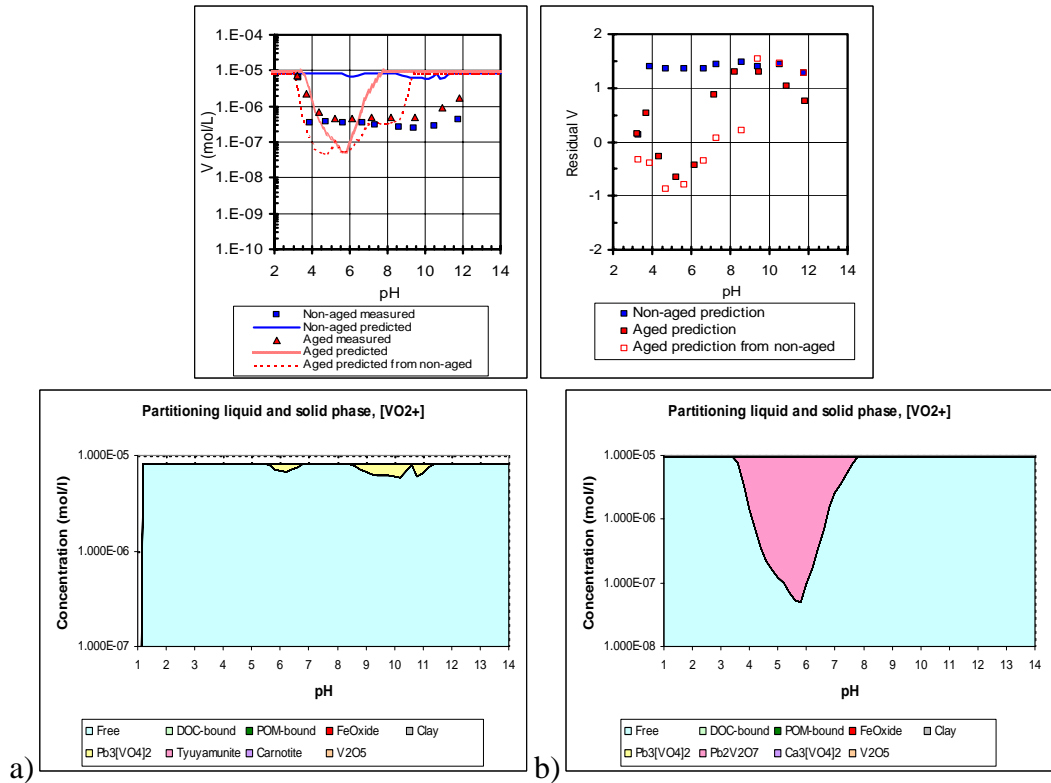


Figure C.27. V solubility prediction and phase partitioning for BA. ((a) NA (b) Carb)

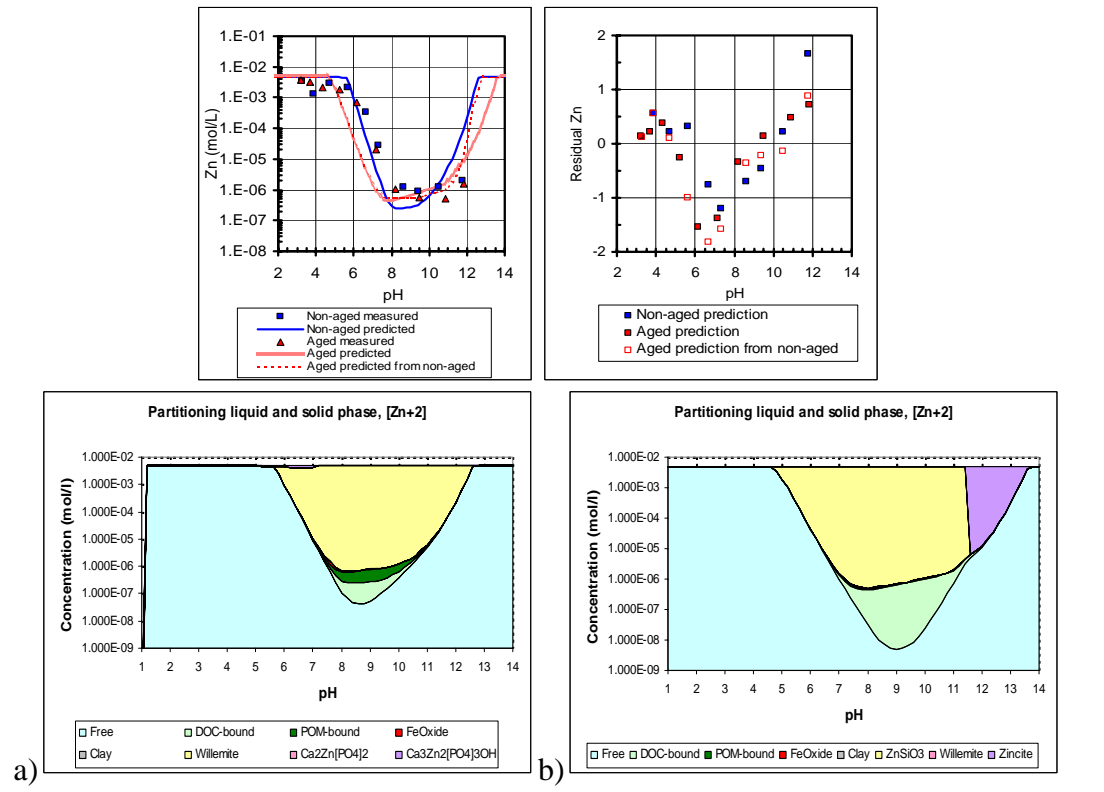


Figure C.28. Zn solubility prediction and phase partitioning for BA. ((a) NA (b) Carb)

Laboratory formulated concrete

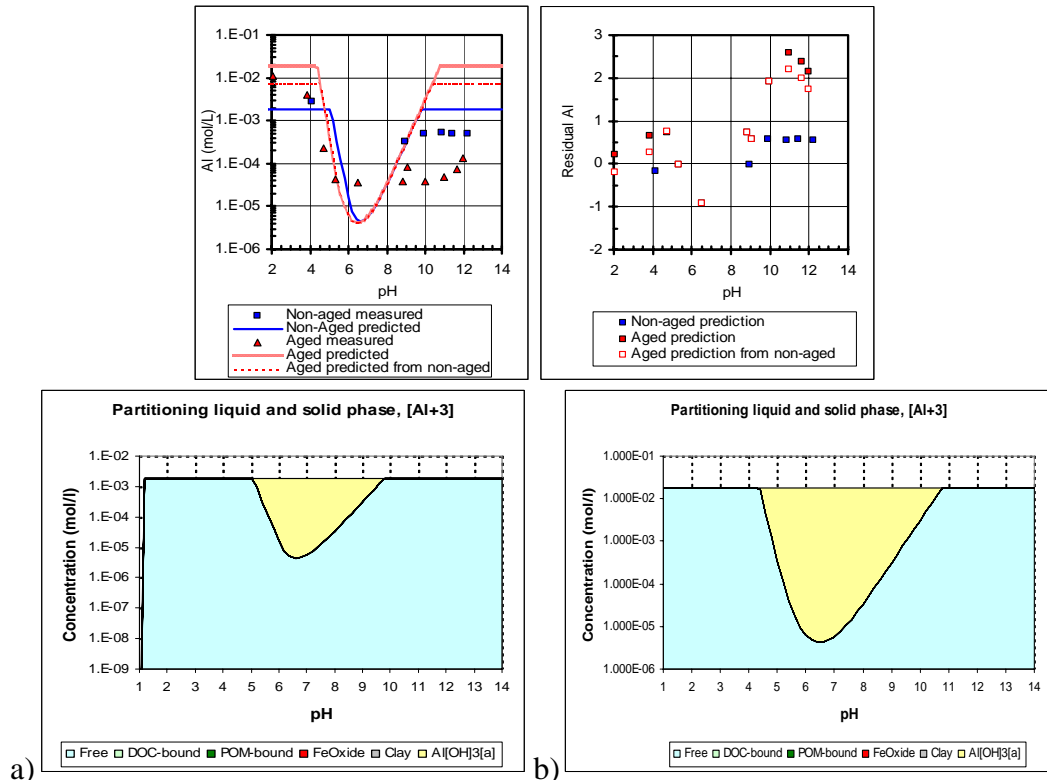


Figure C.29. Al solubility prediction and phase partitioning for LFC. ((a) NA (b) Carb)

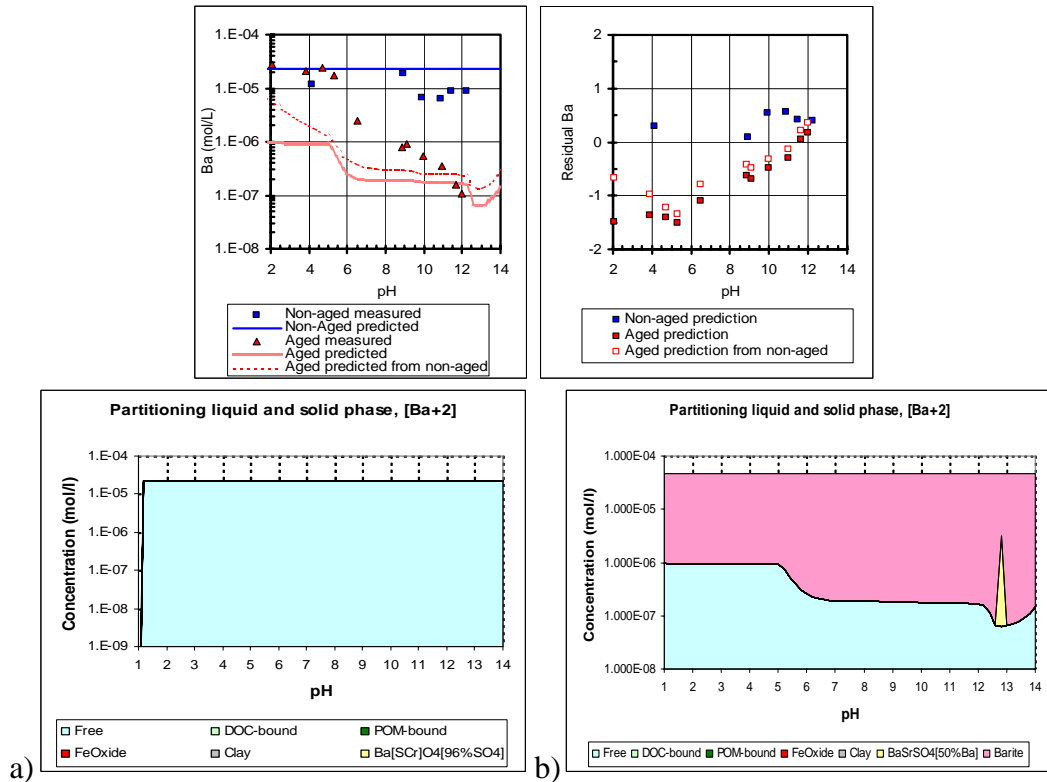


Figure C.30. Ba solubility prediction and phase partitioning for LFC. ((a) NA (b) Carb)

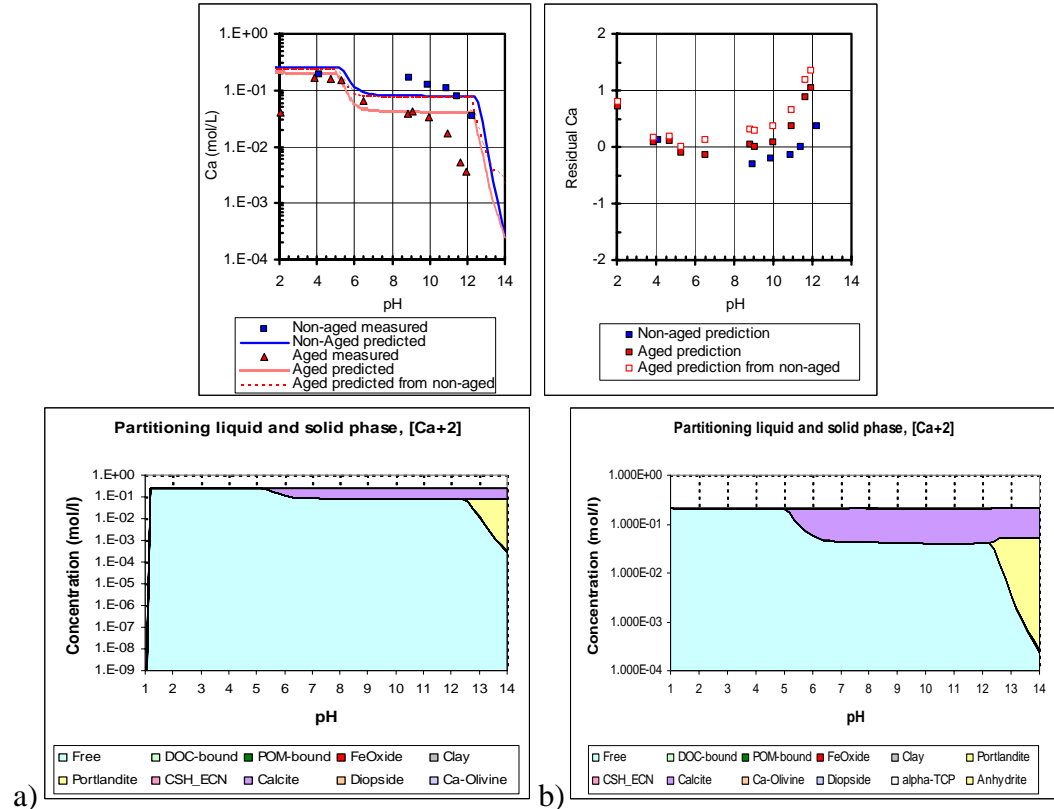


Figure C.31. Ca solubility prediction and phase partitioning for LFC. ((a) NA (b) Carb)

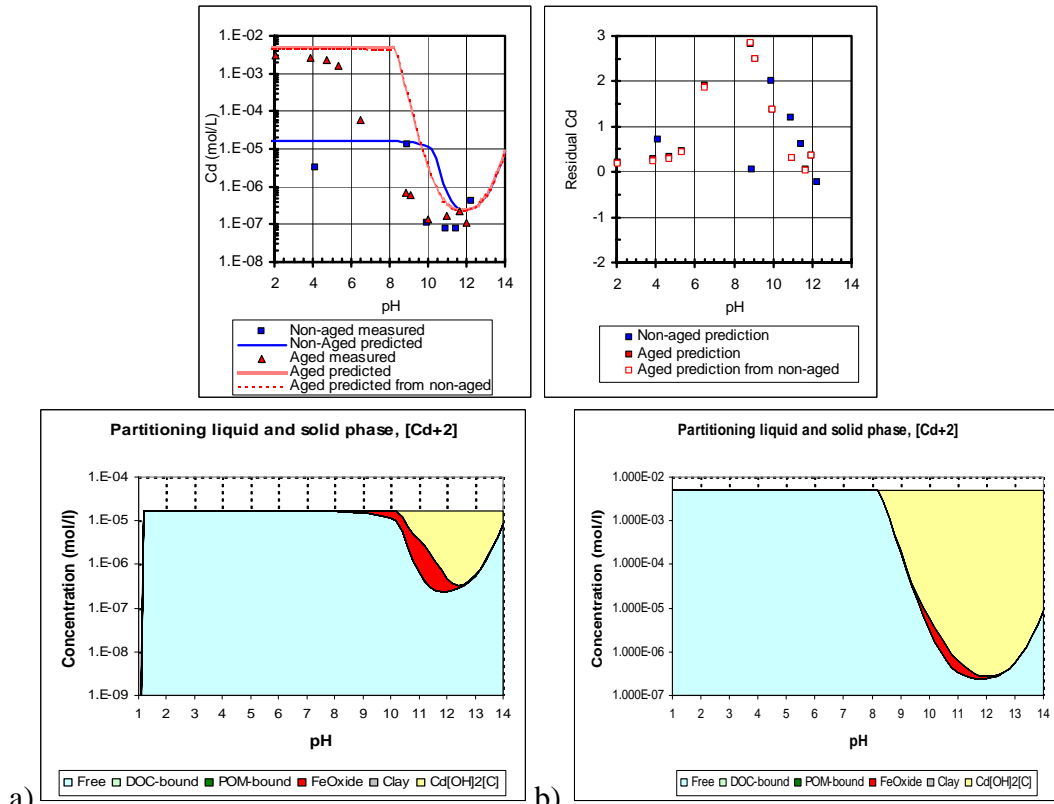


Figure C.32. Cd solubility prediction and phase partitioning for LFC. ((a) NA (b) Carb)

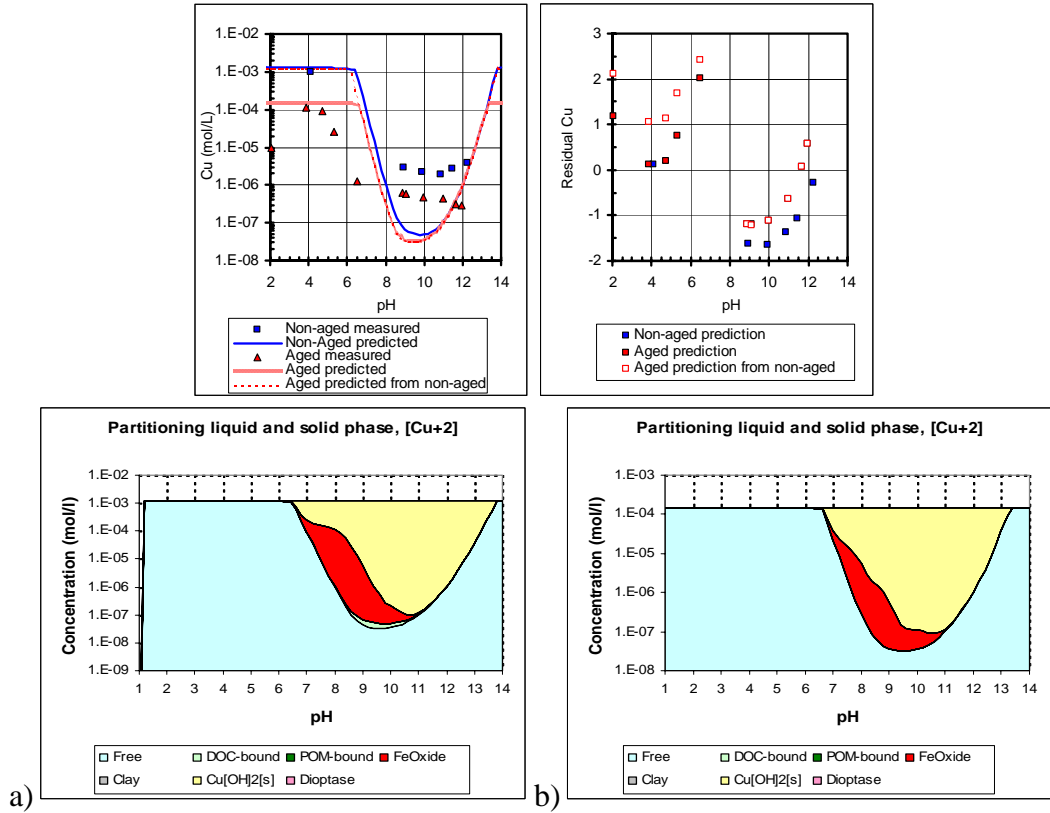


Figure C.33. Cu solubility prediction and phase partitioning for LFC. ((a) NA (b) Carb)

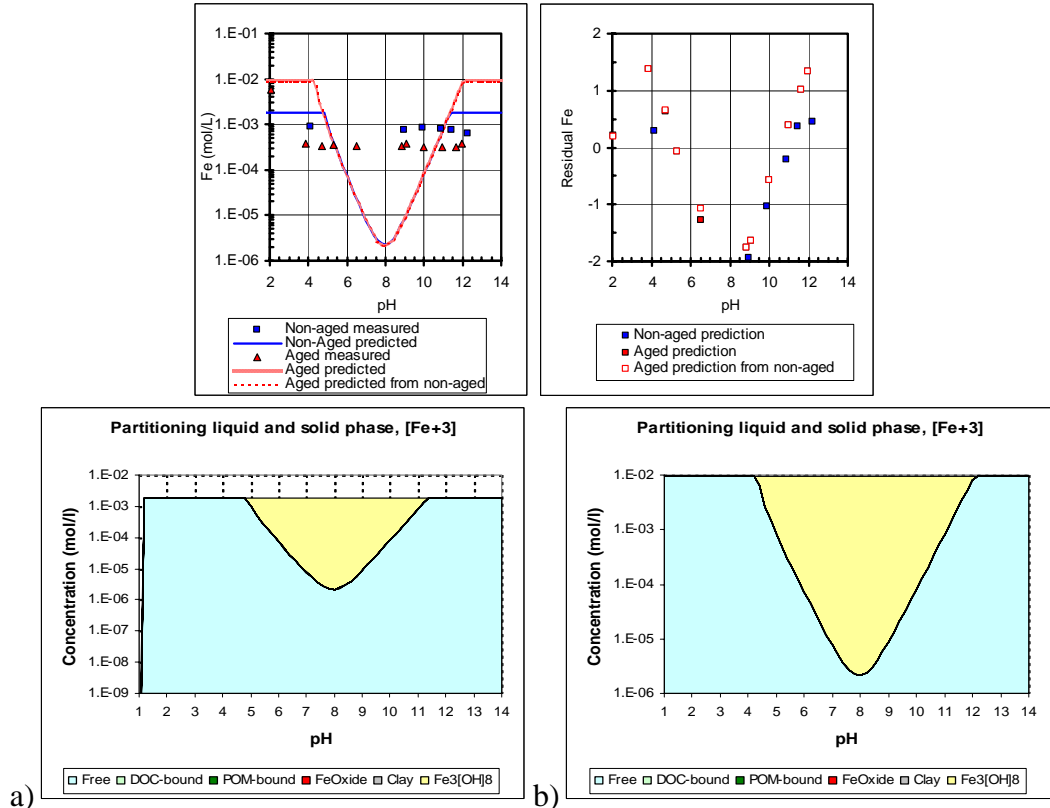


Figure C.34. Fe solubility prediction and phase partitioning for LFC. ((a) NA (b) Carb)

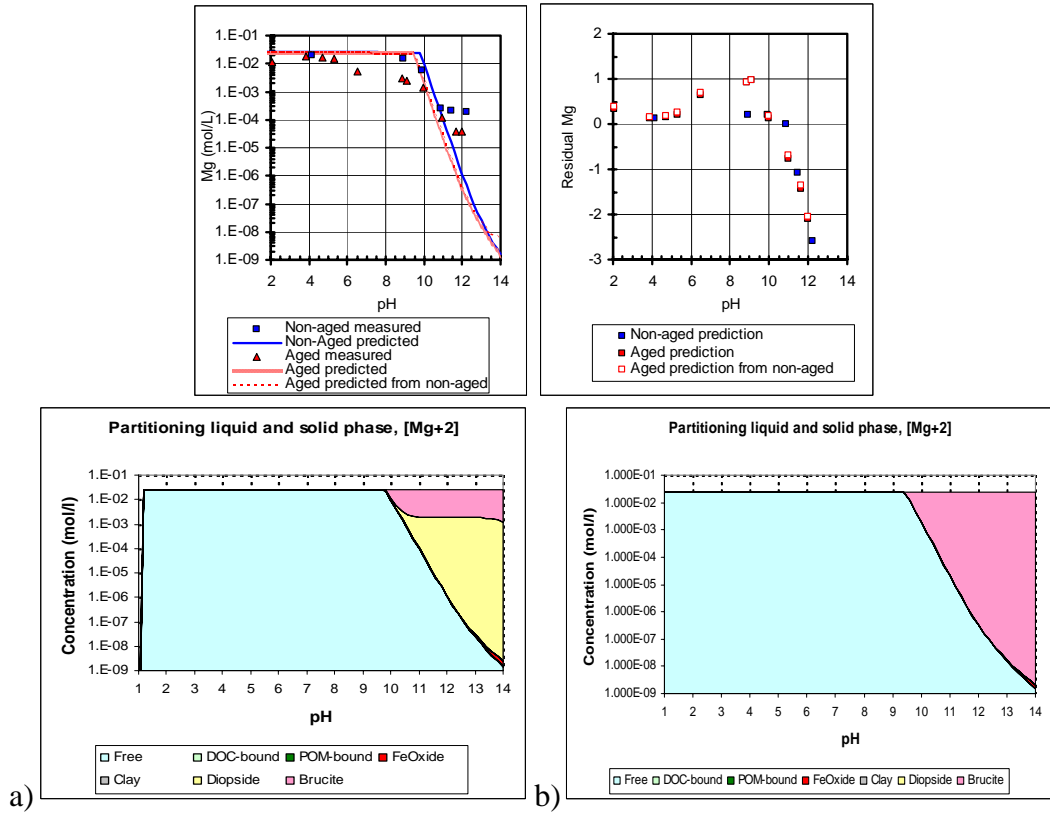


Figure C.35. Mg solubility prediction and phase partitioning for LFC. ((a) NA (b) Carb)

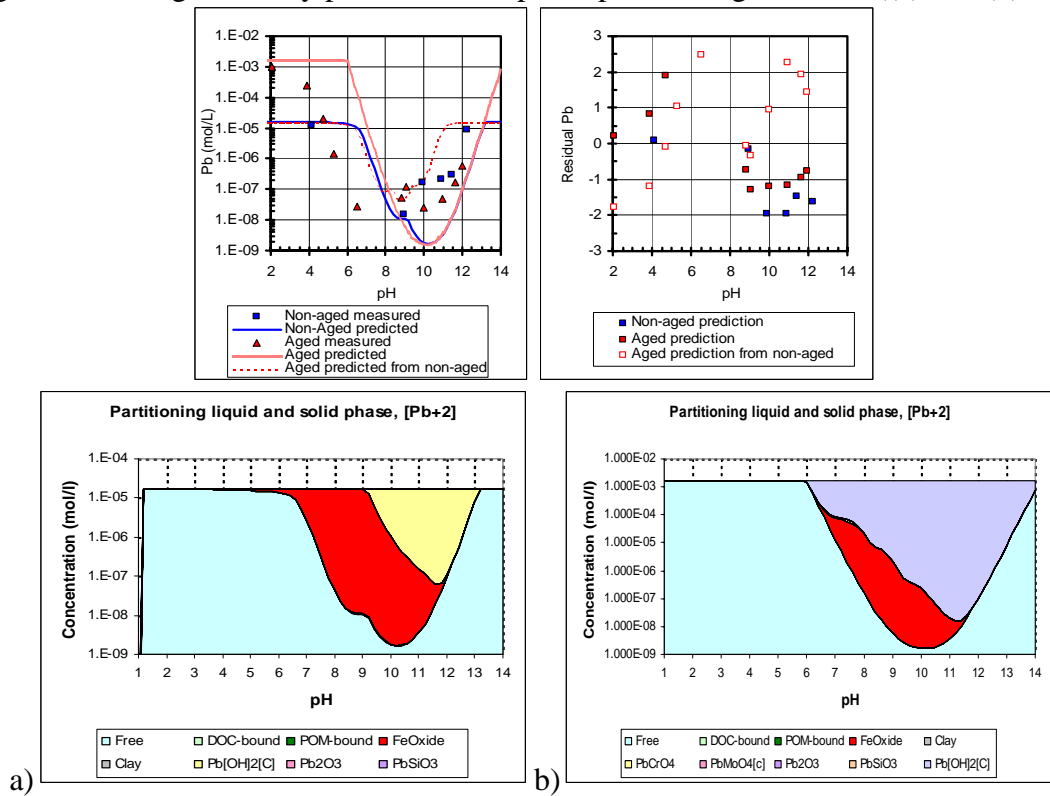


Figure C.36. Pb solubility prediction and phase partitioning for LFC. ((a) NA (b) Carb)

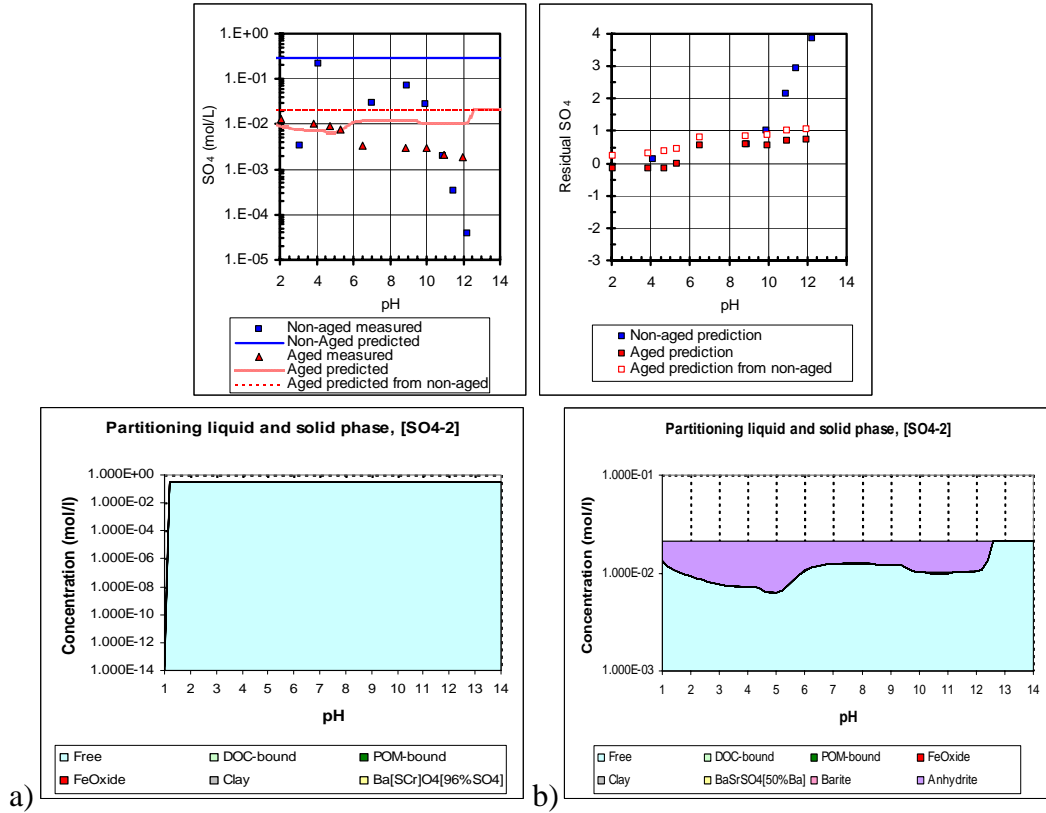


Figure C.37. SO_4 solubility prediction and phase partitioning for LFC. ((a) NA (b) Carb)

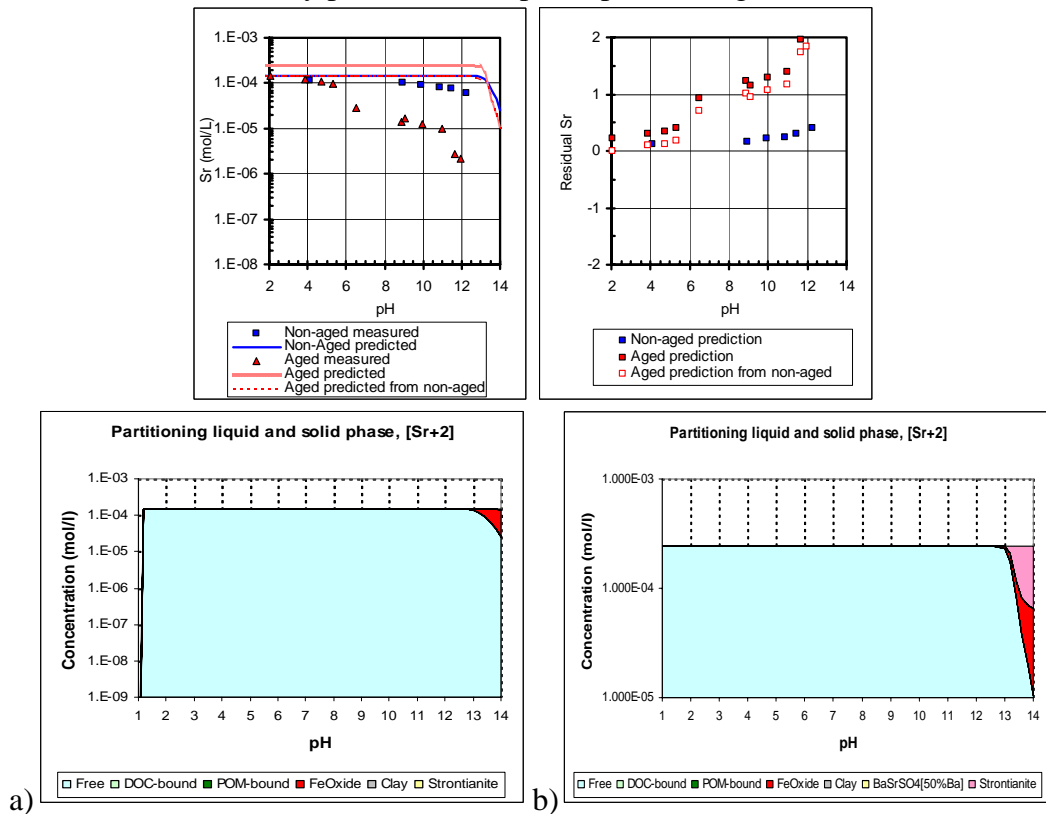


Figure C.38. Sr solubility prediction and phase partitioning for LFC. ((a) NA (b) Carb)

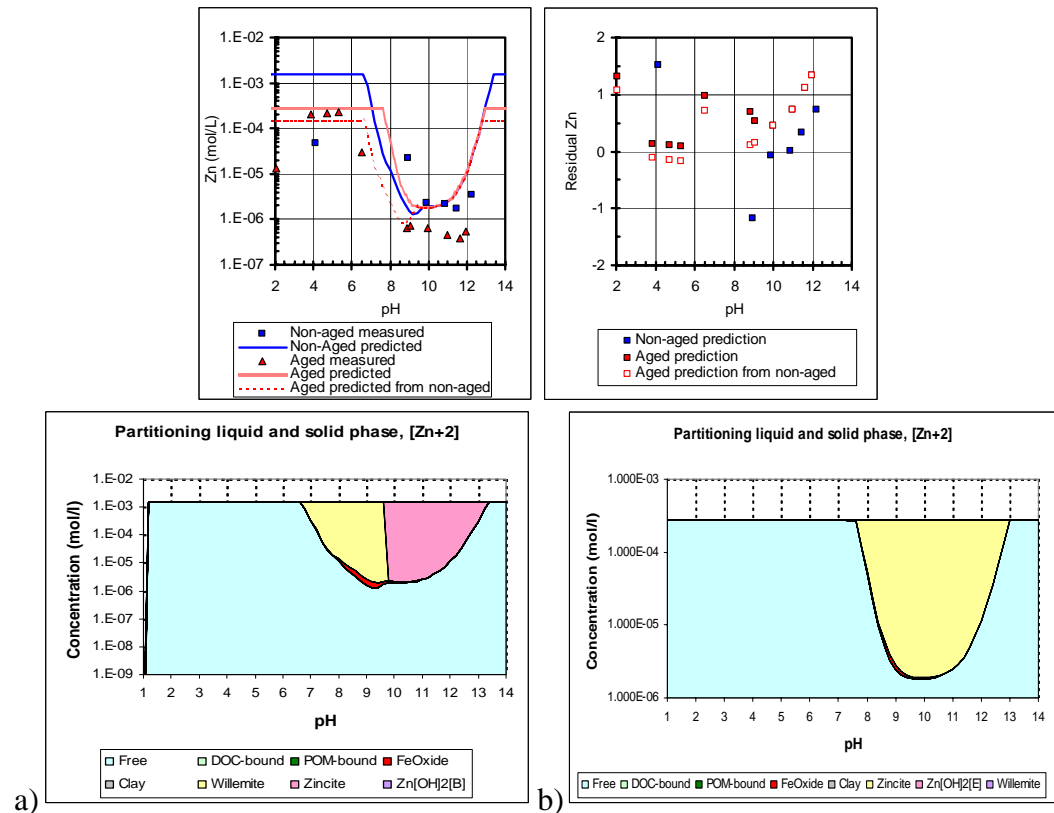


Figure C.39. Zn solubility prediction and phase partitioning for LFC. ((a) NA (b) Carb)

APPENDIX D

MINERAL TABLE

Table D.1. Table of minerals considered for geochemical speciation modeling.

Mineral name	Chemical formula
Albite	NaAlSi ₃ O ₈
Alunite	KAl ₃ (SO ₄) ₂ (OH) ₆
Anglesite	PbSO ₄
Anhydrite	Ca(SO ₄)
Anorthite	CaAl ₂ Si ₂ O ₈
Antlerite	Cu ₃ (SO ₄)(OH) ₄
Atacamite	Cu ₂ Cl(OH) ₃
Barite	Ba(SO ₄)
Birnessite	Na ₄ Mn ₁₄ O ₂₇ ·9H ₂ O
Bixbyite	(Mn,Fe) ₂ O ₃
Boehmite	AlO(OH)
Brucite	Mg(OH) ₂
Bunsenite	NiO
Calcite	CaCO ₃
Carnotite	K ₂ (UO ₂) ₂ (VO ₄) ₂ ·3(H ₂ O)
Celestite (<i>Celestine</i>)	Sr(SO ₄)
Cerrusite	PbCO ₃
Chalcedony	SiO ₂
Corkite	PbFe ³⁺ ₃ (PO ₄)(SO ₄)(OH) ₆
Cristobalite	SiO ₂
CSH	Calcium-silicate-hydrate
Diaspore	AlO(OH)
Diopside	CaMg(Si ₂ O ₆)
Diopside	CuSiO ₂ (OH) ₂

Dolomite	$\text{CaMg}(\text{CO}_3)_2$
Ettringite	$\text{Ca}_6\text{Al}_2(\text{SO}_4)_3(\text{OH})_{12}\cdot 26(\text{H}_2\text{O})$
Fluorite	CaF_2
Goethite	$\text{Fe}^{3+}\text{O}(\text{OH})$
Gibbsite	$\text{Al}(\text{OH})_3$
Gypsum	$\text{Ca}(\text{SO}_4)\cdot 2(\text{H}_2\text{O})$
Hausmannite	Mn_3O_4
Hercynite	$\text{Fe}^{2+}\text{Al}_2\text{O}_4$
Hilgenstockite	$\text{Ca}_4\text{P}_2\text{O}_9$
Hydromagnesite	$\text{Mg}_5(\text{CO}_3)_4(\text{OH})_2\cdot 4(\text{H}_2\text{O})$
Jarosite	$\text{KFe}^{3+}_3(\text{SO}_4)_2(\text{OH})_6$
Kalsilite	KAlSiO_4
Kaolinite	$\text{Al}_2\text{Si}_2\text{O}_5(\text{OH})_4$
Langite	$\text{Cu}_4(\text{SO}_4)(\text{OH})_6\cdot 2(\text{H}_2\text{O})$
Laumontite	$\text{CaAl}_2\text{Si}_4\text{O}_{12}\cdot 4(\text{H}_2\text{O})$
Magnesite	$\text{Mg}(\text{CO}_3)$
Malachite	$\text{Cu}_2(\text{CO}_3)(\text{OH})_2$
Manganite	$\text{Mn}^{3+}\text{O}(\text{OH})$
Mg-Ferrite (<i>Magnesioferrite</i>)	$\text{MgFe}^{3+}_2\text{O}_4$
Montmorillonite	$\text{Na}_{0.2}\text{Ca}_{0.1}\text{Al}_2\text{Si}_4\text{O}_{10}(\text{OH})_2(\text{H}_2\text{O})_{10}$
Muscovite	$\text{KAl}_3\text{Si}_3\text{O}_{10}(\text{OH})_{1.8}\text{F}_{0.2}$
Ca-Olivine (<i>Calcio-Olivine</i>)	Ca_2SiO_4
Otavite	$\text{Cd}(\text{CO}_3)$
Periclase	MgO
Plattnerite	PbO_2
Portlandite	$\text{Ca}(\text{OH})_2$
Pyrolusite	Mn^{4+}O_2
Rhodochrosite	$\text{Mn}^{2+}(\text{CO}_3)$
Sepiolite	$\text{Mg}_4\text{Si}_6\text{O}_{15}(\text{OH})_2\cdot 6(\text{H}_2\text{O})$
Spinel	MgAl_2O_4
Strengite	$\text{Fe}^{3+}(\text{PO}_4)\cdot 2(\text{H}_2\text{O})$
Strontianite	$\text{Sr}(\text{CO}_3)$

α -TCP, β -TCP, OCP	Tricalcium phosphate, ortocalcium phosphate
Tenorite	CuO
Tsumebite	$\text{Pb}_2\text{Cu}(\text{PO}_4)(\text{SO}_4)\text{OH}$
Tyuyamunite	$\text{Ca}(\text{UO}_2)_2(\text{VO}_4)_2 \cdot 6(\text{H}_2\text{O})$
Wairakite	$\text{CaAl}_2\text{Si}_4\text{O}_{12} \cdot 2(\text{H}_2\text{O})$
Willemite	$\text{Zn}_2(\text{SiO}_4)$
Wollastonite	CaSiO_3
Zincate	$\text{Zn}(\text{OH})_2$
Zincite	$(\text{Zn},\text{Mn})\text{O}$
	$\text{Zn}(\text{Mn},\text{Fe})\text{O}$
	$\text{Zn}_5(\text{CO}_3)_2(\text{OH})$ - (<i>hydrozincite</i>)

Mineralogy Database: <http://www.webmineral.com/>

The Mineral Database: <http://www.mindat.org/>

CURRICULUM VITA

SARYNNA LÓPEZ MEZA

Education

- May 2006 **Ph.D. in Environmental Engineering**
Vanderbilt University, Nashville, TN
- June 1999 **M.S. in Environmental Engineering**
December 1996 **B.S. in Chemical Engineering**
Instituto Tecnológico y de Estudios Superiores de Monterrey
(ITESM) Campus Monterrey, Monterrey, N.L., México

Experience

- 2000 – present **Research Assistant**, Advisor: Professor David S. Kosson
Civil and Environmental Engineering, Vanderbilt University
Topic: *Evaluation of the impact of environmental conditions on
constituent leaching from granular materials during intermittent
infiltration.*
- 1997 – 1999 **Research Assistant**, Advisor: Professor Belzahet Treviño Arjona
Environmental Quality Center, ITESM Campus Monterrey
Topic: *Integration of a waste from SrCO₃ production in the
manufacture of construction blocks.*